Clinical Pharmacology of Kinase Inhibitors in Oncology

Optimized and Personalized Dosing

Remy B. Verheijen

The research in this thesis was performed at the Departments of Pharmacy & Pharmacology and Medical Oncology & Clinical Pharmacology of the Netherlands Cancer Institute – Antoni van Leeuwenhoek hospital, Amsterdam, the Netherlands and in collaboration with other institutes.

Printing of this thesis was financially supported by:

The Netherlands Cancer Institute
Utrecht Institute for Pharmaceutical Sciences
Stichting KNMP fondsen

ISBN
978-94-6233-775-6

Design/lay-out
Bregje Jaspers, ProefschriftOntwerp.nl, Nijmegen

Print
Gildeprint, Enschede

Clinical Pharmacology of Kinase Inhibitors in Oncology

Optimized and Personalized Dosing

Klinische Farmacologie van Kinaseremmers in de Oncologie

Dosisoptimalisatie en –personalisatie

(met een samenvatting in het Nederlands)

Proefschrift

ter verkrijging van de graad van doctor aan de Universiteit Utrecht op gezag van de rector magnificus, prof.dr. G.J. van der Zwaan, ingevolge het besluit van het college voor promoties in het openbaar te verdedigen op woensdag 29 november 2017 des middags te 2.30 uur

door

Remy Bob Verheijen

geboren op 27 juli 1989 te De Ronde Venen

Promotoren: Prof.dr. J.H. Beijnen
Prof.dr. J.H.M. Schellens
Prof.dr. A.D.R. Huitema

Copromotor: Dr. N. Steeghs

Contents

Preface

The introduction of targeted anti-cancer therapies has unrecognizably changed and improved the treatment of cancer. Yet, challenges remain in selecting those patients who may benefit most from these treatments and how to best deploy these agents in the treatment of patients.
These targeted agents are generally divided in two main categories: monoclonal antibodies and small molecules. Most of these small molecules inhibit kinases, which are proteins involved in the signal transduction of growth factors that stimulate survival, proliferation and metastasis of tumor cells. Kinase inhibitors have revolutionized the treatment of cancer and are currently used for a wide range of solid and hematological malignancies. This thesis describes a range of clinical pharmacological studies to optimize and personalize the treatment of cancer with kinase inhibitors.

The introduction of these kinase inhibitors to the clinic has widely been hailed as a triumph of personalized or precision medicine. At the moment however, all these drugs are administered using a *one-size-fits-all* fixed dosing schedule, which consists of either a flat dose or a fixed dose based on body surface area (BSA), even though a clear rationale for BSA based dosing is often lacking [2]. This starting dose is then only empirically reduced after the occurrence of intolerable toxicity. **Chapter 1** argues how individualized dosing could improve cancer treatment, for example through adapting the dose based on the concentration of the drug in plasma, generally known as therapeutic drug monitoring.
In **chapter 1.1** we describe the available evidence for individualized dosing through therapeutic drug monitoring of kinase inhibitors in oncology. Furthermore, available data is translated into practical recommendations for dose individualization of these agents.

Chapter 2 focusses on pazopanib, a kinase inhibitor targeting the vascular endothelial growth factor receptor (VEGFR) used for the treatment of advanced renal cancer and soft tissue sarcoma. First in **chapter 2.1** we provide an overview of the available pharmacokinetic and pharmacodynamic data of pazopanib. **Chapters 2.2** and **2.3** provide a description of the bioanalytical validation and clinical application of liquid chromatography tandem mass spectrometry assays to quantify pazopanib in plasma and dried blood spot samples, respectively. **Chapter 2.4** reports on identification of relationships between the pazopanib concentration measured in plasma samples of patients and treatment outcomes in routine care. This chapter is particularly focused on the relationship between pazopanib plasma concentrations and progression free survival. Finally, in **chapter 2.5** we describe a prospective study in cancer patients to evaluate the safety and feasibility of individualized dosing of pazopanib based on measured plasma concentrations.

Chapter 3 provides an outline of bioanalytical and clinical studies with the mammalian target of rapamycin (mTOR) inhibitor everolimus used in the treatment of breast cancer, renal cancer and neuro-endocrine tumors. First, a method to quantify everolimus concentrations in patient samples using a less invasive sampling technique called volumetric absorptive microsampling (VAMS) is described in **chapter 3.1**. Thereafter, **chapter 3.2** describes a randomized pharmacokinetic

crossover study to optimize the pharmacokinetics of everolimus by splitting the dosing schedule from a once daily to a bi-daily schedule in cancer patients. This could reduce the maximum concentrations which are thought to be related to toxicity and, thereby, reduce toxicity without negatively impacting treatment efficacy.

Chapter 4 studies the clinical pharmacological properties of kinase inhibitors by analyzing data from real-world patient cohorts. In **chapter 4.1**, circulating tumor DNA is monitored in a group of patients with non-small cell lung cancer (NSCLC) treated with erlotinib. The quantitative dynamics of circulating tumor DNA of the epidermal growth factor receptor gene were investigated and associated with early treatment failure and disease progression.
In **chapter 4.2**, we report the pharmacokinetics of imatinib in a cohort of gastro-intestinal stromal tumor patients. Analyses included the incidence and predictive factors of low imatinib pharmacokinetics exposure, the change in the exposure over time and the correlation between exposure and response.

In addition to suboptimal and *one-size-fits-all* fixed dosing, another shortcoming of the current application of kinase inhibitors is their limited penetration of the blood-brain barrier, resulting in low concentrations in the central nervous system and suboptimal efficacy in preventing and treating brain tumors and metastases.[4] This is a frequent problem (amongst others) in NSCLC and results in a dismal prognosis for patients. It was hypothesized that the brain concentration of kinase inhibitors routinely used in NSCLC, such as erlotinib, could be increased by co-administration of molecules that inhibit key efflux transporters in the brain, in particular the ATP-binding cassette transporters (ABC) ABCB1 and ABCG2. Specific inhibitors of these transporters have been developed, one example being elacridar. **Chapter 5.1** describes the clinical pharmacokinetics of a novel amorphous solid dispersion formulation of elacridar in a phase I dose-escalation study. **Chapter 5.2** shows the application of this formulation of elacridar in a proof-of-concept study in cancer patients. In this study, patients were subjected to ^{11}C-erlotinib PET scanning, enabling non-invasive visualization of erlotinib in the brain. To evaluate the effect of elacridar on erlotinib brain penetration, patients underwent a PET scan with and without administration of an elacridar dose.

Clinical pharmacological studies could also guide early drug development for example to optimize the posology of drug candidates. The novel focal adhesion kinase inhibitor BI 853520 is such a drug currently under clinical development. **Chapter 6.1** describes two randomized open-label crossover clinical pharmacokinetic studies on the effect of food and formulation as a liquid dispersion.

References

1. Longo DL. Imatinib Changed Everything. N. Engl. J. Med. 2017;376:982–3.
2. Bins S, Ratain MJ, Mathijssen RHJ. Conventional dosing of anticancer agents: precisely wrong or just inaccurate? Clin. Pharmacol. Ther. 2014;95:361–4.
3. Sheiner LB. Learning versus confirming in clinical drug development. Clin. Pharmacol. Ther. 1997;61:275–91.
4. Jacus MO, Daryani VM, Harstead KE, Patel YT, Throm SL, Stewart CF. Pharmacokinetic Properties of Anticancer Agents for the Treatment of Central Nervous System Tumors: Update of the Literature. Clin. Pharmacokinet. 2016;55:297–311.

Chapter 1

Introduction

Chapter 1.1

Practical Recommendations for Therapeutic Drug Monitoring of Kinase Inhibitors in Oncology

R.B. Verheijen[1], H.Yu[1], J.H.M. Schellens[2,3], J.H. Beijnen[1,3], N. Steeghs[2], A.D.R. Huitema[1,4]

[1]Department of Pharmacy & Pharmacology, The Netherlands Cancer Institute - Antoni van Leeuwenhoek, Amsterdam, The Netherlands.
[2]Department of Medical Oncology and Clinical Pharmacology, The Netherlands Cancer Institute - Antoni van Leeuwenhoek, Amsterdam, The Netherlands.
[3]Department of Pharmaceutical Sciences, Utrecht University, Utrecht, The Netherlands.
[4]Department of Clinical Pharmacy, Utrecht University Medical Center, Utrecht, The Netherlands.

Introduction

Despite the fact that pharmacokinetic exposure of kinase inhibitors (KIs) is highly variable and clear relationships exist between exposure and treatment outcomes, fixed dosing is still standard practice. This review aims to summarize the available clinical pharmacokinetic and pharmacodynamic data into practical guidelines for individualized dosing of KIs through therapeutic drug monitoring (TDM). Additionally, we provide an overview of prospective TDM trials and discuss the future steps needed for further implementation of TDM of KIs.

Introduction

Numerous kinase inhibitors (KIs) have become available for the treatment of solid tumors and have improved outcomes for a wide range of malignant diseases. In contrast to most classical cytotoxic drugs, these agents target specific molecular aberrations of cancer cells and are administered orally. Many KIs show exposure-response and exposure-toxicity relationships. As pharmacokinetic (PK) exposure (e.g. area under the plasma concentration time curve (AUC) or plasma trough level (C_{min})) varies highly between patients, some patients may be at risk of treatment related toxicity due to high exposure, while others may experience suboptimal efficacy caused by low exposure.

Therefore, PK is a relevant and obvious biomarker which could be used to optimize treatment through therapeutic drug monitoring (TDM) (figure 1). For some anti-cancer drugs, TDM targets have already been recommended previously[1]. Nonetheless, expansion and an update of these previous works is warranted given the rapid developments in oncology demonstrated by the large volume of new PK and pharmacodynamic (PD) data that has become available and the abundance of new agents in this class that have been approved in recent years.

The purpose of this review is to integrate the available clinical PK and PD data into practical recommendations which can be used to personalize the treatment with KIs approved for the treatment of solid tumors, using TDM. An overview of the selected KIs used in the treatment of solid tumors and their pharmacokinetic properties (most relevant to TDM) are provided in supplemental table 1. A discussion of the available data for each KI is provided below. First, an overview of the available exposure-toxicity studies is given and exposure-response data is discussed. Concentrations for metabolites are taken into account if these have been shown to be pharmacologically active and contribute substantially to the anti-cancer effect. Then, based on these data, TDM recommendations are provided, focusing on the PK target. These TDM recommendations for each drug are summarized in table 1 and 2. Where evidence based target exposure is lacking, the average exposure of the approved efficacious dose will be provided as a proxy (also see figure 2). Additionally, we provide a comprehensive general discussion on a broadly applicable PK-guided dosing algorithm, a weighting of the evidence for TDM of each drug, the use of the mean exposure as proxy for a PK target and an overview of previously conducted prospective TDM trials in oncology.

Practical Recommendations for TDM of KIs in Oncology

Anaplastic Lymphoma Kinase (ALK) inhibitors

Alectinib

In previous studies, no relationships between alectinib exposure and grade 3 toxicity have been found.[2] No relationship between best overall response and the combined average concentration of alectinib and its metabolite M4 was found (n=49). However, in an population pharmacokinetic

analysis, a higher than median steady-state alectinib C_{min} ≥435 ng/mL has been associated with greater reduction in tumor size (n=46).[2]
Based on the available data, the best estimate for a cut-off for efficacy at this time is C_{min} ≥435 ng/mL. Yet, this preliminary finding should be confirmed in future studies.

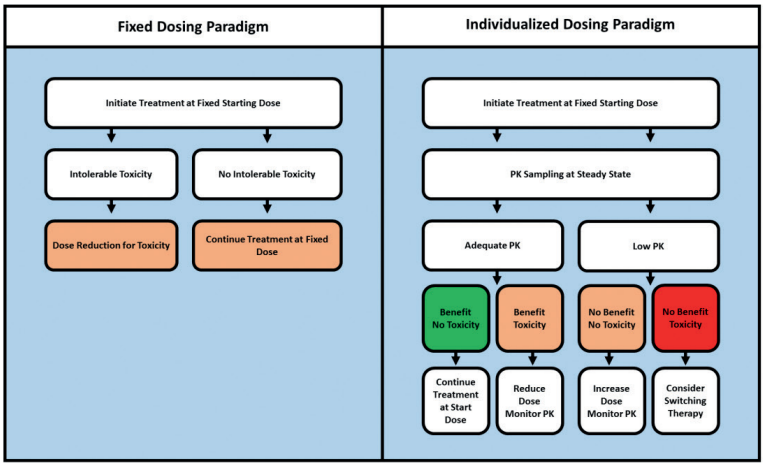

Figure 1: Current fixed dosing paradigm (left) versus the proposed individualized or TDM dosing algorithm (right).

Ceritinib

Higher ceritinib C_{min} has been associated with an increase of grade ≥3 adverse events (AEs) (p=0.002), specifically with grade ≥3 alanine transaminase (ALT) elevation, aspartate transaminase (AST) elevation, grade ≥2 hyperglycemia and probability of dose reduction (all p< 0.01), but not with grade ≥2 diarrhea (p=0.11), grade ≥3 gastro-intestinal tract AEs (p=0.86) or fatigue (p=0.92).[3]
No significant exposure-response relationships were identified for the primary efficacy endpoint objective response rate (ORR) and secondary efficacy endpoint progression free survival (PFS) in the pivotal trial in non-small cell lung cancer (NSCLC),[3] but a trend towards higher ORR with higher C_{min} was reported.[4]
Based on the limited data no specific threshold can be proposed yet. For now, ceritinib concentrations measured for TDM could be interpreted in relation to the mean C_{min} of 871 ng/mL at the approved dose.[3]

Crizotinib

No relationships between exposure and toxicity have been reported for crizotinib, except for a suggested relationship with QTc prolongation.[5] In two trials (n=120 and 114), the ORR was 60% in the patients with a C_{min} in the upper three quartiles (≥235 ng/mL) compared to 47% in the lowest

quartile (<235 ng/mL).[6] An increase in PFS with increasing C_{min} was also found. A stepwise Cox proportional analysis pointed toward a higher hazard of disease progression in the lowest quartile compared to the higher quartiles with a hazard ratio of 3.2 (90% CI: 1.62–6.36).[6] This threshold of >235 ng/mL is in accordance with the EC_{50} of 233 ng/mL found in preclinical models.[7]
Based on these data, it seems reasonable to use the threshold of C_{min} ≥235 ng/mL for TDM of crizotinib.

Break Point Cluster Region - Abelson (Bcr-Abl) oncoprotein inhibitors

Bosutinib

Few exposure-response and exposure-toxicity data have been reported for bosutinib in chronic myelogenous leukemia (CML).[8] PK-PD analyses indicated weak relationships between the incidence (but not severity) of diarrhea and rash and PK described by an E_{max} model.[9] The same study identified limited associations between AUC and C_{min} for both complete cytogenetic response and complete hematological response and between AUC, C_{max} and C_{min} with major molecular response. Moreover, C_{min} was reported to be higher in responders than in non-responders in the pivotal CML trial.[10] Although the limited data point towards both exposure-response and exposure-toxicity relationships, no cut-off values have yet been proposed. Therefore, the most pragmatic PK target for TDM would be the median C_{min} on the approved 500 mg QD dose of 147 ng/mL.[9,11]

Dasatinib

In a population PK-PD analysis of the several clinical trials including the phase III study in CML (n=981), the dasatinib trough concentration was significantly related to pleural effusion ($p < 0.01$).[12]
Moreover, the dasatinib weighted average steady-state concentration was significantly associated with major cytogenetic response, with the odds of response increasing 2.11-fold for every doubling of the average steady-state concentration ($p < 0.001$).[12]
Another study in Japanse patients (n=51) found that the time above the IC_{50} of phosphorylated CT10 regulator of kinase like (p-CrkL) in CD43+ cells was related to early molecular response to dasatinib in CML.[13]
Given the solid relation of exposure (weighted average steady-state concentration) with treatment response, TDM could be of value for dasatinib. However, using an average concentration for TDM is not feasible. Therefore using the geometric mean C_{min} of 2.61 ng/mL may serve as a more practical proxy.

Nilotinib

Large population PK-PD analyses identified several exposure-response and exposure-safety relationships for nilotinib. Higher C_{min} was associated with the occurrence of all-grade elevations in total bilirubin and lipase levels and increases in QTcF changes.[14,15]
Also, patients in the lowest C_{min} quartile had significantly longer time to complete cytogenetic response or major molecular response and shorter time to progression compared with patients in

the higher quartiles.[14] For each of these analyses this Q1-Q2 threshold varied from 469 to 553 ng/mL. Based on the above, nilotinib TDM could be employed with a target of C_{min} ≥ 469 ng/mL.

Table 1: Overview of practical TDM recommendations for KIs approved by the FDA for the treatment of solid tumors.*

Drug	TDM Recommendation	Proposed Target (ng/mL)	Mean / Median Exposure (C_{min} in ng/mL)	Outcome Parameter Associated with TDM Target	References
Afatinib	Exploratory		14.4		
Alectinib	Promising	C_{min} ≥435	572	Increased ORR	[2]
Axitinib	Promising	AUC ≥300†	375†	Increased OS	[42]
Ceritinib	Exploratory		871		
Cabozantinib	Exploratory		1380		
Cobimetinib	Exploratory		127		
Crizotinib	Promising	C_{min} ≥235	274	Increased PFS	[6]
Dabrafenib	Exploratory		96.1		
Erlotinib	Exploratory		1010		
Everolimus	Promising	C_{min} ≥10.0	13.2	Increased PFS	[95]
Gefitinib	Promising	C_{min} ≥200	291	Increased OS	[35]
Imatinib	Viable	C_{min} ≥1100	1193	Increased PFS	[100]
Lapatinib	Exploratory		780		
Lenvatinib	Exploratory		51.5		
Nintedanib	Exploratory		13.1		
Osimertinib	Exploratory		166		
Palbociclib	Exploratory		61		
Pazopanib	Viable	C_{min} ≥20,000	24,000	Increased PFS	[57,64]
Regorafenib	Exploratory		1400		
Sorafenib	Exploratory		3750		
Sunitinib	Viable	C_{min} ≥50 (inter), ≥37.5 (cont)	51.6 (sum of parent & SU12662)	Increased OS	[76]
Trametinib	Promising	C_{min} ≥10.6	12.1	Increased PFS	[110]
Vandetanib	Exploratory		795		
Vemurafenib	Promising	C_{min} ≥42,000	39,000	Increased PFS	[85,89]

** The provided recommendation is considered promising if a pharmacokinetic TDM target is available or viable if a prospective TDM study has been conducted. Otherwise the recommendations should be considered exploratory.*

*† For axitinib the AUC is provided in units of ng*h/mL.*

‡ Average steady state concentr-ation.

AUC: Area under the 0curve; C_{min}: Minimum plasma concentration / trough concentration; ORR: Objective response rate; OS: Overall survival; PFS: Progression-free survival;

Imatinib

Several relationships between imatinib concentrations and toxicity, including C_{min} with thrombocytopenia[16] and AUC (unbound) with absolute neutrophil count decrease have been established.[17] A trend towards higher incidences of hematological grade 3 / 4 adverse events for patients with patients with very high C_{min} (>3180 ng/mL) was reported.[18]

Multiple studies in CML patients point towards increased efficacy of imatinib in CML with higher exposure.

In a subanalysis of the IRIS trial (n=351), significantly reduced incidences of major molecular and complete cytogenetic response and a trend towards reduced event free survival were observed in the lowest C_{min} quartile.[19] Another study in Japanese patients found (n=254) found a significant correlation between C_{min} ≥1,002 ng/ml and higher probability of achieving a major molecular response.[20]

An Israeli study (n=191) also found a significantly higher C_{min} in CML patients who achieved a complete cytogenetic response compared to those without those without (1078 versus 827 ng/mL, p = 0.045).[21]

A study in 353 CML patients found higher incidences of major molecular response and complete cytogenetic response rates for patients with an exposure >1165 ng/mL.[18] A subanalysis of an imatinib adherence study (n=84) also found a statistically significant increased incidence of major molecular response (83.2 versus 60.1%) for patients with C_{min} >1000 ng/mL.[22]

Several other studies have also that patients with better treatment outcomes also had higher C_{min} values.[23,24]

Given the large number of studies reporting the importance of imatinib C_{min}, a prospective TDM study was conducted in 56 CML patients.[25] It set a PK target of 750 – 1500 ng/mL. Due to low adherence to the dosing recommendations this study did not meet its formal endpoint. Yet, in patients who were dosed in accordance with the recommendation experienced significantly fewer unfavorable events (28 versus 77%, p=0.03).[25]

The studies above all seem to support the use of a threshold of ≥1000 ng/mL for efficacy for imatinib in CML. Moreover the feasibility of imatinib dosing based on C_{min} has been established in a prospective study.[25] Future studies are needed to conclusively demonstrate the added benefit of personalized imatinib dosing in CML patients.

Ponatinib

For ponatinib, analyses of the dose intensity-safety relationship (defined as the average ponatinib dose of each subject while on study, which ranged from 0.34 to 45.2 mg) indicated a significant increase in grade ≥ 3 safety events such as AST, ALT and lipase increases, myelosuppression, hypertension, pancreatitis, rash, neutropenia and thrombocytopenia, with increasing dose intensity.[26] A statistically significant relationship between dose intensity and probability of major cytogenetic responses in CML patients has been described.[26]

Given the relation between dose intensity and major cytogenetic response, targeting the geometric mean (CV%) C_{min} of the approved 45 mg QD dose 34.2 (45.4) ng/mL (corresponding to 64.3 nM) seems a reasonable target.[27]

Epidermal Growth Factor Receptor (EGFR) inhibitors

Afatinib

Diarrhea and rash are the most common AEs of afatinib. These toxicities have been correlated to AUC and maximum plasma concentration (C_{max}) ($p < 0.0005$).[28] C_{min} in patients experiencing grade 3 diarrhea was higher (35.8 ng/mL) than those experiencing grade 1-2 diarrhea (25.2 – 31.6 ng/mL). In patients experiencing grade 3 rash, C_{min} was 31.4 ng/mL versus 26.8 – 27.6 ng/mL in those with only grade 1-2 rash.[29] A consistent relationship between exposure and response has not been found yet for afatinib.[30]

Awaiting future exposure-response analyses, TDM of afatinib could focus on targeting a steady state C_{min} of the 40 mg once daily (QD) dose of 14.4 – 27.4 ng/mL.[30]

Erlotinib

Erlotinib exposure has been significantly correlated to rash in several studies.[31] However, there was significant overlap in the range of PK values with patients who had no rash. No correlation was found with diarrhea.[31] Two clinical exposure-response studies have been reported. The first was conducted in head and neck squamous cell carcinoma (HNSCC) patients and found a trend toward increased overall survival (OS) for a C_{min} >950 ng/mL ($p=0.09$). The second found a relationship between the ratio of erlotinib and its O-desmethyl metabolite and PFS and OS (both $p<0.01$).[32] This metabolite ratio was also associated with grade 2 rash ($p=0.02$). This study found no relationships between PFS or OS and erlotinib concentrations. It should be noted however, that these results are based on a pooled analysis of NSCLC and pancreatic cancer patients (n=63 and 33, respectively).

More studies are needed to elaborate the role of erlotinib and O-desmethyl erlotinib concentrations, as no threshold for monitoring of the metabolic ratio is currently available.[32] At the moment, the previously established preclinical threshold of >500 ng/mL still seems the most rational target for TDM.[1,33]

Gefitinib

Gefitinib AUC_{0-24} and C_{min} were higher in patients experiencing diarrhea and hepatotoxicity.[34,35] Rash-based dosing of gefitinib has been explored in head and neck squamous cell carcinoma, but even though this was found to be feasible, it did not result in increased anti-tumor activity, measured as response rate or PFS.[36] This study did find higher gefitinib C_{min} levels in patient with disease control compared to patient with progressive disease as best response, 1,117 ng/ml versus 520 ng/ml ($p=0.01$). In another study, OS was linked to gefitinib C_{min} in NSCLC patients (n=30). Patients with C_{min} <200 ng/mL had an OS of 4.7 months compared to 14.6 months for patients ≥200 ng/mL ($p=0.007$).[35] The available data support TDM of gefitinib in NSCLC using a threshold C_{min} of ≥200 ng/mL.

Lapatinib

No thorough exposure-response or exposure-toxicity studies have been reported for lapatinib. Although one trial found that the majority of responders had a C_{min} in the 300 to 600 ng/ml range.[37] Future studies should focus on establishing exposure-response and exposure-toxicity relationships. Meanwhile, lapatinib C_{min} could be interpreted in reference to the mean C_{min} of 780 ng/mL.[1]

Osimertinib

For osimertinib, a relationship was found between steady state AUC and the probability of rash (p=0.0023) and diarrhea (p=0.0041) in a population of NSCLC patients.[38] However, no evidence of a relationship between exposure and tumor response, duration of response or change in tumor size has been established.[38,39]

In the absence of conclusive exposure-response analyses, C_{min} could be compared to the geometric mean (coefficient of variation (CV)) of the approved 80 mg daily dose of 166 (48.7) ng/mL (corresponding to 332 nM).[39]

Vascular Endothelial Growth Factor Receptor (VEGFR) inhibitors

Axitinib

Exposure-safety analysis has demonstrated that axitinib AUC was significantly related to increased hypertension, proteinuria, fatigue, and diarrhea.[40] Diastolic blood pressure (dBP) ≥90 mm Hg has been associated with increased probability of response, PFS and OS in RCC patients.[41,42] Based on these results, a randomized phase II trial to individualize axitinib dose based on dBP has been performed.[43] In total, 122 RCC patients were randomized to either axitinib or placebo dose titration. The axitinib dose titration group showed an increased ORR compared to the placebo group (p=0.019)[43], but this did not result in improved OS (p=0.162).[44] One small study (n=24) also found a relationship between axitinib C_{min} >5 ng/mL and tumor response and the occurrence of hypertension, hyperthyroidism and proteinuria.[45] In renal cell carcinoma (RCC) patients, an AUC ≥300 ng*h/mL was significantly associated with increased PFS (13.8 versus 7.4 months, p=0.03) and OS (37.4 versus 15.8 months, p<0.01).[42]

The available data support using an AUC ≥300 ng*h/mL as a target for TDM.[42] However, given that prospective studies using dBP are already available, an integrated approach using both PK and dBP to guided dosing may be the most appropriate strategy to optimize treatment, as has been advocated previously.[46] Although more evidence is available to support the AUC target, the more practical C_{min} target of >5 ng/mL could also be considered (as it requires only a single plasma sample). [45]

Cabozantinib

Steady state AUC derived from a population PK model of combined phase I, II, and III studies has been correlated to dose reductions and lower achieved dose intensity. These dose modifications, however, did not appear to impact PFS.[47] Population pharmacodynamic modelling suggested that a concentration of only 59-78 ng/mL would already result in 50% of maximum effect in medullary thyroid cancer patients.[48]

As no PK thresholds for cabozantinib have been reported, future studies should first establish these before TDM of cabozantinib can move forward. Meanwhile, cabozantinib concentrations could be referenced relative to the mean C_{min} in the medullary thyroid cancer phase III trial of 1380 ng/mL (on 140 mg) or 1125 ng/mL in renal cell carcinoma.[49,50]

Lenvatinib

An increase in the incidence of grade 3 or higher hypertension, grade 3 or higher proteinuria, nausea and vomiting with higher lenvatinib dose intensity has been observed.[51] Analyses of the pivotal study in thyroid cancer indicated similar PFS across the full range of exposures (AUC_{0-24} between 1,410 and 10,700 ng*h/mL).[52] However, a model based PKPD analysis indicated that lenvatinib AUC_{0-24} was correlated to reduction in tumor size.[52]

As no exposure-response and exposure-toxicity thresholds are established yet for lenvatinib, TDM could target the mean C_{min} of 51.5 ng/mL.[51]

Nintedanib

Nintedanib has only shown modest relationships between exposure and safety and efficacy.[53] In exploratory analyses, higher nintedanib concentrations have been associated with hepatotoxicity, but not with gastrointestinal AEs. Exposure-response analyses are currently not available for clinical endpoints, except for a statistically significant association between nintedanib exposure and dynamic contrast enhanced MRI response[54] and a decrease in soluble vascular endothelial growth factor (VEGFR) levels with increasing C_{min} in a phase I study (r=-0.46, n=15).[55]

As no specific threshold for nintedanib has been proposed, TDM should focus on targeting the mean C_{min} value of the approved dose (calculated for a 200 mg dose, based on the dose-normalized C_{min} value of 0.0654 ng/mL/mg) of 13.1 ng/mL.[56]

Pazopanib

Pazopanib exposure has been correlated to hypertension.[57] This correlation was stronger for C_{min} than for AUC_{0-t} (R^2 of 0.91,p =0.0075 and 0.25 respectively, p =0.23). Relations were also found between C_{min} and diarrhea, ALT-elevations, hand-foot syndrome and stomatitis.[58] The probability of grade ≥3 ALT increased with higher pazopanib concentration.[59] However, a recent study suggested that pazopanib hepatotoxicity maybe related to genetic mutations in human leukocyte antigen (HLA) and, therefore, unrelated to PK.[60] Analysis of data from 177 RCC patients showed an increased PFS in patients with C_{min} ≥20.5 mg/L compared to patients with a C_{min} below this threshold (52.0 versus 19.6 weeks, p=0.0038).[57] This threshold seems to be in accordance with preclinical data showing optimal VEGFR2 inhibition by pazopanib *in vivo* at a concentration ≥17.5 mg/L.[61] Plasma concentrations have also been correlated with radiographic response in a phase II study of patients with progressive, radioiodine-refractory, metastatic differentiated thyroid cancer.[62] Two trials have investigated individualized dosing of pazopanib in cancer patients. The first used pazopanib AUC_{0-24h} as a target (715-920 mg*h/L) and set a reduction in variability as the primary endpoint.[63] AUC-guided

dosing did not significantly reduce inter-patient variability, probably due to intra-patient variability or sampling time issues. Based on this trial the authors concluded it may be more beneficial to target the C_{min} threshold rather than an AUC window. The second study was a prospective study in 30 patients with advanced solid tumors, using a C_{min} ≥20 mg/L as target.[64] The dosing algorithm, based on dose adjustments after 2, 4 and 6 weeks, led to patients being treated at dosages ranging from 400 to 1800 mg daily. C_{min} in patients whose dose was successfully escalated above 800 mg (n=10) increased significantly from 13.2 (38.0%) mg/L (mean (CV%)) to 22.9 mg/L (44.9%).
This study demonstrated the safety and feasibility of C_{min} (≥20 mg/L) guided dosing for pazopanib and merits further investigation of pazopanib TDM for instance in a randomized clinical trial (RCT) to demonstrate the relevance of individualized over fixed dosing on a clinical endpoint such as PFS or OS.

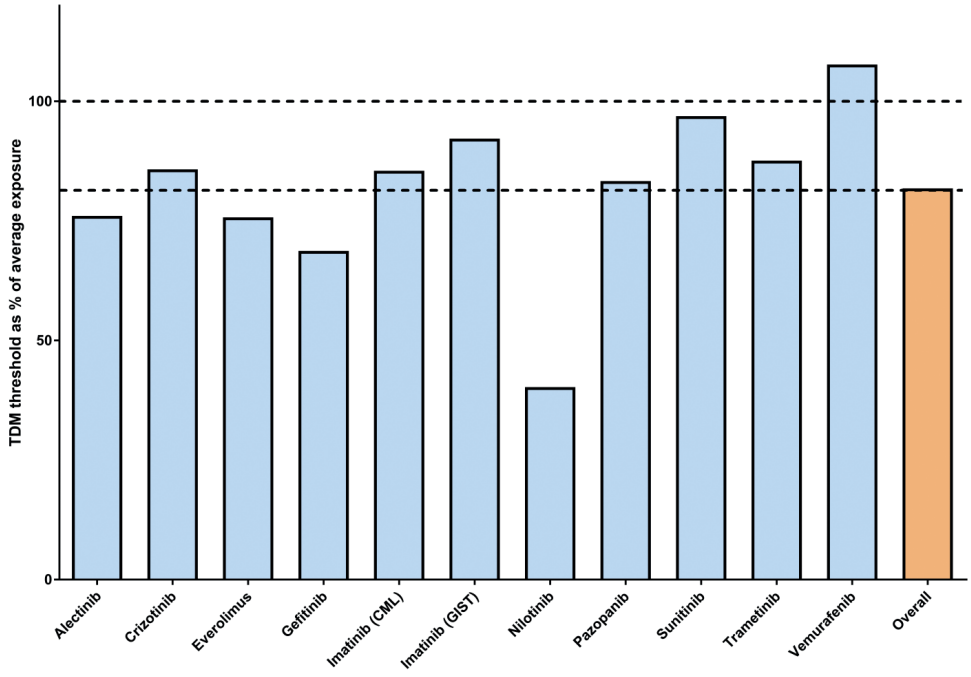

Figure 2: The TDM-thresholds of selected KIs as percent of the mean/median exposure of the approved dose (blue bars). Overall, the thresholds were 81.7 % of the mean exposure across all agents (orange bar), with a standard deviation of 17.4%. Dotted horizontal lines indicate 100% of mean exposure and 81% (the mean of the thresholds). This analysis suggests that across all kinase inhibitors, the target exposure matches with 81.7% of the population exposure and supports the view that targeting the population average could serve as a proxy, in absence of a definitive TDM target.

Regorafenib

Regorafenib is metabolized by CYP3A4 into the active metabolites M2 (N-oxide) and M5 (N-oxide, N-desmethyl), which at steady state form a major component of the total exposure.[65] An exposure-

dependent increase was seen for rash, total bilirubin and median indirect bilirubin in gastro-intestinal stromal tumor (GIST) patients, for parent and total (including M2 and M5) regorafenib exposure.[66] No exposure-response relationships for efficacy have been reported for regorafenib hitherto. [65]

More studies are needed to investigate exposure-response and -toxicity relationships of regorafenib. These should take into account M2 and M5, as these have been shown to be pharmacologically active and present at similar or higher concentrations than the parent compound. Currently, the most appropriate TDM target for regorafenib (parent compound only) is the mean C_{min} of 1.4 mg/L.[65]

Table 2: Overview of practical TDM recommendations for KIs approved by the FDA for the treatment of hematological malignancies.*

Drug	TDM Recommendation	Proposed Target (ng/mL)	Mean / Median Exposure (C_{min} in ng/mL)	Outcome Parameter Associated with TDM Target	References
Bosutinib	Exploratory		147		
Dasatinib	Exploratory		2.61		
Nilotinib	Promising	C_{min} ≥469	1165	Prolonged TTP	[14]
Idelalisib	Exploratory		318		
Ibrutinib	Exploratory		680†		
Imatinib	Viable	C_{min} ≥1000	1170	Improved MMR, CCYR	[19]
Ponatinib	Exploratory		34.2		

** The provided recommendation is considered promising if a pharmacokinetic TDM target is available or viable if a prospective TDM study has been conducted. Otherwise the recommendations should be considered exploratory.*

CCYR: Complete cytogenetic response; MMR: Major molecular response; TTP; Time to progression.

*† For ibrutinib the AUC is provided in ng*h/mL"*

Sorafenib

In a study of patients with advanced solid tumors (n=54), a cut-off at a cumulative AUC (calculated over day 0 to 30) of 3,161 mg*h/L was associated with the highest risk to develop any grade ≥3 toxicity (p=0.018).[67] A patient series found that sorafenib C_{min} was higher in patients who experienced grade 3 AEs (n=8) than those who did not (n=14), 7.7 ± 3.6 mg/L versus 4.4 ± 2.4 mg/L, (p=0.0083).[68] Sorafenib steady state concentrations were found to be higher in patients with grade ≥2 hand-foot syndrome and hypertension than in those not experiencing these AEs (p=0.0045 and 0.0453, respectively). Optimal cut-offs were 5.78 mg/L for hand-foot syndrome and 4.78 mg/L for hypertension.[69] In a small cohort of 25 hepatocellular carcinoma patients, the AUC-ratio of sorafenib and its metabolites resulted in even better prediction of toxicity (p=0.002).[70] The same cohort found that not sorafenib AUC but that of its metabolite seemed significantly associated with dose reduction or discontinuation (p=0.031) and increased PFS (p=0.048).[70] A study in Japanese patients (n=91) found a trend toward increased OS in hepatocellular carcinoma patients at a sorafenib C_{max} of ≥4.78 mg/L (12.0 versus 6.5 months, p=0.08).[69]

Future studies need to confirm the proposed exposure-response and -toxicity relations described in these small patients cohorts, taking into account the N-oxide metabolite. Currently, the most appropriate target for sorafenib TDM is >3.75-4.30 mg/L (parent compound only), based on preclinical experiments and the mean exposure in humans, as was advocated previously.[1]

Table 3: Overview of prospective dose individualization trials of KIs.

Drug	n	Patient Population	PK Parameter	Target	Dose Change	PK-guided dose escalations (↑) or reductions (↓)†	Endpoint	Reference
Everolimus	28	Pediatric SEGA patients	C_{min}	5-15 ng/mL	-	↑ and ↓	PD	[97]
Sunitinib	37	Advanced solid tumors	C_{min}	≥50 ng/mL	After 3 and 5 weeks	↑ only	PK	[78]
Imatinib	56	Chronic myelogenous leukemia patients	C_{min}	750 – 1500 ng/mL	-	↑ and ↓	PK	[25]
Pazopanib	13	Renal cell carcinoma patients	AUC	715-920 mg*h/L	After 2 weeks	↑ and ↓	PK	[63]
Pazopanib	30	Advanced solid tumors	C_{min}	≥20 mg/L	After 2, 4 and 6 weeks	↑ only	PK	[64]

AUC: Area under the curve; C_{min}: Minimum plasma concentration / trough concentration; PD: Pharmacodynamic; PK: Pharmacokinetic; SEGA: Subendymal giant cell astrocytoma

†Per protocol, some trials had dosing algorithms which allowed for dose reductions (in absence of toxicity) based on PK, while others only allowed for dose escalation based on PK. All allowed for dose reductions based on toxicity.

Sunitinib

Sunitinib is metabolized by CYP3A4 into its active metabolite N-desethylsunitinib also known as SU12662. TDM for sunitinib is generally performed using the sum of concentrations (total C_{min}) of both sunitinib and SU12662.[71] Dose limiting and grade ≥3 toxicities of sunitinib have been associated with total C_{min} ≥100 ng/mL.[17,72] Grade ≥2 mucositis and altered taste have also been related to higher total C_{min}.[73] A relationship was also found between sunitinib AUC and grade ≥3 toxicity (p=0.0005).[74] Based on the above, an upper C_{min} cut-off of <100 ng/mL could be considered.

In RCC, increasing AUC has been related to higher response rates, longer PFS and OS.[74–77] A meta-analysis found AUC of sunitinib combined with its active metabolite N-desethylsunitinib to be significantly associated with PFS and OS in both GIST (n=401) and RCC (n=169), all p<0.01.[76] An increased OS was found for an AUC ≥1973 ng*h/mL in another study in RCC patients (n=55).[74] C_{min} correlated with AUC (r^2=0.8-0.9), suggesting C_{min} could be used for TDM as substitute.[76] A PK target of 50-100 ng/mL[17] has been suggested for intermittent dosing in RCC (50 mg daily for 4 weeks in a 6 week cycle) and based on PK linearity a target of ≥37.5 ng/mL was extrapolated for continuous dosing in GIST (37.5 mg daily continuously) .[1]

A TDM-feasibility trial has been conducted in cancer patients using C_{min} ≥50 ng/mL as PK target allowing for dose adjustments after 3 and 5 weeks of treatment.[78] A third of the patients <50 ng/mL at the standard dose, could be treated successfully at an increased dose and additional patients reached the target exposure. This study demonstrates the feasibility using C_{min}≥50 ng/mL (sunitinib + metabolite) as TDM target. Future studies are now needed to confirm the efficacy of TDM over fixed dosing for sunitinib.

Vandetanib

Grade ≥2 diarrhea and fatigue have significantly been associated with steady state vandetanib C_{min} (p=0.03 and 0.02, respectively), but no relationship was found for hypertension or rash.[79] Importantly, a substantial dose and exposure related QTc prolongation has been observed.[79] No clear relationship between PFS and exposure has been found in the pivotal trial in patients with thyroid cancer [79], although multiple studies have used IC_{50} values established *in vitro* (190 ng/mL) to support dose selection in early clinical trials.[80]

In absence of studies that establish specific PK thresholds, current exploratory TDM efforts could focus on targeting the population mean exposure of 795 ng/mL.

Serine/Threonine-Protein kinase B-Raf (BRAF) inhibitors

Dabrafenib

Dabrafenib is metabolized into its carboxy, hydroxyl and desmethyl metabolites.[81] The hydroxyl metabolite showed similar IC_{50} values to dabrafenib *in vitro*. No relationships between AEs and exposure, except for pyrexia, have been reported.[82] Pyrexia seemed to be related to $C_{average}$ dabrafenib and hydroxy-dabrafenib C_{min}, but not to desmethyldabrafenib C_{min}.[83] At the moment, no evident exposure-response relationships have been reported for dabrafenib and/or for any of its metabolites.[84]

In absence of a validated target, current TDM efforts could target the median C_{min} (sum of parent dabrafenib and its hydroxyl metabolite) of 99.6 ng/mL.[84]

Vemurafenib

In melanoma patients, vemurafenib concentrations were significantly higher in those patients who developed grade ≥2 rash compared to those who did not (mean ± standard deviation (SD) of 61.7±25.0 vs. 36.3±17.9 mg/L, p<0.0001).[85] Another study found an exposure-dependent QTc prolongation for vemurafenib.[86] Vemurafenib concentrations have also been related to treatment response. Responders had a mean concentration of 56.4 mg/L, whilst non-responders had a mean of 38.8 mg/L (p=0.013).[87,88] Moreover, melanoma patients in the lowest exposure quartile (<40.4 mg/L) had a PFS of 1.5 months compared to that of 4.5 months of patients in the higher three quartiles (p=0.029).[85] This effect was confirmed in an independent cohort after 12 months of follow up with a threshold of 42 mg/L (p=0.005).[89]

The available data support the use of a threshold C_{min} of >42 mg/L. A real-world study however, found that in routine care only half of patients had a C_{min} <42 mg/L,[90] demonstrating the opportunities for dose optimization.[90]

Mitogen Activated Protein Kinase Kinase (MEK) inhibitors

Cobimetinib

Exploratory exposure-toxicity analyses for safety identified a trend towards increased diarrhea with increasing cobimetinib and vemurafenib exposure.[91] No significant exposure-response relationship has been established for cobimetinib on the primary endpoint of PFS in the pivotal registration trial.[91] On the basis of the available data no clear PK target can yet be identified for cobimetinib. Therefore, the currently most appropriate target would be the mean C_{min} of the approved dose of 127 ng/mL.[91]

Trametinib

No exposure- toxicity relationships have been identified for trametinib. A population analysis was performed to explore the effect of trametinib C_{min} and average concentration on ORR and PFS.[92] The proportion of responders seemed to increase with increasing exposure and reached a plateau at a C_{min} of 10 ng/mL. No relationship between exposure above or below the mean C_{min} of 13.6 ng/mL and PFS has been identified in phase 3 trials. However, in an analysis of the phase 2 study, patients with C_{min} above 10.6 ng/mL, had longer PFS than those below this C_{min} value.[92] Furthermore, the C_{min} threshold of 10.6 ng/mL is supported by preclinical data pointing towards a target of 10.4 ng/mL based on efficacy in BRAF mutant melanoma cell lines.[93]

Given the above, the threshold of a C_{min} ≥10.6 ng/mL seems the most appropriate target to be used for trametinib TDM.

Other Kinase Inhibitors used in Oncology

Everolimus

In transplantation medicine, TDM is routinely applied for everolimus, using a window of 6-10 ng/mL or 3-8 ng/mL in combination therapy.[94] No target for TDM has been validated in oncology. Higher C_{min} has been associated with increased risk of high-grade pulmonary and metabolic (such as hyperglycemia) AEs and stomatitis. However, this meta-analysis of everolimus phase II trials (n=945), found that a 2-fold increase in everolimus C_{min} was associated with improved tumor size reduction, regardless of cancer type.[95] No specific target window has been proposed, but in RCC and pNET cut-offs at ≥10 and 30 ng/mL resulted in numerically higher PFS values than C_{min}<10 ng/mL.[95] A retrospective analysis of 45 RCC patients showed a trend toward increased PFS for patients with a C_{min} ≥14.1 ng/mL of 13.3 versus 3.9 months, p=0.06.[96]

Based on experience in transplant and pediatric patients, everolimus TDM seems feasible.[94,97] Although exposure-response relations are seen for everolimus in oncology, no formal PK-target has been established yet. Based on the available data, a cut-off for efficacy of C_{min} ≥10 ng/mL seems a reasonable target for TDM of everolimus in oncology.

Ibrutinib

For ibrutinib no exposure-safety relationships were found.[98] A phase 1 study indicated maximum Bruton's tyrosine kinase occupancy at doses of ≥ 2.5 mg/kg (corresponding to a 175 mg dose for average weight of 70 kg). This complete target inhibition was already seen at an AUC of 160 ng*h/mL.[99] In absence of a clearly defined pharmacokinetic thresholds for clinical patient outcomes, ibrutinib TDM could target the mean +SD AUC at the approved 560 mg QD dose of 953 ± 705 ng*h/mL for mantle cell lymphoma patients or 680 ± 517 ng*h/mL at 420 mg QD for patients with chronic lymphocytic leukemia (no C_{min} data was reported).[98]

Imatinib

In addition to its use in CML, imatinib is also used as an inhibitor of the stem cell receptor KIT and platelet derived growth factor receptor (PDGFR) in GIST. In an analysis of 73 GIST patients randomized to either 400 or 600 mg QD, an increase in time to disease progression was found for patients with a C_{min} >1100 ng/mL.[100] Another study did not find a relationship between imatinib C_{min} and treatment response, but did find a relationship between free (unbound to plasma proteins) imatinib concentration >20 ng/mL and complete response.[101] Two real-world studies suggest a relationship of imatinib C_{min} and efficacy. The first, found that responders had a median C_{min} of 1271 ng/mL, whilst C_{min} in non-responders was 920 ng/mL (p=0.23).[102] The second, did not find a significant relationship between a C_{min} >1100 ng/mL threshold of imatinib and PFS (p=0.1107). However, a threshold of >760 ng/mL was associated with a significantly longer PFS (p=0.0256).[103]
The available studies point towards different targets for imatinib TDM in GIST patients (≥760 and ≥1100 ng/mL). The more pragmatic approach may be to use the C_{min} >1100 ng/mL threshold, as it is based on PFS data from a RCT [100] and seems to be confirmed by data from an independent observational cohort.[102] Moreover, a retrospective cohort study of 68 GIST patients, indicated the feasibility of dosing imatinib based on the 1100 ng/mL threshold, with more patients reaching the prespecified target exposure.[104]

Idelalisib

No exposure-response or exposure-safety relationships have been identified for idelalisib in chronic lymphocytic leukemia or non-Hodgkin lymphoma, using either AUC or C_{min} as pharmacokinetic parameters.[105] However, dose selection was supported by that fact that the exposure achieved on the approved dose achieved the EC_{90} of 125 ng/mL for inhibition of PI3Kδ in vitro.[105] In absence of more conclusive data, TDM of idelalisib should for now target the median C_{min} at the approved 150 mg QD dose of 318 ng/mL.[105,106]

Palbociclib

A greater reduction in absolute neutrophil count (ANC) appears to be associated with increased palbociclib exposure.[107] No conclusive exposure-response relationship has been found in 81 patients treated at the 125 mg fixed dose.

Based on the limited exposure response and toxicity analyses no specific PK target for palbociclib can be formulated. More thorough PKPD analyses are needed. Until these come available palbociclib concentrations can be compared to the population mean (CV) C_{min} of 61 (42) ng/mL.[107]

Discussion

Currently, KIs are administered at a fixed starting dose which is only adjusted in case of intolerable toxicity (figure 1, left). As many KIs show an exposure-response and exposure-toxicity relationship and exposure varies highly between patients, we propose that an individualized PK-guided dosing or TDM algorithm should be explored for KIs (figure 1, right).

Based on the PK targets discussed above, dose increments could be considered for patients with low exposure in absence of significant toxicity. These dose increments could for instance follow the dose-escalation schedule explored in the phase I dose-escalation study of the respective drug. Yet if available, a prospectively validated and safe TDM-dose algorithm would be preferred (see table 3).

For patients with a high plasma concentration not experiencing toxicity, dose reductions could be considered. However, in contrast to for example TDM of aminoglycosides in infectious diseases, in oncology the main focus of TDM will probably be directed towards improving efficacy by increasing the dose in low exposure patients. Concerns for lasting side-effects may in most cases be less relevant.

Nonetheless, monitoring of plasma concentrations may be useful in patients requiring dose reductions for toxicity. Here, it could be used to differentiate between patients who had toxicity due to high exposure (who might be successfully treated at the lower dose) and those who do not tolerate treatment despite an exposure below the efficacious concentration (red box, figure 1). Taking together the considerations above, a proposal for a generic decision tree for PK-guided dosing is provided in figure 1.

Ideally, individualized dosing should be based on thorough exposure-response and exposure-toxicity analyses. A weighting of the robustness of the evidence has been provided for each of the proposed TDM recommendations in table 1 and 2 as either *negative, exploratory*, *promising*, *viable or standard of care*.

None of the included drugs has been qualified as *negative*. Based on the mechanism of action of KIs and the clinical pharmacological properties, exposure-response relationships are to be expected for most of these drugs. A fully negative recommendation can only be provided if evidence from a adequately sized and powered study demonstrates that at the recommended dose no relationship between drug exposure and response exist.

For the drugs in the *exploratory* category (table 1 and 2), no PK-targets have been specified yet. Therefore it is too early to recommend implementation of TDM for these drugs. Further PK sampling in clinical trials and routine patient care could help to identify exposure-response and exposure-toxicity relationships.

TDM, however, could already be of value in specific patient populations, such as patients with hepatic impairment, patients not able to swallow medication or patients having possible drug interactions and compliance issues. The mean population exposure could be used as reference for interpretation of the exposure of these individual patients.[1] An updated analysis of the relationship between available TDM targets and the average population exposure support this (figure 2). Overall the targets (n=11) amounted to 81.7% of the population exposure, with a relatively small SD of 17.4%. Although this is no substitute for thorough exposure-response analyses, the data support the view that targeting the mean or median exposure will generally result in efficacious concentrations for KIs in oncology.

If an exposure-outcome relationship and a PK target have been established, TDM could be considered a promising strategy for treatment optimization. The agents for which a TDM target is available are therefore classified as *promising* in table 1 and 2. For these drugs, the feasibility of individualized dosing based on this target should preferably be demonstrated in a prospective clinical trial.

For KIs where feasibility studies have already been conducted (table 3), TDM is classified as *viable* (table 1 and 2). All but one of these studies have used PK endpoints, aiming to establish the safety and feasibility of reaching the target exposure.[25,63,64,78,108] One study used a PD endpoint, a one-armed trial with the purpose to show efficacy in a rare pediatric tumor (subependymal giant cell astrocytoma).[97]

Currently, for none of the discussed agents TDM is performed as the standard of care. Before TDM can become standard for drugs in the *viable* category, the relevance of this dosing strategy over fixed dosing should, if feasible, be clinically validated in a prospective randomized trial. Such studies are scarce, but have been conducted previously for TDM of cytotoxic drugs such as paclitaxel,[109] indicating the feasibility of conducting randomized individualized dosing trials in cancer patients. This type of trials should now be initiated to demonstrate an effect of TDM for targeted anti-cancer agents on relevant clinical endpoints in oncology.

Conclusion

For KIs with an exposure-response and/or exposure-toxicity relationship and high inter-patient variability in exposure, a PK parameter such as C_{min} is an obvious and relevant biomarker for dose individualization through TDM.

Several clinical trials demonstrate the safety and feasibility of TDM of KIs, such as imatinib, pazopanib, tamoxifen, everolimus and sunitinib. Randomized clinical trials are now needed to confirm an effect of TDM over fixed dosing on relevant clinical efficacy endpoints such as PFS and OS, before TDM can become universally implemented as standard care of cancer patients treated with KIs.

Disclosures

The authors declare they have no conflicts to disclose.

References

1. Yu, H. *et al.* Practical guidelines for therapeutic drug monitoring of anticancer tyrosine kinase inhibitors: focus on the pharmacokinetic targets. *Clin. Pharmacokinet.* **53**, 305–25 (2014).
2. Food and Drug Administration. Center for Drug Evaluation and Research Alectinib Clinical Pharmacology and Biopharmaceutics Review. (2016).<http://www.accessdata.fda.gov/drugsatfda_docs/nda/2015/208434Orig1s000ClinPharmR.pdf>
3. Food and Drug Administration. Center for Drug Evaluation and Research Ceritinib Clinical Pharmacology and Biopharmaceutics Review. (2014). <http://www.accessdata.fda.gov/drugsatfda_docs/nda/2014/205755Orig1s000ClinPharmR.pdf>
4. Committee for Medicinal Products for Human Use (CHMP) European Medicines Agency Ceritinib European Public Assessment report. **44**, (2015).
5. European Medicines Agency Committee for Medicinal Products For Human Use (CHMP) Crizotinib European Public Assessment Report. (2012).<http://www.ema.europa.eu/docs/en_GB/document_library/EPAR_-_Public_assessment_report/human/002489/WC500134761.pdf>
6. Food and Drug Administration. Center for Drug Evaluation and Research Crizotinib Clinical Pharmacology and Biopharmaceutics Review. (2011). <http://www.accessdata.fda.gov/drugsatfda_docs/nda/2011/202570Orig1s000ClinPharmR.pdf>
7. Yamazaki, S. Translational pharmacokinetic-pharmacodynamic modeling from nonclinical to clinical development: a case study of anticancer drug, crizotinib. *AAPS J.* **15**, 354–66 (2013).
8. Abbas, R. & Hsyu, P.-H. Clinical Pharmacokinetics and Pharmacodynamics of Bosutinib. *Clin. Pharmacokinet.* **55**, 1191–1204 (2016).
9. Hsyu, P.-H., Mould, D. R., Upton, R. N. & Amantea, M. Pharmacokinetic-pharmacodynamic relationship of bosutinib in patients with chronic phase chronic myeloid leukemia. *Cancer Chemother. Pharmacol.* **71**, 209–18 (2013).
10. Committee for Medicinal Products for Human Use (CHMP) European Medicines Evaluation Agency Bosutinib European Public Assessment Report. (2013). <http://www.ema.europa.eu/docs/en_GB/document_library/EPAR_-_Public_assessment_report/human/002373/WC500141745.pdf>
11. Hsyu, P., Mould, D. R., Abbas, R. & Amantea, M. Population Pharmacokinetic and Pharmacodynamic Analysis of Bosutinib. *Drug Metab Pharmacokinet* **Epub**, 1–43 (2014).
12. Wang, X. *et al.* Differential effects of dosing regimen on the safety and efficacy of dasatinib: retrospective exposure-response analysis of a Phase III study. *Clin. Pharmacol.* **5**, 85–97 (2013).
13. Ishida, Y. *et al.* Pharmacokinetics and pharmacodynamics of dasatinib in the chronic phase of newly diagnosed chronic myeloid leukemia. *Eur. J. Clin. Pharmacol.* **72**, 185–193 (2016).
14. Giles, F. J. *et al.* Nilotinib population pharmacokinetics and exposure-response analysis in patients with imatinib-resistant or -intolerant chronic myeloid leukemia. *Eur. J. Clin. Pharmacol.* **69**, 813–823 (2013).
15. Larson, R. A. *et al.* Population pharmacokinetic and exposure-response analysis of nilotinib in patients with newly diagnosed Ph+ chronic myeloid leukemia in chronic phase. *Eur. J. Clin. Pharmacol.* **68**, 723–733 (2012).
16. Francis, J., Dubashi, B., Sundaram, R., Pradhan, S. C. & Chandrasekaran, A. A study to explore the correlation of ABCB1, ABCG2, OCT1 genetic polymorphisms and trough level concentration with imatinib mesylate-induced thrombocytopenia in chronic myeloid leukemia patients. *Cancer Chemother. Pharmacol.* **76**, 1185–1189 (2015).
17. Faivre, S. *et al.* Safety, pharmacokinetic, and antitumor activity of SU11248, a novel oral multitarget tyrosine kinase inhibitor, in patients with cancer. *J. Clin. Oncol.* **24**, 25–35 (2006).
18. Guilhot, F. *et al.* Plasma exposure of imatinib and its correlation with clinical response in the Tyrosine Kinase Inhibitor OPtimization and Selectivity trial. *Haematologica* **97**, 731–738 (2012).
19. Larson, R. A. *et al.* Imatinib pharmacokinetics and its correlation with response and safety in chronic-phase chronic myeloid leukemia: A subanalysis of the IRIS study. *Blood* **111**, 4022–4028 (2008).

20. Takahashi, N. *et al.* Correlation between imatinib pharmacokinetics and clinical response in Japanese patients with chronic-phase chronic myeloid leukemia. *Clin. Pharmacol. Ther.* **88**, 809–13 (2010).
21. Koren-Michowitz, M. *et al.* Imatinib plasma trough levels in chronic myeloid leukaemia: results of a multicentre study CSTI571AIL11TGLIVEC. *Hematol. Oncol.* **30**, 200–205 (2012).
22. Marin, D. *et al.* Adherence is the critical factor for achieving molecular responses in patients with chronic myeloid leukemia who achieve complete cytogenetic responses on imatinib. *J. Clin. Oncol.* **28**, 2381–2388 (2010).
23. Obbergh, F. Van *et al.* The clinical relevance of imatinib plasma trough concentrations in chronic myeloid leukemia. A Belgian study. *Clin. Biochem.* 10–12 (2016).doi:10.1016/j.clinbiochem.2016.12.006
24. Singh, N., Kumar, L., Meena, R. & Velpandian, T. Drug monitoring of imatinib levels in patients undergoing therapy for chronic myeloid leukaemia: comparing plasma levels of responders and non-responders. *Eur. J. Clin. Pharmacol.* **65**, 545–9 (2009).
25. Gotta, V. *et al.* Clinical usefulness of therapeutic concentration monitoring for imatinib dosage individualization: results from a randomized controlled trial. *Cancer Chemother. Pharmacol.* **74**, 1307–19 (2014).
26. Food and Drug Administration. Center for Drug Evaluation and Research Ponatinib Clinical Pharmacology and Biopharmaceutics Review. <https://www.accessdata.fda.gov/drugsatfda_docs/nda/2012/203469Orig1s000ClinPharmR.pdf>
27. Cortes, J. E. *et al.* Ponatinib in refractory Philadelphia chromosome-positive leukemias. *N. Engl. J. Med.* **367**, 2075–88 (2012).
28. Wind, S., Schmid, M., Erhardt, J., Goeldner, R. G. & Stopfer, P. Pharmacokinetics of afatinib, a selective irreversible ErbB family blocker, in patients with advanced solid tumours. *Clin. Pharmacokinet.* **52**, 1101–1109 (2013).
29. Wind, S., Schnell, D., Ebner, T., Freiwald, M. & Stopfer, P. Clinical Pharmacokinetics and Pharmacodynamics of Afatinib. *Clin. Pharmacokinet.* **Jul 28.**, [Epub ahead of print] (2016).
30. Food and Drug Administration. Center for Drug Evaluation and Research Afatinib Clinical Pharmacology and Biopharmaceutics Review. (2012). <http://www.accessdata.fda.gov/drugsatfda_docs/nda/2013/201292Orig1s000ClinPharmR.pdf>
31. Lu, J.-F. *et al.* Clinical pharmacokinetics of erlotinib in patients with solid tumors and exposure-safety relationship in patients with non-small cell lung cancer. *Clin. Pharmacol. Ther.* **80**, 136–145 (2006).
32. Steffens, M. *et al.* Dosing to rash? - The role of erlotinib metabolic ratio from patient serum in the search of predictive biomarkers for EGFR inhibitor-mediated skin rash. *Eur. J. Cancer* **55**, 131–139 (2016).
33. Hidalgo, M. *et al.* Phase I and pharmacologic study of OSI-774, an epidermal growth factor receptor tyrosine kinase inhibitor, in patients with advanced solid malignancies. *J Clin Oncol* **19**, 3267–3279 (2001).
34. Kobayashi, H. *et al.* Relationship Among Gefitinib Exposure, Polymorphisms of Its Metabolizing Enzymes and Transporters, and Side Effects in Japanese Patients With Non-Small-Cell Lung Cancer. *Clin. Lung Cancer* **16**, 274–81 (2015).
35. Zhao, Y.-Y. *et al.* The relationship between drug exposure and clinical outcomes of non-small cell lung cancer patients treated with gefitinib. *Med. Oncol.* **28**, 697–702 (2011).
36. Perez, C. A. *et al.* Phase II study of gefitinib adaptive dose escalation to skin toxicity in recurrent or metastatic squamous cell carcinoma of the head and neck. *Oral Oncol.* **48**, 887–892 (2012).
37. Burris, H. A. *et al.* Phase I safety, pharmacokinetics, and clinical activity study of lapatinib (GW572016), a reversible dual inhibitor of epidermal growth factor receptor tyrosine kinases, in heavily pretreated patients with metastatic carcinomas. *J. Clin. Oncol.* **23**, 5305–5313 (2005).
38. Food and Drug Administration. Center for Drug Evaluation and Research Osimertinib Clinical Pharmacology and Biopharmaceutics Review. (2015). <http://www.accessdata.fda.gov/drugsatfda_docs/nda/2015/208065Orig1s000ClinPharmR.pdf>
39. Committee for Medicinal Products for Human Use (CHMP) European Medicines Agency Osimertinib European Public Assessment Report. (2015). <http://www.ema.europa.eu/docs/en_GB/document_library/EPAR_-_Public_assessment_report/human/004124/WC500202024.pdf>

40. Food and Drug Administration. Center for Drug Evaluation and Research Axitinib Clinical Pharmacology and Biopharmaceutics Review. (2012). <http://www.accessdata.fda.gov/drugsatfda_docs/nda/2012/202324Orig1s000ClinPharmR.pdf>

41. Rini, B. I. *et al.* Diastolic blood pressure as a biomarker of axitinib efficacy in solid tumors. *Clin. Cancer Res.* **17**, 3841–3849 (2011).

42. Rini, B. I. *et al.* Axitinib in metastatic renal cell carcinoma: Results of a pharmacokinetic and pharmacodynamic analysis. *J. Clin. Pharmacol.* **53**, 491–504 (2013).

43. Rini, B. I. *et al.* Axitinib with or without dose titration for first-line metastatic renal-cell carcinoma: A randomised double-blind phase 2 trial. *Lancet Oncol.* **14**, 1233–1242 (2013).

44. Rini, B. I. *et al.* Overall Survival Analysis From a Randomized Phase II Study of Axitinib With or Without Dose Titration in First-Line Metastatic Renal Cell Carcinoma. *Clin. Genitourin. Cancer* 1–5 (2016).doi:10.1016/j.clgc.2016.04.005

45. Tsuchiya, N. *et al.* Association of pharmacokinetics of axitinib with treatment outcome and adverse events in advanced renal cell carcinoma patients. In *Genitourin. Cancers Symp.* J Clin Oncol 33, 2015 (suppl 7; abstr 506) (2015).

46. Rini, B. I. *et al.* Axitinib dose titration: analyses of exposure, blood pressure and clinical response from a randomized phase II study in metastatic renal cell carcinoma. *Ann. Oncol.* **26**, 1372–1377 (2015).

47. Miles, D., Jumbe, N. L., Lacy, S. & Nguyen, L. Population Pharmacokinetic Model of Cabozantinib in Patients with Medullary Thyroid Carcinoma and Its Application to an Exposure-Response Analysis. *Clin. Pharmacokinet.* **55**, 93–105 (2016).

48. Miles, D. R., Wada, D. R., Jumbe, N. L., Lacy, S. A. & Nguyen, L. T. Population pharmacokinetic/pharmacodynamic modeling of tumor growth kinetics in medullary thyroid cancer patients receiving cabozantinib. *Anticancer. Drugs* **27**, 328–341 (2016).

49. Food and Drug Administration. Center for Drug Evaluation and Research Cabozantinib Clinical Pharmacology and Biopharmaceutics Review. (2012). <http://www.accessdata.fda.gov/drugsatfda_docs/nda/2012/203756Orig1s000ClinPharmR.pdf>

50. Singh, H. *et al.* U.S. Food and Drug Administration Approval: Cabozantinib for the Treatment of Advanced Renal Cell Carcinoma. *Clin. Cancer Res.* **23**, 330–335 (2017).

51. Food and Drug Administration. Center for Drug Evaluation and Research Lenvatinib Clinical Pharmacology and Biopharmaceutics Review. (2014). <http://www.accessdata.fda.gov/drugsatfda_docs/nda/2015/206947Orig1s000ClinPharmR.pdf>

52. Committee for Medicinal Products for Human Use (CHMP) European Medicines Agency Lenvatinib European Public Assessment report. (2015). <http://www.ema.europa.eu/docs/en_GB/document_library/EPAR_-_Public_assessment_report/human/003727/WC500188676.pdf>

53. Committee for Medicinal Products for Human Use (CHMP) European Medicines Agency Nintedanib European Public Assessment Report. (2014). <http://www.ema.europa.eu/docs/en_GB/document_library/EPAR_-_Public_assessment_report/human/002569/WC500179972.pdf>

54. Committee for Medicinal Products for Human Use (CHMP) European Medicines Agency Nintedanib Summary of Product Characteristics. (2014). <http://www.ema.europa.eu/docs/en_GB/document_library/EPAR_-_Product_Information/human/002569/WC500179970.pdf>

55. Okamoto, I. *et al.* Phase I safety, pharmacokinetic, and biomarker study of BIBF 1120, an oral triple tyrosine kinase inhibitor in patients with advanced solid tumors. *Mol. Cancer Ther.* **9**, 2825–33 (2010).

56. Food and Drug Administration. Center for Drug Evaluation and Research Nintedanib Clinical Pharmacology and Biopharmaceutics Review. (2009). <http://www.accessdata.fda.gov/drugsatfda_docs/nda/2014/205832Orig1s000ClinPharmR.pdf>

57. Suttle, A. B. *et al.* Relationships between pazopanib exposure and clinical safety and efficacy in patients with advanced renal cell carcinoma. *Br. J. Cancer* **111**, 1–8 (2014).

58. Lin, Y. *et al.* Relationship between plasma pazopanib concentration and incidence of adverse events in renal cell carcinoma. In *J Clin Oncol 29* (suppl 7; abstr 345) (2011).

59. Food and Drug Administration. Center for Drug Evaluation and Research Pazopanib Clinical Pharmacology and Biopharmaceutics Review. (2008). <http://www.accessdata.fda.gov/drugsatfda_docs/nda/2009/022465s000_ClinPharmR.pdf>

60. Xu, C.-F. *et al.* HLA-B*57:01 Confers Susceptibility to Pazopanib-Associated Liver Injury in Patients With Cancer. *Clin. Cancer Res.* **22**, 1371–7 (2016).

61. Kumar, R. *et al.* Pharmacokinetic-pharmacodynamic correlation from mouse to human with pazopanib, a multikinase angiogenesis inhibitor with potent antitumor and antiangiogenic activity. *Mol. Cancer Ther.* **6**, 2012–2021 (2007).

62. Bible, K. C. *et al.* Efficacy of pazopanib in progressive, radioiodine-refractory, metastatic differentiated thyroid cancers: Results of a phase 2 consortium study. *Lancet Oncol.* **11**, 962–972 (2010).

63. Wit, D. de *et al.* Therapeutic Drug Monitoring to individualize the dosing of pazopanib: a pharmacokinetic feasibility study. *Ther. Drug Monit.* **37**, 331–338 (2014).

64. Verheijen, R. B. *et al.* Individualized Pazopanib Dosing: A Prospective Feasibility Study in Cancer Patients. *Clin. Cancer Res.* **22**, 5738–5746 (2016).

65. Food and Drug Administration. Center for Drug Evaluation and Research Regorafenib Clinical Pharmacology and Biopharmaceutics Review. (2012). <http://www.accessdata.fda.gov/drugsatfda_docs/nda/2012/203085Orig1s000ClinPharmR.pdf>

66. Committee for Medicinal Products for Human Use (CHMP) European Medicines Agency Regorafenib CHMP Extension of Indication Variation Assessment Report. (2014). <http://www.ema.europa.eu/docs/en_GB/document_library/EPAR_-_Assessment_Report_-_Variation/human/000701/WC500215995.pdf>

67. Boudou-Rouquette, P. *et al.* Early Sorafenib-induced toxicity is associated with drug exposure and UGTIA9 genetic polymorphism in patients with solid tumors: A preliminary study. *PLoS One* **7**, 1–9 (2012).

68. Blanchet, B. *et al.* Validation of an HPLC-UV method for sorafenib determination in human plasma and application to cancer patients in routine clinical practice. *J. Pharm. Biomed. Anal.* **49**, 1109–1114 (2009).

69. Fukudo, M. *et al.* Exposure-toxicity relationship of sorafenib in Japanese patients with renal cell carcinoma and hepatocellular carcinoma. *Clin. Pharmacokinet.* **53**, 185–196 (2014).

70. Shimada, M. *et al.* Monitoring Serum Levels of Sorafenib and Its N-Oxide Is Essential for Long-Term Sorafenib Treatment of Patients with Hepatocellular Carcinoma. *Tohoku J. Exp. Med.* **237**, 173–82 (2015).

71. Yu, H. *et al.* Integrated semi-physiological pharmacokinetic model for both sunitinib and its active metabolite SU12662. *Br. J. Clin. Pharmacol.* **79**, 809–819 (2015).

72. Noda, S. *et al.* Assessment of Sunitinib-Induced Toxicities and Clinical Outcomes Based on Therapeutic Drug Monitoring of Sunitinib for Patients with Renal Cell Carcinoma. *Clin. Genitourin. Cancer* **13**, 350–358 (2015).

73. Teo, Y. L. *et al.* Association of drug exposure with toxicity and clinical response in metastatic renal cell carcinoma patients receiving an attenuated dosing regimen of sunitinib. *Target. Oncol.* **10**, 429–437 (2015).

74. Narjoz, C. *et al.* Role of the lean body mass and of pharmacogenetic variants on the pharmacokinetics and pharmacodynamics of sunitinib in cancer patients. *Invest. New Drugs* **33**, 257–268 (2015).

75. Ravaud, A. & Bello, C. L. Exposure-response relationships in patients with metastatic renal cell carcinoma receiving sunitinib: maintaining optimum efficacy in clinical practice. *Anticancer. Drugs* **22**, 377–383 (2011).

76. Houk, B. E. *et al.* Relationship between exposure to sunitinib and efficacy and tolerability endpoints in patients with cancer: Results of a pharmacokinetic/pharmacodynamic meta-analysis. *Cancer Chemother. Pharmacol.* **66**, 357–371 (2010).

77. Houk, B. E., Bello, C. L., Kang, D. & Amantea, M. A population pharmacokinetic meta-analysis of sunitinib malate (SU11248) and its primary metabolite (SU12662) in healthy volunteers and oncology patients. *Clin. Cancer Res.* **15**, 2497–2506 (2009).

78. Lankheet, N. A. G. *et al.* Pharmacokinetically guided sunitinib dosing: a feasibility study in patients with advanced solid tumours. *Br. J. Cancer* **110**, 2441–9 (2014).

79. Food and Drug Administration. Center for Drug Evaluation and Research Vandetanib Clinical Pharmacology and Biopharmaceutics Review. (2010). <http://www.accessdata.fda.gov/drugsatfda_docs/nda/2011/022405Orig1s000ClinPharmR.pdf>

80. Holden, S. N. *et al.* Clinical evaluation of ZD6474, an orally active inhibitor of VEGF and EGF receptor signaling, in patients with solid,

malignant tumors. *Ann. Oncol.* **16**, 1391–1397 (2005).

81. Bershas, D. A. *et al.* Metabolism and disposition of oral dabrafenib in cancer patients: Proposed participation of aryl nitrogen in carbon-carbon bond cleavage via decarboxylation following enzymatic oxidation. *Drug Metab. Dispos.* **41**, 2215–2224 (2013).
82. Committee for Medicinal Products for Human Use (CHMP) European Medicines Agency Dabrafenib European Public Assessment Report. (2013). <http://www.ema.europa.eu/docs/en_GB/document_library/EPAR_-_Public_assessment_report/human/002604/WC500149673.pdf>
83. Menzies, A. M. *et al.* Characteristics of pyrexia in BRAFV600E/K metastatic melanoma patients treated with combined dabrafenib and trametinib in a phase I/II clinical trial. *Ann. Oncol.* **26**, 415–421 (2015).
84. Food and Drug Administration. Center for Drug Evaluation and Research Dabrafenib Clinical Pharmacology and Biopharmaceutics Review. (2013). <http://www.accessdata.fda.gov/drugsatfda_docs/nda/2013/202806Orig1s000ClinPharmR.pdf>
85. Kramkimel, N. *et al.* Vemurafenib pharmacokinetics and its correlation with efficacy and safety in outpatients with advanced BRAF-mutated melanoma. *Target. Oncol.* **11**, 59–69 (2016).
86. Committee for Medicinal Products for Human Use (CHMP) European Medicines Agency Vemurafenib European Public Assessment Report. (2011). <http://www.ema.europa.eu/docs/en_GB/document_library/EPAR_-_Public_assessment_report/human/002409/WC500124400.pdf>
87. Funck-Brentano, E. *et al.* Plasma vemurafenib concentrations in advanced BRAFV600mut melanoma patients: Impact on tumour response and tolerance. *Ann. Oncol.* **26**, 1470–1475 (2015).
88. Funck-Brentano, E. *et al.* Is there a plasma vemurafenib concentration which predicts outcome in advanced BRAFV600 melanoma patients? *Ann. Oncol.* 2–6 (2015).
89. Goldwirt, L. *et al.* Reply to 'Plasma vemurafenib concentrations in advanced BRAFV600mut melanoma patients: impact on tumour response and tolerance' by Funck-Brentano et al. *Ann. Oncol.* **27**, 363.1-364 (2016).
90. Nijenhuis, C. M. *et al.* Clinical Pharmacokinetics of Vemurafenib in BRAF-Mutated Melanoma Patients. *J. Clin. Pharmacol.* (2016).doi:10.1002/jcph.788
91. Food and Drug Administration. Center for Drug Evaluation and Research Cobimetinib Clinical Pharmacology and Biopharmaceutics Review. (2014). <http://www.accessdata.fda.gov/drugsatfda_docs/nda/2015/206192Orig1s000ClinPharmR.pdf>
92. Ouellet, D. *et al.* Population pharmacokinetics and exposure-response of trametinib, a MEK inhibitor, in patients with BRAF V600 mutation-positive melanoma. *Cancer Chemother. Pharmacol.* **77**, 807–817 (2016).
93. Committee for Medicinal Products for Human Use (CHMP) European Medicines Agency Trametinib European Public Assessment Report. (2014). <http://www.ema.europa.eu/docs/en_GB/document_library/EPAR_-_Public_assessment_report/human/002643/WC500169708.pdf>
94. Shipkova, M. *et al.* Therapeutic Drug Monitoring of Everolimus: A Consensus Report. *Ther. Drug Monit.* **38**, 143–169 (2016).
95. Ravaud, A. *et al.* Relationship between everolimus exposure and safety and efficacy: Meta-analysis of clinical trials in oncology. *Eur. J. Cancer* **50**, 486–495 (2014).
96. Thiery-Vuillemin, A. *et al.* Impact of everolimus blood concentration on its anti-cancer activity in patients with metastatic renal cell carcinoma. *Cancer Chemother. Pharmacol.* **73**, 999–1007 (2014).
97. Krueger, D. A. *et al.* Everolimus for Subependymal Giant-Cell Astrocytomas in Tuberous Sclerosis. *N Engl J Med* **363**, 1801–1811 (2010).
98. Food and Drug Administration. Center for Drug Evaluation and Research Ibrutinib Clinical Pharmacology and Biopharmaceutics Review. (2013). <https://www.accessdata.fda.gov/drugsatfda_docs/nda/2013/205552Orig1s000ClinPharmR.pdf>
99. Advani, R. H. *et al.* Bruton tyrosine kinase inhibitor ibrutinib (PCI-32765) has significant activity in patients with relapsed/refractory B-cell malignancies. *J. Clin. Oncol.* **31**, 88–94 (2013).
100. Demetri, G. D. *et al.* Imatinib plasma levels are correlated with clinical benefit in patients with unresectable/metastatic gastrointestinal stromal tumors. *J. Clin. Oncol.* **27**, 3141–7 (2009).

101. Widmer, N. *et al.* Imatinib plasma levels: correlation with clinical benefit in GIST patients. *Br. J. Cancer* **102**, 1198–9 (2010).

102. Farag, S. *et al.* Imatinib Pharmacokinetics in a Large Observational Cohort of Gastrointestinal Stromal Tumour Patients. *Clin. Pharmacokinet.* **Jul 19**, [Epub ahead of print] (2016).

103. Bouchet, S. *et al.* Relationship between imatinib trough concentration and outcomes in the treatment of advanced gastrointestinal stromal tumours in a real-life setting. *Eur. J. Cancer* **57**, 31–38 (2016).

104. Lankheet, N. A. G. *et al.* Optimizing the dose in cancer patients treated with imatinib, sunitinib and pazopanib. *Br. J. Clin. Pharmacol.* (2017). doi:10.1111/bcp.13327

105. Ramanathan, S., Jin, F., Sharma, S. & Kearney, B. P. Clinical Pharmacokinetic and Pharmacodynamic Profile of Idelalisib. *Clin. Pharmacokinet.* **55**, 33–45 (2016).

106. Jin, F., Robeson, M., Zhou, H., Hisoire, G. & Ramanathan, S. The pharmacokinetics and safety of idelalisib in subjects with severe renal impairment. *Cancer Chemother. Pharmacol.* **76**, 1133–1141 (2015).

107. Food and Drug Administration. Center for Drug Evaluation and Research Palbociclib Clinical Pharmacology and Biopharmaceutics Review. (2014). <http://www.accessdata.fda.gov/drugsatfda_docs/nda/2015/207103Orig1s000ClinPharmR.pdf>

108. Fox, P. *et al.* Dose escalation of tamoxifen in patients with low endoxifen level: evidence for therapeutic drug monitoring - The TADE Study. *Clin. cancer Res.* **22**, 3164–71 (2016).

109. Joerger, M. *et al.* Open-label, randomised study of individualized, pharmacokinetically (PK)-guided dosing of paclitaxel combined with carboplatin or cisplatin in patients with advanced non-small cell lung cancer (NSCLC). *Ann. Oncol.* 1–22 (2016).doi:10.1093/annonc/mdw290

110. Food and Drug Administration. Center for Drug Evaluation and Research Trametinib Clinical Pharmacology and Biopharmaceutics Review. (2013). <http://www.accessdata.fda.gov/drugsatfda_docs/nda/2013/204114Orig1s000ClinPharmR.pdf>

Supplemental table 1: Overview of KIs approved by the FDA for oncological indications with selected (steady state) pharmacokinetic parameters.

Drug	Indication	(Primary) Target	Approved Dose	T_{max} (h)	C_{min} (ng/mL plus ± SD, (CV%) or [range]	$T_{1/2}$ (h)	Refs
Afatinib	NSCLC	EGFR	40 mg QD	3	14.4 (70)	36	[1]
Alectinib	NSCLC	ALK	600 mg BID	4	572 (48)	32	[2,3]
Axitinib	RCC	VEGFR	5 mg BID	3	NR	4	[4]
Bosutinib	CML	Bcr-Abl	500 mg QD	6	147 [16-841]	34	[5,6]
Cabozantinib	TC, RCC	VEGFR	140 mg QD / 60 mg QD	3	1380 (53)	55	[7]
Ceritinib	NSCLC	ALK	750 mg QD	6	871 (46)	40	[8,9]
Cobimetinib	Mel	MEK	60 mg QD	2	127 (87)	44	[10]
Crizotinib	NSCLC	ALK	250 mg BID	5	274	42	[11,12]
Dabrafenib	Mel	BRAF	150 mg BID	2	99.6*	10	[13,14]
Dasatinib	CML	Bcr-Abl	100 mg QD	1	2.61 (26)	6	[15]
Erlotinib	NSCLC, Pan	EGFR	150 mg QD	4	1010 [75-5542]	36	[16,17]
Everolimus	RCC, NET, BC	mTOR	10 mg QD	1	13.2 ± 7.9	38	[18]
Gefitinib	NSCLC	EGFR	250 mg QD	5	291(67)	41	[19,20]
Ibrutinib	CLL, MCL	BTK	420 mg QD / 560 mg QD	1	680 ± 517 †	9	[21]
Idelalisib	CLL, FL	PI3Kδ	150 mg BID	3	318 [97 – 700]	8	[22]
Imatinib	GIST, CML	KIT, PDGFR, Bcr-Abl	400 mg QD	3	1193 [227 – 2606]	19	[23,24]
Lapatinib	BC	HER2	1250 mg QD	4	780 (22)	24	[25,26]
Lenvatinib	TC	VEGFR	24 mg QD	2	51.5	29	[27,28]
Nilotinib	CML	Bcr-Abl	300 mg BID	3	1123 (64)	17	[29,30]
Nintedanib	NSCLC	VEGFR	200 mg BID	3	13.1(81)	20	[31]
Osimertinib	NSCLC	EGFR	80 mg QD	6	166 (49)	55	[32,33]
Palbociclib	BC	CDK4/6	125 QD	4	61(42)	27	[34,35]
Pazopanib	RCC, STS	VEGFR	800 mg QD	4	24,000 (67)	31	[36]
Ponatinib	CML	Bcr-Abl	45 mg QD	4	34.2 (45)	22	[37]
Regorafenib	CRC, GIST	VEGFR	160 mg QD	4	1400 (57)	28	[38]
Sorafenib	HCC, TC	VEGFR	400 mg BID	8	3750 (104)	26	[39]
Sunitinib	RCC, HCC	VEGFR	50 mg QD (inter) 37.5 mg QD (cont)	5 (parent)	51.6 [15 -94] (sum of parent & SU12662)	50 (parent), 95 (SU12662)	[16,40,41]
Trametinib	Mel	MEK	2 mg QD	2	12.1	96	[42]
Vandetanib	TC	VEGFR	300 mg QD	6	795	456	[43]
Vemurafenib	Mel	BRAF	960 mg BID	5	38,900 (41)	34	[44,45]

** Sum of the C_{min} of dabrafenib and its hydroxyl metabolite*

*†For ibrutinib the area under the plasma concentration-time curve in ng*h/mL is provided as no C_{min} data was reported.*

ALK: Anaplastic lymphoma kinase; AR: androgen receptor; BC: Breast cancer; BCR-Abl: Break point cluster region – Abelson fusion oncoprotein; BRAF: Serine/threonine-protein kinase B-Raf; BTK: Bruton's tyrosine kinase; CDK4/6: Cycline dependent Kinase 4/6; CML: Chronic myelogenous leukemia; C_{min}: Minimum plasma concentration / trough concentration; CLL: Chronic lymphocytic leukemia; CRC: Colorectal cancer; CV: coefficient of variation; EGFR: Epidermal growth factor receptor; ER: Estrogen receptor; FL: Follicular lymphoma; GIST: Gastro-intestinal stromal tumors; HCC: Hepatocellular carcinoma; HER: Human epidermal growth factor receptor; KIT: CD117; MCL: Mantle cell lymphoma; MEK: Mitogen-activated protein kinase kinase; Mel: Melanoma; mTOR: Mammalian target of rapamycin; NET: Neuro-endocrine tumors; NSCLC: Non-small cell lung cancer; NR: Not reported; PC: Pancreatic cancer; PDGFR: Platelet derived growth factor receptor; PI3Kδ:phosphoinositide 3 kinase delta; RCC: Renal cell cancer; SD: standard deviation; STS: Soft tissue sarcoma; TC: Thyroid cancer; VEGFR: Vascular endothelial growth factor receptor.

Supplemental references

1. Food and Drug Administration. Center for Drug Evaluation and Research Afatinib Clinical Pharmacology and Biopharmaceutics Review. (2012). <http://www.accessdata.fda.gov/drugsatfda_docs/nda/2013/201292Orig1s000ClinPharmR.pdf>
2. Seto, T. *et al.* CH5424802 (RO5424802) for patients with ALK-rearranged advanced non-small-cell lung cancer (AF-001JP study): A single-arm, open-label, phase 1-2 study. *Lancet Oncol.* **14**, 590–598 (2013).
3. Food and Drug Administration. Center for Drug Evaluation and Research Alectinib Clinical Pharmacology and Biopharmaceutics Review. (2016). <http://www.accessdata.fda.gov/drugsatfda_docs/nda/2015/208434Orig1s000ClinPharmR.pdf>
4. Food and Drug Administration. Center for Drug Evaluation and Research Axitinib Clinical Pharmacology and Biopharmaceutics Review. (2012). <http://www.accessdata.fda.gov/drugsatfda_docs/nda/2012/202324Orig1s000ClinPharmR.pdf>
5. Committee for Medicinal Products for Human Use (CHMP) European Medicines Evaluation Agency Bosutinib Summary of Product Characteristics. (2016). <http://www.ema.europa.eu/docs/en_GB/document_library/EPAR_-_Product_Information/human/002373/WC500141721.pdf>
6. Hsyu, P.-H., Mould, D. R., Upton, R. N. & Amantea, M. Pharmacokinetic-pharmacodynamic relationship of bosutinib in patients with chronic phase chronic myeloid leukemia. *Cancer Chemother. Pharmacol.* **71**, 209–18 (2013).
7. Food and Drug Administration. Center for Drug Evaluation and Research Cabozantinib Clinical Pharmacology and Biopharmaceutics Review. (2012). <http://www.accessdata.fda.gov/drugsatfda_docs/nda/2012/203756Orig1s000ClinPharmR.pdf>
8. Food and Drug Administration. Center for Drug Evaluation and Research Ceritinib Clinical Pharmacology and Biopharmaceutics Review. (2014).at <http://www.accessdata.fda.gov/drugsatfda_docs/nda/2014/205755Orig1s000ClinPharmR.pdf>
9. Shaw, A. T. *et al.* Ceritinib in ALK -Rearranged Non–Small-Cell Lung Cancer. *N. Engl. J. Med.* **370**, 1189–1197 (2014).
10. Food and Drug Administration. Center for Drug Evaluation and Research Cobimetinib Clinical Pharmacology and Biopharmaceutics Review. (2014). <http://www.accessdata.fda.gov/drugsatfda_docs/nda/2015/206192Orig1s000ClinPharmR.pdf>
11. Food and Drug Administration. Center for Drug Evaluation and Research Crizotinib Clinical Pharmacology and Biopharmaceutics Review. (2011). <http://www.accessdata.fda.gov/drugsatfda_docs/nda/2011/202570Orig1s000ClinPharmR.pdf>
12. Ou, S.-H. I., Bartlett, C. H., Mino-Kenudson, M., Cui, J. & Iafrate, A. J. Crizotinib for the treatment of ALK-rearranged non-small cell lung cancer: a success story to usher in the second decade of molecular targeted therapy in oncology. *Oncologist* **17**, 1351–75 (2012).
13. Food and Drug Administration. Center for Drug Evaluation and Research Dabrafenib Clinical Pharmacology and Biopharmaceutics Review. (2013). <http://www.accessdata.fda.gov/drugsatfda_docs/nda/2013/202806Orig1s000ClinPharmR.pdf>
14. Falchook, G. S. *et al.* Dose selection, pharmacokinetics, and pharmacodynamics of BRAF inhibitor dabrafenib (GSK2118436). *Clin. Cancer Res.* **20**, 4449–4458 (2014).
15. Committee for Medicinal Products for Human Use (CHMP) European Medicines Evaluation Agency Dasatinib Summary of Product Characteristics. (2011). <http://www.ema.europa.eu/docs/en_GB/document_library/EPAR_-_Product_Information/human/000709/WC500056998.pdf>
16. Lankheet, N. A. G. *et al.* Plasma concentrations of tyrosine kinase inhibitors imatinib, erlotinib, and sunitinib in routine clinical outpatient cancer care. *Ther. Drug Monit.* **36**, 326–34 (2014).
17. Committee for Medicinal Products for Human Use (CHMP) European Medicines Agency

Erlotinib Summary of Product Characteristics. (2010). <http://www.ema.europa.eu/docs/en_GB/document_library/EPAR_-_Product_Information/human/000618/WC500033994.pdf>

18. O'Donnell, A. *et al.* Phase I pharmacokinetic and pharmacodynamic study of the oral mammalian target of rapamycin inhibitor everolimus in patients with advanced solid tumors. *J. Clin. Oncol.* **26**, 1588–1595 (2008).
19. Committee for Medicinal Products for Human Use (CHMP) European Medicines Agency Gefitinib Summary of Product Characteristics. (2014). <http://www.ema.europa.eu/docs/en_GB/document_library/EPAR_-_Product_Information/human/001016/WC500036358.pdf>
20. Horak, J. *et al.* The effect of different etiologies of hepatic impairment on the pharmacokinetics of gefitinib. *Cancer Chemother. Pharmacol.* **68**, 1485–1495 (2011).
21. Food and Drug Administration. Center for Drug Evaluation and Research Ibrutinib Clinical Pharmacology and Biopharmaceutics Review. (2013). <https://www.accessdata.fda.gov/drugsatfda_docs/nda/2013/205552Orig1s000ClinPharmR.pdf>
22. Committee for Medicinal Products for Human Use (CHMP) European Medicines Evaluation Agency Idelalisib Summary of Product Characteristics. (2014). <http://www.ema.europa.eu/docs/en_GB/document_library/EPAR_-_Product_Information/human/003843/WC500175377.pdf>
23. Peng, B., Lloyd, P. & Schran, H. Clinical Pharmacokinetics of Imatinib. **44**, 879–894 (2005).
24. Farag, S. *et al.* Imatinib Pharmacokinetics in a Large Observational Cohort of Gastrointestinal Stromal Tumour Patients. *Clin. Pharmacokinet.* **Jul 19**, [Epub ahead of print] (2016).
25. Yu, H. *et al.* Practical guidelines for therapeutic drug monitoring of anticancer tyrosine kinase inhibitors: focus on the pharmacokinetic targets. *Clin. Pharmacokinet.* **53**, 305–25 (2014).
26. Burris, H. A. *et al.* Phase I safety, pharmacokinetics, and clinical activity study of lapatinib (GW572016), a reversible dual inhibitor of epidermal growth factor receptor tyrosine kinases, in heavily pretreated patients with metastatic carcinomas. *J. Clin. Oncol.* **23**, 5305–5313 (2005).
27. Hong, D. S. *et al.* Phase I dose-escalation study of the multikinase inhibitor lenvatinib in patients with advanced solid tumors and in an expanded cohort of patients with melanoma. *Clin. Cancer Res.* **21**, 4801–4810 (2015).
28. Committee for Medicinal Products for Human Use (CHMP) European Medicines Agency Lenvatinib European Public Assessment report. (2015). <http://www.ema.europa.eu/docs/en_GB/document_library/EPAR_-_Public_assessment_report/human/003727/WC500188676.pdf>
29. Committee for Medicinal Products for Human Use (CHMP) European Medicines Evaluation Agency Nilotinib Summary of Product Characteristics. (2012).t <http://www.ema.europa.eu/docs/en_GB/document_library/EPAR_-_Product_Information/human/000798/WC500034394.pdf>
30. Larson, R. A. *et al.* Population pharmacokinetic and exposure-response analysis of nilotinib in patients with newly diagnosed Ph+ chronic myeloid leukemia in chronic phase. *Eur. J. Clin. Pharmacol.* **68**, 723–733 (2012).
31. Dallinger, C. *et al.* Pharmacokinetic Properties of Nintedanib in Healthy Volunteers and Patients With Advanced Cancer. *J. Clin. Pharmacol.* (2016). doi:10.1002/jcph.752
32. Committee for Medicinal Products for Human Use (CHMP) European Medicines Agency Osimertinib European Public Assessment Report. (2015). <http://www.ema.europa.eu/docs/en_GB/document_library/EPAR_-_Public_assessment_report/human/004124/WC500202024.pdf>
33. Jänne, P. a *et al.* AZD9291 in EGFR Inhibitor-Resistant Non-Small-Cell Lung Cancer. *N. Engl. J. Med.* **372**, 1689–1699 (2015).
34. Schwartz, G. K. *et al.* Phase I study of PD 0332991, a cyclin-dependent kinase inhibitor, administered in 3-week cycles (Schedule 2/1). *Br J Cancer* **104**, 1862–1868 (2011).
35. Food and Drug Administration. Center for Drug Evaluation and Research Palbociclib Clinical Pharmacology and Biopharmaceutics Review. (2014). <http://www.accessdata.fda.gov/drugsatfda_docs/nda/2015/207103Orig1s000ClinPharmR.pdf>
36. Hurwitz, H. I. *et al.* Phase I trial of pazopanib in patients with advanced cancer. *Clin. Cancer Res.* **15**, 4220–4227 (2009).
37. Committee for Medicinal Products for Human Use (CHMP) European Medicines Evaluation

Agency Ponatinib Summary of Product Characteristics. (2013). <http://www.ema.europa.eu/docs/en_GB/document_library/EPAR_-_Product_Information/human/002695/WC500145646.pdf>

38. Food and Drug Administration. Center for Drug Evaluation and Research Regorafenib Clinical Pharmacology and Biopharmaceutics Review. (2012). <http://www.accessdata.fda.gov/drugsatfda_docs/nda/2012/203085Orig1s000ClinPharmR.pdf>
39. Minami, H. *et al.* Phase I and pharmacokinetic study of sorafenib, an oral multikinase inhibitor, in Japanese patients with advanced refractory solid tumors. *Cancer Sci.* **99**, 1492–1498 (2008).
40. Faivre, S. *et al.* Safety, pharmacokinetic, and antitumor activity of SU11248, a novel oral multitarget tyrosine kinase inhibitor, in patients with cancer. *J. Clin. Oncol.* **24**, 25–35 (2006).
41. Committee for Medicinal Products for Human Use (CHMP) European Medicines Agency Sunitinib Summary of Product Characteristics. (2012). <http://www.ema.europa.eu/docs/en_GB/document_library/EPAR_-_Product_Information/human/000687/WC500057737.pdf>
42. Food and Drug Administration. Center for Drug Evaluation and Research Trametinib Clinical Pharmacology and Biopharmaceutics Review. (2013). <http://www.accessdata.fda.gov/drugsatfda_docs/nda/2013/204114Orig1s000ClinPharmR.pdf>
43. Food and Drug Administration. Center for Drug Evaluation and Research Vandetanib Clinical Pharmacology and Biopharmaceutics Review. (2010). <http://www.accessdata.fda.gov/drugsatfda_docs/nda/2011/022405Orig1s000ClinPharmR.pdf>
44. Grippo, J. F. *et al.* A phase I, randomized, open-label study of the multiple-dose pharmacokinetics of vemurafenib in patients with BRAF V600E mutation-positive metastatic melanoma. *Cancer Chemother. Pharmacol.* **73**, 103–111 (2014).
45. Nijenhuis, C. M. *et al.* Clinical Pharmacokinetics of Vemurafenib in BRAF-Mutated Melanoma Patients. *J. Clin. Pharmacol.* (2016).doi:10.1002/jcph.788

Chapter 2

Clinical Pharmacology & Bioanalysis of Pazopanib

Chapter 2.1

Clinical Pharmacokinetics & Pharmacodynamics of Pazopanib: Towards Optimized Dosing

R.B. Verheijen[1], J.H. Beijnen[1,2], J.H.M. Schellens[2,3], A.D.R. Huitema[1,4],N. Steeghs[2]

[1]Department of Pharmacy & Pharmacology, The Netherlands Cancer Institute - Antoni van Leeuwenhoek, Louwesweg 6, 1066 EC Amsterdam, The Netherlands.
[2]Department of Pharmaceutical Sciences, Utrecht University, Utrecht, The Netherlands.
[3]Department of Medical Oncology and Clinical Pharmacology, The Netherlands Cancer Institute - Antoni van Leeuwenhoek, Amsterdam, The Netherlands.
[4]Department of Clinical Pharmacy, Utrecht University Medical Center, Utrecht, The Netherlands.

Abstract

Pazopanib is an inhibitor of VEGFR, PDGFR, FGFR and c-Kit, approved for the treatment of renal cell carcinoma and soft tissue sarcoma.

The pharmacokinetics of pazopanib are complex and characterized by pH-dependent solubility, large interpatient variability and low, non-linear and time-dependent bioavailability. Exposure to pazopanib is increased by food and co-administration of ketoconazole, but drastically reduced by proton-pump inhibitors.

Studies have demonstrated relationships between systemic exposure to pazopanib and toxicity, such as hypertension. Furthermore, a strong relationship between pazopanib trough level ≥20 mg/L and both tumor shrinkage and progression free survival has been established. At the currently approved daily dose of 800 mg, approximately 20% of patients do not reach this threshold and may be at risk of suboptimal treatment.

Because of this, clinical trials have explored individualized pazopanib dosing. These demonstrate the safety and feasibility of individualized pazopanib dosing based on trough levels.

In summary, we provide an overview of the complex pharmacokinetic and pharmacodynamic profiles of pazopanib and based on the available data we propose optimized dosing strategies.

Introduction

Pazopanib is an inhibitor of the Vascular Endothelial Growth Factor Receptor (VEGFR), Platelet Derived Growth Factor Receptor (PDGFR), Fibroblast Growth Factor Receptor (FGFR) and the stem cell receptor (c-Kit), approved for the treatment of renal cell carcinoma (RCC) and soft tissue sarcoma (STS).[1–3]

In patients with locally advanced or metastatic RCC, pazopanib increased progression free survival (PFS) from 4.2 to 9.2 months compared to placebo, with a hazard ratio (HR) of 0.46 (95% CI, 0.34-0.62; p<0.0001). [2] In the phase III trial in STS patients, PFS was 4.6 months in the pazopanib treated group versus only 1.6 months in the placebo group, corresponding to a HR of 0.31 (95% CI 0.24-0.40; p<0.0001).[3]

Treatment with pazopanib has also been explored in a range of other tumor types such as thyroid cancer[4], gastro-intestinal stromal tumors [5] and ovarian cancer.[6]

The most common adverse events related to pazopanib included fatigue, nausea, diarrhea, hypertension, anorexia and hair depigmentation, aspartate transaminase (AST) and alanine transaminase (ALT) elevations.[2,3]

The purpose of this review is to provide an overview of the available clinical pharmacokinetic and pharmacodynamic data for pazopanib. In addition, we describe population pharmacokinetic models that have been developed for pazopanib and the clinical trials studying adaptive dosing strategies in an effort to optimize treatment outcomes of patients treated with this drug.

Physiochemical properties & Preclinical Pharmacology

Physiochemical properties

Pazopanib is a synthetic 5-[[4-[(2,3-Dimethyl-2H-indazol-6-yl)methylamino]-2-pyrimidinyl]amino]-2-methyl-benzenesulfonamide and part of the group of indazolylpyrimidines.[7] The chemical structure of pazopanib is shown in figure 1. Pazopanib has three pKa values of 2.1, 6.4, and 10.2. Commercially, pazopanib is formulated as a hydrochloride salt. This salt is slightly soluble at very low pH (1) but practically insoluble at pH values ≥4 in aqueous matrices.[8] The permeability of pazopanib was measured *in vitro* by Caco-2 monolayers experiments. The results pointed towards dissolution rate limited permeability. Given the above pazopanib was classified as a class II compound, according to the Biopharmaceutics Classification System.[8]

Mechanism of Action and Preclinical Pharmacology

Angiogenesis is one of the hallmarks of cancer and is controlled partly by the Vascular Endothelial Growth Factor (VEGF).[9] VEGF and its receptor VEGFR mediate numerous changes within the tumor vasculature and inhibition of this pathway affects vascular function (including both flow and permeability) in addition to inhibition of further new blood vessel growth.[10]

In vitro, pazopanib has shown to inhibit VEGFR 1, 2 and 3 with an IC_{50} of 10, 30 and 47 nM respectively. [7] Pazopanib has also shown affinity for other proteins such as PDGFR α and β (with an IC_{50} of 71 and 81 nM), c-Kit (74 nM) and FGFR 1, 3 and 4 (140, 130 and 800 nM respectively).[1]
The activity of pazopanib based on these kinase assays was further confirmed in cell-based assays where it inhibited ligand-induced autophosphorylation of VEGFR2, PDGFR β and c-Kit in human umbilical vein endothelial cells, human foreskin fibroblasts and NCI-H526 cells respectively.[1]

In vivo, pazopanib has been shown to have a dose dependent anti-tumor activity in a variety of tumor xenograft models based on colon, melanoma, prostate, renal, breast and lung cancer cell lines.[1] To establish the pazopanib concentration required for optimal efficacy, VEGF-induced VEGFR2 phosphorylation was assessed in mice lungs after oral doses of pazopanib. Results indicated maximal inhibition at a concentration of approximately 40 µmol/L, which corresponds to a steady state C_{min} of 17.5 mg/L.[1]

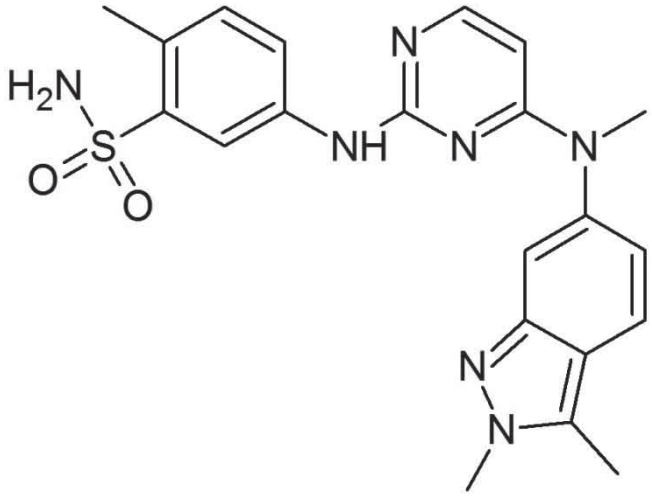

Figure 1: Chemical structure of pazopanib ((5-[[4-[(2,3-Dimethyl-2H-indazol-6-yl)methylamino]-2-pyrimidinyl] amino]-2-methyl-benzenesulfonamide).

Clinical Pharmacokinetics

Pharmacokinetics in Cancer Patients

In a phase I study (n=63), pazopanib doses ranging from 50 to 2000 mg have been explored.[11] Pazopanib pharmacokinetics did not increase linearly with dose. Although the highest exposure after single administration was seen at the 2000 mg dose, steady-state exposure to pazopanib seemed to plateau at doses above 800 mg.[11]

Four patients experienced dose-limiting toxicities (DLTs): gastrointestinal hemorrhage, extrapyramidal involuntary movements, hypertension and fatigue. The maximum tolerated dose (MTD) was not reached, but based on a plateau in exposure at the 800 mg once daily (QD) dose, this dose was selected for further clinical development.

A single 800 mg dose (n=10) resulted in a mean (CV%) C_{max} of 19.46 (176) mg/L, AUC_{0-24} of 275.1 (203) mg*h/L, C_{min} of 9.4 (240) mg/L and T_{max} of 3 hours. Pazopanib was eliminated with a $t_{1/2}$ of 31.1 hours, resulting in accumulation with repeated daily dosing. At steady state (day 22, n=10) C_{max}, AUC_{0-24}, C_{min} and T_{max} were 45.1 (68.8) mg/L, 743.3 (76.1) mg*h/L, 24.0 (67.4) mg/L, 2 hours, respectively.[11]

Administration of pazopanib as a crushed tablet or oral suspension increased C_{max} by 2.09 and 1.29 fold and AUC_{0-72} by 1.46 and 1.33 fold, respectively. [12]

Pazopanib is bound to plasma proteins to a very large extent (>99.9%), with an unbound fraction of on average 0.011±0.0013%. Protein binding seemed not influenced by the total pazopanib plasma concentration. Pazopanib was mainly bound to albumin and to a lesser extend to α1 glycoprotein or other plasma proteins.[13]

The bioavailability (F), metabolism and disposition of pazopanib were studied in cancer patients using ^{14}C-labeled pazopanib.[14] Absolute F was determined by comparing the dose-normalized ratio of AUC_{0-24} on day 15 at a 800 mg QD tablet dose to the AUC_{0-inf} of a 5 mg i.v. dose. Mean F was estimated to be 21.4% ranging from 13.5 to 38.9%.[14]

Seven metabolites were identified, M1 to M7. Two of these were hydroxylated metabolites, M1 (or GSK1268992) and M2 (or GSK1268997) and one N-demethylated metabolite M3 (or GSK1071306). Pazopanib was also directly glucuronidated to form M4. The hydroxylated metabolites M1 and M2 were subsequently glucuronidated to form M5 and M6, respectively. Lastly M7 was thought to be the carboxylic acid derivative of pazopanib.

In total, pazopanib metabolites accounted for ≤10% of plasma radioactivity and the contribution to the effect of parent compound was shown to be low based on their low relative concentrations and *in vitro* potency.[14]

Pazopanib was primarily excreted with feces (82.2%), with unchanged pazopanib being the most abundant compound excreted following oral administration. Only 2.6% of radioactivity was found in urine.

Pharmacokinetics in Special Populations

Pediatric Cancer Patients

A phase I study was conducted in children with STS or other treatment refractory solid tumors (n=51).[15] Pazopanib was administered as a tablet formulation at doses of 275, 350, 450 and 600 mg/m^2 and as a suspension for oral use at 160 and 225 mg/m^2.

DLTs included lipase, amylase and ALT elevations, proteinuria, hypertension and intracranial hemorrhage (the last occurred in a patient with brain metastases).

The MTD was reached at 450 mg/m^2 (for the tablet formulation). At steady state this dose resulted in a mean (CV%) C_{min} of 23.9 (13.5) mg/L,[15] which was very similar to the average (CV%) C_{min} observed in the adult phase I trial at 800 mg of 24.0 (67.4) mg/L.[11]

Patients with Renal Impairment

As pazopanib was only excreted in urine to a very limited extent (2.6%)[14], no dedicated clinical trial was performed to assess the pharmacokinetics of pazopanib in patients with impaired renal function.

However, in a small cohort of end-stage renal disease (ESRD) patients, 9 patients with metastatic renal cell cancer were treated with pazopanib.[16] Five patients received 800 mg QD and four patients received 600 mg QD. Two of the 800 mg QD treated patients required a dose reduction to 400 mg, while all patients who started at 600 mg QD were reduced to 400 mg QD. Median time on treatment was 11.6 months.[16] Unfortunately no pharmacokinetic data was available in this study. Further sporadic case reports are available of patients treated with pazopanib during dialysis.[17,18] However, no pharmacokinetic sampling in patients with severe renal impairment or those undergoing dialysis has been reported.

In a population pharmacokinetic analysis, creatinine clearance (values ranging from 30 to 150 mL/min) did not show an effect on the clearance of pazopanib (n=408).[8]

Currently, no dose adjustments are recommended for patients with a creatinine clearance ≥30 mL/min, but caution is advised in patients with lower clearance values.[19]

Patients with Hepatic Impairment

To study the effect of hepatic impairment on the pharmacokinetics of pazopanib, a phase 1 study was conducted in 89 patients with solid tumors. Patients were stratified into 4 groups [A (normal), B (mild), C (moderate), and D (severe)], using the National Cancer Institute Organ Dysfunction Working Group (NCI-ODWG) categories of liver dysfunction.[20]

Patients in the mild group tolerated 800 mg QD, while patients in the moderate and severe groups only tolerated 200 mg QD. At steady state, the 800 mg QD dose led to a median (range) C_{min} and AUC_{0-24} of 24.0 (8.3–74.6) mg/L and 774.2 (214.7–2034.4) mg*h/L in patients with mild hepatic dysfunction (n=12).

The 200 mg dose was associated with a median (range) C_{min} and AUC_{0-24} of 16.2 (3.1–24.2) mg/L and 256.8 (65.7–487.7) mg*h/L in patients with moderate dysfunction (n=11) and 5.7 (1.5–18.4) mg/L and 130.6 (46.9–473.2) mg*h/L with severe dysfunction (n=14).

Based on this study, a dose of 800 mg is advised in patients with mild and a 200 mg dose for patients with moderate hepatic impairment. Use of pazopanib is not recommend in patients with severe liver impairment.[19]

Although patients with moderate impairment were shown to tolerate doses of 200 mg QD, it should be taken into account that the mean C_{min} value in these patients of 16.2 mg/L was below

the concentrations found to be efficacious in preclinical models (≥17.5 mg/L),[1] and clinical trials (≥20.5 mg/L).[21]

Food Effect

Pazopanib pharmacokinetics were investigated in a fasted state and with high fat or low fat meal in an open-label, randomized, crossover, phase I study (n=35).[22] Compared to a fasted state AUC_{0-72} and C_{max} increased 2.34 and 2.08 fold, respectively, with administration of a single dose of pazopanib with a high-fat meal and 1.92 and 2.10 fold, respectively, with a low-fat meal. $T_{1/2}$ was not affected by either a high or low fat meal. Although the PK of metabolites was also altered, the AUC_{0-72} and C_{max} of these remained below 5% of that of pazopanib.

Based on this study the authors advocated that food increased pazopanib exposure, but that pazopanib should be administered in a fasted state, at least 1 hour before or 2 hours after a meal, to reduce variability in pazopanib exposure that may be caused by the variability of food intake in cancer patients.

Given the clear food effect, it has been hypothesized that pazopanib's large PK variability may be partially caused by intake of food.[23] A larger fasted interval around ingestion could therefore theoretically reduce variability, however this hypothesis has not been confirmed in a clinical trial.

Drug-Drug Interaction Studies

Pazopanib has been studied in a range of combination regimens, including combinations with chemotherapy [24,25], hormonal agents [26] and other targeted therapies.[27] In general, efforts to combine tyrosine kinase inhibitors such as pazopanib with other anti-cancer drugs have been unsuccessful due to limited tolerability. As none of these combinations with pazopanib are currently approved by the Food and Drug Administration (FDA) or the European Medicines Agency (EMA), only dedicated pharmacokinetics interaction studies will be discussed in detail here.

To study the potential of pazopanib for drug-drug interactions, a trial in patients with advanced solid tumors (n=24) evaluated the effect of pazopanib on CYP450 isoforms using a cocktail of probe drugs.[28] The probes used were midazolam (CYP3A), warfarin (CYP2C9), omeprazole (CYP2C19), caffeine (CYP1A2) and dextromethorphan (CYP2D6).

Pazopanib did not have a significant effect on the AUC_{0-24} or C_{max} of warfarin, omeprazole or caffeine.

The AUC_{0-24} and C_{max} of midazolam however, were increased 1.3 fold from 53 ng*h/mL and 21 ng/mL to 71 ng*h/mL and 27 ng/mL, respectively. This demonstrates that pazopanib is a weak inhibitor of CYP3A4.

When pazopanib was co-administered with dextromethorphan, it increased the dextromethorphan/dextrorphan ratio in urine by 1.33-1.64 fold, indicating only moderate inhibition of CYP2D6.

Although inhibition of CYP3A and CYP2D6 was weak, the authors concluded it might be necessary to closely monitor when co-administrating CYP3A and CYP2D6 substrates with a narrow therapeutic index.

Table 1: Biomarkers related to pazopanib treatment efficacy.

Study	Tumor Type	N	Matrix	Biomarker	Association	p
Sleijfer et al.[29]	STS	142	Serum	High sVEGFR2 (12 weeks)‡	PFS_{12wks} ↑	0.0039
				Low PlGF (12 weeks)	PFS_{12wks} ↑	0.0318
					OS ↑	0.0009
				Low IL12 p40	PFS_{12wks} ↑	0.0305
				Low MPC3	PFS_{12wks} ↑	0.0271
				Low HGF	PFS ↑	0.0079
				Low bNGF	PFS ↑	0.0044
				Low Ilra2	OS ↑	0.0078
				ICAM-1	OS ↑	0.0072
Tran et al.[31]	RCC	129	Plasma	Low IL8	PFS ↑	0.006
				Low HGF	PFS ↑	0.0004
				Low TIMP-1	PFS ↑	0.010
				Low Osteopontin	PFS ↑	0.006
				High IL6	PFS ↑	0.009
Xu et al. [33]	RCC	397	Whole blood	IL8 2767A>T	PFS	0.009
				IL8 251 T>A	PFS	0.01
				HIF1A 1790 G>A	PFS	0.03
					RR	0.02
				NR1I2 25385 C>T	RR	0.03
				VEGFA 2578 A>C	RR	0.02
				VEGFA 1498 C>T	RR	0.02
				VEGFA 634 G>C	RR	0.03
Sweis et al.[35]	RCC	18	DCE-MRI	High K^{trans}	PFS ↑	0.036

‡High and low biomarker levels were defined based on the median.
bNGF: basic nerve growth factor
HGF: hepatocyte growth factor
HIF1a: hypoxia-inducible factor 1A
ICAM-1: intercellular adhesion molecule-1
IL12 p40: interleukin 12 p40 subunit
IL8: interleukin 8
NR1I2: nuclear receptor subfamily 1, group I, member 2
OS: overall survival
PFS: progression free survival
PFS_{12wks}: probability of PFS at 12 weeks
PlGF; placental growth factor
RCC: renal cell carcinoma
RR: response rate
STS: soft tissue sarcoma
sVEGFR2: soluble vascular endothelial growth factor receptor 2
TIMP-1: tissue inhibitor of metalloproteinases-1
VEGFA: vascular endothelial growth factor A

A dedicated drug-drug interaction study was performed with pazopanib and the CYP3A4 inhibitor ketoconazole.[29] In total, 21 patients were treated with a 400 mg dose of pazopanib and 400 mg of ketoconazole. After 5 days of co-administration, pazopanib AUC_{0-24} increased 1.66-fold and C_{max} 1.45-fold. The formation of metabolites was inhibited to a 0.39-fold lower AUC of GSK1268997 (M2) and 0.56-fold of GSK1071306 (M3). GSK1268992 (M1) was less affected with an AUC-ratio of 1.06, suggesting that this metabolite it is not formed through CYP3A4 metabolism.[29]
The pazopanib exposure at 400 mg QD pazopanib in combination with 400 mg QD of ketoconazole was approximately similar to that of the 800 mg QD pazopanib dose in the phase I monotherapy study (geometric mean (95% CI) C_{max} of 59.2 (45.1-77.6) mg/L and 1300 (1030-1620) mg*h/L versus mean (CV%) 45.1 (68.8) mg/L and 743.3* (76.1) mg*h/L). Therefore, it is now recommended to lower the dose of pazopanib to 400 mg when co-administration with a strong CYP3A4-inhibitor is therapeutically necessary. [19,29]

The pharmacokinetics of pazopanib were also studied in 13 patients who were treated with 800 mg pazopanib (QD 1 hour before or 2 hours after breakfast) and 40 mg esomeprazole (QD before bedtime) for 7 days. Pazopanib exposure was markedly reduced by the proton pump inhibitor (PPI), with an AUC-ratio of 0.60 and C_{max}-ratio of 0.58. Mean C_{min} was also reduced from 27.2 mg/L under control condition to 17.3 mg/L. If concomitant use of a PPI is unavoidable, pazopanib should be administered when gastric pH is expected to be lowest (i.e. in the evening) and together with the PPI.[29,30] The current recommendation therefore is to avoid the use of gastric acid reducing agents and if unavoidable take pazopanib without food once daily in the evening concomitantly with the PPI. [19] If the concomitant use of an H2-receptor antagonist is necessary, pazopanib could best be taken without food at least 2 hours before or at least 10 hours after a dose of an H2-receptor antagonist. For short-acting antacids, the interval can be shorted to at least 1 hour before or 2 hours after administration of the antacid.[19]

Clinical Pharmacodynamics

Pharmacodynamic markers

An overview of all pharmacodynamic biomarkers significantly related to pazopanib treatment efficacy is provided in table 1.

Pharmacodynamics in Soft Tissue Sarcoma

Hypertension is generally considered a relevant biomarker for response of angiogenesis inhibitors,[31] an often studied example of this is bevacizumab.[32] Yet, for pazopanib a retrospective analysis of 337 sarcoma patients did not find any significant relationship between hypertension and PFS (HR 0.88; 95% CI 0.64-1.23;p=0.467) or OS (HR 0.76; 95% CI 0.54-1.08; p=0.123).[33]

Cytokines and circulating angiogenic factors in serum were investigated as predictors of pazopanib efficacy and toxicity in STS patients.[34] For efficacy, increased interleukin 12 (IL12) and mitochondrial pyruvate carrier 3 (MPC3) levels at baseline were related to a higher probability of PFS after 12 weeks. Low (≤7000) sVEGFR2 and high (>50) placental growth factor (PlGF) levels were related to lower PFS after 12 weeks. Moreover, PlGF levels were also significantly related to shorter OS.[34] A full overview of all associations is provided in table 1. Low sVEGFR2 and high PlGF levels were also related to increased grades of hypertension and elevations of thyroid stimulating hormone.[34]

Pharmacodynamics in Renal cell Carcinoma

In RCC patients, change in blood pressure was not significantly related to PFS. A trend toward increased PFS was seen for higher systolic blood pressure at week 4 and 12, p=0.06 and 0.07, respectively.[35]

A retrospective analysis of pazopanib phase II and III trials in RCC assessed the prognostic and predictive value of plasma concentrations of cytokine and angiogenic factors.[36]
Pazopanib treated patients with high concentrations of interleukin 8 (IL8) (p=0.006), osteopontin (p=0.0004), hepatocyte growth factor (HGF) (p=0.010), and tissue inhibitor of metalloproteinases-1 (TIMP-1) (p=0.006) had shorter PFS than did those with low concentrations, while high interleukin 6 (IL6), VEGF and E-selectin concentrations were not predictive of PFS (p=0.445, 0.689 and 0.844, respectively).[36]
In the placebo treated group, higher IL6 and osteopontin were related with shorter PFS, which could suggest a relationship between progression in RCC instead of a relationship with pazopanib pharmacodynamics. [36]

Analysis of VEGF genotypes in RCC biopsies, suggested increased benefit of pazopanib compared to sunitinib for the s833061 TT, rs2010963 CC and rs699947 CC genotypes.[37] However this was based on only 19 pazopanib treated patients of which RCC nephrectomy or biopsy tissue was available.

An analysis of germline pharmacogenetic markers in peripheral blood was performed on samples of 397 patients with RCC from pazopanib phase II and III trials. Three polymorphisms in the IL8 gene and hypoxia-inducible factor 1A (HIF1A) showed a significant relation with PFS.[38] Response rate was significantly associated with polymorphisms in HIF1A, nuclear receptor subfamily 1, group I, member 2 (NR1I2) and VEGFA genes.[38] A complete overview of all relationships found for the genotypes and PFS and response rate is provided in table 1.

A randomized trial comparing pazopanib with sunitinib in RCC patients found a shorter PFS for pazopanib treated patients with a higher (>55) H-score for programmed death ligand 1 (PD-L1) in immunohistochemical stainings of tumor biopsies (15.1 versus 35.6 months, p=0.03).[39] However, since a similar effect (15.3 versus 27.8 months, p=0.03) was seen in the sunitinib arm, it

seems possible that this is a prognostic marker in RCC rather than a marker specific for pazopanib pharmacodynamics.

Dynamic contrast enhanced magnetic resonance imaging (DCE-MRI) is a modality used for imaging of tumor vasculature and angiogenesis and DCE-MRI parameters, such as K^{trans} which reflects perfusion rate and capillary permeability, have been related to treatment response of other VEGFR-inhibitors.[40] DCE-MRI was also explored as potential biomarker for PFS in a cohort of RCC patients treated with pazopanib.[41] The parameter K^{trans} was tested dichotomously (above or below the median of 0.472/min) in a survival analysis. Patients with high K^{trans} values had a longer PFS in univariate analysis (p=0.036). However, this was not significant anymore in multivariate cox regression including prognostic markers and previous treatments (p=0.83).[41]

Table 2: Pharmacokinetic parameters significantly related to pazopanib treatment efficacy and toxicity.

Relationship	Pharmacokinetic Parameter	n	Tumor Type	Value	Association	p	Reference
Efficacy	C_{max}	36	Thyroid cancer	r=–0.40†	Maximum change in tumor size ↑	0.021	[4]
	C_{min}	177	Renal Cancer	≥20.5 mg/L threshold	PFS ↑	0.0038	[21]
	C_{min}	177	Renal Cancer	≥20.5 mg/L threshold	Maximum change in tumor size ↑	<0.001	[21]
	C_{min} *	30	Advanced solid tumors	≥20.0 mg/L threshold	Maximum change in tumor size ↑	0.01	[36]
Toxicity	C_{min}	54	Renal Cancer	r=0.95‡	Blood Pressure ↑	0.0075	[21]
	C_{min}	59	Pediatric advanced solid tumors	C_{min} 38.8±11.1 versus 29.6±13.6 mg/L	Any DLT ↑	0.04	[15]
	C_{min}	38	Pediatric advanced solid tumors	C_{min} 43.7±13.3 versus 29.4±13.0 mg/L	Blood Pressure ↑	0.004	[15]
	AUC_{0-24}	29	Pediatric advanced solid tumors	r=0.595‡	DLT cycle 1 ↑	0.01	[15]

AUC_{0-24}: Area under the plasma time curve from 0 to 24 hours

C_{max}: Maximum plasma concentration (during the first cycle)

C_{min}: Minimum plasma concentration / trough level (at steady state)

DLT: Dose limiting toxicity

PFS: Progression free survival

r: Spearman's rank correlation coefficient† or correlation coefficient‡

**Mean of all available C_{min} samples*

It should be noted, that although many of the proposed biomarkers discussed above were numerically significant at the p<0.05 or even <0.01 level, many of these associations are likely to be considered statistically negligible after correction for multiple testing given the multitude of biomarkers, sampling times and endpoints tested in several of these studies. Therefore, further prospective confirmation of these proposed biomarkers is necessary before treatment of patients could be guided by these markers.

Exposure-Response Analyses

An overview of all pharmacokinetic parameters significantly related to pazopanib treatment efficacy and toxicity is provided in table 2. Most exposure-response studies have used C_{min} as PK parameter instead of AUC_{0-24}. However, for pazopanib C_{min} correlated significantly with AUC_{0-24}. Interestingly, this relation was better for the concentration exactly 24 hours after intake than the concentration just before intake of the next tablet (R^2=0.940 versus 0.596).[23]

In the phase 1 trial, 5 of the 6 RCC patients with PR or SD had a steady-state C_{min} of ≥15 mg/L, while all patients with PD as best response had a C_{min} of <15 mg/L.[11]
In a retrospective analysis of 177 RCC patients, relationships between exposure and response were explored. A threshold C_{min} of ≥20.5 mg/L was significantly related to both tumor shrinkage and PFS. Patients below the threshold had a median tumor shrinkage of 6.9% versus 37.9% for patients with pazopanib C_{min} above the threshold (p<0.001). PFS was also strongly associated with C_{min}, with patients with a pazopanib C_{min} level <20.5 mg/L having a PFS of only 19.6 weeks compared to 52.0 weeks for patients with a pazopanib C_{min} level ≥20.5 mg/L (p=0.0038).

Exposure-response relationships have also been studied in other tumor types. A post-hoc subgroup analysis in a randomized phase II study of pazopanib versus best supportive care in gastro-intestinal stromal tumor (GIST) patients, found a 4-months PFS of 42.5% in patients with a pazopanib C_{min} level <20 mg/L versus 71.1% in patients with a pazopanib C_{min} level ≥20 mg/L (n=26; p=0.17).[5]
In patients with metastatic, rapidly progressive, radioiodine-refractory differentiated thyroid cancers, pazopanib C_{max} correlated with tumor response (maximum change in tumor size, p=0.021) and was significantly higher in responders than in patients with no tumor response (p=0.009).
In a pediatric phase 1 trial in STS and advanced solid tumors, all but one patient with clinical benefit had C_{min} ≥20 mg/L, and all five patients who received therapy for a year or more had a C_{min} ≥30mg/L.[15]
Unfortunately, no pharmacokinetic samples were taken in the pivotal study of pazopanib in STS.[3] Therefore, the threshold of ≥20 mg/L was not clinically validated for STS patients.
However, a trial in advanced solid tumors found a trend towards improved tumor size reduction for (-6.01 versus +13.5%, p=0.28) and PFS (47.9 versus 11.5 weeks, p=0.06) in a subset of STS patients (n=7) for patients with an average C_{min} ≥20.0 mg/L.[42]

The same trial did find a significant relationship using the same threshold and tumor size reduction in the overall population of patients with advanced solid tumors (-6.49% versus +14.6%; n=30; p=0.01).[42]

In summary, there are multiple studies that support the use of a pazopanib C_{min} of ≥20 mg/L as a pharmacokinetic threshold for efficacy.

Exposure-Toxicity Analyses

In a retrospective analysis of exposure as a predictor of toxicity in RCC patients (n=205), the frequency of hypertension, diarrhea, hair color change, ALT elevations, stomatitis, and hand–foot syndrome increased with increasing pazopanib C_{min}. However, other adverse events such as vomiting, fatigue, nausea, dysgeusia, and rash displayed no obvious relationship with exposure.[21]

The relationship between pharmacokinetic exposure and toxicity was studied further and interestingly, the correlation between exposure and hypertension was stronger for C_{min} than for AUC_{0-24}, r^2 of 0.91 (p=0.0075) and 0.25 (p=0.23) respectively.[21]

In pediatric cancer patients, C_{min} was related to the occurrence of DLTs. Patients experiencing a DLT had a mean ±SD C_{min} of 38.8±11.1 versus only 29.6±13.6 mg/L for patients who did not (p=0.04). C_{min} was also related to grade ≥2 hypertension. Here C_{min} was 43.7±13.3 mg/L (n=11) in hypertensive compared to only 29.4±13.0 mg/mL (n=27) in normotensive patients (p=0.004). There also was a strong association between AUC_{0-24} and the occurrence of DLTs in cycle 1. (n=29; r=0.595; p=0.001).[15]

A randomized, double-blind, placebo-controlled trial comparing pazopanib to placebo and moxifloxacin (as positive control) did not find an effect of pazopanib or its metabolites on the QTcF interval.[43]

In the registration trials, the probability of grade ≥3 ALT elevation has been reported to increase with higher pazopanib C_{min}.[8] However, a recent study suggested that the mechanism of this hepatotoxicity may be related to genetic mutations in the human leukocyte antigen (HLA), specifically with the HLA-B*57:01 genotype. It may therefore be the case that hepatotoxicity is mediated by an immunological reaction which would most likely be unrelated to pazopanib exposure or dose.[44]

Pazopanib related ALT-elevations have also been shown to be associated to the rs2858996 and rs707889 polymorphisms in the hemochromatosis HFE-gene.[45] Moreover, the risk of ALT-elevations in cancer patients treated with pazopanib was shown to be higher in those patients who concomitantly used simvastatin.[46]

Interestingly, case reports show that administration of a starting dose of 30 mg prednisolone (which is subsequently slowly tapered down) is a promising treatment strategy for pazopanib related transaminase elevations.[47] The suggestion that immunosuppressive drugs are effective

in treating this form of toxicity further support the hypothesis that this drug-induced liver injury is immunologically mediated.

Population Pharmacokinetic & Pharmacodynamic Studies

Several pharmacometric models have been developed for pazopanib to date. Two models focused on tumor growth kinetics and two on pharmacokinetic modelling.
The first tumor growth model quantified the effect of pazopanib in clinical data from phase II (n=220) and phase III studies (n=423). This study quantified the tumor inhibition of pazopanib using a modified Wang model and identified prognostic markers (including prior radiotherapy, baseline tumor size, tumor shrinkage rate and tumor regrowth rate) as predictors for the formation of new lesions.[48]
The second tumor growth model used both preclinical and clinical (n=47) data. This semi-mechanistic model also described the role of tumor vasculature (based on preclinical experiments) in tumor growth and shrinkage. This study suggested the antitumor effect of pazopanib might be comprized of two separate mechanisms, the first a direct cytotoxic effect and the second a slower antiangiogenic effect.[49]

At present, two model-based pharmacokinetic studies have been reported.
The first is a one-compartment model with first-order absorption and elimination based pharmacokinetic data obtained from a phase I study of pazopanib in combination with bevacizumab (n=15).[50] Co-administration of bevacizumab did not influence pazopanib C_{min}. Inter-individual variability in this study was quantified at 40% and an inter-occasion variability at 27%. However, in these 15 patients, no significant relationships were found between measures of exposure and either DLTs or treatment response (measured by RECIST 1.1).[50]

The second population pharmacokinetic model was based on a larger data set from three clinical studies (n=96).[51] The pH-limited solubility of pazopanib[8] was best described by a two-phase first-order absorption.[51]
To account for the non-linear F, a relative bioavailability parameter (rF) was introduced as a function of dose (rFd) and of time (rFt). rFd was set at 1 for the (lowest) 200 mg dose and decreased in an E_{max} manner. The influence of time on rFt was best described by an first-order decay. [51]
Simulation studies were performed to quantify the effect of time on pazopanib pharmacokinetics. When comparing exposure in week 2 to week 4, both the C_{min} and AUC dropped by 11 %. A decrease in exposure has also been reported for other tyrosine kinase inhibitors such as imatinib.[52] The mechanism behind this effect is unclear.[53] For pazopanib it is hypothesized that this reduced exposure could be caused by auto-induction of CYP3A4 as it has been reported that pazopanib

induces CYP3A4 *in vitro* through an interaction with the human pregnane X receptor,[8,51] but this theory has not yet been confirmed in clinical studies.

Simulations also indicated that the non-linear F could be leveraged to increase C_{min} in low exposure patients, by switching from a once to a twice daily dosing (BID) regimen. At steady state, C_{min} on the 400 mg BID dose level was 75 % higher at the 800 mg QD dose level, 39 compared to 22 mg/L, respectively. AUC increased by 59 % from 665 to 1056 mg*h/L by switching from 800 QD to 400 mg BID.[51]

This strategy of splitting intake moments, has the advantage of increasing exposure without increasing the overall daily dose and cost of therapy. However, future prospective clinical trials are needed to confirm this hypothesis, before such a strategy can be implemented.

Individualizing Pazopanib Therapy

Several studies have identified pharmacokinetic and pharmacodynamic biomarkers for pazopanib treatment efficacy in cancer patients (tables 1 and 2).

Moreover, it has been shown that at the currently approved dose of 800 mg QD, approximately 20% of patients do not reach the pharmacokinetic threshold of C_{min} ≥20 mg/L and are therefore at risk of suboptimal efficacy.[21] Furthermore, intrapatient variability in pharmacokinetics (25-27%)[23,50] was markedly smaller than interpatient variability (67-72%)[11,42].

Because of this, two clinical trials have investigated individualized pharmacokinetically-guided dosing of pazopanib in cancer patients.[23,42]

The first was a study in advanced solid tumors (n=13) and used an AUC_{0-24h} range of 715 to 920 mg*h/L as the pharmacokinetic target and set a reduction in variability as the primary endpoint.[23] All patients were treated for 3 consecutive periods of 2 weeks. In the first period, all patients received 800 mg pazopanib once daily to reach steady-state exposure. In the second, patients either received a PK-guided dose or the fixed 800 mg dose. During the last period, the regimens were switched.

AUC-guided dosing did not significantly reduce inter-patient variability in this trial. Interpatient variability in C_{min} was 36.9% and 31.9% in the AUC-guided and fixed-dose arm respectively. In the AUC-guided dosing arm 53.9% of patients and in the fixed dosing arm 46.2% of patients achieved the target exposure. Based on these results the authors concluded that it might be more beneficial to target the C_{min} threshold rather than an AUC range.

The second study was a prospective trial in 30 patients with advanced solid tumors. It set C_{min} ≥20.0 mg/L as target exposure.[42] At weeks 3, 5, and 7, the pazopanib dose was increased if C_{min} was <20.0 mg/L. Patients with a C_{min} <15.0 mg/L received a dose increase of 400 mg in the absence of grade ≥2 toxicity or 200 mg when experiencing grade 2 toxicity. Patients with a C_{min} of 15.0 to 19.9 mg/L received a 200 mg dose increase if toxicity was below grade 3. No patients would be treated above the prespecified limit of 2000 mg QD. The dose would be reduced in case of grade ≥3 toxicity. This dosing algorithm led to patients being treated at dosages ranging from 400 to 1800 mg daily.

Mean C_{min} in patients whose dose was successfully increased above 800 mg (n=10) rose significantly from only 13.2 to 22.9 mg/L (above the pre-specified target of ≥20 mg/L). Patients with a high C_{min} who experienced ≥ grade 3 toxicity (n=9) and required a dose reduction initially had a mean C_{min} 51.3 mg/L, but even after subsequent dose reductions, mean C_{min} was still above the >20 mg/L target at 28.2 mg/L.[42]

The overall variability in C_{min} was reduced from 71.9% on the fixed dose schedule (week 2) to 33.9% (week 8) after applying the pharmacokinetically-guided dosing algorithm.

This trial demonstrated the feasibility of individualized C_{min}-guided dosing. Future prospective clinical trials to validate this dosing strategy on clinically relevant endpoints are warranted.

Furthermore given its evident exposure-response relationship, pazopanib C_{min} monitoring in routine care is already of clear importance in specific clinical situations, such as hepatic impairment,[54] or co-administration of PPIs or CYP3A4-inhibitors/inducers[29].

To facilitate pharmacokinetic monitoring of pazopanib in routine care, dried blood spot sampling could be used as a less invasive alternative to venous blood sampling. Multiple validated bioanalytical assays are already available for this purpose.[55,56]

Conclusions

In conclusion, we provide an overview of the complex pharmacokinetic and pharmacodynamic profile of pazopanib. We critically reviewed the published (population) pharmacokinetic and pharmacodynamic data on pazopanib in patients and special patient populations.

The pharmacokinetics of pazopanib are described by a low, non-linear and time-dependent bioavailability and large interpatient variability.

A multitude of pharmacokinetic and pharmacodynamic biomarkers has been proposed for pazopanib, but only AUC and C_{min} have been studied prospectively to individualize treatment.

There are opportunities to optimize pazopanib dosing through monitoring of C_{min} and by switching to BID dosing in selected patients. These strategies hold promise to optimize pazopanib dose selection and individualization and improve treatment outcomes for cancer patients.

Disclosures

Dr. N. Steeghs received an unrestricted grant (funding and study medication) from GlaxoSmithKline as Principal Investigator for an investigator initiated study with Pazopanib. Pazopanib is an asset of Novartis as of June 2015.

The other authors declare they have no conflicts of interest to disclose.

References

1. Kumar R, Knick VB, Rudolph SK, Johnson JH, Crosby RM, Crouthamel M-C, et al. Pharmacokinetic-pharmacodynamic correlation from mouse to human with pazopanib, a multikinase angiogenesis inhibitor with potent antitumor and antiangiogenic activity. Mol. Cancer Ther. 2007;6:2012–21.
2. Sternberg CN, Davis ID, Mardiak J, Szczylik C, Lee E, Wagstaff J, et al. Pazopanib in locally advanced or metastatic renal cell carcinoma: Results of a randomized phase III trial. J. Clin. Oncol. 2010;28:1061–8.
3. van der Graaf WT, Blay JY, Chawla SP, Kim DW, Bui-Nguyen B, Casali PG, et al. Pazopanib for metastatic soft-tissue sarcoma (PALETTE): a randomised, double-blind, placebo-controlled phase 3 trial. Lancet. 2012;379:1879–86.
4. Bible KC, Suman VJ, Molina JR, Smallridge RC, Maples WJ, Menefee ME, et al. Efficacy of pazopanib in progressive, radioiodine-refractory, metastatic differentiated thyroid cancers: Results of a phase 2 consortium study. Lancet Oncol. Elsevier Ltd; 2010;11:962–72.
5. Mir O, Cropet C, Toulmonde M, Cesne A Le, Molimard M, Bompas E, et al. Pazopanib plus best supportive care versus best supportive care alone in advanced gastrointestinal stromal tumours resistant to imatinib and sunitinib (PAZOGIST): A randomised, multicentre, open-label phase 2 trial. Lancet Oncol. 2016;17:632–41.
6. du Bois A, Floquet A, Kim J-W, Rau J, del Campo JM, Friedlander M, et al. Incorporation of pazopanib in maintenance therapy of ovarian cancer. J. Clin. Oncol. 2014;32:3374–82.
7. Harris P, Boloor A, Cheung M, Kumar R, Crosby RM, Davis-Ward RG, et al. Discovery of 5-[[4-[(2,3-dimethyl-2H-indazol-6-yl) methylamino]-2-pyrimidinyl]amino]-2-methyl-benzenesulfonamide (Pazopanib), a novel and potent vascular endothelial growth factor receptor inhibitor. J. Med. Chem. 2008;51:4632–40.
8. Food and Drug Administration. Center for Drug Evaluation and Research. Pazopanib Clinical Pharmacology and Biopharmaceutics Review. 2008; Available from: http://www.accessdata.fda.gov/drugsatfda_docs/nda/2009/022465s000_ClinPharmR.pdf
9. Hanahan D, Weinberg RA. Hallmarks of cancer: The next generation. Cell. Elsevier Inc.; 2011;144:646–74.
10. Ellis LM, Hicklin DJ. VEGF-targeted therapy: mechanisms of anti-tumour activity. Nat. Rev. Cancer. 2008;8:579–91.
11. Hurwitz HI, Dowlati A, Saini S, Savage S, Suttle AB, Gibson DM, et al. Phase I trial of pazopanib in patients with advanced cancer. Clin. Cancer Res. 2009;15:4220–7.
12. Heath EI, Forman K, Malburg L, Gainer S, Suttle AB, Adams L, et al. A phase i pharmacokinetic and safety evaluation of oral pazopanib dosing administered as crushed tablet or oral suspension in patients with advanced solid tumors. Invest. New Drugs. 2012;30:1566–74.
13. Imbs DC, Paludetto MN, Négrier S, Powell H, Lafont T, White-Koning M, et al. Determination of unbound fraction of pazopanib in vitro and in cancer patients reveals albumin as the main binding site. Invest. New Drugs. 2016;34:41–8.
14. Deng Y, Sychterz C, Suttle AB, Dar MM, Bershas D, Negash K, et al. Bioavailability, metabolism and disposition of oral pazopanib in patients with advanced cancer. Xenobiotica. 2013;43:443–53.
15. Glade Bender JL, Lee A, Reid JM, Baruchel S, Roberts T, Voss SD, et al. Phase I pharmacokinetic and pharmacodynamic study of pazopanib in children with soft tissue sarcoma and other refractory solid tumors: a children's oncology group phase I consortium report. J. Clin. Oncol. 2013;31:3034–43.
16. Shetty A V., Matrana MR, Atkinson BJ, Flaherty AL, Jonasch E, Tannir NM. Outcomes of patients with metastatic renal cell carcinoma and end-stage renal disease receiving dialysis and targeted therapies: A single institution experience. Clin. Genitourin. Cancer. Elsevier Inc; 2014;12:348–53.
17. Czarnecka AM, Kawecki M, Lian F, Korniluk J, Szczylik C. Feasibility, efficacy and safety of tyrosine kinase inhibitor treatment in hemodialyzed patients with renal cell cancer: 10 years of experience. Futur. Oncol. 2015;11:2267–82.
18. Bersanelli M, Facchinetti F, Tiseo M, Maiorana M, Buti S. Pazopanib in Renal Cell Carcinoma Dialysis Patients: a Mini-Review and a Case Report. Curr. Drug Targets. 2016;
19. Committee for Medicinal Products for Human Use (CHMP) European Medicines Agency.

Pazopanib Summary of Product Characteristics. 2013;

20. Shibata SI, Chung V, Synold TW, Longmate JA, Suttle AB, Ottesen LH, et al. Phase i study of pazopanib in patients with advanced solid tumors and hepatic dysfunction: A national cancer institute organ dysfunction working group study. Clin. Cancer Res. 2013;19:3631–9.
21. Suttle AB, Ball H, Molimard M, Hutson T, Carpenter C, Rajagopalan D, et al. Relationships between pazopanib exposure and clinical safety and efficacy in patients with advanced renal cell carcinoma. Br. J. Cancer. Nature Publishing Group; 2014;111:1–8.
22. Heath EI, Chiorean EG, Sweeney CJ, Hodge JP, Lager JJ, Forman K, et al. A phase I study of the pharmacokinetic and safety profiles of oral pazopanib with a high-fat or low-fat meal in patients with advanced solid tumors. Clin Pharmacol Ther. Nature Publishing Group; 2010;88:818–23.
23. de Wit D, van Erp NP, den Hartigh J, Wolterbeek R, den Hollander-van Deursen M, Labots M, et al. Therapeutic Drug Monitoring to individualize the dosing of pazopanib: a pharmacokinetic feasibility study. Ther. Drug Monit. 2014;37:331–8.
24. Hamberg P, Boers-Sonderen MJ, van der Graaf WTA, de Bruijn P, Suttle AB, Eskens FALM, et al. Pazopanib exposure decreases as a result of an ifosfamide-dependent drug-drug interaction: results of a phase I study. Br. J. Cancer. Nature Publishing Group; 2014;110:888–93.
25. Imbs DC, Diéras V, Bachelot T, Campone M, Isambert N, Joly F, et al. Pharmacokinetic interaction between pazopanib and cisplatin regimen. Cancer Chemother. Pharmacol. Springer Berlin Heidelberg; 2016;77:385–92.
26. Sridhar SS, Joshua AM, Gregg R, Booth CM, Murray N, Golubovic J, et al. A phase II study of GW786034 (Pazopanib) with or without bicalutamide in patients with castration-resistant prostate cancer. Clin. Genitourin. Cancer. Elsevier Inc; 2015;13:124–9.
27. Monk BJ, Lopez LM, Zarba JJ, Oaknin A, Tarpin C, Termrungruanglert W, et al. Phase II, open-label study of pazopanib or lapatinib monotherapy compared with pazopanib plus lapatinib combination therapy in patients with advanced and recurrent cervical cancer. J. Clin. Oncol. 2010;28:3562–9.
28. Goh BC, Reddy NJ, Dandamudi UB, Laubscher KH, Peckham T, Hodge JP, et al. An evaluation of the drug interaction potential of pazopanib, an oral vascular endothelial growth factor receptor tyrosine kinase inhibitor, using a modified Cooperstown 5+1 cocktail in patients with advanced solid tumors. Clin. Pharmacol. Ther. 2010;88:652–9.
29. Tan AR, Gibbon DG, Stein MN, Lindquist D, Edenfield JW, Martin JC, et al. Effects of ketoconazole and esomeprazole on the pharmacokinetics of pazopanib in patients with solid tumors. Cancer Chemother. Pharmacol. 2013;71:1635–43.
30. Warrington S, Baisley K, Boyce M, Tejura B, Morocutti A, Miller N. Effects of rabeprazole, 20 mg, or esomeprazole, 20 mg, on 24-h intragastric pH and serum gastrin in healthy subjects. Aliment. Pharmacol. Ther. 2002;16:1301–7.
31. Murukesh N, Dive C, Jayson GC. Biomarkers of angiogenesis and their role in the development of VEGF inhibitors. Br. J. Cancer [Internet]. Nature Publishing Group; 2010;102:8–18. Available from: http://www.pubmedcentral.nih.gov/articlerender.fcgi?artid=2813747&tool=pmcentrez&rendertype=abstract
32. Zhong J, Ali AN, Voloschin AD, Liu Y, Curran WJ, Crocker IR, et al. Bevacizumab-induced hypertension is a predictive marker for improved outcomes in patients with recurrent glioblastoma treated with bevacizumab. Cancer. 2015;121:1456–62.
33. Duffaud F, Sleijfer S, Litière S, Ray-Coquard I, Le Cesne A, Papai Z, et al. Hypertension (HTN) as a potential biomarker of efficacy in pazopanib-treated patients with advanced non-adipocytic soft tissue sarcoma. A retrospective study based on European Organisation for Research and Treatment of Cancer (EORTC) 62043 and 62072 trial. Eur. J. Cancer. 2015;51:2615–23.
34. Sleijfer S, Gorlia T, Lamers C, Burger H, Blay J-Y, Le Cesne A, et al. Cytokine and angiogenic factors associated with efficacy and toxicity of pazopanib in advanced soft-tissue sarcoma: an EORTC-STBSG study. Br. J. Cancer. Nature Publishing Group; 2012;107:639–45.
35. Goldstein D, Rosenberg JE, Figlin RA, Townsend RR, Mccann L, Carpenter C, et al. Is change in blood pressure a biomarker of pazopanib and sunitinib efficacy in advanced / metastatic renal cell carcinoma ? 2016;53:96–104.

36. Tran HT, Liu Y, Zurita AJ, Lin Y, Baker-Neblett KL, Martin AM, et al. Prognostic or predictive plasma cytokines and angiogenic factors for patients treated with pazopanib for metastatic renal-cell cancer: A retrospective analysis of phase 2 and phase 3 trials. Lancet Oncol. Elsevier Ltd; 2012;13:827–37.

37. Bianconi M, Faloppi L, Loretelli C, Zizzi A, Bittoni A, Andrikou K, et al. Angiogenesis genotyping in the selection of first-line treatment with either sunitinib or pazopanib for advanced renal cell carcinoma. Oncotarget. 2016;7:37599–607.

38. Xu CF, Bing NX, Ball HA, Rajagopalan D, Sternberg CN, Hutson TE, et al. Pazopanib efficacy in renal cell carcinoma: Evidence for predictive genetic markers in angiogenesis-related and exposure-related genes. J. Clin. Oncol. 2011;29:2557–64.

39. Choueiri TK, Figueroa DJ, Fay AP, Signoretti S, Liu Y, Gagnon R, et al. Correlation of PD-L1 tumor expression and treatment outcomes in patients with renal cell carcinoma receiving sunitinib or pazopanib: Results from COMPARZ, a randomized controlled trial. Clin. Cancer Res. 2015;21:1071–7.

40. Hahn OM, Yang C, Medved M, Karczmar G, Kistner E, Karrison T, et al. Dynamic contrast-enhanced magnetic resonance imaging pharmacodynamic biomarker study of sorafenib in metastatic renal carcinoma. J. Clin. Oncol. 2008;26:4572–8.

41. Sweis RF, Medved M, Towey S, Karczmar GS, Oto A, Szmulewitz RZ, et al. Dynamic Contrast-Enhanced Magnetic Resonance Imaging as a Pharmacodynamic Biomarker for Pazopanib in Metastatic Renal Carcinoma. Clin. Genitourin. Cancer. Elsevier Inc.; 2016;1–6.

42. Verheijen RB, Bins S, Mathijssen RHJ, Lolkema MP, van Doorn L, Schellens JHM, et al. Individualized Pazopanib Dosing: A Prospective Feasibility Study in Cancer Patients. Clin. Cancer Res. 2016;22:5738–46.

43. Heath EI, Infante J, Lewis LD, Luu T, Stephenson J, Tan AR, et al. A randomized, double-blind, placebo-controlled study to evaluate the effect of repeated oral doses of pazopanib on cardiac conduction in patients with solid tumors. Cancer Chemother. Pharmacol. 2013;71:565–73.

44. Xu C-F, Johnson T, Wang X, Carpenter C, Graves A, Warren L, et al. HLA-B*57:01 Confers Susceptibility to Pazopanib-Associated Liver Injury in Patients With Cancer. Clin. Cancer Res. 2015;

45. Xu CF, Reck BH, Goodman VL, Xue Z, Huang L, Barnes MR, et al. Association of the hemochromatosis gene with pazopanib-induced transaminase elevation in renal cell carcinoma. J. Hepatol. European Association for the Study of the Liver; 2011;54:1237–43.

46. Xu CF, Xue Z, Bing N, King KS, Mccann LA, De souza PL, et al. Concomitant use of pazopanib and simvastatin increases the risk of transaminase elevations in patients with cancer. Ann. Oncol. 2012;23:2470–1.

47. Vlenterie M, van Erp NP, van der Graaf WT a. Promising management of pazopanib-induced liver toxicity. Acta Oncol. (Madr). 2015;54:7:1–3.

48. Bonate PL, Suttle AB. Modeling tumor growth kinetics after treatment with pazopanib or placebo in patients with renal cell carcinoma. Cancer Chemother. Pharmacol. 2013;72:231–40.

49. Ouerdani A, Struemper H, Suttle A, Ouellet D, Ribba B. Preclinical Modeling of Tumor Growth and Angiogenesis Inhibition to Describe Pazopanib Clinical Effects in Renal Cell Carcinoma. CPT Pharmacometrics Syst. Pharmacol. 2015;4:660–8.

50. Imbs DC, Négrier S, Cassier P, Hollebecque A, Varga A, Blanc E, et al. Pharmacokinetics of pazopanib administered in combination with bevacizumab. Cancer Chemother. Pharmacol. 2014;73:1189–96.

51. Yu H, van Erp N, Bins S, Mathijssen RHJ, Schellens JHM, Beijnen JH, et al. Development of a Pharmacokinetic Model to Describe the Complex Pharmacokinetics of Pazopanib in Cancer Patients. Clin. Pharmacokinet. 2016;

52. Eechoute K, Fransson MN, Reyners AK, de Jong F a, Sparreboom A, van der Graaf WT a, et al. A long-term prospective population pharmacokinetic study on imatinib plasma concentrations in GIST patients. Clin. Cancer Res. 2012;18:5780–7.

53. Bins S, Eechoute K, Kloth JSL, de Man FM, Oosten AW, de Bruijn P, et al. Prospective Analysis in GIST Patients on the Role of Alpha-1 Acid Glycoprotein in Imatinib Exposure. Clin. Pharmacokinet. Springer International Publishing; 2016;1–6.

54. Yau T, Chen PJ, Chan P, Curtis CM, Murphy PS, Suttle AB, et al. Phase I dose-finding study of pazopanib in hepatocellular carcinoma: Evaluation of early efficacy, pharmacokinetics, and pharmacodynamics. Clin. Cancer Res. 2011;17:6914–23.

55. Verheijen RB, Bins S, Thijssen B, Rosing H, Nan L, Schellens JH, et al. Development and clinical validation of an LC – MS / MS method for the quantification of pazopanib in DBS. Bioanalysis. 2016;369–74.

56. de Wit, D, den hartigh, J, Gelderdblom, H, Qian, Y, den Hollander, M, Verheul, H, Guchelaar, HJ, van Erp N. Dried blood spot analysis for therapeutic drug monitoring of pazopanib. J. Clin. Pharmacol. 2015;doi: 10.1002/jcph.558. [Epub ahead of print].

Chapter 2.2

Fast and Straightforward Method for the Quantification of Pazopanib in Human Plasma Using LC-MS/MS

Remy B. Verheijen[1], Bas Thijssen[1], Hilde Rosing[1], Jan H.M. Schellens[2,3], Lianda Nan[1], Nikkie Venekamp[1], Jos H. Beijnen[1,3], Neeltje Steeghs[2], Alwin D.R. Huitema[1,4]

[1]Department of Pharmacy & Pharmacology, The Netherlands Cancer Institute - Antoni van Leeuwenhoek, Plesmanlaan 121, 1066 CX, Amsterdam, The Netherlands.
[2]Department of Medical Oncology and Clinical Pharmacology, The Netherlands Cancer Institute - Antoni van Leeuwenhoek, Amsterdam, Amsterdam, The Netherlands.
[3]Department of Pharmaceutical Sciences, Utrecht University, Utrecht, The Netherlands.
[4]Department of Clinical Pharmacy, Utrecht University Medical Center, Utrecht, The Netherlands

Abstract

Background: Pazopanib is an angiogenesis inhibitor approved for renal cell carcinoma and soft tissue sarcoma. Studies indicate that treatment with pazopanib could be optimized by adapting the dose based on measured pazopanib plasma concentrations.

Methods: This study describes the validation and clinical application of a fast and straightforward method for the quantification of pazopanib in human plasma for the purpose of therapeutic drug monitoring and bioanalytical support of clinical trials.

Stable isotopically labeled $^{13}C,^{2}H_3$-pazopanib was used as internal standard. Plasma samples were prepared for analysis by protein precipitation using methanol and diluted with 10 mM ammonium hydroxide buffer. Chromatographic separation was performed on a C18 column using isocratic elution with ammonium hydroxide in water and methanol. For detection an tandem mass spectrometer, equipped with a turbo ionspray interface was used in positive ion mode at *m/z* 438 → *m/z* 357 for pazopanib and *m/z* 442 → *m/z* 361 for the internal standard.

Results: All validated parameters were within pre-established limits and fulfilled the FDA and EMA requirements for bioanalytical method validation. Final runtime was 2.5 minutes. After completion of the validation, the routine application of the method was tested by analyzing clinical study samples which were collected for the purpose of therapeutic drug monitoring.

Conclusions: In conclusion, the described method was successfully validated and was found to be robust for routine application to analyze samples from cancer patients treated with pazopanib.

Introduction

Pazopanib is a potent and selective multi-targeted receptor tyrosine kinase inhibitor of the vascular endothelial growth factor receptor 1 (VEGFR-1), VEGFR-2, VEGFR-3, Platelet derived growth factor receptor α and β, and c-kit.[1] Through blocking the kinase activity of these receptors, pazopanib blocks tumor growth and inhibits angiogenesis [2]. Pazopanib is currently approved by the Food and Drug Administration (FDA) and European Medicines Agency (EMA) for the treatment of renal cell carcinoma (RCC) and soft tissue sarcoma (STS) [3,4]. A retrospective analysis showed increased tumor shrinkage and longer median progression free survival in patients with pazopanib plasma trough concentrations ≥20.5 μg/mL compared to patients with lower concentrations (52.0 weeks vs. 19.6 weeks) [5].

Pazopanib pharmacokinetics show large inter-individual variability in plasma concentrations. This results in a subset of patients at risk of receiving less than optimal exposure [6–9]. In routine clinical care this variability may be even greater as these patients are not selected and are likely to have more comorbidities and concomitant medication, may be older, may have impaired renal or hepatic function and may have suboptimal therapy adherence.

The factors above may influence pazopanib pharmacokinetics, for example absorption of pazopanib depends on gastric acidity and intake with food [10] and it is a substrate for various CYP isoenzymes which may be inhibited by concomitant medication and subject to genetic polymorphisms [11].

Based on the observations above, a prospective study in cancer patients was conducted to study pazopanib dose individualization based on plasma trough concentrations.[12] This trial found that individualized pazopanib dosing was feasible, safe and lead to more patients reaching an adequate pharmacokinetic exposure. Therefore, measurement pazopanib plasma concentrations in routine care, also known as therapeutic drug monitoring, could be an effective way to estimate the influence of all these factors and assess if patients would require therapy adjustments based on suboptimal exposure.

Previously, methods for the quantification of pazopanib in plasma have been reported [13,14]. However, these methods were only validated for mouse plasma and tissue or suffered from long run time (7 minutes per sample) due to the large number of analytes, making them suboptimal for application to routine (e.g. weekly) therapeutic drug monitoring measurements in cancer patients.

We describe the development, validation and clinical application of a fast and straightforward liquid chromatography tandem mass spectrometry (LC-MS/MS) method for the quantification of pazopanib in human plasma specifically designed for the purpose of therapeutic drug monitoring and bioanalytical support of clinical trials.

Materials & Methods

Chemicals

Pazopanib (as hydrochloride) and stable isotopically labeled internal standard (IS) $^{13}C,^{2}H_3$-pazopanib were supplied by GlaxoSmithKline (Zeist, The Netherlands). Dimethyl sulfoxide (DMSO) was purchased from Merck (Darmstadt, Germany), ammonia (Empure® 25%) and methanol (HPLC grade) from BioSolve Ltd (Valkenswaard, The Netherlands). Control human EDTA-plasma was obtained from healthy volunteers and used for preparation of quality control samples (QC), calibration standards and matrix blanks.

Stock solutions, calibration standards and quality control samples

Stock solutions of pazopanib were prepared in DMSO at a concentration of 2 mg/mL. Working solutions were prepared by diluting stock solutions with methanol. The IS stock solution was prepared in methanol at a concentration of 1 mg/mL. The IS working solution was prepared by further dilution with methanol to a concentration of 0.1 µg /mL. All stock and working solutions were stored at -20 °C, except for the IS working solution which was stored at 2 – 8 °C.

Calibration standards and QC samples were prepared by addition of an 10 µL aliquot of working solution to 190 µL of control plasma. Concentrations of 1.00, 3.00, 15.0 and 37.5 µg/mL were used for the QC samples (lower limit of quantification (LLOQ), Low, Mid and High concentrations respectively). The concentrations for the calibration standards were: 1.00, 2.00, 5.00, 10.0, 20.0, 30.0, 40.0 and 50.0 µg/mL.

Table 1: Optimized Mass Spectrometer Settings

Parameter	Value
Nebulizer gas	7 a.u.
Turbo gas	7 L/min
Curtian gas	15 a.u.
Collision gas	10 a.u.
Ion spray voltage	3000 V
Ionization temperature	400 ^{0}C
Dwell time	200 ms
Declustering Potential	41 V
Collision Energy	57 V
Collision Cell Exit Potential	18 V
Entrance Potential	10 V

a.u.: arbitrary units.

Liquid chromatography tandem mass spectrometry

All LC-MS/MS experiments were performed using an 1100 series binary pump, degasser, column oven and autosampler from Agilent Technologies (Santa Clara, CA, United USA) and an API3000 triple quadrupole equipped with Turbo ionspray interface, and Analyst™ software was used for data analysis (Sciex Framigham, MA, USA). Mass transitions of precursor and product ions, fragmentor voltage, nebulizer, tubro, curtain and collision gases, ion spray voltage, ionization temperature, declustering potential, collision energy, collision cell exit and entrance potential were optimized. An overview of the optimized mass spectrometer settings is provided in **table 1**.

Quantification was performed in positive ion mode using the *m/z* 438 → *m/z* 357 transition for pazopanib and *m/z* 442 → m/z 361 for $^{13}C,^{2}H_3$-pazopanib. Proposed fragmentation patterns of these transitions are provided in **figure 1**.

Separation was performed on Gemini C18 Column, 50 x 2.0 mm ID, 5 µm particle size with a Gemini SecurityGuard, 4.0 x 2.0 mm ID guard column by Phenomenex (Torrance, CA, USA) using an 0.2 µm in-line filter.

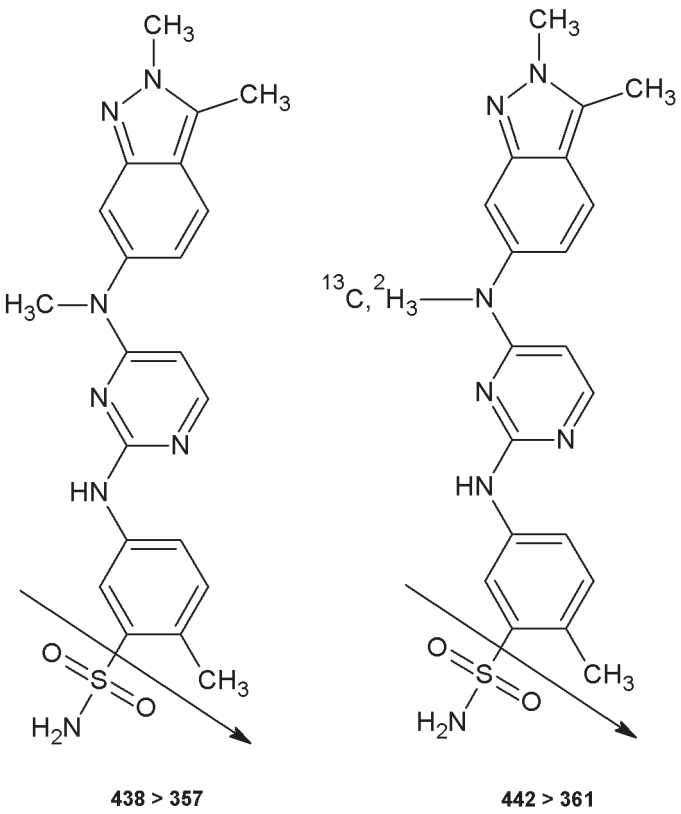

Figure 1: Chemical structures of pazopanib (left) and $^{13}C,^{2}H_3$-pazopanib (right), including the proposed fragmentation patterns (m/z 438 → 357 and 442 → 361, respectively).

The column oven was set at 55 °C and the tray temperature of the autosampler at 5 °C. Isocratic elution was achieved using a mixture of 10 mM ammonium hydroxide in water and 1 mM ammonium hydroxide in methanol (45:55, v/v) at flow of 0.4 mL/min. The total runtime was 2.5 minutes.

Sample preparation

A 10 µL aliquot of plasma was transferred to an eppendorf tube of 1.5 mL. A total of 500 µL of methanol containing 0.1 µg/mL IS was added and the sample was vortex mixed. The corresponding IS concentration is thus 5.00 µg per mL of plasma. Hereafter, 500 µL of 10 mM ammonium hydroxide in water was added. The samples were briefly mixed and centrifuged for 5 minutes at 15,000 rpm. Then 800 µL of the clear supernatant was transferred to an autosampler vial and 5 µL was injected into the LC-MS/MS system.

Validation

The method was validated in accordance with FDA and EMA guidelines for bioanalytical method validation [15,16].

The following validation parameters were assessed: calibration model, accuracy and precision, LLOQ, dilution integrity, selectivity, instrument carry-over, matrix factor and recovery. Furthermore, the stability of pazopanib was studied in various matrices.

Calibration

Weighted linear regression (1/concentration) was applied to fit the calibration plots (area ratio vs concentration). At least 75% of the non-zero standards (including at least one LLOQ and upper limit of quantification (ULOQ)) in each run had to be within ±15% of the nominal value (±20% for the LLOQ). For the LLOQ and ULOQ level at least 50% should meet these criteria. The regression coefficient was calculated for each analytical run.

Accuracy and precision

The assays accuracy and precision were determined in three separate validation runs by injecting five replicates of QC samples at the LLOQ, Low, Mid and High concentrations. Intra-run and overall accuracy was expressed as the bias in %, The intra-run and overall precision were calculated as the coefficient of variation (CV) in %. At each concentration level, the bias had to be within ±15% and the precision is not allowed to exceed 15%. For the LLOQ concentrations level bias had to be within ±20% and the precision would not allowed to exceed 20%.

LLOQ

The LLOQ of the method was evaluated in each analytical run. It was quantified as the ratio of the peak height of the 1.00 µg/mL calibration standard (the signal) to the peak height of a double blank sample (the noise). A predefined limit of ≥5 was set for this ratio.

Dilution integrity

The dilution integrity was studied by analyzing five replicate samples at concentration of 100 µg/mL. These were diluted 20 times with blank EDTA-plasma (10 µL sample plus 190 µL matrix) and compared with the nominal concentration. Predefined limits for bias and precision were set at ±15% and ≤15% respectively.

Selectivity

The selectivity of the assay was determined for Cross analyte/IS interference. The internal standard interference was assessed by analyzing a pazopanib ULOQ sample without adding the IS and by spiking IS separately to a double blank sample at the concentration used in the assay.

The possibility of endogenous interferences was assessed by analyzing double blank samples from six different individuals and comparing the peak area in the blank with the peak area of the LLOQ in the same analytical run.

The endogenous and IS interferences were considered acceptable if it was less than or equal to 20% of the response of the LLOQ of the analyte and less than or equal to 5% of the response of the IS.

Carry-over

The instrumentation carry-over was tested by injecting two double blank samples after an ULOQ sample in each validation run. The carry-over was calculated as the ratio (in %) of the peak area in the blanks and the peak area of the LLOQ. The carry-over was considered acceptable if the response at the retention time of the analyte (for both pazopanib and the IS) was less than or equal to 20% of the response of the LLOQ in the first blank.

Matrix factor

The matrix factor (MF) was determined in six different batches of plasma spiked at both the QC Low and QC High concentration. The MF was calculated by dividing the pazopanib and IS peak area in presence of matrix by the peak area ratio at the same concentration in a neat solution. The IS-normalized MF was calculated for six different batches of control human plasma and the IS-normalized MF was considered acceptable if the coefficient of variation was less than or equal to 15%.

Sample pretreatment recovery

The pazopanib recovery was determined by dividing the peak area of pazopanib in processed validation samples at QC low and high concentrations (n=5) by the peak area of pazopanib in presence of matrix (a double blank sample to which pazopanib was spiked after processing). No specific requirement for recovery was predefined except that it should be reproducible.

Stability

The stability of pazopanib in processed samples (final extract) was determined after being stored at nominally 2 – 8 °C. The stability in plasma samples was assessed at ambient temperatures and at -20 °C. All these stability analyses were carried out in triplicate at the QC Low and High concentrations. Samples were considered to be stable if the measured concentration was within ±15% of the nominal concentration. Stability of pazopanib in DSMO (stock) and methanol (working solutions) was studied (also in triplicate) at concentrations of 2 mg/mL and 300 µg/mL respectively. For these solutions the limit for the deviation was set at within ±5%.

Clinical application

The described method was used to support pharmacokinetic analyses in a clinical trial where pazopanib trough samples were collected (trial registry identifier: NTR3967)[12]. This trial was conducted in accordance with the World Medical Organization declaration of Helsinki, compliant with Good Clinical Practice and approved by the Medical Ethics Committee of each of the participating medical centers. All patients provided written informed consent before enrollment.

Table 2: Summary of validation results. All tested parameters met their predefined criteria (predefined acceptance criteria are reported in text).

Parameter	Result
Calibration model	Weighted (1/x) linear regression, coefficients all >0.99
Calibration range	1.00 to 50.0 µg/mL
Intra-run accuracy (%)	±19.2% (LLOQ) ±4.4% (QC Low, Mid, High)
Overall accuracy (%)	±7.8% (LLOQ) ±2.0% (QC Low, Mid, High)
Intra-run precision (CV)	≤3.8% (LLOQ) ≤8.4% (QC Low, Mid, High)
Overall precision (CV)	≤9.6% (LLOQ) ≤1.7% (QC Low, Mid, High)
Lower limit of quantification (S/N)	>176
Dilution integrity (Mean, CV)	bias ±2.2%, CV 2.6%
Selectivity (cross analyte and endogenous interference)	≤0.5% and 0.0%
Instrument carry-over	0.7% of the LLOQ
IS-normalized matrix factor (mean, CV)	0.984, 3.1% (QC Low) 0.948, 1.5% (QC High)
Recovery (mean, CV)	102%, 3.1% (QC Low) 101%, 1.2% (QC High)

CV: Coefficient of variation; IS: Internal standard; LLOQ: lower limit of quantitation; QC: Quality control sample; S/N: Signal to noise ratio

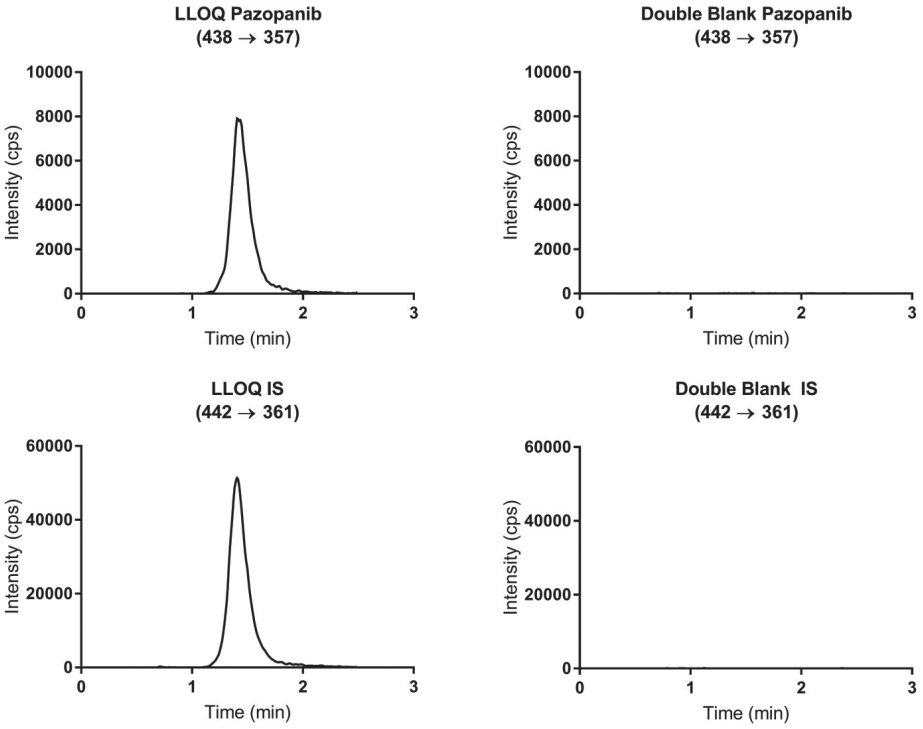

Figure 2: Representative lower limited of quantitation (LLOQ) chromatograms of pazopanib (438 → 357) at 1.00 µg/mL and the internal standard (IS) $^{13}C,^{2}H_3$-pazopanib (442 → 361) at 5.00 µg/mL (from the same LLOQ sample).

Results

Validation

A complete overview of all the validation results is provided in **table 2**. All validated parameters were within their pre-established limits. A representative chromatogram of pazopanib at the LLOQ level, the internal standard and a double blank are provided in **figure 2**. A full overview of the analytical performance data (accuracy and precision) of the method is depicted in **table 3**.

Stability

Results for the stability measurements of pazopanib in the various matrices are provided in **table 4**. All deviations where within ±15% and CVs were also all within 15%.

Clinical application

After completing the bioanalytical validation, the described method was used to support pharmacokinetic analyses in a clinical trial. Plasma samples were stored at -20 °C and then processed and analyzed using the method described in this manuscript.

As displayed in **figure 3**, 327 plasma trough samples were measured from patients who received pazopanib dosages ranging from 400 to 1800 mg daily. Of these 96.9% were within the validated range (0.9% <LLOQ and 2.1% >ULOQ), with a mean of 24.4 µg/mL and a CV of 49.5%. All samples above the ULOQ were successfully re-analyzed after applying the validated 20-fold dilution.

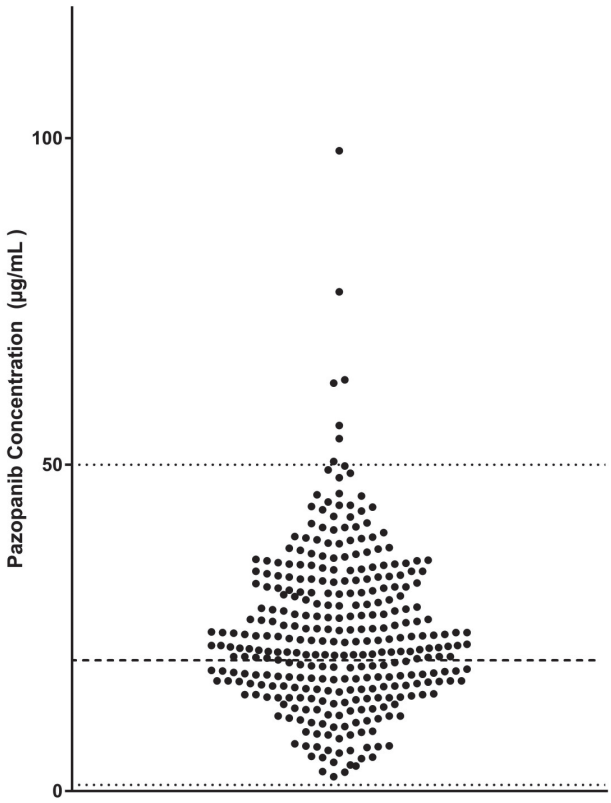

Figure 3: Distribution of clinical plasma samples measured using the described LC-MS/MS method. Of all samples (n=327), only 3 (0.9%) were below LLOQ (not displayed), 7 (2.1%) were above ULOQ. The mean concentration of (non <LLOQ) samples was 24.4 µg/mL. Dotted lines indicate the LLOQ (1 µg/mL) and ULOQ (50 µg/mL), the dashed line indicated the therapeutic threshold of ≥20.5 mg/L proposed by Suttle et al.

Table 3: Analytical performance data, for the LLOQ (1.00 µg/mL), QC Low (3.00 µg/mL), QC Mid (15.0 µg/mL) and QC High (37.5 µg/mL) concentration levels.

Run	Nominal concentration (µg/mL)	Mean measured concentration (µg/mL)	Accuracy (% deviation)	Precision (% CV)	Replicates (n)
1	1.00	0.808	-19.2	3.2	5
2	1.00	0.973	-2.7	3.1	5
3	1.00	0.983	-1.7	3.8	5
Overall	1.00	**0.922**	**-7.8**	**9.6**	**15**
1	3.00	2.94	-1.9	6.4	5
2	3.00	2.94	-0.2	1.9	5
3	3.00	2.88	-4.0	3.1	5
Overall	3.00	**2.94**	**-2.0**	**4.3**	**15**
1	15.0	15.3	1.9	3.1	5
2	15.0	15.1	0.5	1.3	5
3	15.0	14.7	-2.1	2.3	5
Overall	15.0	**15.0**	**0.1**	**2.8**	**15**
1	37.5	37.3	-0.5	8.4	5
2	37.5	36.4	-2.8	1.7	5
3	37.5	35.8	-4.4	2.2	5
Overall	37.5	**36.5**	**-2.6**	**5.1**	**15**

CV: Coefficient of variation; LLOQ: lower limit of quantitation

Table 4: Stability data for pazopanib in various matrices. All analyses were performed in triplicate.

Sample type	Condition & Interval (days)	Concentration (µg/mL)	Deviation (% deviation)	CV (%)
Final Extract	70 days at 2 - 8 °C	3.00 37.5	-4.0 -4.2	1.3 10.4
Plasma Sample	5 days at ambient temperatures	3.03 37.8	-6.8 -6.0	0.7 2.8
Plasma Sample	111 days at -20 °C	3.00 37.5	-3.1 -2.0	5.2 3.4
Plasma Sample	3 freeze/thaw cycles (-20 °C/ambient)	3.00 37.5	-0.4 -0.2	1.5 3.1
Working Solution (MeOH)	38 days at -20 °C	300	1.0	8.0
Stock Solution (DMSO)	30 days at -20 °C	$2.00 \cdot 10^3$	1.8	2.6

CV: Coefficient of variation; DMSO: Dimethyl sulfoxide; MeOH: Methanol.

Discussion

The method described in this manuscript is robust and was fast and easy to implement in routine pazopanib plasma concentration monitoring to support clinical trials and therapeutic drug monitoring. The method was fully validated in accordance with EMA and FDA guidelines and met all pre-established validation criteria (**table 2**).

The runtime was only 2.5 minutes and the sample preparation was straightforward consisting only of protein precipitation and dilution. Moreover, chromatographic separation was performed using isocratic elution.
To further reduce analytical workload and facilitate sample handling, extensive stability testing was performed. Pazopanib samples appeared to be very stable (**table 4**). Samples were shown to be stable in the final extract for at least 70 days when stored at 2 – 8 °C. This could reduce the need to prepare calibration standards for each analytical run, making the method more suitable to application in routine therapeutic drug monitoring. Moreover, concentrations in plasma samples were within specifications for at least 5 days at room temperature, forgoing the need to send samples to the bioanalytical laboratory on ice or dry ice.

Protein precipitation was used as sample pretreatment and despite the limited sample clean-up, the method resulted in reliable quantification, demonstrated by its robust analytical performance (**table 2 & 3**). At our institute the described method is now routinely applied to support clinical trials and to guide the treatment of patients treated with pazopanib. The described method has been used to quantify a large set of over 300 clinical samples, supporting its clinical applicability.

Pazopanib plasma concentrations have been shown to be a relevant parameter related to treatment efficacy and toxicity.[5,9] Moreover, a prospective trial in cancer patients has established the safety and feasibility of individualizing the dose of pazopanib based on plasma concentrations.[12] Ultimately, future randomized clinical studies are needed to show the added value of individualized dosing of pazopanib on a relevant clinical endpoint such as progression free survival or overall survival.

Conclusion

We describe the bioanalytical validation and clinical application of a fast and straightforward method for the quantification of pazopanib in human plasma using LC-MS/MS. All validated parameters were within the FDA and EMA requirements for bioanalytical method validation. The method has been applied to over 300 clinical samples, demonstrating that it is suitable to support therapeutic drug monitoring and clinical trials of cancer patients treated with pazopanib.

Acknowledgements

This study was funded by Fonds NutsOhra and GlaxoSmithKline; Pazopanib is an asset of Novartis AG as of March, 2015. The funding sources had no involvement in the study design, collection, analysis and interpretation of data, the writing of the report or in the decision to submit the article for publication.

Compliance with Ethical Standards:

Funding
No funding was received for this research.

Disclosures
Neeltje Steeghs received an unrestricted grant (funding and study medication) from GlaxoSmithKline as Principal Investigator for an investigator initiated study with Pazopanib. Pazopanib is an asset of Novartis as of June 2015.
Remy B. Verheijen, Bas Thijssen, Hilde Rosing, Jan H.M. Schellens, Lianda Nan, Nikkie Venekamp, Jos H. Beijnen and Alwin D.R. Huitema declare they have no conflicts to disclose.

Ethical approval
All procedures performed in this study involving human participants were in accordance with the ethical standards of the institutional and/or national research committee and with the 1964 Helsinki declaration and its later amendments or comparable ethical standards.

References

1. Kumar R, Knick VB, Rudolph SK, et al. Pharmacokinetic-pharmacodynamic correlation from mouse to human with pazopanib, a multikinase angiogenesis inhibitor with potent antitumor and antiangiogenic activity. *Mol. Cancer Ther.* 2007;6:2012–21.
2. Hamberg P, Verweij J, Sleijfer S. (Pre-)clinical pharmacology and activity of pazopanib, a novel multikinase angiogenesis inhibitor. *Oncologist.* 2010;15:539–47.
3. Sternberg CN, Davis ID, Mardiak J, et al. Pazopanib in locally advanced or metastatic renal cell carcinoma: Results of a randomized phase III trial. *J. Clin. Oncol.* 2010;28:1061–8.
4. van der Graaf WT, Blay JY, Chawla SP, et al. Pazopanib for metastatic soft-tissue sarcoma (PALETTE): a randomised, double-blind, placebo-controlled phase 3 trial. *Lancet.* 2012;379:1879–86.
5. Suttle AB, Ball H, Molimard M, et al. Relationships between pazopanib exposure and clinical safety and efficacy in patients with advanced renal cell carcinoma. *Br. J. Cancer.* 2014;111:1–8.
6. Hurwitz HI, Dowlati A, Saini S, et al. Phase I trial of pazopanib in patients with advanced cancer. *Clin. Cancer Res.* 2009;15:4220–7.
7. de Wit D, van Erp NP, den Hartigh J, et al. Therapeutic Drug Monitoring to individualize the dosing of pazopanib: a pharmacokinetic feasibility study. *Ther. Drug Monit.* 2014;37:331–8.
8. Deng Y, Sychterz C, Suttle AB, et al. Bioavailability, metabolism and disposition of oral pazopanib in patients with advanced cancer. *Xenobiotica.* 2013;43:443–53.
9. Verheijen RB, Beijnen JH, Schellens JHM,et al. Clinical Pharmacokinetics and Pharmacodynamics of Pazopanib: Towards Optimized Dosing. *Clin. Pharmacokinet.* 2017;
10. Gion P Di, Kanefendt F, Lindauer A, et al. Clinical Pharmacokinetics of Tyrosine Kinase Inhibitors. *Clin. Pharmacokinet.* 2011;50:551–603.
11. Tan AR, Gibbon DG, Stein MN, et al. Effects of ketoconazole and esomeprazole on the pharmacokinetics of pazopanib in patients with solid tumors. *Cancer Chemother. Pharmacol.* 2013;71:1635–43.
12. Verheijen RB, Bins S, Mathijssen RHJ, et al. Individualized Pazopanib Dosing: A Prospective Feasibility Study in Cancer Patients. *Clin. Cancer Res.* 2016;22:5738–46.
13. Minocha M, Khurana V, Mitra AK. Determination of pazopanib (GW-786034) in mouse plasma and brain tissue by liquid chromatography-tandem mass spectrometry (LC/MS-MS). *J. Chromatogr. B;* 2012;901:85–92.
14. van Erp NP, de Wit D, Guchelaar H-J, et al. A validated assay for the simultaneous quantification of six tyrosine kinase inhibitors and two active metabolites in human serum using liquid chromatography coupled with tandem mass spectrometry. *J. Chromatogr. B.* ; 2013;937:33–43.
15. Committee for Medicinal Products for Human Use (CHMP) European Medicines Evaluation Agency. Guideline on Bioanalytical Method Validation. 2011. Available from: http://www.ema.europa.eu/docs/en_GB/document_library/Scientific_guideline/2011/08/WC500109686.pdf Accessed July 18th 2017
16. Center for Drug Evaluation and Research (CDER) Food and Drug Administration. Guidance for Industry Bioanalytical Method Validation. 2001. Available from: http://www.fda.gov/downloads/Drugs/Guidance/ucm070107.pdf Accessed July 18th 2017

Chapter 2.3

Development and Clinical Validation of an LC-MS/MS Method for the Quantification of Pazopanib in Dried Blood Spots

Remy B. Verheijen[1], Sander Bins[2], Bas Thijssen[1], Hilde Rosing[1], Lianda Nan[1], Jan H.M. Schellens[3,4], Ron H.J. Mathijssen[2], Martijn P. Lolkema[2,5], Jos H. Beijnen[1,4], Neeltje Steeghs[3,5], Alwin D.R. Huitema[1]

[1]Department of Pharmacy & Pharmacology, The Netherlands Cancer Institute - Antoni van Leeuwenhoek, Plesmanlaan 121, 1066 CX, Amsterdam, The Netherlands.

[2]Department of Medical Oncology, Erasmus MC Cancer Institute, Rotterdam, 's-Gravendijkwal 230, 3015 CE Rotterdam, The Netherlands.

[3]Department of Medical Oncology and Clinical Pharmacology, The Netherlands Cancer Institute - Antoni van Leeuwenhoek, Amsterdam, Plesmanlaan 121, 1066 CX, Amsterdam, The Netherlands.

[4]Dept. of Pharmaceutical Sciences, Utrecht University, Universiteitsweg 99, 3584 CG, Utrecht, The Netherlands.

[5]Department of Medical Oncology, University Medical Center Utrecht, Heidelberglaan 100 3584 CX Utrecht, The Netherlands.

Abstract

Background: Pazopanib is approved for the treatment of renal cell carcinoma and soft tissue sarcoma. Analyses show increased benefit in patients with plasma trough concentrations ≥20.5 µg/mL compared to patients with lower concentrations. **Methods & Results:** We developed a dried blood spot assay as a patient friendly approach to guide treatment. The method was validated according to FDA and EMA guidelines and EBF recommendations. Influence of spot homogeneity, spot volume and hematocrit were shown to be within acceptable limits. Analysis of paired clinical samples showed a good correlation between the measured plasma and DBS concentrations (R^2 of 0.872). **Conclusion:** The method was successfully validated, applied to paired clinical samples and is suitable for application to therapeutic drug monitoring of pazopanib.

Introduction

Pazopanib is an angiogenesis inhibitor targeting the vascular endothelial growth factor receptor (VEGFR)-1,2,3, platelet derived growth factor receptor (PDGFR) α/β, fibroblast growth factor receptor (FGFR) and the stem cell receptor/ c-Kit [1]. Pazopanib has shown efficacy in advanced renal cell carcinoma and soft tissue sarcoma in a fixed dose of 800 mg once daily [2,3]. A recent retrospective analysis of a trial of 177 patients treated with pazopanib showed a markedly increased median progression free survival (PFS) in patients with (steady state) plasma trough concentrations (C_{min}) ≥20.5 µg/mL compared to patients with lower C_{min} (50.2 weeks vs. 19.6 weeks) [4]. In addition, pazopanib shows large inter-individual variability in plasma exposure, resulting in a subset of patients at risk of receiving less than optimal exposure [4–7].

Given the established exposure response relationship and large inter-individual variability in exposure, patients might benefit from pharmacokinetically guided dosing, also known as therapeutic drug monitoring (TDM), based on a measured C_{min}. A quantitative assay is needed to identify patients with a low C_{min} that might benefit from treatment at a higher dose. Several assays to quantify pazopanib in (mouse and human) plasma have been described, both using diode array detection (DAD) [8] and liquid chromatography tandem mass spectrometry (LC-MS/MS) [9–11].

Last year, a review article by Wilhelm et al discussed the application of dried blood spots (DBS) to support TDM [12]. A DBS method would allow patients to take a sample themselves using a simple finger prick. Compared to plasma methods, DBS sampling could be more patient friendly and lead to increased sample stability, limited sample volume, convenient storage and shipping.

Additionally DBS methods may be ideally suited to measure C_{min} concentrations, because a blood sample can be obtained at the planned time point by the patients themselves and will not be dependent on the time of the visit to an out-patient clinic. This may be relevant for pazopanib as De Wit et al found a strong correlation (R^2 of 0.940) between the trough sample (exactly C_{24h}) and pazopanib area under the curve (AUC)[7].

Measurement of pazopanib concentrations in DBS may therefore be an ideal method for guiding the systemic exposure to this drug.

However, quantification in DBS samples may be more challenging for several reasons. Patients or nurses will need additional training to provide good quality samples and additional validation tests need to be performed, such as the influences of blood hematocrit, spot volume, punch carry-over and blood spot homogeneity on analytical outcome [13]. Moreover, a clinical validation study to investigate the relationship between the plasma and DBS concentrations is needed [14,15] But once a comprehensively validated method is available and patients and nurses are familiar with the sampling technique, a DBS method will be optimally suited to pharmacokinetically guided dosing of pazopanib.

Here, we describe the development, analytical and clinical validation of an LC-MS/MS method for the quantification of pazopanib in DBS.

Materials, methods and patients

Chemicals and reagents

Pazopanib hydrochloride and stable isotopically labeled internal standard (IS) $^{13}C,^{2}H_{3}$-pazopanib hydrochloride, with purities as free base of 92.3% and 92.6% respectively were supplied by GlaxoSmithKline (Zeist, The Netherlands). Formic acid and dimethyl sulfoxide were purchased from Merck (Darmstadt, Germany) and methanol (analytical grade) and water (LC-MS grade) from BioSolve Ltd (Valkenswaard, The Netherlands). Blank human whole K_2EDTA blood was obtained from healthy volunteers and used for preparation of the quality control samples (QC), calibration standards and matrix blanks .

Stock solutions, calibration standards and quality control samples

Stock solutions of pazopanib (2 mg/mL) were prepared in dimethyl sulfoxide. Working solutions were prepared by dilution from stocks with methanol. The IS stock solution (1 mg/mL) was prepared in methanol. The IS working solution was prepared by further dilution with methanol to a concentration of 0.1 µg /mL. All stock and working solutions were stored at -20 °C, the IS working solution at 2 – 8 °C.

Calibration standards and QC samples were prepared by spiking 30 µL of the working solutions to 570 µL of control whole blood. Concentrations of 1.00, 3.00, 15.0 and 37.5 µg/mL were used for the QC samples (lower limit of quantification (LLOQ), low, mid and high concentrations respectively). The concentrations for the calibration standards were: 1.00, 2.00, 5.00, 10.0, 20.0, 30.0, 40.0 and 50.0 µg/mL. From the blanks, calibration standards and QC samples a volume of 15 µL whole blood was spotted on the DBS cards. The blood spots were dried at ambient temperatures (20-25 °C) for at least 3 hours after which the samples were stored at ambient temperature with desiccant in a sealed foil bag. Hematocrit values of calibration standards and QC samples were not standardized in each run.

Equipment and conditions

Blood was spotted on Whatman™ 903 protein saver cards and punches from these cards were made using a Harris Uni-Core™ 3.0 mm puncher both purchased from GE Healthcare Europe GmbH (Diegem, Belgium). Samples were shaken using a L45 shaker by Labinco (Breda, The Netherlands).

All LC-MS/MS experiments were performed using an 1100 series binary pump, degasser, column oven and autosampler from Agilent Technologies (Santa Clara, CA, United USA) and an API3000 triple quadrupole equipped with Turbo ionspray interface operating in positive ion-mode, on Analyst™ software for data analysis from Sciex (Framigham, MA, USA). Mass transitions of precursor and product ions and other MS parameters were optimized. Final settings were: ,tubro, nebulizer, curtain and collision gases 7 lL/min 7 , 8 and 12 a.u., ion spray voltage 3000 V, ionization temperature 500 °C, declustering potential 41 V, collision energy 43 V, collision cell exit and entrance potential 24 V and 10 V. Quantification was performed using the *m/z* 438.2 à *m/z* 357.3 transition for pazopanib and *m/z* 442.2 à *m/z* 361.2 for $^{13}C,^{2}H_{3}$-pazopanib (see figure 1).

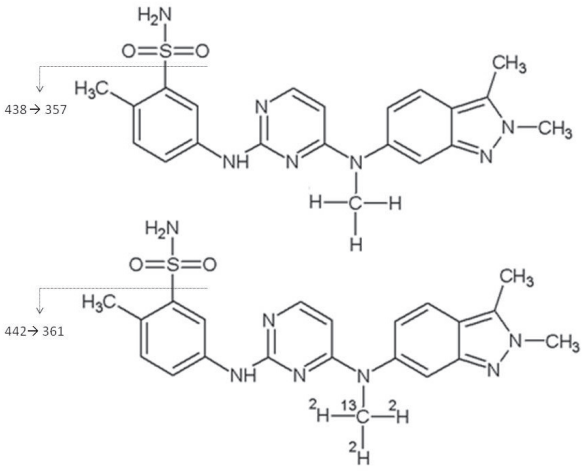

Figure 1: Chemical structure and proposed mass transition of pazopanib and $^{13}C,^{2}H_{3}$ pazopanib.

Table 1: Summary of validation Results. All tested parameters met their predefined criteria (predefined acceptance criteria are mentioned in the text).

Parameter	Result
Calibration model	Linear regression coefficients all >0.99
Validated range	1.00 to 50.0 µg/mL
Overall (in)accuracy	bias ±4.0%
Inter and intra run precision (CV)	≤8.6%
Lower limit of quantification (S/N)	>27
Dilution integrity	bias ±1.0%, CV 10.7%
Selectivity (endogenous and cross analyte)	≤0.6%
Instrument carry-over	0.6% of the LLOQ
IS normalized matrix factor (mean, CV)	1.01, 1.6% (QC low) 0.980, 1.9%(QC high)
Recovery	97.6% (QC low) 103.7% (QC high), CV ≤2.7%
Spot-to-spot carry-over	6.4% of the LLOQ
Blood spot homogeneity	bias ±3.5%, CV ≤4.6%
Effect of blood spot volume	bias ±9.5%, CV ≤4.8%
Effect of blood hematocrit	bias ±14.2%, CV ≤10.2%
Final extract stability (2 – 8 °C)	168 days
DBS stability (ambient temperatures)	398 days

Separation was performed on a Sunfire C18 Column, 2.1 x 50 mm, 5 µm from Waters (Milford, MA, USA) with a Gemini SecurityGuard, 2.0 x 4.0 mm guard column by Phenomenex (Torrance, CA, USA). The column oven was set at 55 °C and the tray temperature of the autosampler at 5 °C. Elution was achieved by using a gradient of methanol and 0.1% formic acid in water. The gradient started at a flow of 0.4 mL/min at a percentage of 27% methanol, after 1.5 minutes the gradient was increased to 80% methanol. At 2 minutes, the flow increased to 0.6 mL/min and at 2.5 min the percentage of methanol was returned to 27% for 1.5 minutes. The total runtime was 4 minutes.

Sample preparation

On the day of analysis a 3 mm diameter punch was taken from the blood spots and transferred to an eppendorf tube. A total of 50 µL of concentrated formic acid (99%) was added to the spot and the sample was vortex mixed and consequently shaken for 10 minutes at 1250 rpm. Hereafter, 500 µL of methanol containing the IS (at a concentration of 0.1 µg/mL) was added and the samples were again vortexed and shaken for 10 minutes at 1,250 rpm. After centrifugation at 23100 g and 300 µL of the supernatant was transferred to a clean vial containing 300 µL of water. These vials were then vortex mixed and 5 µL was injected into the LC-MS/MS system.

For plasma samples, a 10 µL aliquot was used, to which 500 µL of IS containing methanol and 500 µL eluent was added. This solution was then centrifuged at 23100 rpm and 5 µL of the supernatant was analyzed by LC-MS/MS.

Table 2: Analytical performance data for pazopanib in dried blood spots

Run	Nominal concentration (µg/mL)	Mean measured concentration (µg/mL)	(In)accuracy (% deviation)	Precision (% CV)	Replicates (n)
1	1.01	1.09	8.1	5.6	5
2	1.01	1.02	1.2	5.9	5
3	1.01	1.00	-0.8	6.1	5
Overall	**1.01**	**1.04**	**2.8**	**3.7**	**15**
1	3.03	3.04	0.2	5.1	5
2	3.03	2.95	-2.7	5.3	5
3	3.03	3.20	5.7	7.1	5
Overall	**3.03**	**3.06**	**1.1**	**3.4**	**15**
1	15.1	15.9	5.0	3.0	5
2	15.1	14.8	-2.3	8.6	5
3	15.1	16.5	9.3	3.8	5
Overall	**15.1**	**15.7**	**4.0**	**5.0**	**15**
1	37.9	38.5	1.6	5.8	5
2	37.9	36.6	-3.5	4.9	5
3	37.9	40.3	6.4	3.2	5
Overall	**37.9**	**38.5**	**1.5**	**4.4**	**15**

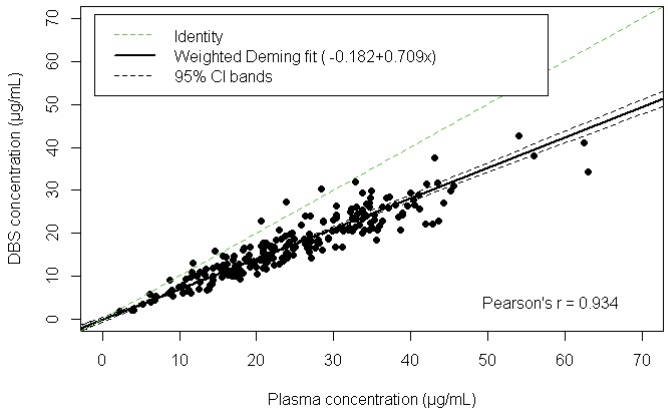

Figure 2: Measured DBS concentration versus the measured plasma concentration (n=221). The filled black line represents the weighted Deming fit, the dotted black lines represent the 95% confidence interval of the Deming fit, the green dotted line is the line of unity.

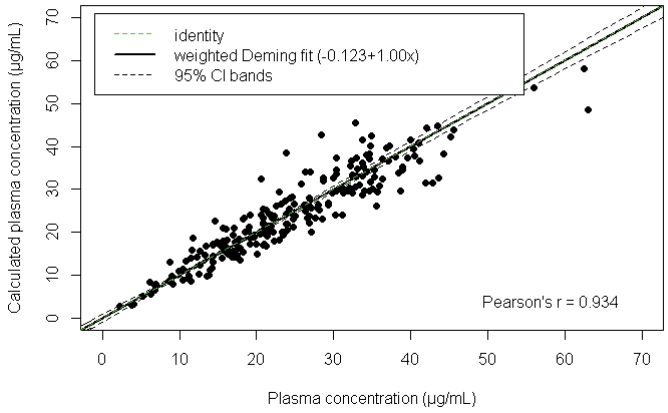

Figure 3: Calculated plasma versus the measured plasma concentration (n=221). The filled black line represents the weighted Deming fit, the dotted black lines represent the 95% confidence interval of the Deming fit, the green dotted line is the line of unity.

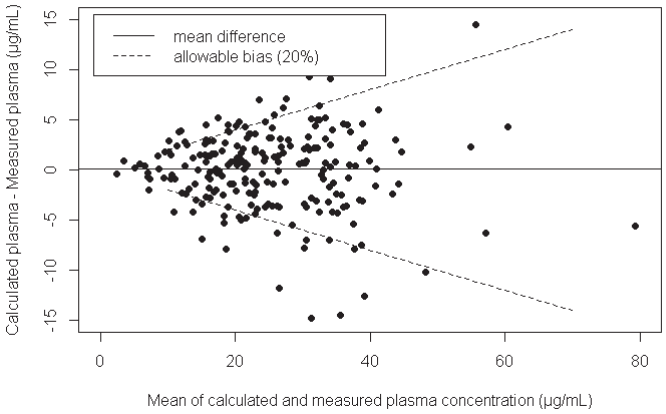

Figure 4: Bland-Altman plot showing the difference between the calculated and measured pazopanib plasma concentration (n=221). The mean difference between the two methods was 0.08 µg/mL.

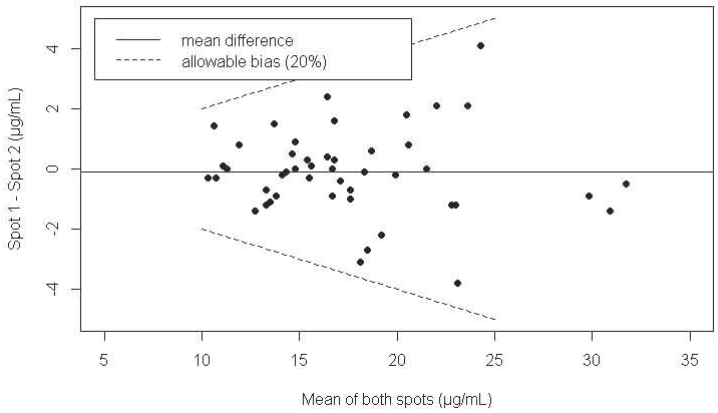

Figure 5: Bland-Altman plot showing the difference between the measured pazopanib spots in the subset of samples of which two spots provided by the same patient at the same time were measured (n=47). The mean difference between the two methods was -0.105 µg/mL.

Validation

The method was validated in accordance with Food and Drug Administration (FDA) and European Medicines Agency (EMA) guidelines on bioanalytical method validation and Good Laboratory Practices [16,17]. DBS specific validation tests were performed, as recommended by the European Bioanalysis Forum (EBF)[18,19].

Analytical validation

Three separate validation runs were executed on separate days and the following validation parameters were assessed: LLOQ, calibration model, accuracy and precision, dilution integrity, selectivity, instrumentation carry-over, matrix effect and recovery.

Linear regression was applied. Non-weighted, 1/x and 1/x2 weighted regression were evaluated (where x equals the peak area ratio). In every run at least 75% of the non-zero standards (including at least one LLOQ and upper limit of quantification (ULOQ)) should be within ±15% of the nominal value (or ±20% for the LLOQ), additionally for the LLOQ and ULOQ level at least 50% should meet these criteria. Regression coefficients were calculated in each run.

Accuracy and precision of the method were assessed by injecting five replicates of LLOQ, QC low, mid and high samples in three separate validation runs. Intra- and inter-run accuracy was expressed as the bias in % and intra- and inter-run precision as the coefficient of variation (CV) in %. At each of the QC levels the bias should be within ±15% and the precision should not exceed 15%.

The LLOQ was evaluated in each run using the signal to noise ratio (S/N) expressed as the signal (peak height of the 1.00 µg/mL calibration standard) to the noise (peak height) of a blank sample. This ratio should be at least 5.

Dilution integrity was calculated by analyzing five replicates of samples with a concentration of 100 µg/mL, diluted 10 times with a processed controlled matrix and comparing the measured concentration with the nominal concentration. This bias should be within ±15% and the precision should not exceed 15%.

For selectivity, the effect of endogenous interferences and IS interference were determined. Six different batches of human whole blood were processed both as blanks and spiked at the LLOQ concentration to investigate possible endogenous interferences. Cross analyte interference was assessed by extracting pazopanib without the addition of the IS and by spiking IS separately to a double blank sample (a matrix sample; 3 mm punch from a blood spot without spiking analyte or IS) at the concentration used in the assay. The interference should be less than 20% of the response of the LLOQ of the analyte and less than 5% of the response of the IS.

Instrumentation carry-over was tested by injecting two double blank samples after injecting an ULOQ sample in each validation run and expressed as the peak area in the blanks as a percentage of the LLOQ peak area. Carry-over was considered acceptable when the response in the first blank at the retention time of the analyte is less than 20% of the response of the LLOQ.

The matrix factor (MF) was calculated by dividing the analyte and IS peak area in presence of matrix by the peak area of the analyte and IS in a neat solution, using six different batches of whole blood

spiked at both the QC low and QC high concentration. The IS-normalized MF was calculated by dividing the MF of pazopanib by the MF of the IS of which the CV was calculated. This CV was considered acceptable if it was less than 15%.

The (sample pretreatment) recovery was determined by comparing peak area of pazopanib in processed validation samples to peak area of pazopanib area in presence of matrix, at QC low and high concentrations in triplicate. No specific requirement for recovery was predefined except that it should be reproducible.

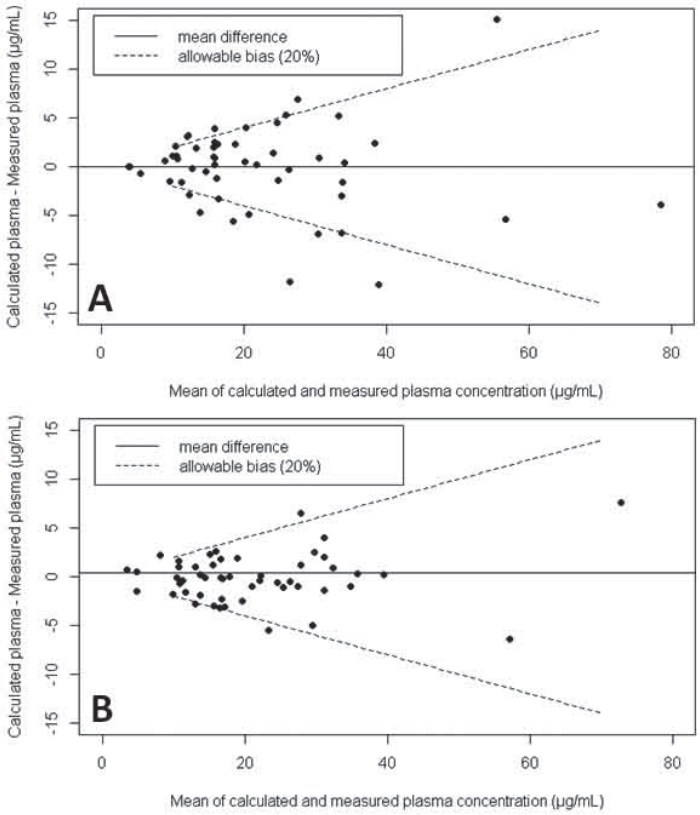

Figure 6A and B: Bland-Altman plots showing the difference between the measured pazopanib spots in the subset of samples (n=51) which were measured after a 3mm punch (A) and a 6 mm punch (B) from the DBS card. The mean difference was -0.09 µg/mL and 0.44 µg/mL for the 3 mm and 6 mm punched samples respectively.

DBS specific validation

The influence of spot (in)homogeneity, spot volume, blood hematocrit and spot-to-spot carry-over was investigated. The spot-to-spot carry-over was tested by punching a double blank sample after an ULOQ sample. Carry-over was considered acceptable as the response in this blank sample at the retention time of the analyte was ≤20% of the mean (n=5) response at the LLOQ.

The effect of (in)homogeneity within the blood spot was examined in triplicate by taking punches from the edge of the blood spot and comparing the measured concentration with the nominal concentration, at low and high QC concentrations.

The effect of spot volume and blood hematocrit was investigated in triplicate at QC low and QC high concentrations, by spotting a range of volumes on the DBS cards (10, 15, 30 µL). The effect of the hematocrit was determined by preparing batches of whole blood with different hematocrit values in the range from nominally 35% to 50% (tested values: 34.1%, 42.4% and 49.7%).

The effect of spot volume, inhomogeneity and hematocrit was considered acceptable if bias and precision were within ±15% and ≤15% respectively.

Stability

Stability of processed samples stored at nominally 2 – 8 °C and samples on the DBS cards at ambient temperature (in a foil bag with desiccant) was investigated in triplicate at both low and high QC concentrations. Samples were considered stable if the bias was within ±15% of the nominal concentration and the CV was ≤15%.

Clinical validation

Paired DBS and (venous) plasma samples were obtained from patients with advanced solid tumors treated with pazopanib (n=30) recruited from three centers (the Netherlands Cancer Institute, Amsterdam, Utrecht University Medical Center, Utrecht and Erasmus MC Cancer Institute, Rotterdam). Doses administered ranged from 400 mg to 1800 mg daily following protocol and within patient adjustments of the dose were possible [20]. The trial was approved by the independent ethics committee of each participating hospital (Dutch Trial Registry; trial identifier NTR3967) and all patients provided written informed consent before enrolment. DBS samples were taken by a finger prick under the supervision of a study nurse and the obtained blood spots were dried at ambient temperatures for at least 3 hours, after which the samples were stored with desiccant in a sealed foil bag and sent to the analytical laboratory.

Weighted Deming fit was used to investigate the relationship between the plasma and DBS concentration. Using the observed slope and intercept the plasma concentration were calculated. Bland-Altman plots were made to investigate the bias between the calculated and measured plasma concentrations. These analyses were all performed in R (version 3.0.0) [21].

An arbitrarily selected subset of DBS samples (n=47) was measured in duplicate (two separate blood spots on the same card, obtained from the same patient at the same date and time) to investigate the variability during the spotting procedure in clinical practice. Another subset of DBS samples was

measured in duplicate with one punch of 3 mm and another of 6 mm (n=51), to assess the effect of punch size in the clinical samples. In this separate analysis the calibration standards and QC samples were also analyzed using a 6 mm punch for the DBS.

Table 3: Effect of spot volume on the quantification of pazopanib (n=3)

Spot Volume	QC low Bias (%)	CV (%)	QC high Bias (%)	CV (%)
10 µL	-9.0	4.7	-5.0	0.7
20 µL	5.2	4.8	-0.7	1.8
30 µL	9.5	3.1	5.5	1.9

Table 4: Effect of blood hematocrit on the quantification of pazopanib (n=3)

Blood Hematocrit	QC low Bias (%)	CV (%)	QC high Bias (%)	CV (%)
34.1%	-14.2	7.1	-10.0	10.2
42.4%	-4.2	4.4	-7.4	2.4
49.7%	7.4	3.9	1.0	1.3

Results & Discussion

Analytical validation results

An overview of the validated parameters is shown in table 1. Analytical performance data for pazopanib in DBS are shown in table 2. All tested parameters met their predefined acceptance criteria. As 1/x weighted regression resulted in the lowest total bias this was selected for the calibration model.

DBS specific validation results

The spot-to-spot carry-over was 6.4% of the mean (n=5) LLOQ level for pazopanib and 0.0% for $^{13}C,^{2}H_{3}$-pazopanib. Spot (in)homogeneity resulted in a bias of 3.5% and 2.2% for low and high QC levels with CV percentages of 1.3 and 4.6, respectively.

Data for the effect of spot volume are presented in table 3. The biases for all tested volumes were ≤9.5% of the nominal concentration and the CV was ≤4.8%, indicating that the influence of spot volume was within the requirements.

Results for the influence of hematocrit are shown in table 4. The calibration standards used in the analysis had a hematocrit value of 43.8%. The effect of the hematocrit was within the predefined limits as the mean measured concentration was ≤14.2% of the nominal concentration, with a CV of ≤10.2%.

Stability

QC samples at low and high concentrations (n=3), deviated ≤15% of the nominal concentration after being stored at ambient temperatures (in a foil bag with desiccant) at 398 days. Therefore pazopanib was considered to be stable for at least 398 days on the DBS cards. Processed samples stored at nominally 2 – 8 °C deviated ≤15% of the nominal concentration and were therefore considered stable at nominally 2 – 8 °C for at least 168 days.

Clinical validation

The method was applied to clinical samples taken approximately 24 hours after the last dose (at steady state) from cancer patients treated with pazopanib. In total, 329 paired DBS and plasma samples were obtained from the 30 enrolled patients. Irregular, very large (larger than the printed ring on the DBS card), very small (smaller than the punch diameter) spots were excluded. Samples resulting in concentrations below the LLOQ (15) were also excluded. In total, 221 spots were used for the analysis. As shown in Figure 2, a good correlation between the DBS and the plasma concentration was found (R^2 of 0.872 with a slope of 0.709 and an intercept of -0.182).

The plasma concentration was back calculated based on the measured DBS concentration, using $[\text{pazopanib}_{\text{calculated plasma}}] = ([\text{pazopanib}_{\text{dried blood spot}}] + 0.182) / 0.709$. The plotted calculated versus measured plasma concentrations are shown in figure 3. The difference between the calculated and measured plasma concentrations versus the measured plasma concentration is shown in a Bland-Altman plot in figure 4. Back calculated plasma concentrations were within 20% of measured plasma concentrations for 79.2% of the DBS samples.

Correction for patient specific hematocrit when calculating the plasma concentration (using the formula proposed by Kromdijk et al [14], $[\text{pazopanib}_{\text{calculated plasma (hmtcrt corrected)}}] = [\text{pazopanib}_{\text{dried blood spot}}]/(1\text{-hematocrit})*\text{fraction bound to plasma protein}$) did not improve the correlation between the calculated and measured plasma concentrations compared to the empirically found Deming regression. The hematocrit values of the patients used for this sub analysis were within the validated range, the mean was 40%, ranging from 36% to 48%.

When used to identify patients above or below the 20 µg/mL threshold the plasma and DBS methods were in agreement in 91.4% of the cases.

A Bland-Altman plot of the difference between two spots taken at the same time as a function of the mean of the two measurements is given in figure 5. The Bland-Altman plot showing the deviations of clinical samples punched with both a 3 and a 6 mm diameter punch is shown in figure 6.

Our method was successfully developed to quantify pazopanib in DBS and validated in accordance with FDA and EMA guidelines on bioanalytical method validation and Good Laboratory Practices [16,17].

With a run time of only 4 minutes, the developed method is suitable for routine analyses of patient samples. Moreover processed samples were shown to be stable for at least 168 days, therefore calibration standards can be re-used several times, reducing the time needed to perform an analytical run.

Spot volume resulted in a small positive bias for large volumes and a small negative bias for small volumes (both within the predefined requirements). No clear mechanism for this effect has been reported. The same trend was found for the tyrosine kinase inhibitor vemurafenib [22] and other compounds such as everolimus, tacrolimus and sirolimus [23].

Spot-to-spot carry-over was shown to be only 6.4% of the LLOQ and will therefore have no relevant effect on the analytical outcome when applying this method.

The influence of spot homogeneity was assessed in the laboratory and showed a bias within ±3.5% and a CV of ≤4.6%. In practice however it is likely that this effect will be larger, as samples provided by patients will be less uniform than those made using a pipette.

During the DBS specific validation experiments, hematocrit values from 35-50% were tested and the bias and variability were within predefined limits. Low hematocrit values resulted in a negative bias, while high hematocrit resulted in a positive bias. This might be explained by the higher viscosity with higher hematocrit and, consequently, less spreading on paper. The effect of hematocrit seems to be dependent on the analyte tested. For example, a trend similar to that of pazopanib was found for vemurafenib, everolimus and sirolimus, no clear trend was observed for tamoxifen, endoxifen, tacrolimus and an opposite trend was found for cyclosporine A [22–24].

A good correlation was observed between the DBS concentration and the plasma concentration ($R^2 = 0.872$), with a slope of 0.709 and intercept of -0.182 (figure 2). The lower DBS concentration probably results from pazopanib's high plasma protein binding causing a higher concentration in the plasma relative to blood cells.

Based on this weighted Deming fit, the plasma concentration could be back calculated using the formula: $[\text{pazopanib}_{\text{calculated plasma}}] = ([\text{pazopanib}_{\text{dried blood spot}}] + 0.182) / 0.709$ (figure 3). Correction for patient specific hematocrit when calculating the plasma concentration, did not improve the correlation between the calculated and measured plasma concentrations compared to the empirical Deming regression formula. This suggests that even though hematocrit influences the analytical results (as seen in the DBS specific validation tests) in the clinical setting it is not the most important factor driving the variability between the two methods.

Despite the good correlation between plasma and DBS samples, 20.8% of the calculated plasma concentrations deviated more than 20% from the measured plasma concentration (figure 4). Taking into account the excellent analytical performance of the assay during the validation with the laboratory spots (table 2) it is likely that the variability arises during the clinical spotting procedure. This is supported by the results of the DBS samples measured in duplicate. As even in these samples, which were taken from the same patient at the same time, differences of up to 17.2% were observed (figure 5). Spot quality, volume and (in)homogeneity are the likely factors that cause this variability. Since these samples were taken from the same patient at the same time, blood hematocrit could not explain this difference. Using a larger 6 mm punch resulted in a small reduction of the imprecision (figure 6). But using the 6 mm punch would require patients to produce larger spots, leading to use of larger blood volumes and most likely to a larger number of samples smaller than the punch size.

Acknowledging the above, care should be taken to inspect the quality of the spot before measurement. Very large, very small or irregular spots should not be used, as parameters such as spot homogeneity and volume seemed more important than hematocrit during the clinical validation study. Careful instruction and training of patients in the sampling procedure should thus considered important when using this method, but a recent study in breast cancer patients treated with tamoxifen shows the feasibility of DBS self-sampling [25].

In guiding pazopanib therapy it will be particularly important to identify patients above or below the pharmacokinetic target of ≥20 µg/mL. When the calculated pazopanib plasma concentration was used to identify patients below the pharmacokinetic target level of ≥20 µg/mL, the DBS method was in agreement with the plasma method in 91.4% of the cases. This makes the DBS method acceptable for the proposed purpose of guiding pazopanib therapy, with relevant practical advantages over the plasma method. Furthermore in light of the intra-patient variability (CV) of pazopanib of 24.7% [7], the discrepancy between the two analytical methods will have little effect on the clinical application. As patients with a C_{min} around the 20 µg/mL threshold (for example 15 – 25 µg/mL) would require repeated measurements of the pazopanib concentration, regardless of the analytical method used.

An earlier method for the quantification of pazopanib in DBS has been described [26], when this method was used to compare calculated versus measured plasma pazopanib concentrations in paired samples, 92.6% of the samples were within the predefined deviation of ±25% in the Bland-Altman analysis. When applying these (wider) acceptance criteria to our current method a similar percentage of 88.2% was found.

However the earlier method used the patient's hematocrit in calculating the plasma concentration. This is a major disadvantage if the method is to be applied to patient self-sampling, as calculation of the pazopanib plasma level would still require a visit to the clinic to measure a patient's hematocrit. With the current method there was no need to use the patient's hematocrit and no such correction was used during our clinical validation study, making it more suited to a patient self-sampling approach.

Given the well established exposure response relationship of pazopanib, a fast and minimally invasive DBS method might help implementation of an individualized dosing approach or TDM. Patients would be able to take DBS samples at home and send these at ambient temperatures (these were shown to be stable for at least 398 days) to the analytical laboratory.

The pazopanib DBS concentration could then be measured before the next visit to the clinic and the plasma concentration could be calculated using $[\text{pazopanib}_{\text{calculated plasma}}] = ([\text{pazopanib}_{\text{dried blood spot}}] + 0.182) / 0.709$. Subsequently an assessment of the C_{min} could be made by the treating physician and a dose adjustment could be considered for patients with a low pazopanib exposure, to optimize their treatment.

Conclusion

An LC-MS/MS method for the quantitative determination of pazopanib in DBS was developed and successfully validated in accordance with FDA and EMA guidelines and EBF recommendations for DBS method validation. The DBS concentrations showed a good correlation with the plasma concentrations (R^2 of 0.872) and could be used to determine a calculated plasma concentration. The DBS method can be used for pharmacokinetically guided dosing of pazopanib therapy.

Future perspectives

The described method is suitable for the application to therapeutic drug monitoring of pazopanib, with relevant advantages over plasma quantification (e.g. patient friendly sampling and sample stability) and no need to correct for patient hematocrit. The availability of this assay facilitates further implementation of therapeutic drug monitoring of pazopanib and enables more personalized treatment with this drug. But further prospective clinical trials are needed to demonstrate the added value of an individualized dosing strategy for pazopanib based a measured drug concentration.

References

[1] Hamberg P, Verweij J, Sleijfer S, (Pre-)clinical pharmacology and activity of pazopanib, a novel multikinase angiogenesis inhibitor, *Oncologist* 15, 539–47 (2010).

[2] Sternberg CN, Davis ID, Mardiak J *et al.* Pazopanib in locally advanced or metastatic renal cell carcinoma: results of a randomized phase III trial, *J. Clin. Oncol.* 28, 1061–8 (2010).

[3] Van der Graaf WT, Blay JY, Chawla SP *et al*. Pazopanib for metastatic soft-tissue sarcoma (PALETTE): a randomised, double-blind, placebo-controlled phase 3 trial, *Lancet* 379, 1879–86 (2012).

[4] Suttle AB, Ball HA, Molimard M *et al.* Relationships between pazopanib exposure and clinical safety and efficacy in patients with advanced renal cell carcinoma, *Br. J. Cancer* 111, 1909–16 (2014).

[5] Hurwitz HI, Dowlati A, Saini S, *et al.* Phase I Trial of Pazopanib in Patients with Advanced Cancer, *Clin. Cancer Res.* 15, 4220–4227 (2009).

[6] Deng Y, Sychterz C, Suttle AB et al., Bioavailability, metabolism and disposition of oral pazopanib in patients with advanced cancer, *Xenobiotica* 43, 443–53 (2013).

[7] De Wit D, Van Erp NP, Den Hartigh J et al. Therapeutic Drug Monitoring to individualize the dosing of pazopanib: a pharmacokinetic feasibility study, *Ther. Drug Monit.* 37, 331-338 (2015).

[8] Dziadosz M, Lessig R, Bartels H, HPLC-DAD protein kinase inhibitor analysis in human serum, *J. Chromatogr. B Biomed. Sci. Appl.*893-894, 77–81 (2012).

[9] Van Erp NP, De Wit D, Guchelaar HJ, Gelderblom H, Hessing TJ, Den Hartigh J, A validated assay for the simultaneous quantification of six tyrosine kinase inhibitors and two active metabolites in human serum using liquid chromatography coupled with tandem mass spectrometry, *J. Chromatogr. B Biomed. Sci. Appl.* 937, 33–43 (2013).

[10] Sparidans RW, Ahmed TTA, Muilwijk EW, Welzen MEB, Schellens JHM, Beijnen JH, Liquid chromatography-tandem mass spectrometric assay for therapeutic drug monitoring of the tyrosine kinase inhibitor pazopanib in human plasma, *J. Chromatogr. B Biomed. Sci. Appl.* 905, 137–40 (2012).

[11] Minocha M, Khurana V, Mitra AK, Determination of pazopanib (GW-786034) in mouse plasma and brain tissue by liquid chromatography-tandem mass spectrometry (LC/MS-MS), *J. Chromatogr. B Biomed. Sci. Appl.* 901, 85–92 (2012).

[12] Wilhelm AJ, Den Burger JCG, Swart EL, Therapeutic drug monitoring by dried blood spot: progress to date and future directions, *Clin. Pharmacokinet*. 53, 961–73 (2014).

[13] Jager NGL, Rosing H, Schellens JHM, Beijnen JH, Procedures and practices for the validation of bioanalytical methods using dried blood spots: a review, *Bioanalysis* 6, 2481–2514 (2014).

[14] Kromdijk W, Mulder JW, Rosing H, Smit PM, Beijnen JH, Huitema ADR, Use of dried blood spots for the determination of plasma concentrations of nevirapine and efavirenz, J. *Antimicrob Chemother.* 67, 1211–1216 (2012).

[15] Jager NGL, Rosing H, Schellens JHM, Beijnen JH, Linn SC, Use of dried blood spots for the determination of serum concentrations of tamoxifen and endoxifen, *Breast Cancer Res. Treat.* 146, 137–144 (2014).

[16] *Guideline on bioanalytical method validation.* European Medicines Agency, London, UK (2011).

[17] *Guidance for Industry Bioanalytical Method Validation, Draft Guidance,* .US Department of Health and Human Services, US FDA, Rockville, MD, USA (2013).

[18] Timmerman P, White S, Cobb Z, *et al.* Updates from the EBF DBS – microsampling consortium, *Bioanalysis* 4, 1969–1970 (2012).

[19] Timmerman P, White S, Cobb Z, De Vries R, Van Baar B, White Paper Update of the EBF recommendation for the use of DBS in regulated bioanalysis integrating the conclusions from the EBF DBS-microsampling consortium, *Bioanalysis* 5, 2129–2136 (2013).

[20] Verheijen RB, Bins S, Gadellaa-van Hooijdonk CG *et al.* Individualized PK-guided pazopanib dosing: A feasibility study in cancer patients. Presented at: European Society of Medical Oncology Annual Congress . Marid Spain, 26-30 September 2014.

[21] The R Project for Statistical Computing. www.R-project.org (Accessed 22 May 2015)

[22] Nijenhuis CM, Rosing H, Schellens JHM, Quantifying vemurafenib in dried blood

spots using high-performance LC – MS / MS, *Bioanalysis* 6, 3215–3224 (2014).

[23] Koster RA, Alffenaar JWC, Greijdanus B, Uges DRA, Fast LC-MS/MS analysis of tacrolimus, sirolimus, everolimus and cyclosporin A in dried blood spots and the influence of the hematocrit and immunosuppressant concentration on recovery, *Talanta* 115, 47–54 (2013).

[24] Jager NGL, Rosing H, Schellens JHM, Beijnen JH, Determination of tamoxifen and endoxifen in dried blood spots using LC – MS / MS and the effect of coated DBS cards on recovery and matrix effects, *Bioanalysis* 6, 2999–3009 (2014).

[25] Jager NGL, Rosing H, Linn SC, Schellens JHM, Beijnen JH, Dried blood spot self-sampling at home for the individualization of tamoxifen treatment: a feasibility study., *Ther. Drug Monit*. (2015) [Epub ahead of print].

[26] N. de Wit, D, den hartigh, J, Gelderdblom, H, Qian, Y, den Hollander, M, Verheul, H, Guchelaar, HJ, van Erp, Dried blood spot analysis for therapeutic drug monitoring of pazopanib, J. of Clin. Pharmacol. (2015) [Epub ahead of print].

Chapter 2.4

Exposure-Survival Analyses of Pazopanib in Renal Cell Carcinoma and Soft Tissue Sarcoma Patients: Opportunities for Dose Optimization

R.B. Verheijen[1], L.E. Swart[1], J.H. Beijnen[1,2], J.H.M. Schellens[2,3], A.D.R. Huitema[1,4], N. Steeghs[3]

[1]Department of Pharmacy & Pharmacology, The Netherlands Cancer Institute - Antoni van Leeuwenhoek, Louwesweg 6, 1066 EC Amsterdam, The Netherlands.

[2]Department of Pharmaceutical Sciences, Utrecht University, Utrecht, The Netherlands.

[3]Department of Medical Oncology and Clinical Pharmacology, The Netherlands Cancer Institute - Antoni van Leeuwenhoek, Amsterdam, The Netherlands.

[4]Department of Clinical Pharmacy, University Medical Center Utrecht, Utrecht, The Netherlands.

Abstract

Background

Pazopanib is an angiogenesis inhibitor approved for the treatment of renal cell carcinoma and soft tissue sarcoma. Post hoc analysis of a clinical trial demonstrated a relationship between pazopanib trough concentrations (C_{min}) and treatment efficacy. The aim of this study was to explore the pharmacokinetics and exposure-survival relationships of pazopanib in a real-world patient cohort.

Patients and methods

Renal cell cancer and soft tissue sarcoma patients who had at least one pazopanib plasma concentration available were included. Using calculated C_{min} values and a threshold of >20 mg/L, univariate and multivariate exposure-survival analyses were performed.

Results

Sixty-one patients were included, of which 16.4% were underexposed (mean C_{min} <20 mg/L) using the 800 mg fixed-dosed schedule.

In univariate analysis C_{min} >20 mg/L was related to longer progression free survival in renal cell cancer patients (34.1 versus 12.5 weeks, n=35, p=0.027) and the overall population (25.0 versus 8.8 weeks, n=61, p=0.012), but not in the sarcoma subgroup (18.7 versus 8.8 weeks, n=26, p=0.142). In multivariate analysis C_{min} >20 mg/L was associated with hazard ratios of 0.25 (p=0.021) in renal cancer, 0.12 (p=0.011) in sarcoma and 0.38 (p=0.017) in a pooled analysis.

Conclusion

This study confirms that pazopanib C_{min} >20 mg/L relates to better progression free survival in renal cancer and points towards a similar trend in sarcoma patients. C_{min} monitoring of pazopanib can help identify patients with low C_{min} for whom individualized treatment at a higher dose may be appropriate.

Introduction

Pazopanib is an angiogenesis inhibitor, targeting the vascular endothelial growth factor receptor (VEGFR)-1,2,3, platelet derived growth factor receptor (PDGFR) α/β, fibroblast growth factor receptor (FGFR) and the stem cell receptor/ c-Kit.[1, 2]

Pazopanib increased progression free survival in renal cell carcinoma and in soft tissue sarcoma compared to placebo, resulting in market approval for both tumor types by the Food and Drug Administration and European Medicine Agency.[3, 4] A retrospective analysis from clinical trial data showed an increased median progression free survival in patients with pazopanib plasma trough concentrations (C_{min}) ≥20.5 mg/L compared to patients with lower concentrations (52.0 versus 19.6 weeks, n=177, p=0.004). [5]

Pazopanib has a complex pharmacokinetic profile, described by low, non-linear and time-dependent bioavailability and large inter-individual variability.[6–9] This results in a subset of patients receiving less than optimal exposure.[5] It has been estimated in clinical trials that on the approved 800 mg dose, approximately 20% of patients may not reach the >20 mg/L threshold.[5]

In routine clinical care pharmacokinetic variability may be even greater, as patients are likely to have more comorbidities and concomitant medication, may be older, have impaired renal or hepatic function and have suboptimal therapy adherence.[10] In particular the elderly are known to be underrepresented in clinical trials. [11] Moreover, it has been reported that only 39.0% of renal cancer patients treated with targeted therapies in routine clinical practice would be eligible for enrolment in the pivotal phase III trials of their respective therapy.[12]

The above underscores the need for exploration of the proportion of patients that risk suboptimal efficacy due to low exposure in real-word patient cohorts. Especially, since it has been shown that increasing the pazopanib dose based on a low C_{min} is a feasible and safe option that could lead to improved treatment outcomes.[13]

We now report an observational unselected cohort study in renal cell carcinoma and soft tissue sarcoma patients to identify the number of patients at risk of suboptimal treatment due to low exposure. Additionally, we perform exposure-response and exposure-toxicity analyses and explore if patient characteristics could predict the occurrence of low pazopanib C_{min}.

Materials and methods

Patient Inclusion and Data Collection

An observational study was performed in the outpatient clinic of the Netherlands Cancer Institute, Amsterdam, The Netherlands. Plasma sampling for concentration monitoring was performed as part of routine care in all patients treated with pazopanib at this hospital (however, no dose increments above 800 mg based on low C_{min} were performed during the study period). In the current study, data

from routine clinical care including pazopanib plasma concentrations were used retrospectively, which has been authorized in the institute.
Renal cell carcinoma and soft tissue sarcoma patients who received pazopanib treatment as part of standard of care and who had at least one pazopanib plasma concentration measured were included. Visits were planned according to standard of care in accordance with respective treatment guidelines. Clinical characteristics including demographic data, medical history, pazopanib dose, treatment duration, reason for discontinuation and progression free survival were collected retrospectively from medical records.

Pharmacokinetics

Blood samples were drawn at routinely scheduled visits to the outpatient clinic. Date and time of last intake of pazopanib dose and the time of blood sampling were recorded. Plasma pazopanib levels were determined using a validated liquid chromatography tandem mass spectrometry assay.[14] C_{min} values were calculated based on the measured concentration and interval between last ingested dose and sample time using the algorithm developed previously for imatinib[15]. Samples drawn before T_{max} (2 hours)[8] or more than 24 hours after the last dose were excluded from the analysis.
Relationships between C_{min} and available patient characteristics were explored, including tumor type, age, weight, gender, (lowest) pazopanib dose and World Health Origination (WHO) performance status. Binary variables were tested using two-sided t-tests, categorical variables using analysis of variance, numerical variables using linear regression. P-values <0.05 were considered significant. All statistical analyses were performed in R 3.3.1.[16]

Exposure-Survival Analysis

For the purpose of exposure-survival analyses the mean of all available C_{min} levels per patient was used as parameter for exposure during the entire treatment period, as described previously. [13] Progression free survival of patients with a mean C_{min} above or below the pharmacokinetic threshold of >20 mg/L was analyzed in univariate (Kaplan-Meier analysis plus log-rank test) and multivariate analyses using Cox regression. In multivariate analysis performances status, (lowest) pazopanib dose, number of prior lines of therapy, age and sex were included as covariates. For the exposure-survival analyses in sarcoma, the tumor subtype (leiomyosarcoma, synovial sarcoma or other) was included as an additional covariate. Results are reported as hazard ratios plus 95% confidence intervals (95% CI). A pooled analysis of all patients was also performed. Here, tumor type (renal cancer versus sarcoma) was also included in the multivariate Cox regression.

Exposure-Toxicity Analysis

Pharmacokinetic exposure was compared between patients who discontinued pazopanib therapy due to toxicity and those who did not. Both the average C_{min} per patient and the last C_{min} closest to the discontinuation event (due to toxicity or progressive disease) were analyzed.

Results

Evaluable Patients

From April 2013 to November 2016, 61 patients were included in the analysis, of whom 35 had renal cell carcinoma and 26 soft tissue sarcoma. A full overview of patient characteristics, including WHO performance status, pazopanib dose, previous lines of therapy, age, weight, sex and number of samples is given in table 1.

The subtypes of the sarcoma patients included leiomyosarcoma (n=12), synovial sarcoma (n=6), pleomorphic sarcoma (n=2) epithelioid sarcoma, malignant peripheral nerve sheath tumor, angiosarcoma, solitary fibrous tumor, myxofibrosarcoma and undifferentiated spindle cell sarcoma (all n=1).

Pharmacokinetics

In total, 227 plasma samples were included. Overall, a mean (range) of 4 (1-17) samples were available per patient, 3 (1-9) for the sarcoma and 4 (1-17) for the renal cancer patients. In aggregate, mean (coefficient of variation (CV%)) pazopanib C_{min} was 28.1 (39.7) mg/L, ranging from 6.90 to 77.8 mg/L. Median [range] sampling time was 6 [1 – 44] months since start of therapy. With 5% of samples taken <4 weeks after start. Median interpatient variability (quantified as CV% of the multiple C_{min} values per patient on the same dose) was 24.8%.

An overview of the distribution of average C_{min} per patients per tumor type is provided in figure 1 and table 1. In renal cancer patients mean (CV%) C_{min} per patient was 26.9 (36.4) mg/L compared to 31.9 (36.3) mg/L in the sarcoma patients. The overall average C_{min} per patient was 29.0 (37.1) mg/L. Although C_{min} was higher in sarcoma compared to renal cancer patients (table 1), this difference was not statistically significant (p=0.081). In renal cell carcinoma 6 (17.1%) and in soft tissue sarcoma 4 (15.4%) patients were underexposed (mean C_{min} <20 mg/L) using the 800 mg fixed-dose schedule.

Of all explored clinical parameters, none were found to be significantly predictive of low pazopanib C_{min} except gender in renal cell cancer patients and age in sarcoma patients. Female sex was associated with a higher C_{min} (mean (CV%) of 33.1 (32.5) mg/L versus 23.2 (30.1) p=0.005). Of the 6 renal cancer patients with low C_{min} only 1 was female.

In sarcoma patients, linear regression indicated that patients with higher age had lower C_{min} and was associated with a slope of -0.454 and Pearson's r of -0.414 (p=0.035).

Table 1: Characteristics of included patients.

	Renal Cell Carcinoma	Soft Tissue Sarcoma	Overall
Patients (n)	35	26	61
Gender (n (%))			
Male	22 (62.9)	14 (53.8)	36 (59.0)
Female	13 (37.1)	12 (46.2)	25 (41.0)
Age (mean (range))	62 (45 – 77)	61 (32 – 91)	61 (32 – 91)
Weight (mean (CV%))	84 (23.1)	77 (17.5)	81 (21.6)
Performance Status (n (%))			
0	13 (37.1)	11(42.3)	24 (39.3)
1	16 (45.7)	14 (53.8)	30 (49.2)
2	6 (17.1)	1 (3.8)	7 (11.5)
Pazopanib Dose† (n (%))			
200 mg	3 (8.6)	1 (3.8)	4 (6.6)
400 mg	5 (14.3)	2 (7.7)	7 (11.5)
600 mg	6 (17.1)	2 (7.7)	8 (13.1)
800 mg	21 (60.0)	21 (80.8)	42 (68.9)
Previous Lines of Systemic Therapy (median (range))	1 (1 – 4)	1 (0 – 2)	1 (0 – 4)
Number of samples (n)	151	76	227
Samples per patients (mean (range))	4 (1-17)	3 (1-9)	4 (1-17)
Mean (CV%) C_{min} per patient (mg/L)	26.9 (36.4)	31.9 (36.3)	29.0 (37.1)
Patients with mean C_{min} < 20 mg/L (n (%))	6 (17.1)	4 (15.4)	10 (16.4)

C_{min}: Pazopanib trough level / minimum concentration

CV%: Coefficient of variation

†Lowest dose per patient

Exposure-Survival Analysis

In renal cell carcinoma, C_{min} >20 mg/L was significantly related to improved progression free survival in univariate analysis (p=0.027, see figure 2 and table 2). Median progression free survival was 34.1 weeks for patients with high and 12.5 weeks for patients with low exposure.

In multivariate analysis, C_{min} above or below 20 mg/L resulted in a hazard ratio of 0.25 (95% CI 0.076-0.81, p=0.021). Female gender was also significantly related to increased progression free survival (p=0.008).

In soft tissue sarcoma, median progression free survival was 18.7 weeks for patients with high and 8.8 weeks for patients with low C_{min} (p=0.142, log-rank test, see figure 3 and table 2). In Cox regression, C_{min} >20 mg/L was significantly related to progression free survival and associated with an hazard ratio of 0.12 (95% CI 0.024-0.61, p=0.011). In the sarcoma subgroup, worse performance status (p=0.035) and lower age (p=0.017) were also associated with shorter progression free survival.

In the pooled analysis, C_{min} >20 mg/L was related to improved survival in univariate analysis (25.0 versus 8.8 weeks, p=0.012, see figure 4 and table 2). Here, multivariate analysis resulted in a hazard ratio of 0.38 (95% CI 0.17-0.92, p=0.017) for C_{min} >20 mg/L. Worse WHO performance status and sarcoma as tumor type were also both associated with worse treatment outcome in the Cox model, p=0.004 and p<0.001, respectively.
An overview of the main univariate and multivariate exposure-survival outcomes is provided in table 2.

Table 2: Overview of exposure-survival analysis outcomes.

	Renal Cell Carcinoma	Soft Tissue Sarcoma	Overall
Patients (n)	35	26	61
Median PFS (weeks)	29.9	18.3	24.4
Median PFS C_{min} >20 mg/L (weeks)	34.1	18.7	25.0
Median PFS C_{min} < 20 mg/L (weeks)	12.5	8.8	8.8
Univariate p-value (Log-rank test)	0.027	0.142	0.012
Hazard ratio† (95% CI)	0.25 (0.076-0.81)	0.12 (0.024-0.61)	0.38 (0.17-0.84)
Multivariate p-value (Cox Regression)	0.021	0.011	0.017

C_{min}: Pazopanib trough level / minimum plasma concentration
PFS: Progression free survival
95% CI: 95% Confidence interval
†Hazard ratios are based on the multivariate Cox regression analysis.

Exposure-Toxicity Analysis

Of the 61 included patients, 44 discontinued treatment due to progressive disease and 5 due to toxicity. Reasons for discontinuation included, hepatotoxicity, hypertension, pancreatitis, dyspnea and multiple grade 2 toxicities (all n=1). Mean C_{min} was 37.3 mg/L in those who discontinued due to toxicity, compared to 27.5 mg/L in those had experienced progressive disease. However, this

difference was not statistically significant (p=0.176). Mean (CV%) last C_{min} (the last available sample) was 37.7 (36.4) mg/L compared to 26.4 (46.9) mg/L (p=0.177).

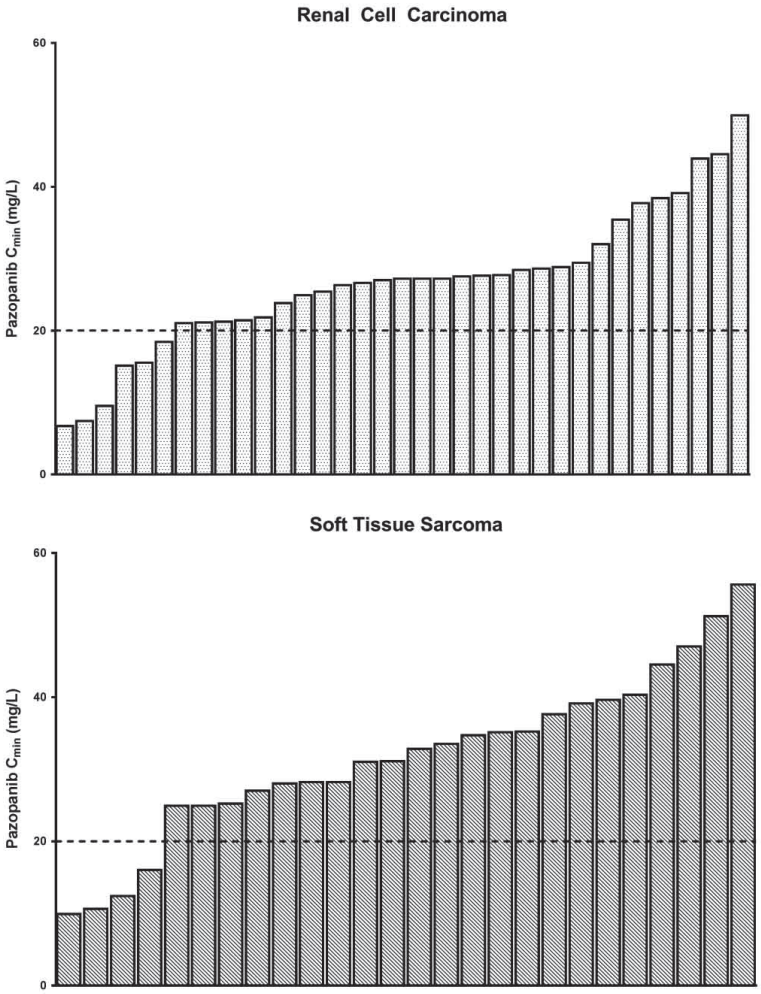

Figure 1: Distribution of the mean calculated pazopanib C_{min} per patient for renal cell carcinoma n=35 (upper panel) and soft tissue sarcoma patients n=26 (lower panel). The dotted line indicates the threshold of 20 mg/L. In renal cell carcinoma 6 (17.1%) of patients and in soft tissue sarcoma 4 (15.4%) of patients seem underexposed using the 800 mg fixed-dosed schedule.

Discussion

Pazopanib is administered at a fixed 800 mg dose, which is only adjusted in case of severe toxicity. Yet, based on the available data this may lead to suboptimal treatment outcomes in a subset of patients. [5] We now show in an unselected cohort that approximately 16.4% of patients is underexposed using the pazopanib fixed-dosing schedule applying the predefined C_{min} target of >20 mg/L. (figure 1, table 1).

No clinical characteristics, except for gender and age were found to be significantly related to pazopanib C_{min}. In general, the ability of clinical characteristics to predict which patients experienced low C_{min} was limited. This underscores the relevance of routine pazopanib C_{min} monitoring, as the subgroup at risk of lower efficacy cannot be identified employing clinical and demographic characteristics. Furthermore, the use of potential interacting medication is carefully monitored during routine care and, therefore, no effects of concomitantly used medication on PK exposure could be identified.

We demonstrate that in renal cancer patients C_{min} >20 mg/L was significantly related to longer progression free survival (34.1 versus 12.5 weeks, table 2 and figure 2). Our data therefore confirm the findings of Suttle et al in an independent patient cohort.[5]

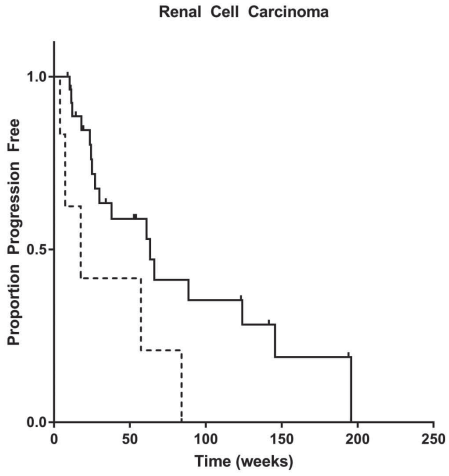

Figure 2: Kaplan-Meier plot of progression free survival (weeks) for renal cell carcinoma patients with an average C_{min} above (n=29, solid line) or below (n=6, dashed line) the exposure target of >20 mg/L. Median progression free survival was 34.1 weeks for patients with high and 12.5 weeks for patients with low exposure, p=0.027 (log-rank test).

As no pharmacokinetic sampling was performed in the pivotal phase II trial in soft tissue sarcoma,[4] no pazopanib exposure threshold has been proposed yet in sarcoma. This is the first study to investigate a relationship between exposure and survival in sarcoma. However, possibly due to the limited size of the sarcoma subgroup in our cohort and the relatively lower effect size of pazopanib in sarcoma, our result did not reach statistical significance in univariate analysis (progression free survival of 18.7 versus 8.8 weeks, p=0.142, figure 3). Another possible explanation for the lack of significance in the univariate exposure-survival analysis could be the diversity of sarcoma subtypes. This heterogeneity may, therefore, explain differences in response rates and response duration between disease subtypes. However, in the multivariate analysis in sarcoma this difference in PFS for patients with C_{min} >20 mg/L was statistically significant (p=0.011).

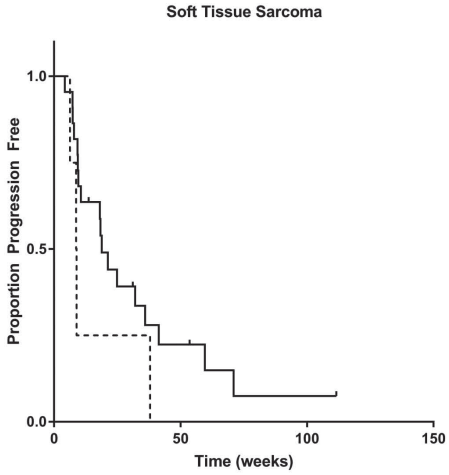

Figure 3: Kaplan-Meier plot of progression free survival (weeks) for soft tissue sarcoma patients with an average C_{min} above (n=22, solid line) or below (n=4, dashed line) the exposure target of >20 mg/L. Median progression free survival was 18.7 weeks for patients with high and 8.80 weeks for patients with low exposure, p=0.142 (log-rank test).

In a pooled exposure-survival analysis (figure 4) higher pazopanib C_{min} was significantly related to improved treatment outcomes. Furthermore, the existence of a similar exposure-response relationship is theoretically supported by the fact that efficacy of pazopanib is mediated by inhibition of the same target proteins (mainly VEGFR) in both tumor types. However, this exploratory pooled analysis should be interpreted with caution given the variability in sensitivity of the different tumor types.

Previous exposure-toxicity relationships have been reported for pazopanib related adverse events such as hepatotoxicity and hypertension and dose-limiting toxicity in pediatric patients.[5, 17, 18] Although not statistically significant, in this cohort we did find a numerically higher exposure in patients discontinuing due to toxicity (n=5), this result was not statistically significant (37.3 mg/L versus 27.5 mg/L, p=0.176).

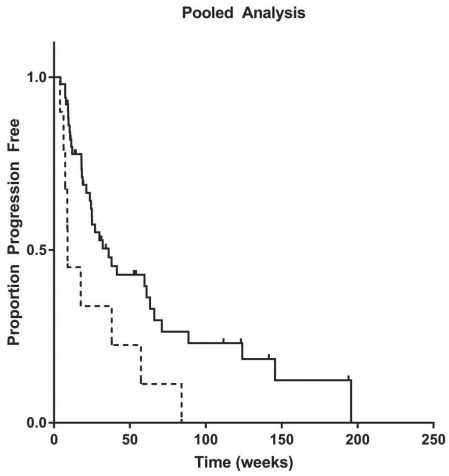

Figure 4: Kaplan-Meier plot of progression free survival (weeks) in a pooled analysis of both renal cell carcinoma and soft tissue sarcoma patients with an average C_{min} above (n=51, solid line) or below (n=10, dashed line) the exposure target of >20 mg/L. Median progression free survival was 25.0 weeks for patients with high and 8.80 weeks for patients with low exposure, p=0.012 (log-rank test).

Drawbacks of this study are its retrospective nature, relatively limited number of patients in each tumor type and the heterogeneity in the availability and timing of plasma samples. Furthermore not actual but calculated C_{min} values (using an therapeutic drug monitoring algorithm as validated for imatinib) were used. However, this algorithm describes a general exponential decline in exposure with a specified plasma half-life and would therefore also be suitable for pazopanib.
Yet despite these limitations, it is the first pharmacokinetic study that reports exposure-survival and exposure-toxicity relationships for pazopanib in a real-world cohort of renal cell carcinoma and soft tissue sarcoma patients and identifies a subgroup of approximately 16.4% of patients which may benefit from individualized C_{min}-guided pazopanib dosing.

Given the currently presented results and the previous work by Suttle et al[5], one could argue that a fixed dosing strategy for pazopanib is becoming increasingly inappropriate in the era of personalized medicine.[19, 20] Recommendations for individualized dosing of pazopanib and other tyrosine kinase inhibitors have been made previously.[21, 22] Moreover, specifically for pazopanib the safety and feasibility of individualized dosing has been established in a prospective clinical trial.[13]
Collectively, the current study and data available in the literature [5, 13] point towards the need to validate the strategy of individualized pazopanib dosing in a prospective randomized clinical trial.

Conclusion

In conclusion, at the currently approved fixed dose regimen a relevant subgroup of 16.4% of patients treated with pazopanib is underexposed in routine care and may be at risk of suboptimal treatment efficacy.

Our study further confirms that the previously established threshold of C_{min} >20 mg/L is related to longer progression free survival in renal cell carcinoma patients (34.1 versus 12.5 weeks, n=35, p=0.027). Moreover, exploratory analyses point towards a similar association of increased progression free survival with higher exposure in soft tissue sarcoma patients (18.7 versus 8.8 weeks, n=26, p=0.142).

Plasma C_{min} monitoring of pazopanib can help identify patients with low C_{min} for whom treatment at a higher dose may be appropriate.

Compliance with Ethical Standards:

Funding

No funding was received for this research.

Disclosures

N. Steeghs received an unrestricted grant (funding and study medication) from GlaxoSmithKline as Principal Investigator for an investigator initiated study with Pazopanib. Pazopanib is an asset of Novartis as of June 2015.

R.B. Verheijen, L.E. Swart, J.H. Beijnen, J.H.M. Schellens and A.D.R. Huitema declare they have no conflicts of interest to disclose.

Ethical approval

All procedures performed in this study involving human participants were in accordance with the ethical standards of the institutional and/or national research committee and with the 1964 Helsinki declaration and its later amendments or comparable ethical standards.

Informed consent

For this type of retrospective study formal consent was not required.

References

1. Kumar R, Knick VB, Rudolph SK, et al (2007) Pharmacokinetic-pharmacodynamic correlation from mouse to human with pazopanib, a multikinase angiogenesis inhibitor with potent antitumor and antiangiogenic activity. Mol Cancer Ther 6:2012–2021. doi: 10.1158/1535-7163.MCT-07-0193
2. Hamberg P, Verweij J, Sleijfer S (2010) (Pre-) clinical pharmacology and activity of pazopanib, a novel multikinase angiogenesis inhibitor. Oncologist 15:539–47. doi: 10.1634/theoncologist.2009-0274
3. Sternberg CN, Davis ID, Mardiak J, et al (2010) Pazopanib in locally advanced or metastatic renal cell carcinoma: Results of a randomized phase III trial. J Clin Oncol 28:1061–1068. doi: 10.1200/JCO.2009.23.9764
4. van der Graaf WT, Blay JY, Chawla SP, et al (2012) Pazopanib for metastatic soft-tissue sarcoma (PALETTE): a randomised, double-blind, placebo-controlled phase 3 trial. Lancet 379:1879–1886. doi: 10.1016/S0140-6736(12)60651-5
5. Suttle AB, Ball H, Molimard M, et al (2014) Relationships between pazopanib exposure and clinical safety and efficacy in patients with advanced renal cell carcinoma. Br J Cancer 111:1–8. doi: 10.1038/bjc.2014.503
6. Yu H, van Erp N, Bins S, et al (2016) Development of a Pharmacokinetic Model to Describe the Complex Pharmacokinetics of Pazopanib in Cancer Patients. Clin Pharmacokinet. doi: 10.1007/s40262-016-0443-y
7. Deng Y, Sychterz C, Suttle AB, et al (2013) Bioavailability, metabolism and disposition of oral pazopanib in patients with advanced cancer. Xenobiotica 43:443–53. doi: 10.3109/00498254.2012.734642
8. Hurwitz HI, Dowlati A, Saini S, et al (2009) Phase I trial of pazopanib in patients with advanced cancer. Clin Cancer Res 15:4220–4227. doi: 10.1158/1078-0432.CCR-08-2740
9. Verheijen RB, Beijnen JH, Schellens JHM, et al (2017) Clinical Pharmacokinetics and Pharmacodynamics of Pazopanib: Towards Optimized Dosing. Clin Pharmacokinet. doi: 10.1007/s40262-017-0510-z
10. Marin D, Bazeos A, Mahon FX, et al (2010) Adherence is the critical factor for achieving molecular responses in patients with chronic myeloid leukemia who achieve complete cytogenetic responses on imatinib. J Clin Oncol 28:2381–2388. doi: 10.1200/JCO.2009.26.3087
11. Lewis JH, Kilgore ML, Goldman DP, et al (2003) Participation of patients 65 years of age or older in cancer clinical trials. J Clin Oncol 21:1383–1389. doi: 10.1200/JCO.2003.08.010
12. Mitchell AP, Harrison MR, Walker MS, et al (2015) Clinical Trial Participants With Metastatic Renal Cell Carcinoma Differ From Patients Treated in Real-World Practice. J Oncol Pract 11:491–7. doi: 10.1200/JOP.2015.004929
13. Verheijen RB, Bins S, Mathijssen RHJ, et al (2016) Individualized Pazopanib Dosing: A Prospective Feasibility Study in Cancer Patients. Clin Cancer Res 22:5738–5746. doi: 10.1158/1078-0432.CCR-16-1255
14. Herbrink M, de Vries N, Rosing H, et al (2016) Quantification of 11 therapeutic kinase inhibitors in human plasma for therapeutic drug monitoring using liquid chromatography coupled with tandem mass spectrometry. Ther Drug Monit 38:649–656. doi: 10.1097/FTD.0000000000000349
15. Wang Y, Chia YL, Nedelman J, Schran H (2009) A Therapeutic Drug Monitoring Algorithm for Refining the Imatinib Trough Level Obtained at Different Sampling Times. Ther Drug Monit 31:579–584.
16. R Core Development Team (2016) A Language and Environment for Statistical Computing. In: Vienna, Austria R Found. Stat. Comput. https://www.r-project.org/.
17. Food and Drug Administration. Center for Drug Evaluation and Research (2008) Pazopanib Clinical Pharmacology and Biopharmaceutics Review.
18. Glade Bender JL, Lee A, Reid JM, et al (2013) Phase I pharmacokinetic and pharmacodynamic study of pazopanib in children with soft tissue sarcoma and other refractory solid tumors: a children's oncology group phase I consortium report. J Clin Oncol 31:3034–3043. doi: 10.1200/JCO.2012.47.0914
19. Ornstein MC, Rini BI (2016) Pharmacokinetically-guided dosing of oral drugs: true precision oncology? Clin Cancer Res 22:5626–5628. doi: 10.1158/1078-0432.CCR-16-1833

20. Beumer JH (2013) Without therapeutic drug monitoring, there is no personalized cancer care. Clin Pharmacol Ther 93:228–230. doi: 10.1038/clpt.2012.243

21. Yu H, Steeghs N, Nijenhuis CM, et al (2014) Practical guidelines for therapeutic drug monitoring of anticancer tyrosine kinase inhibitors: focus on the pharmacokinetic targets. Clin Pharmacokinet 53:305–25. doi: 10.1007/s40262-014-0137-2

22. de Wit D, Guchelaar H-J, den Hartigh J, et al (2015) Individualized dosing of tyrosine kinase inhibitors: are we there yet? Drug Discov Today 20:18–36. doi: 10.1016/j.drudis.2014.09.007

Chapter 2.5

Individualized Pazopanib Dosing: a Prospective Feasibility Study in Cancer Patients

Remy B. Verheijen[1*], Sander Bins[2*], Ron H.J. Mathijssen[2], Martijn P. Lolkema[2,3], Leni van Doorn[2] Jan H.M. Schellens[4,5], Jos H. Beijnen[1,5], Marlies H.G. Langenberg[3], Alwin D.R. Huitema[1], Neeltje Steeghs[3,4]. On behalf of the Dutch Pharmacology Oncology Group.

[1]Department of Pharmacy & Pharmacology, The Netherlands Cancer Institute - Antoni van Leeuwenhoek, Louwesweg 6, 1066 EC Amsterdam, The Netherlands.
[2]Department of Medical Oncology, Erasmus MC Cancer Institute, Wytemaweg 80, 3015 CN Rotterdam, The Netherlands.
[3]Department of Medical Oncology, UMC Utrecht Cancer Center, University Medical Center Utrecht, Heidelberglaan 100, 3584 CX Utrecht, The Netherlands.
[4]Department of Medical Oncology and Clinical Pharmacology, The Netherlands Cancer Institute - Antoni van Leeuwenhoek, Plesmanlaan 121, 1066 CX Amsterdam, The Netherlands.
[5]Department of Pharmaceutical Sciences, Utrecht University, Universiteitsweg 99, Utrecht, The Netherlands.
** Both authors contributed equally to this study*

Abstract

Purpose: Pazopanib is a tyrosine kinase inhibitor approved for the treatment of renal cell carcinoma and soft tissue sarcoma. Retrospective analyses have shown that an increased median PFS and tumor shrinkage appears in patients with higher plasma trough levels (C_{min}). Therefore, patients with low C_{min} might benefit from pharmacokinetically-guided individualized dosing.

Experimental design: We conducted a prospective multicenter trial in 30 patients with advanced solid tumors. Pazopanib C_{min} was measured weekly by LC-MS/MS. At week 3, 5 and 7 the pazopanib dose was increased if the measured C_{min} was <20 mg/L and toxicity was < grade 3.

Results: In total, 17 patients had at least one C_{min} <20 mg/L at week 3, 5 and 7. Of these, 10 were successfully treated with a pharmacokinetically-guided dose escalation, leading to daily dosages ranging from 1000 to 1800 mg daily. C_{min} in these patients increased significantly from 13.2 (38.0%) mg/L (mean (CV%)) to 22.9 mg/L (44.9%). Thirteen patients had all C_{min} levels ≥20.0 mg/L. Of these, nine patients with a high C_{min} of 51.3 mg/L (45.1%) experienced ≥ grade 3 toxicity and subsequently required a dose reduction to 600 or 400 mg daily, yet in these patients C_{min} remained above the threshold at 28.2 mg/L (25.3%).

Conclusions: A pharmacokinetically-guided individualized dosing algorithm was successfully applied and evaluated. The dosing algorithm led to patients being treated at dosages ranging from 400 to 1800 mg daily. Further studies are needed to show a benefit of individualized dosing on clinical outcomes such as progression free survival.

Introduction

Pazopanib is a tyrosine kinase inhibitor targeting VEGFR-1,2,3, PDGFR α/β, FGFR and c-Kit (1). Pazopanib increased progression free survival (PFS) from 4.2 to 9.2 months in renal cell carcinoma (RCC) and from 1.6 to 4.6 months in soft tissue sarcoma (STS) compared to placebo (2,3).

A retrospective analysis in 177 RCC patients by Suttle et al. showed an increased tumor shrinkage and longer PFS in patients with plasma trough levels (C_{min}) ≥20.5 mg/L compared to patients with a C_{min} below this threshold (4). Median PFS was found to be 50.2 weeks in patients with higher pazopanib C_{min} versus 19.6 weeks in patients with lower C_{min}. Median tumor shrinkage was 37.9% in the high versus 6.9% in the low exposure group. No further increase in PFS or tumor shrinkage was found above a pazopanib plasma concentration of 20.5 mg/L.

This threshold for efficacy seems to be in accordance with preclinical data showing optimal VEGFR2 inhibition by pazopanib in vivo at a concentration ≥17.5 mg/L (40 µmol/L) in mouse models (5). Additionally, in the phase I trial hypertension, a pharmacodynamic biomarker for response to anti-angiogenic agents, correlated with C_{24h} values above 15 mg/L at day 22 (6). Plasma concentrations were also correlated with radiographic response in a phase II study of patients with progressive, radioiodine-refractory, metastatic differentiated thyroid cancers treated with pazopanib (7). The above indicates that efficacy of pazopanib is strongly associated with pharmacokinetic (PK) exposure in many tumor types.

Pazopanib PK shows significant inter-individual variability in plasma exposure (6,8,9) and may be affected by various factors, such as concomitant medication (e.g. drugs increasing gastric pH or inhibiting/inducing CYP3A4), intake of food, patient compliance and (exact) time of tablet ingestion and blood sampling (9–12).

Despite the large variability in exposure, pazopanib is currently still administered at a fixed dose of 800 mg daily. This may however result in suboptimal treatment in a subset of patients who have a low C_{min}. In a retrospective analysis performed by the manufacturer of pazopanib, 20% of patients had a C_{min} below 20.5 mg/L and might have had benefit from an increased dose (4).

The feasibility of PK-guided dosing has already been shown in prospective clinical trials for tamoxifen (13) and another tyrosine kinase inhibitor with similar properties, sunitinib (14). Therefore, we now conducted a prospective feasibility trial to investigate whether the dose of pazopanib could be safely increased in patients who have a low C_{min} on the fixed 800 mg dose of pazopanib and whether this led to increased drug exposure, without intolerable toxicity.

Materials and methods

Patient population

Cancer patients for whom pazopanib was considered standard of care, or for whom no remaining standard treatment options were available, were eligible for enrollment. Patients also had to be at

least 18 years of age, had to have a WHO performance score of 0 or 1, needed to have evaluable disease according to RECIST 1.1 and also had to have an adequate organ function at baseline defined as: absolute neutrophil count ≥ 1.5x10^9/L, hemoglobin ≥ 5.6 mmol/L, platelets ≥ 100x10^9/L, prothrombin time or international normalized ratio ≤ 1.2x ULN, activated partial thromboplastin time ≤ 1.2x ULN, total bilirubin ≤ 1.5x ULN, alanine amino transferase and aspartate aminotransferase ≤ 2.5x ULN, serum creatinine ≤ 133 µmol/L or, if >133 µmol/L a calculated creatinine clearance of 30 to 50 mL/min, urinary protein (on dipstick) <2 + or <1 gram in 24-hour urine.
Exclusion criteria were: corrected QT interval (QTc) > 480 milliseconds, history of any relevant cardiovascular conditions, cerebrovascular accidents, transient ischemic attack, pulmonary embolisms or untreated deep venous thrombosis (DVT) within the past 6 months, poorly controlled hypertension (defined as systolic blood pressure (SBP) of ≥140 mmHg or diastolic blood pressure (DBP) of ≥ 90mmHg), clinically significant gastrointestinal abnormalities that might increase the risk for gastrointestinal bleeding, major surgery or trauma within 28 days prior to first pazopanib dose, evidence of active bleeding or bleeding diathesis, known endobronchial lesions and/or lesions infiltrating major pulmonary vessels, recent hemoptysis within 8 weeks before the first dose, any anti-cancer therapy within 14 days or five half-lives of the previous anti-cancer drug (whichever was longer) prior to first pazopanib dose, any ongoing toxicity from prior anti-cancer therapy that was grade >1 and/or that was progressing in severity, except for alopecia.

Pharmacokinetically guided dosing
All patients started at the approved pazopanib dose of 800 mg once daily (QD). Plasma samples for C_{min} measurements were collected weekly in the first 8 weeks of pazopanib treatment and every 4 weeks thereafter. Pazopanib concentrations were measured using a validated LC-MS/MS assay.
A 10 µL plasma aliquot was used, to which 500 µL of methanol containing $^{13}C,^{2}H_3$-pazopanib as internal standard and 500 µL of 10 mM ammonium hydroxide in water were added. This solution was then centrifuged at 15.000 rpm and 5 µL of the supernatant was injected into the LC-MS/MS system (LC-system from Agilent Technologies (Santa Clara, CA) and API3000 MS by AB Sciex (Framingham, MA). Elution was performed using an isocratic gradient of 45% 10 mM ammonium hydroxide in water and 55% methanol on a Gemini C18 column, 2.0 x 50 mm, 5 µm by Phenomenex (Torrance, CA). This assay was validated and fulfilled all requirements of the FDA and EMA guidelines for bioanalytical method validation. C_{min} results were reported to the treating physician within 1 week.

At week 3, day 1 (Day 15); week 5, day 1 (Day 29) and week 7, day 1 (Day 43), the dose could be adapted, based on the measured C_{min} collected a week earlier and observed toxicity was graded according to the National Cancer Institute's Common Terminology Criteria for Adverse Events (NCI-CTCAE v4.02).
The target exposure for efficacy used during this trial was a C_{min} ≥20.0 mg/L. Patients with a C_{min} <15.0 mg/L received a dose increase of 400 mg daily in the absence of ≥ grade 2 toxicity or 200 mg

daily when experiencing grade 2 toxicity, but not ≥ grade 3 adverse events (AEs). Patients with a C_{min} of 15.0-19.9 mg/L received a 200 mg dose increase if toxicity was below grade 3. No patients would be treated above the prespecified dose limit of 2,000 mg QD, as this was the highest dose previously tested in humans (6). In case of severe (≥ grade 3) treatment related toxicity the dose was lowered by 1 dose level, or to the previous dose level in case of an earlier dose increment.

Safety assessments

Recording of AEs, physical examination, hematology and blood chemistry assessments were performed weekly during the first 8 weeks and monthly thereafter. The incidence, severity, start and end dates of all serious AEs (SAEs) and of non-serious AEs related to pazopanib were recorded.

Efficacy assessments

CT-scan and/or MRI-scans were performed every 8 weeks after initiation of therapy until documented disease progression according to the Response Evaluation Criteria in Solid Tumors (RECIST) version 1.1. Data on best response and time to progression was collected.

Statistical methods

All statistical analyses were performed in R version 3.2.2 (15). For exposure-response relationships the mean of all measured C_{min} levels for each patient during the entire treatment period (from start of treatment to discontinuation) was used as the measure of pazopanib exposure. For the purpose of exposure-toxicity relationships, the C_{min} measurement closest to the first presentation of the toxicity was used. Unless otherwise specified, hypotheses were tested using a two-sided independent sample t-test. P-values <0.05 were considered significant.

Study Conduct and registry

This trial was conducted in accordance with the World Medical Organization declaration of Helsinki, compliant with Good Clinical Practice and approved by the Medical Ethics Committee of the each participating medical centers. All patients provided written informed consent before enrollment. This trial was registered in the EudraCT database (2013-001567-24) and the Netherlands Trial Registry (NTR3967).

Results

Patient population

A total of 30 patients were included from September 2013 until March 2014 in 3 Dutch cancer centers. Characteristics of included patients are shown in table 1. Tumor types of included patients were soft tissue sarcoma (n=7), colorectal carcinoma (n=6), cancer of unknown primary (n=4), neuroendocrine carcinoma (n=2), thymus carcinoid, hepatocellular carcinoma, ovarian carcinoma,

mesothelioma, esophageal carcinoma, meningeoma, perivascular epithelial tumor, renal cell carcinoma, choroidal melanoma, endometrial carcinoma and cholangiocarcinoma (all n=1).
All patients received at least one dose of pazopanib, underwent at least one C_{min} measurement and were eligible for PK evaluation. Median study follow up was 34 weeks.

Table 1: Demographics of included patients.

Characteristic	**Patients (n=30)**
Gender (n (%))	
Male	14 (47)
Female	16 (53)
Age (median (range))	
	58 (33– 88)
Steady state C_{min} (mg/L) at 800 mg dose (W2D1) (mean (CV %))	
	30.0 (71.9)
Performance status (n (%))	
0	7 (23)
1	23 (77)
Previous lines of systemic therapy (median (range))	
	2 (1-5)
Type (n (%))	
Chemotherapy	24 (80)
Targeted therapy	7 (23)
Endocrine therapy	3 (10)
Primary tumor (n (%))	
Soft tissue sarcoma	7 (23)
Colorectal carcinoma	6 (20)
Cancer of unknown primary	4 (13)
Neuroendocrine carcinoma	2 (6)
Miscellaneous*	11 (33)

** Hepatocellular carcinoma, ovarian carcinoma, mesothelioma, esophageal carcinoma, meningeoma, perivascular epithelial tumor, renal cell carcinoma, choroidal melanoma, endometrial carcinoma, cholangiocarcinoma and thymus carcinoid (all n=1).*

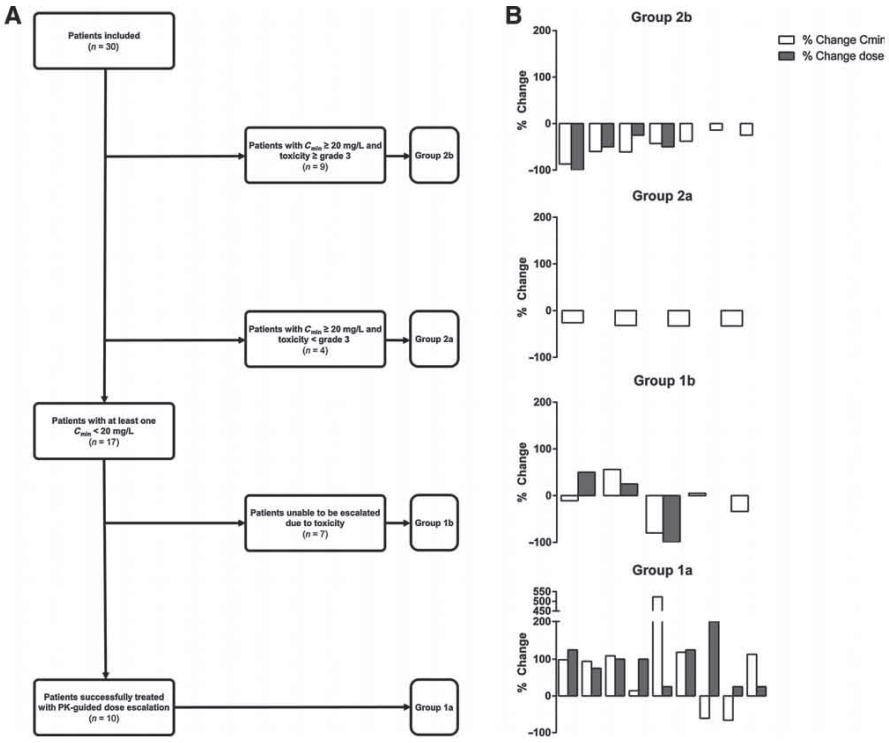

Figure 1: *Left Panel:* Trial outcome flowchart. Toxicity for the purposes of this chart is defined as any adverse event requiring a dose interruption or reduction in the first 8 weeks of treatment. C_{min} below or above the target of ≥20.0 mg/L is based on samples from week 2, 4 or 6 as per protocol dose escalations were based on these samples. *Right Panel:* Percent change in dose from baseline (steady state at W2D1) to the end of the dose algorithm period (Last dose change (W7D1) and corresponding steady state C_{min} W8D1). Grey bars represent % change in pazopanib dose (mg QD) white bars represent % change in pazopanib C_{min} (mg/L). Each patient is represented by adjacent bars, plotted per treatment outcome group, only patients evaluable at both week 2 and week 8 are shown.

Pharmacokinetic guided dosing

Based on treatment outcome patients were divided into four groups, see figure 1. Patients who had at least one C_{min} below 20.0 mg/L at day 15, 29 or 43 were appointed group 1, patients who had all these C_{min} measurement above the target were appointed group 2. Patients who did not experience any toxicity requiring a dose reduction or interruption during the dose escalation period (the first 8 weeks of treatment) were classified as group a (no severe toxicity), those who did were classed as group b (severe toxicity). Based on this classification the distribution of patients was 10 in group 1a (eligible for a dose escalation), 7 in 1b (no dose escalation possible due to toxicity), 4 in group 2a (adequate C_{min}, no toxicity) and 9 in group 2b (adequate C_{min}, severe toxicity) (figure 1). A

full overview of treatment outcomes (C_{min} measurements, dose received and percentage of patients above the C_{min} target) is provided in table 2. Plots of the C_{min} over time per treatment outcome group are shown in figure 2.

Table 2: Pazopanib C_{min}, percentage of patients above target and dose per treatment outcome group‡.

Outcome	Group 1a	Group 1b	Group 2a	Group 2b	Total
	TOX - C_{min} <20.0 mg/L	TOX + C_{min} <20.0 mg/L	TOX - C_{min} ≥20.0 mg/L	TOX + C_{min} ≥20.0 mg/L	
	n = 10	n = 7	n = 4	n = 9	n = 30
Mean pazopanib C_{min} (mg/L (CV %))					
W2D1	13.2 (38.0)	19.7 (56.6)	37.4 (19.4)	51.3 (45.1)	30.0 (71.9)
W4D1	15.5 (52.8)	16.2 (39.6)	31.8 (8.1)	39.4 (29.5)	24.8 (54.8)
W6D1	19.7 (27.4)	13.3 (39.6)	26.8 (29.2)	33.2 (30.5)	22.8 (43.2)
W8D1	22.9 (44.9)	18.9 (40.5)	25.9 (18.8)	28.2 (25.3)	24.1 (33.9)
% of pts above the target C_{min} of ≥20.0 mg/L†					
W2D1	10.0	42.8	100.0	100	56.7
W4D1	20.0	14.3	100.0	88.6	50.0
W6D1	40.0	14.3	100.0	66.6	50.0
W8D1	40.0*	28.6	100.0	55.6	50.0
Mean daily pazopanib Dose (mg)					
W3D1	1040	933	800	725	893
W5D1	1280	1000	800	667	1000
W7D1	1378	950	800	633	1009

**40% of patients in group 1a achieved the target in week 8. During study follow up, 7 patients in group 1a (70%) achieved target exposure of > 20.0 mg/L within 3 months since start of treatment.*

†Patients for whom no C_{min} was available or who discontinued treatment are scored as below the target.

‡Toxicity for the purposes of grouping is defined as any adverse event requiring a dose interruption or reduction in the first 8 weeks of treatment. C_{min} below or above the target of ≥20.0 mg/L is based on samples from week 2, 4 or 6.

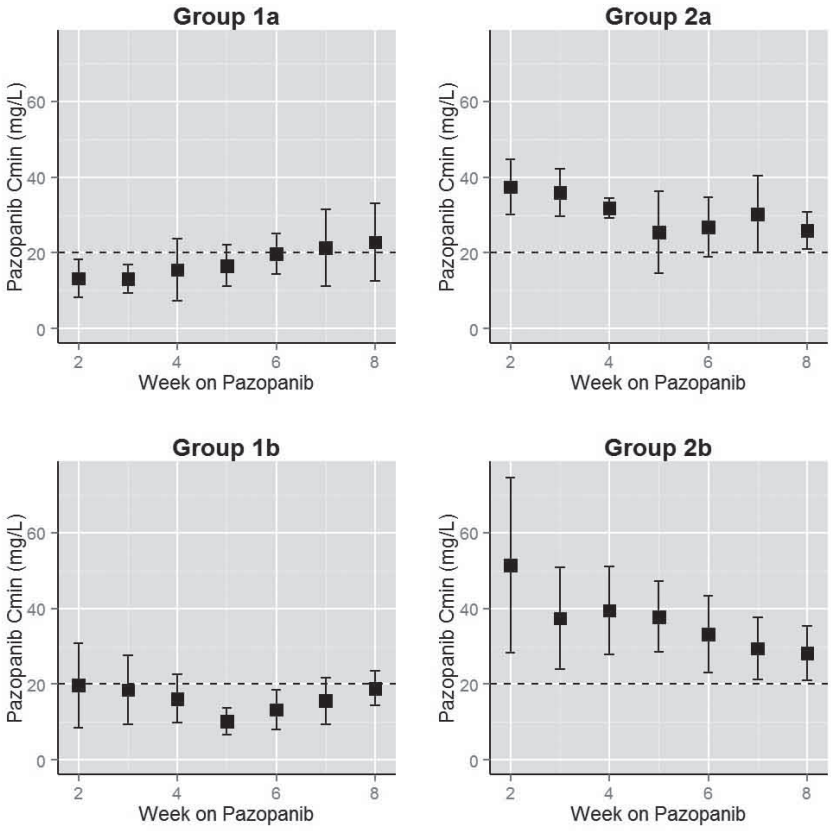

Figure 2: Pazopanib exposure over time per outcome group (mean C_{min} ± standard deviation). The dotted line indicates the threshold of 20 mg/L. C_{min} did not change in group 1b (p=0.89). In group 2a and 2b C_{min} declined significantly (p=0.04 and 0.04 respectively). Group 1a showed a significant increase in C_{min} from 13.2 mg/L to 22.9 mg/L (p=0.02).

Group1a: Group 1a (patients with low drug exposure, and no severe toxicity) consisted of 10 patients who were sustainably treated at an increased dose. The C_{min} in this group increased from 13.2 (CV 38.0%) mg/L in week 2 to 22.9 (CV 44.9%) mg/L in week 8 (p=0.02). Only two patients did not show an increase in C_{min} after the dose escalation. Four patients reached the target at the end of the dose escalation period (week 8) and 7 patients reached the target exposure of ≥20 mg/L within 3 months of treatment. After the last dose escalation (day 43), patients in group 1a were treated at a mean dose of 1,378 mg, ranging from 1,000 to 1,800 mg. One patient was treated with 1,800 mg QD for over 33 weeks, with acceptable (<grade 3) toxicity.

Group 1b: Patients in group 1b (patients with low drug exposure, but with toxicity requiring a dose interruption or reduction, n=7) had a stable C_{min} during the dose escalation phase. In this group, one patient could not have a dose escalation because of toxicity (ASAT/ALAT increase) at the prespecified

dose escalation moments. Another patient required a dose interruption but could later continue treatment on 800 mg QD. Five patients experienced toxicity after an initial escalation and required a subsequent dose reduction. Four of these five could hereafter be treated successfully until disease progression at a dose of 800 mg (n=3) or 1,000 mg (n=1) daily. One patient discontinued treatment due to toxicity after dose escalation (fatigue, grade 3).Their C_{min} was 19.7 (CV 56.6%) mg/L at week 2 and 18.9 (CV 40.5%) mg/L at week 8 (p=0.89).

Group 2a: Four patients (group 2a, patients with high drug exposure, and no severe toxicity) could be treated on the fixed 800 mg dose with adequate C_{min} without the need for a dose reduction or interruption in the first 8 weeks. Surprisingly, the C_{min} decreased in these patients from 37.4 mg/L (CV 19.4%) at week 2 to 25.9 mg/L (CV 18.8%) at week 8 (p=0.04).

Group 2b: Patients in group 2b (patients with a high drug exposure, but also severe toxicity, n=9) had a decrease in C_{min} from week 2 to week 8 from 51.3 mg/L (CV 45.1%) to 28.2 mg/L (CV 25.3%) (p=0.04). The mean dose was reduced from 800 mg to 600 mg in the same interval.

Use of gastric acid reducing agents was discouraged but not prohibited during this trial. Of patients in the low exposure groups 9 (7 in group 1a and 2 in 1b) and in the high exposure groups 4 (all in 2b) used a PPI at any point during treatment. Patients were instructed to take the PPI concomitantly with pazopanib as recommended in the summary of product characteristics.

Adverse Events

An overview of the observed AEs related to pazopanib with a frequency of ≥10% is shown in table 3. The most common severe (≥ grade 3) AEs were hypertension, fatigue, ASAT/ALAT increase.

Less patients experienced ≥ grade 3 AEs in the low exposure groups (1a and 1b), with 41.2% of patients experiencing at least one ≥ grade 3 AE, compared to 76.9% in the high exposure groups (2a and b). The percentage of patients discontinuing due to toxicity was similar between the high and low exposure groups, 11.8% in 1a plus 1b and 15.4% in 2a plus 2b.

Of patients with a high exposure requiring a dose reduction (group 2b, n=9), all but 2 (both cases fatigue grade 3) could be successfully treated at a lower dose until disease progression.

Overall, events causing the discontinuation were fatigue (n=3) and ASAT/ALAT increase (n=1). Remarkably, the C_{min} at week 2 appeared higher in patients in group 1 experiencing toxicity (19.7 mg/L versus 13.2 mg/L (p=0.19), respectively) and the same trend was observed in group 2 (37.4 mg/L for patients without toxicity versus 51.3 mg/L for patients with toxicity (p=0.27), respectively). Patients who experienced fatigue (n=3) or ASAT/ALAT increase (n=2) had a C_{min} (at first presentation of grade 3 toxicity) 51.4 mg/L (range 21.4 - 98.1) and 8.9 mg/L (range 7.3 – 10.5) respectively. Patients with grade 3 hypertension (n=11) had a C_{min} at presentation of 37.3 mg/L (range 7.0 - 76.5) while that patients who experienced grade 2 hypertension (n=10) was 27.8 mg/L (range 16.7 – 43.8).

Table 3: Toxicity data per outcome group‡, only toxicities related to pazopanib with a frequency of ≥10% are shown. Data are presented as number patients (n).

Adverse event	Group 1a		Group 1b		Group 2a		Group 2b		Total	
	TOX - C_{min} ↓ n = 10		TOX + C_{min} ↓ n = 7		TOX - C_{min} ↑ n = 4		TOX + C_{min} ↑ n = 9		n=30	
	Any grade	Grade ≥ 3	Any grade	Grade ≥ 3	Any grade	Grade ≥ 3	Any grade	Grade ≥ 3	Any grade	Grade ≥ 3
Hypertension	4	2*	3	2	1	1*	7	6	15	11
Fatigue	3	0	3	1	1	0	6	2	13	3
Diarrhea	4	1*	4	0	2	0	2	0	12	1
Nausea	2	0	0	0	1	0	6	0	9	0
Rash	2	0	3	1	0	0	3	0	8	1
Hair depigmentation	3	0	2	0	3	0	0	0	8	0
ASAT increase	1	0	2	2	2	0	1	0	6	2
ALAT increase	1	0	2	2	0	0	2	0	5	2
Anorexia	2	0	1	0	0	0	1	0	4	0
Weight loss	1	0	1	0	0	0	2	0	4	0
Dysgeusia	0	0	0	0	2	0	2	0	4	0
Vomiting	1	0	0	0	1	0	2	0	4	0
Edema	0	0	1	0	1	0	1	0	3	0
Proteinuria	1	0	0	0	0	0	2	0	3	0
Dyspnea	1	0	0	0	1	0	1	0	3	0

**These grade 3 toxicities did not result in a dose reduction or discontinuation or occurred after the 8 week dose escalation period.*

‡Toxicity for the purposes of grouping is defined as any adverse event requiring a dose interruption or reduction in the first 8 weeks of treatment. C_{min} below or above the target of ≥20.0 mg/L is based on samples from week 2, 4 or 6.

Efficacy

From 27 patients at least one response evaluation was available. Of these, 3 patients had a partial response (perivascular epithelial tumor, renal cell carcinoma and soft tissue sarcoma, all n=1), 18 had stable disease, and 6 had progressive disease as best response.

The mean of all measured C_{min} levels per patient (from start of treatment to discontinuation) was calculated as a measure of exposure during pazopanib therapy for the purpose of exposure-response relationships. Overall, the average of the mean C_{min} of each patient was 24.4 mg/L (CV 39.1%). In total, 19 patients had a mean C_{min} above and 11 below the target of 20 mg/L. A waterfall plot of the maximum decrease in tumor size from baseline is shown in figure 3. All three patients who had a partial response had a mean C_{min} above the 20 mg/L threshold (with an average of 27.6 mg/L (CV 14.4%). In non-prespecified, exploratory analyses of all evaluable patients (n=27), tumor response was associated with mean C_{min} of pazopanib. An average change from baseline for patients above and below the PK threshold of -6.49% and +14.6% respectively, (p=0.01). In soft tissue sarcoma patients (n=7), mean change from baseline was -6.01% (n=5) for patients above the threshold and +13.5% for patients below (n=2)(p=0.28). In sarcoma patients PFS was 47.9 weeks (range 8 - 60, n=5) and 11.5 weeks (range 7 - 16, n=2) for patients below the PK threshold (p=0.06, log-rank test).

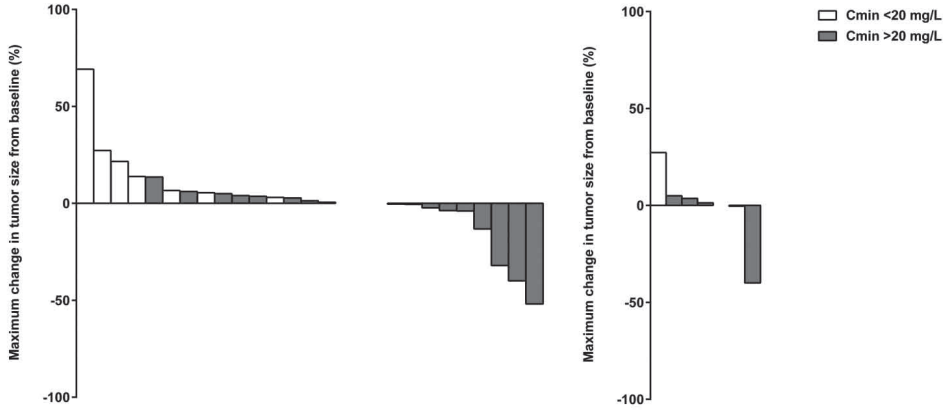

Figure 3: *Left panel*: Waterfall plot showing the maximum change in tumor size from baseline in all evaluable patients (n = 27). Grey bars represent patients with a mean C_{min} ≥20.0 mg/L (n=17), white bars represent patients with a C_{min} <20.0 mg/L (n=10). Mean change from baseline for all evaluable patients (n=27) above and below the PK threshold was -6.49% and +14.6%, (p=0.01). *Right Panel:* Mean change from baseline in soft tissue sarcoma patients (n=7) above and below the PK threshold was -6.01% (n=5) and +13.5% (n=2), (p=0.28).

Discussion

We performed a prospective multicenter clinical trial to assess the safety and feasibility of PK-guided individualized dosing of pazopanib in 30 patients with advanced solid tumors.

With the PK-guided dosing algorithm, 33.3% of all patients could be treated at a higher dose (1000 – 1800 mg daily) with acceptable toxicity (figure 1). Most of these patients achieved the target C_{min} of 20.0 mg/L within study follow up. Furthermore, overall variability in pazopanib C_{min} was reduced from 71.9% before the dose escalation period to 33.9% thereafter (table 2).

An equal number of patients discontinued treatment in the low C_{min} versus the high C_{min} group and only one patient discontinued treatment after a dose escalation. This suggests PK-guided increasing of the dose does not lead to more severe toxicity or higher rates of treatment discontinuation. Meanwhile, a reduction of the dose in case of very high systemic concentrations, may lead to less toxicity and still maintain therapeutic C_{min} levels (group 2b, figure 2).
High pazopanib exposure seemed predictive of dose reductions for toxicity in patients not eligible for a dose escalation (group 2a en 2b). The C_{min} at week 2 was higher (though not significantly) in the patients that would require a dose reduction (2b) than those who would not (2a), (mean of 51.3 versus 37.4 mg/L, table 2, figure 2). This implies that patients are unlikely to tolerate a very high trough level for a longer period of time and could support strategies to prevent toxicity by implementing dose reduction in patients with C_{min} >50 mg/L, although this is based on limited data. No clear relations between C_{min} and specific grade ≥ 3 toxicities were found. The most common severe AE was hypertension. This is thought to be related to higher pazopanib exposure (6), our study found a mean C_{min} at occurrence of hypertension 37.3 and 27.8 mg/L in patients experiencing grade 3 (n=11) and 2 (n=10) hypertension respectively. But this was not significantly higher than the overall mean C_{min}. It might be the case however, that another pharmacokinetic parameter (e.g. C_{max}) may be more appropriate to study exposure-toxicity relationships than C_{min}, the one used in the current trial.
Two patients experienced severe hepatotoxicity, in one case leading to ASAT and ALAT values of over 13 times the upper limit of normal and discontinuation of treatment. This seemed unrelated to high exposure, as the mean C_{min} of these patients (in the sample closest in time to occurrence) was only 8.9 mg/L. This finding is corroborated by a recent study suggesting the mechanism of pazopanib hepatotoxicity may be immunological and therefore unrelated to pazopanib PK or dose (16).

A significant reduction in pazopanib C_{min} was seen in patients treated continuously at the 800 mg fixed dose (group 2a, figure 2).Though in our trial this group consisted of only a small number of patients, the same effect was observed in a population pharmacokinetic analysis of previously published clinical trials (17). A time dependent decrease in exposure was also observed for another tyrosine kinase inhibitor, imatinib (18). For imatinib, upregulation of drug transporters or CYP3A4 have been suggested as possible explanations, which could also be the case for pazopanib as it is a known substrate of both.

In addition to PK-guided dosing of pazopanib other dose individualization strategies could be explored. Pharmacodynamic biomarkers could be used for example, such as interleukin 12 (IL12) or soluble VEGFR2 (sVEGFR2) (19). However given that for pazopanib the relation between C_{min} and PFS was very significant at p=0.0038 and resulted in a remarkable median PFS difference of 32.4 weeks in RCC patients (4), C_{min} might be a more appropriate biomarker for pazopanib than sVEGFR2 or IL12. Toxicity based dosing could also be proposed as a dose individualization approach and has been explored previously for erlotinib (using rash), sorafenib and axitinib (both using hypertension) (20–22). A drawback of this strategy is that it, per definition, would lead to more toxicity. The PK-guided approach applied in this trial with pazopanib did not seem to lead to less tolerability.

Another trial was performed to assess PK-guided dosing of pazopanib by De Wit et al (9). In that trial, pazopanib area under the curve ($AUC_{0\text{-}24h}$) was used as the pharmacokinetic parameter to individualize dosing and a target window of 715-920 $mg{\cdot}h{\cdot}L^{-1}$ (corresponding to C_{min} values of 20.5 – 46.0 mg/L) was specified. The primary endpoint of that study in 13 patients was a reduction in variability and, per protocol, only one dose change was allowed. AUC-guided dosing did not significantly reduce inter-patient variability, probably due to intra-patient variability or sampling time issues. Based on this trial the authors concluded it may be more beneficial to target the C_{min} threshold rather than an AUC window (4,9).
In addition, dosing base on C_{min} will also be more practical to implement in routine care, as it requires just one instead of multiple samples. Moreover, as target inhibition is thought to be concentration dependent, dosing should strive to keep the drug concentration above a certain minimally efficacious concentration during the whole dose interval, which is most accurately reflected by C_{min}. Most importantly, studies relating pazopanib exposure to response have used $C_{min,}$ rather than AUC, further strengthening the case for C_{min} threshold monitoring (4,6).
Finally, self-sampling approaches facilitated by dried blood spot sampling may further enable the use of PK-guided dosing in routine care and several assays have already been developed for this purpose (23,24).

The number of patients who had a C_{min} below the target at a moment of possible dose modification was 56.7%, which is markedly higher than the 20% found by Suttle et al (4). This may partly be explained by the combination of repeated measurements and relatively large intra-individual variability in C_{min}. The large number of patients with low drug exposure may also partially be caused by use of proton pump inhibitors (PPI), which are known to decrease the pH-dependent absorption of pazopanib (25). 9 patients in the low exposure groups (1a and 1b) used a PPI. The use of gastric-pH increasing agents was discouraged but not prohibited during this trial. On the other hand, it also shows that PK-guided dosing may overcome the problem of pH-limited absorption of pazopanib in patients for whom treatment with PPIs is medically necessary.

A drawback of the current study is that dose modification was limited to three pre-specified time points. If later dose increments would have been allowed, more patients in the low exposure group might have achieved the target threshold.
Another limitation is that our study was performed in patients with a wide range of advanced solid tumors. Therefore, a satisfying analysis of the effect of individualized dosing on tumor response or PFS is impossible. Nonetheless, all patients who had a partial response had a C_{min} above the 20.0 mg/L threshold and in a non-prespecified analysis, we found significant association between tumor response (measured as maximum change in tumor size from baseline) and pazopanib C_{min}, which would provide further support for targeting a C_{min} of ≥20.0 mg/L. Interestingly, in a subgroup analysis of STS patients (n=7), a trend toward increased response and longer PFS with higher C_{min} was found. Yet, perhaps due to the small size of this subgroup, these results were not significant.
The results of this trial merit further investigation of individualized pazopanib dosing in cancer patients. A similar design to the one that was previously used for axitinib dose titration in RCC patients could be explored (21,26). As the ideal form of for future studies would be a prospective randomized placebo controlled trial in either STS or RCC patients.

Conclusion

In summary, this prospective multicenter trial in patients with advanced solid tumors showed that pazopanib dose could safely be escalated in selected patients with a C_{min} <20.0 mg/L and that pazopanib exposure increased significantly in patients whose dose was escalated based on a low C_{min}. Moreover, a significant association between C_{min} and tumor response was found.
The outcomes of this trial support further investigation of individualized pazopanib dosing, using the here described dosing algorithm, ideally in a large prospective randomized clinical trial using PFS or overall survival as an endpoint.

Acknowledgements

This investigator initiated study was supported by an unrestricted grant (funding and study medication) from GlaxoSmithKline and by a grant (funding) by Fund Nuts-Ohra**.** The funding sources had no involvement in the study design, collection, analysis and interpretation of data, the writing of the report or in the decision to submit the article for publication. Pazopanib is an asset of Novartis as of June 2015.
We would like to thank all patients for their participation in this study.

References

1. Hamberg P, Verweij J, Sleijfer S. (Pre-)clinical pharmacology and activity of pazopanib, a novel multikinase angiogenesis inhibitor. Oncologist. 2010;15:539–47.
2. Sternberg CN, Davis ID, Mardiak J, Szczylik C, Lee E, Wagstaff J, et al. Pazopanib in locally advanced or metastatic renal cell carcinoma: results of a randomized phase III trial. J Clin Oncol. 2010;28:1061–8.
3. van der Graaf WTA, Blay J-Y, Chawla SP, Kim D-W, Bui-Nguyen B, Casali PG, et al. Pazopanib for metastatic soft-tissue sarcoma (PALETTE): a randomised, double-blind, placebo-controlled phase 3 trial. Lancet. 2012;379:1879–86.
4. Suttle AB, Ball HA, Molimard M, Hutson TE, Carpenter C, Rajagopalan D, et al. Relationships between pazopanib exposure and clinical safety and efficacy in patients with advanced renal cell carcinoma. Br J Cancer. 2014;111:1909–16.
5. Kumar R, Knick VB, Rudolph SK, Johnson JH, Crosby RM, Crouthamel M-C, et al. Pharmacokinetic-pharmacodynamic correlation from mouse to human with pazopanib, a multikinase angiogenesis inhibitor with potent antitumor and antiangiogenic activity. Mol Cancer Ther. 2007;6:2012–21.
6. Hurwitz HI, Dowlati A, Saini S, Savage S, Suttle AB, Gibson DM, et al. Phase I Trial of Pazopanib in Patients with Advanced Cancer rial of Pazopanib in Patients with Advanced Cancer. Clin Cancer Res. 2009;4220–7.
7. Bible KC, Suman VJ, Molina JR, Smallridge RC, Maples WJ, Menefee ME, et al. Efficacy of pazopanib in progressive, radioiodine-refractory, metastatic differentiated thyroid cancers: results of a phase 2 consortium study. Lancet Oncol. 2010;11:962–72.
8. Deng Y, Sychterz C, Suttle AB, Dar MM, Bershas D, Negash K, et al. Bioavailability, metabolism and disposition of oral pazopanib in patients with advanced cancer. Xenobiotica. 2013;43:443–53.
9. de Wit D, van Erp NP, den Hartigh J, Wolterbeek R, den Hollander-van Deursen M, Labots M, et al. Therapeutic Drug Monitoring to individualize the dosing of pazopanib: a pharmacokinetic feasibility study. Ther Drug Monit. 2015 Jun;37(3):331-8
10. Heath EI, Chiorean EG, Sweeney CJ, Hodge JP, Lager JJ, Forman K, et al. A phase I study of the pharmacokinetic and safety profiles of oral pazopanib with a high-fat or low-fat meal in patients with advanced solid tumors. Clin Pharmacol Ther. 2010;88:818–23.
11. Tan AR, Gibbon DG, Stein MN, Lindquist D, Edenfield JW, Martin JC, et al. Effects of ketoconazole and esomeprazole on the pharmacokinetics of pazopanib in patients with solid tumors. Cancer Chemother Pharmacol. 2013;71:1635–43.
12. Xu CF, Xue Z, Bing N, King KS, McCann LA, de Souza PL, et al. Concomitant use of pazopanib and simvastatin increases the risk of transaminase elevations in patients with cancer. Ann Oncol. 2012;23:2470–1.
13. Fox P, Balleine R, Lee C, Gao B, Balakrishnar B, Menzies AM, et al. Dose escalation of tamoxifen in patients with low endoxifen level: evidence for therapeutic drug monitoring - The TADE Study. Clin Cancer Res. 2016;1078–0432.
14. Lankheet NAG, Kloth JSL, Gadellaa-van Hooijdonk CGM, Cirkel GA, Mathijssen RHJ, Lolkema MPJK, et al. Pharmacokinetically guided sunitinib dosing: a feasibility study in patients with advanced solid tumours. Br J Cancer; 2014;110:2441–9.
15. R Development Core Team (2011), R: A Language and Environment for Statistical Computing. Vienna, Austria: the R Foundation for Statistical Computing.

ISBN: 3-900051-07-0. Available online at http://www.R-project.org/.

16. Xu C-F, Johnson T, Wang X, Carpenter C, Graves A, Warren L, et al. HLA-B*57:01 Confers Susceptibility to Pazopanib-Associated Liver Injury in Patients with Cancer. Clin Cancer Res. 2016;22(6):1371-7.

17. Yu H. van Erp NP, Bins S, Mathijssen RHJ, Schellens JHM, Beijnen JHM, Steeghs N, Huitema ADR, Development of a Pharmacokinetic Model for Pazopanib – a Tyrosine Kinase Inhibitor used for the Treatment of Solid Tumours, Annual Meeting of the Population Approach Group in Europe, PAGE 25 Lisbon, (2016) Abstr 5926.

18. Eechoute K, Fransson MN, Reyners AK, de Jong FA, Sparreboom A, van der Graaf WTA, et al. A long-term prospective population pharmacokinetic study on imatinib plasma concentrations in GIST patients. Clin Cancer Res. 2012;18:5780–7.

19. Nikolinakos PG, Altorki N, Yankelevitz D, Tran HT, Yan S, Rajagopalan D, et al. Plasma cytokine and angiogenic factor profiling identifies markers associated with tumor shrinkage in early-stage non-small cell lung cancer patients treated with pazopanib. Cancer Res. 2010;70:2171–9.

20. Brahmer JR, Lee JW, Traynor AM, Hidalgo MM, Kolesar JM, Siegfried JM, et al. Dosing to rash: A phase II trial of the first-line erlotinib for patients with advanced non-small-cell lung cancer an Eastern Cooperative Oncology Group Study (E3503). Eur J Cancer; 2014;50:302–8.

21. Rini BI, Melichar B, Ueda T, Grünwald V, Fishman MN, Arranz JA, et al. Axitinib with or without dose titration for first-line metastatic renal-cell carcinoma: A randomised double-blind phase 2 trial. Lancet Oncol. 2013;14:1233–42.

22. Karovic S, Wen Y, Karrison TG, Bakris GL, Levine MR, House LK, et al. Sorafenib dose escalation is not uniformly associated with blood pressure elevations in normotensive patients with advanced malignancies. Clin Pharmacol Ther. 2014;96:27–35.

23. Verheijen RB, Bins S, Thijssen B, Rosing H, Nan L, Schellens JH, et al. Development and clinical validation of an LC – MS / MS method for the quantification of pazopanib in DBS. Bioanalysis. 2016;369–74.

24. de Wit, D, den hartigh, J, Gelderdblom, H, Qian, Y, den Hollander, M, Verheul, H, Guchelaar, HJ, van Erp N. Dried blood spot analysis for therapeutic drug monitoring of pazopanib. J Clin Pharmacol. 2015;55(12):1344-50

25. van Leeuwen RWF, van Gelder T, Mathijssen RHJ, Jansman FGA. Drug-drug interactions with tyrosine-kinase inhibitors: A clinical perspective. Lancet Oncol.; 2014;15:e315–26.

26. Rini BI, Melichar B, Fishman MN, Oya M, Pithavala YK, Chen Y, et al. Axitinib dose titration: analyses of exposure, blood pressure and clinical response from a randomized phase II study in metastatic renal cell carcinoma. Ann Oncol. 2015;26:1372–7.

Chapter 3

Clinical Pharmacology & Bioanalysis of Everolimus

Chapter 3.1

Validation and Clinical Application of an LC-MS/MS Method for the Quantification of Everolimus using Volumetric Absorptive Microsampling

R.B. Verheijen[1], B. Thijssen[1], F. Atrafi[2], J.H.M. Schellens[3,4], H.Rosing[1], N. de Vries[1], J.H. Beijnen[1,4], R.H.J. Mathijssen[2], N. Steeghs[3], A.D.R. Huitema[1,5]

[1]Department of Pharmacy & Pharmacology, The Netherlands Cancer Institute - Antoni van Leeuwenhoek, Louwesweg 6, 1066 EC Amsterdam, The Netherlands.
[2]Department of Medical Oncology, Erasmus MC Cancer Institute, Rotterdam, The Netherlands.
[3]Department of Medical Oncology and Clinical Pharmacology, The Netherlands Cancer Institute - Antoni van Leeuwenhoek, Amsterdam, The Netherlands.
[4]Department of Pharmaceutical Sciences, Utrecht University, Utrecht, The Netherlands.
[5]Department of Clinical Pharmacy, University Medical Center Utrecht, Utrecht, The Netherlands.

Abstract

Everolimus is a mammalian target of rapamycin inhibitor approved for the treatment of various tumor types. Less invasive measurement of everolimus concentrations could facilitate pharmacokinetic studies and personalized dosing based on whole blood concentrations, known as therapeutic drug monitoring.

Volumetric Absorptive Microsampling (VAMS) has been introduced as a patient friendly, less invasive sampling technique to obtain a dried blood sample of an accurate blood volume regardless of hematocrit value. We describe the bioanalytical validation and clinical application of an liquid chromatography tandem mass spectrometry (LC-MS/MS) method to quantify everolimus using VAMS.

$^{13}C_2D_4$-Everolimus was used as internal standard (IS). Everolimus and the IS were extracted with methanol, which was evaporated after ultrasonification and shaking. The residue was reconstituted in 20mM ammonium formate buffer and methanol of which 5 µL was injected into the MS/MS system. Quantification was performed for the ammonium adduct of everolimus in positive electrospray ion mode

The VAMS method met all pre-defined validation criteria. Overall accuracy and precision were within 11.1% and ≤14.6%, respectively. Samples were shown to be stable on the VAMS device for 362 days at ambient temperatures. Considerable biases from -20 to 31% were observed over a 30-50% hematocrit range. Although the method fulfilled all validation criteria, the perceived advantage of VAMS over DBS sampling could not be demonstrated. Despite the effect of hematocrit, using an empirically derived formula the whole blood everolimus concentration could be back calculated with acceptable accuracy in the clinical application study.

Introduction

Everolimus is a mammalian target of rapamycin (mTOR)-inhibitor approved for the treatment of renal cell carcinoma [1], neuroendocrine tumors [2] and hormone receptor positive, human epidermal growth factor receptor 2 (HER2) negative, breast cancer [3]. In all these tumor types, everolimus is currently administered using a 10 mg once daily dosing regimen. Yet in transplantation medicine (where everolimus is used to as an immunosuppressant following renal, heart of liver transplantations) personalized dosing based on measured blood concentrations, known as therapeutic drug monitoring is applied routinely.[4] Increasingly, personalized dosing of everolimus is also being advocated for in oncology.[5–7] A possible hurdle to the implementation of therapeutic drug monitoring could be the need for additional invasive blood sampling to enable drug concentration measurements. Dried blood spots (DBS) have been proposed as a patient friendly, less invasive alternative to standard blood sampling[8,9] and has been applied to the quantification of everolimus.[10–12] However, analyses on DBS need to validated using additional test to specifically investigate the influence of hematocrit, spot volume and other factors such as sample homogeneity on the analytical results.[13]

Volumetric Absorptive Microsampling (VAMS) has been introduced as an alternative dried blood sampling technique specifically designed to overcome these perceived disadvantages.[14] Specifically, it has been shown that using the VAMS method exactly 10 µL samples could be collected and the influence of hematocrit was reduced, if not completely eliminated for selected analytes. [14,15] Everolimus is an ideal candidate drug for VAMS sampling as everolimus is normally measured in whole blood and methods using DBS have demonstrated a clear influence of hematocrit.[12]

Given these theoretical advantages of this sample collection method, we developed and validated a liquid chromatography tandem mass spectrometry (LC-MS/MS) method for the quantification of everolimus using VAMS. After the bioanalytical validation we investigated the analytical performance of the VAMS system over a range of hematocrit values. Finally, we also applied the VAMS method to a collection of clinical samples for pharmacokinetic measurements in cancer patients treated with everolimus.

Materials & Methods

Chemicals

Everolimus and stable isotopically labeled internal standard (IS) $^{13}C_2D_4$-Everolimus were supplied by Alsachim (Illkrich Graffenstaden, France). Dimethyl sulfoxide (DMSO) was purchased from Merck (Darmstadt, Germany), ammonia (Empure® 25%) and methanol (UPLC grade) from BioSolve Ltd (Valkenswaard, The Netherlands). Control human EDTA whole blood was obtained from healthy volunteers and used for preparation of quality control samples (QC), calibration standards and

matrix blanks. Mitra®, VAMS microsampling devices were obtained from Neoteryx, LLC (Torrance, CA, USA).

Stock solutions, calibration standards and quality control samples

Stock solutions of everolimus were prepared in DMSO at a concentration of 1 mg/mL. Working solutions were prepared by diluting stock solutions with methanol. The IS stock solution was prepared in methanol at a concentration of 1 mg/mL. The IS working solution was prepared by further dilution with methanol to a concentration of 10 ng /mL. All stock and working solutions were stored at -20 °C.

Calibration standards and QC samples were prepared by addition of an 10 µL aliquot of working solution to 190 µL of control whole blood, of which 10 µL was subsequently absorbed using the VAMS device. Nominal concentrations of 2.50, 7.50, 25.0 and 80.0 ng/mL were used for the QC samples (lower limit of quantification (LLOQ), Low, Mid and High concentrations, respectively) and 2.50, 5.00, 10.0, 25.0, 50.0, 75.0, 90.0 and 100 ng/mL for the 8 calibrations standards.

Liquid chromatography tandem mass spectrometry

All LC-MS/MS experiments were performed using the I-class Acquity UPLC system, consisting of a autosampler, pump and column oven by Waters (Milford, MA, USA) and a QTRAP® 5500 MS system equipped with a turboinonspray, and Analyst™ software was used for data analysis by Sciex (Framigham, USA). Final optimized MS settings for these were 5000 V for the ion spray voltage, 350 ºC for the ionization temperature, 25 and 7 arbitrary units for the curtain gas and collision, gas respectively. Declustering potential was set at 56 V, collision energy at 31 V, collision cell exit potential at 40 V and entrance potential at 10 V. Quantification was performed on the ammonium adduct of everolimus[11,12,16] in positive ion mode using the *m/z* 975.6 à *m/z* 908.8 transition for everolimus and *m/z* 981.6 à m/z 914.5 for $^{13}C_2D_4$-everolimus. The chemical structures of everolimus and $^{13}C_2D_4$-Everolimus are provided in **figure 1**.

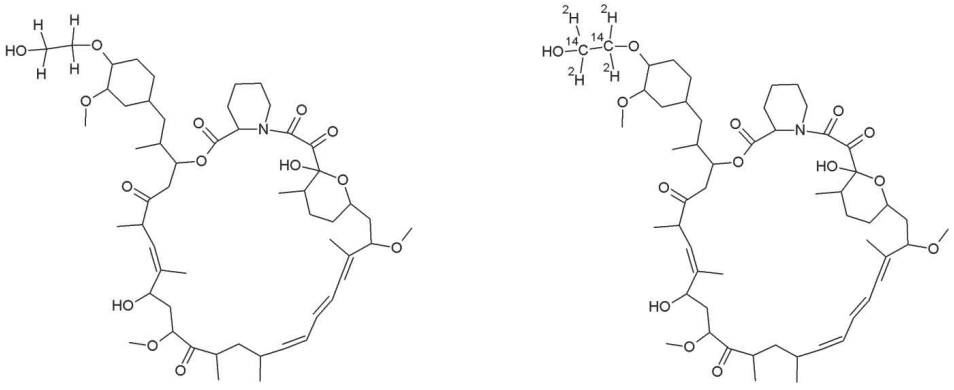

Figure 1: The chemical structures of everolimus and $^{13}C_2D_4$-Everolimus.

Chromatographic separation is performed on a Acquity BEH C18 analytical column, 100 x 2.1 mm ID, 1.7 µm particle size (Waters) using an 0.2 µm in-line filter. The column oven was set at 40 °C and the autosampler tray at 8 °C. Elution was achieved using a mixture of 20 mM ammonium formate in water (eluent A) and methanol (eluent B) at flow of 0.4 mL/min. The gradient would start at 50% methanol and would rise linearly to 95% methanol from 0.20 to 0.45 minutes. After 1.5 minutes the gradient would return to 50% methanol, until the end of the run at 2.0 minutes.

Sample preparation

The tip of the sampling device was transferred to an eppendorf tube of 2.0 mL. A volume of 10 µL of IS working solution and 500 µL of methanol were added and the sample was vortex mixed. The samples were ultrasonicated for 5 minutes and shaken at 500 rpm for 5 minutes. The methanol was then evaporated under a gentle stream of nitrogen. The residue was reconstituted in 50 µL of reconstitution solvent (20 mM ammonium formate : methanol, 1:1, v/v), vortexed and centrifuged for 3 minutes at 15000 rpm. Finally, the solution was transferred to an autosampler vial and 5 µL was injected into the LC-MS/MS system.

Bioanalytical validation

The bioanalytical method validation was conducted in accordance with guidelines for bioanalytical method validation by the Food and Drug Administration (FDA) and European Medicines Agency (EMA)[17,18]. The following validation parameters were assessed: calibration model, accuracy and precision, LLOQ, dilution integrity, selectivity, instrument carry-over, matrix factor, recovery and stability in final extract and on the dried blood sample using the VAMS device.

Calibration

Weighted linear regression (1/concentration^2) was applied to fit the calibration plots (area ratio vs square of the concentration). At least 75% of the non-zero standards (including at least one LLOQ and upper limit of quantification (ULOQ)) in each run had to be within ±15% of the nominal value (±20% for the LLOQ). For the LLOQ and ULOQ levels at least 50% had to meet these criteria. The regression coefficient was calculated for each analytical run.

Accuracy and precision

Accuracy and precision were determined in three separate validation runs by injecting five replicates of QC samples at the LLOQ, Low, Mid and High concentrations. Intra-run and overall accuracy was expressed as the relative bias. The intra-run and overall precision were calculated as the coefficient of variation (CV). At each concentration level, the bias had to be within ±15% and the precision ≤15%. For the LLOQ concentrations bias had to be within ±20% and the precision≤20%.

LLOQ

The LLOQ of the method was evaluated in each analytical run. It was quantified as the ratio of the peak height of the 2.50 ng/mL calibration standard (the signal) to the peak height of a double blank sample (the noise). A predefined limit of ≥5 was set for this ratio.

Dilution integrity

The dilution integrity was studied by analyzing five replicate samples at concentration of 150 ng/mL. These samples were diluted 2 times with final extract from a blanc sample (to which IS has been added before processing). Predefined limits for bias and precision were set at ±15% and ≤15% respectively.

Selectivity

The selectivity of the assay was determined for cross analyte/IS interference. The internal standard interference was assessed by analyzing an everolimus ULOQ sample without adding the IS and by spiking IS separately to a double blank sample at the concentration used in the assay.

The possibility of endogenous interferences was assessed by analyzing double blank samples from six different individuals and comparing the peak area in the blank with the peak area of the LLOQ in the same analytical run.

The endogenous and IS interferences were considered acceptable if it was ≤20% of the response of the LLOQ of the analyte and ≤5% of the response of the IS.

Instrument carry-over

The instrumentation carry-over was tested by injecting two double blank samples after an ULOQ sample in each validation run. The carry-over was calculated as the ratio of the peak area in the blanks and the peak area of the LLOQ. The carry-over was considered acceptable if the response at the retention time of the analyte (for both everolimus and the IS) was ≤20% of the response of the LLOQ in the first blank.

Matrix factor

The matrix factor (MF) was determined in six different batches of plasma spiked at both the QC Low and QC High concentration. The MF was calculated by dividing the everolimus peak area in presence of matrix by the peak area ratio at the same concentration in a neat solution. The MF was calculated for six different batches of control human plasma and was considered acceptable if the coefficient of variation of the MF across the six batches was ≤15%.

Sample pretreatment recovery

Recovery was determined by dividing the peak area of everolimus in processed validation samples at QC low and high concentrations (n=5) by the peak area of everolimus in presence of matrix (a double blank sample to which everolimus was spiked after processing).

Stability

The stability of VAMS samples was assessed at ambient temperatures. The stability of everolimus in processed samples (final extract) was determined after being stored at nominally 2 – 8 °C.

All these stability analyses were carried out in triplicate at the QC Low and High concentrations. Samples were considered to be stable if the measured concentration was within ±15% of the nominal concentration.

Influence of hematocrit

To determine the relative influence of hematocrit on quantification, VAMS samples were analyzed in duplicate on the QC Low, Mid and High concentrations in whole blood at nominal hematocrit concentrations of 30, 40 and 50% (±1%).

Relative deviations were calculated, normalized to the respective (Low, Mid or High) QC at a hematocrit of 40%. The hematocrit value of the calibration standards used to quantify the VAMS samples was 44%. Hematocrit measurements were performed using the Mission Plus (Acon Laboratories Inc, San Diego, USA).

Clinical application

Paired VAMS and whole blood clinical samples were obtained in a pharmacokinetic study in cancer patients. This trial was registered in the EudraCT database (2014-004833-25) and the Netherlands Trial Registry (NTR4908).[19] This trial was conducted in accordance with the World Medical Organization declaration of Helsinki, compliant with Good Clinical Practice and approved by the Medical Ethics Committee of each of the participating medical centers. All patients provided written informed consent before enrollment.

Whole blood samples were drawn by venipuncture performed by a trained nurse or physician. VAMS samples were taken by the patient under supervision of a researcher, in accordance with the manufacturers instruction. VAMS samples were prepared and analyzed by the methods described in this manuscript and whole blood concentrations were quantified using a previously developed and validated LC-MS/MS method.[19] Weighted Deming regression was applied to compare the VAMS with the whole blood everolimus concentrations. Based on the empirical correlation found, the back calculated whole blood concentrations would be determined and compared to the actual whole blood concentration, as described previously.[20,21]

Results

Validation

The method was successfully validated in accordance with the FDA and EMA guidelines and met all pre-specified acceptance criteria. An overview of the validation parameters is provided in **table 1**.

Influence of hematocrit

The influence of hematocrit on the quantification of everolimus using VAMS was investigated. The results are displayed in **figure 2**. The VAMS assay showed a marked influence of hematocrit: at the lower hematocrit value (31%) relative biases were 24%, 31% and 13% for the Low, Mid and High concentration respectively (shown as normalized response ratios of 1.24, 1.31 and 1.13 in **figure 2**). The high hematocrit values (49%) resulted in relative biases of -16%, -20% and -20%, respectively, (depicted as ratios of 0.84, 0.80 and 0.80).

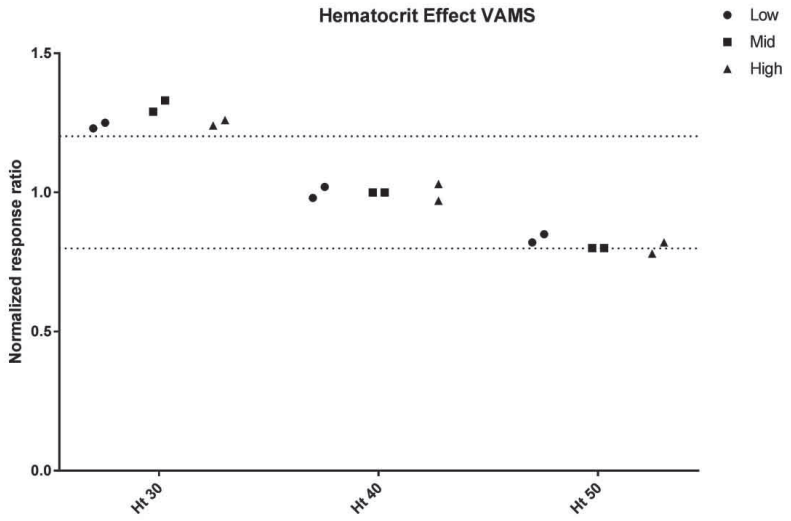

Figure 2: Relative analytical response ratios for everolimus quantified at QC Low, Mid and High concentrations for three different hematocrit values. Analyte/internal standard response ratios were normalized to the QC at the 40% hematocrit. Dotted lines indicate ±20% deviation.

Clinical application

Overall, 25 clinical samples were available from 10 patients. Of these, all but one were taken in duplicate. The VAMS everolimus concentrations are plotted versus the corresponding whole blood concentrations in **figure 3**. Weighted Deming regression was used to compare the VAMS and the whole blood LC-MS/MS methods. The relation was described quantitatively by the formula of y=0.691x+0.158. According to this formula the whole blood concentration could be back calculated based on the VAMS results. These calculated whole blood concentrations are plotted versus the actual measured whole blood concentrations in **figure 4**.

The average absolute deviation between the VAMS samples taken in duplicate was 6.4%. The bias between the calculated and actual whole blood concentrations of everolimus was 0.6% and the mean absolute difference was 14.1%. Mean (CV%) hematocrit of the patients enrolled in this trial was 36% (11).

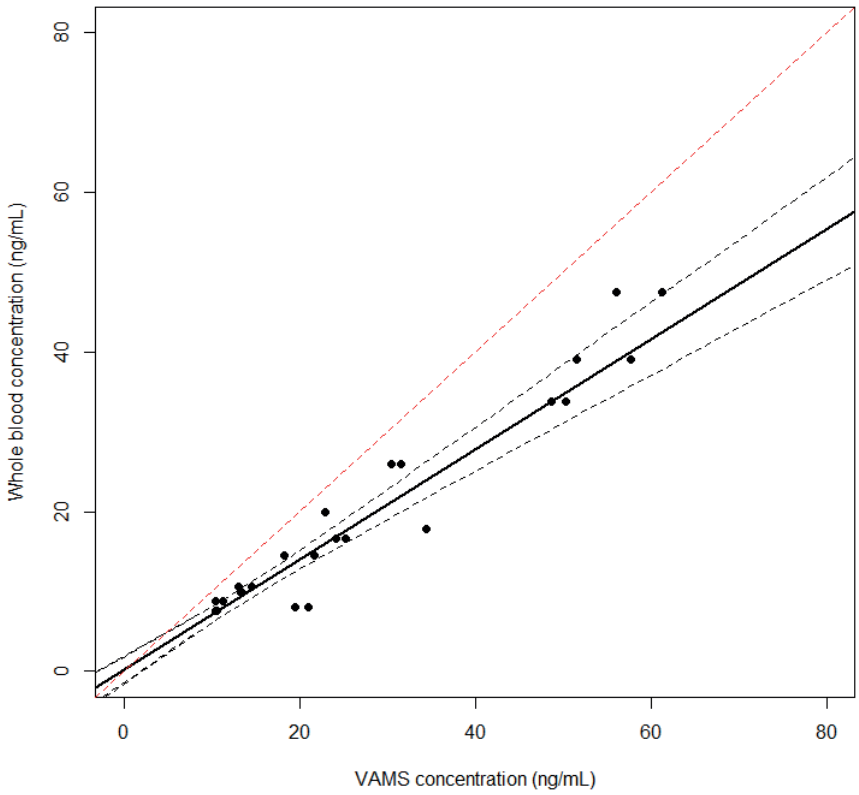

Figure 3: Everolimus concentration determined by volumetric absorptive microsampling (VAMS) and whole blood analysis, with weighted linear Deming regression (black line) and 95% confidence interval (dotted black line). The red dotted line indicates unity. The relation between VAMS and whole blood was described by y=0.691x+0.158.

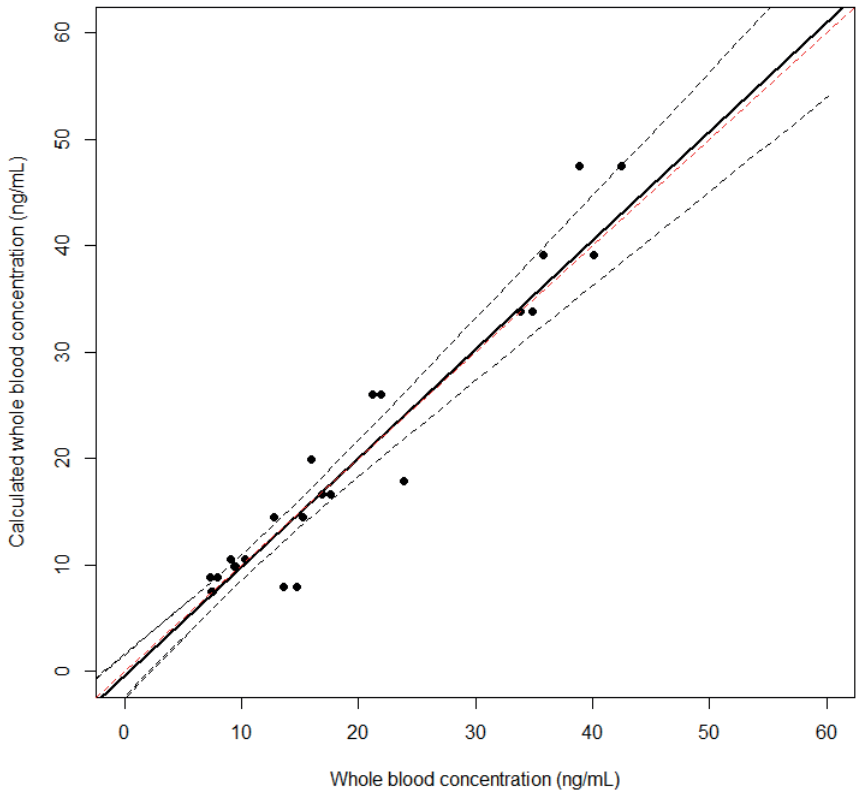

Figure 4: Everolimus concentration determined in whole blood compared to the back calculated whole blood concentration based on the VAMS analysis, with weighted linear Deming regression (black line) and 95% confidence interval (dotted black line). The red dotted line indicates unity. The relation between The calculated whole blood concentration was determined using y=0.691x+0.158 (see figure 3).

Discussion

We describe the bioanalytical validation and clinical application of an LC-MS/MS method to quantify everolimus using VAMS. The method met all pre-specified acceptance criteria although the matrix factor and recovery of the method were low at only 0.64 and 20.2-23.1%, respectively. The perceived major advantage of VAMS over DBS sampling is the volumetric collection of a fixed volume, which should be independent of hematocrit. However, we clearly showed a large impact of hematocrit on analytical performance.

Previous studies have found that VAMS eliminated an effect of hematocrit on the analysis of caffeine and paraxanthine,[15] In the current study for everolimus, biases of -20 to 31% were found over the tested hematocrit range. Comparable deviations were also found in previously published methods e.g. the quantification of miltefosine.[22] Moreover, the inversely correlated direction of the

observed effect was the same, i.e. positive bias for low and negative bias for high hematocrit values. It is hypothesized that this phenomenon is due to the presence of a larger amount of erythrocytes which entrap the analyte in the pores of the VAMS device tip, hindering analyte extraction.[15]
DBS analysis of everolimus has also been shown to be strongly influenced by blood hematocrit in a concentration dependent manner.[12] Interestingly, for the VAMS analysis of everolimus the hematocrit driven relative bias seemed independent of the everolimus concentration (**figure 2**), whilst a considerable effect of concentration was found for DBS quantification of everolimus at varying hematocrit values.[12] Yet, based on our data it must be concluded that no superiority of VAMS over DBS in reducing the effect of hematocrit on everolimus quantification could be demonstrated.

Everolimus concentrations in clinical VAMS samples were consistently higher than the whole blood concentrations (**figure 3**). These results are consistent with previous reports regarding caffeine, paraxanthine and paracetamol, where VAMS systematically overestimated the whole blood concentration [15,23] The underlying explanation of this effect is not clearly understood, but in our study it could be due to the higher hematocrit level (44%) of the calibration standard compared to that of the enrolled patients (36%). Even though considerable effects of hematocrit were found for VAMS, using an empirically determined back calculation the method did result in acceptable estimation of the whole blood concentration (**figure 4**). The current study is the first clinical validation study to use this backward calculation method based on the empirical relation for estimating whole blood concentration of everolimus using VAMS and whole blood samples. However, this calculation has been reported to be successful in DBS analysis for other small molecules both in oncology and infectious diseases such as pazopanib, vemurafenib and miltefosine.[20,21,24]

A possible drawback of the VAMS could be the between-operator variability,[14] but the small variation between the samples drawn in duplicate of 6.4% seem to diminish this concern. Possible advantages of VAMS over DBS sampling would be the accurate whole blood volume sampling regardless of hematocrit value and reducing homogeneity issues.[14] Based on these theoretical advantages, we developed the currently described method. However, specifically for the case of everolimus, we demonstrate that this theoretical advantage of VAMS could not be demonstrated in practice. Although whole blood concentrations can be back calculated, VAMS sampling does not offer advantages over regular DBS sampling.

Conclusion

We describe the bioanalytical validation of an LC-MS/MS method to quantify everolimus using VAMS. The method met all pre-defined bioanalytical validation criteria and samples were shown to be stable for nearly a year (362 days) at ambient temperatures. The analytical performance of the

VAMS method was studied over a 30-50% hematocrit range, where large relative biases were found. Therefore, no superiority of the VAMS over DBS sampling was demonstrated. Despite the effect of hematocrit, using an empirically derived formula the whole blood everolimus concentration could be back calculated with acceptable accuracy in the clinical application study.

Table 1: Overview of the bioanalytical validation outcome data. All tested parameters met their predefined criteria.†

Validation parameter	Outcome
Calibration model	$1/x^2$ weighted linear regression, all regression coefficients > 0.99
Calibration range	2.50 – 100 ng/mL
Intra-run accuracy (%)	LLOQ: -16.8% Other: 11.1%
Overall accuracy (%)	LLOQ: -0.2% Other: 11.1%
Intra-run precision (CV)	LLOQ: 8.6% Other: 9.7%
Overall precision (CV)	LLOQ: 14.6% Other: 9.0%
Lower limit of quantitation (signal/noise ratio)	5
Dilution integrity (bias, CV)	-7.6%, 15.0%
Cross analyte/IS interference	0.0%
Endogenous interferences	0.0%
Instrument carry-over	0.0%
Matrix factor (CV)	QC Low: 0.640, 3.7% QC High: 0.636, 4.3%
Recovery (mean, CV)	QC Low: 23.1%, 7.3% QC High: 20.2%, 9.8%
Stability in final extract at 2 – 8 °C after 48 hours (bias, CV)	QC Low: 9.8%, 3.3% QC High: -1.9%, 6.2%
Stability of dried VAMS samples at ambient temperatures after 362 days (bias, CV)	Low: 12.1%, 0.9% High: -1.6%, 6.2%

CV: coefficient of variation; LLOQ: Lower limit of quantification.

† Predefined acceptance criteria are reported in the text.

Compliance with Ethical Standards

This research was conducted in accordance with the World Medical Organization declaration of Helsinki, compliant with Good Clinical Practice and approved by the Medical Ethics Committee of the each participating medical center (The Netherlands Cancer Institute and Erasmus MC Cancer Institute). All patients provided written informed consent before enrollment. This trial was registered in the EudraCT database (2014-004833-25) and the Netherlands Trial Registry (NTR4908).

Funding Statement

No funding was received for this research.

Conflicts of Interest

N. Steeghs received funding from Novartis as principal investigator for this investigator initiated study. R.B. Verheijen, B. Thijssen, F. Atrafi, J.H.M. Schellens, H. Rosing, N. de Vries, J.H. Beijnen, R.H.J. Mathijssen and A.D.R. Huitema all declare they have no conflicts to disclose.

References

[1] R.J. Motzer, B. Escudier, S. Oudard, T.E. Hutson, C. Porta, S. Bracarda, V. Grunwald, J.A. Thompson, R.A. Figlin, N. Hollaender, G. Urbanowitz, W.J. Berg, A. Kay, D. Lebwohl, A. Ravaud, Efficacy of everolimus in advanced renal cell carcinoma: a double-blind, randomised, placebo-controlled phase III trial, Lancet. 372 (2008) 449–456. doi:10.1016/S0140-6736(08)61039-9.

[2] J.C. Yao, M.H. Shah, T. Ito, C.L. Bohas, E.M. Wolin, E. Van Cutsem, T.J. Hobday, T. Okusaka, J. Capdevila, E.G. de Vries, P. Tomassetti, M.E. Pavel, S. Hoosen, T. Haas, J. Lincy, D. Lebwohl, K. Oberg, T.T.S.G. Rad001 in Advanced Neuroendocrine Tumors, Everolimus for advanced pancreatic neuroendocrine tumors, N Engl J Med. 364 (2011) 514–523. doi:10.1056/NEJMoa1009290.

[3] J. Baselga, M. Campone, M. Piccart, H.A. 3rd Burris, H.S. Rugo, T. Sahmoud, S. Noguchi, M. Gnant, K.I. Pritchard, F. Lebrun, J.T. Beck, Y. Ito, D. Yardley, I. Deleu, A. Perez, T. Bachelot, L. Vittori, Z. Xu, P. Mukhopadhyay, D. Lebwohl, G.N. Hortobagyi, Everolimus in postmenopausal hormone-receptor-positive advanced breast cancer., N. Engl. J. Med. 366 (2012) 520–529. doi:10.1056/NEJMoa1109653.

[4] M. Shipkova, D.A. Hesselink, D.W. Holt, E.M. Billaud, T. van Gelder, P.K. Kunicki, M. Brunet, K. Budde, M.J. Barten, P. De Simone, E. Wieland, O.M. Lopez, S. Masuda, C. Seger, N. Picard, M. Oellerich, L.J. Langman, P. Wallemacq, R.G. Morris, C. Thompson, P. Marquet, Therapeutic Drug Monitoring of Everolimus: A Consensus Report., Ther. Drug Monit. 38 (2016) 143–169. doi:10.1097/FTD.0000000000000260.

[5] R.B. Verheijen, H. Yu, J.H.M. Schellens, J.H. Beijnen, N. Steeghs, A.D.R. Huitema, Practical Recommendations for Therapeutic Drug Monitoring of Kinase Inhibitors in Oncology., Clin. Pharmacol. Ther. (2017). doi:10.1002/cpt.787.

[6] D. de Wit, T.C. Schneider, D.J.A.R. Moes, C.F.M. Roozen, J. den Hartigh, H. Gelderblom, H.J. Guchelaar, J.J. van der Hoeven, T.P. Links, E. Kapiteijn, N.P. van Erp, Everolimus pharmacokinetics and its exposure–toxicity relationship in patients with thyroid cancer, Cancer Chemother. Pharmacol. 78 (2016) 63–71. doi:10.1007/s00280-016-3050-6.

[7] A. Thiery-Vuillemin, G. Mouillet, T. Nguyen Tan Hon, P. Montcuquet, T. Maurina, H. Almotlak, U. Stein, D. Montange, A. Foubert, V. Nerich, X. Pivot, B. Royer, Impact of everolimus blood concentration on its anti-cancer activity in patients with metastatic renal cell carcinoma, Cancer Chemother. Pharmacol. 73 (2014) 999–1007. doi:10.1007/s00280-014-2435-7.

[8] A.J. Wilhelm, J.C.G. den Burger, E.L. Swart, Therapeutic Drug Monitoring by Dried Blood Spot: Progress to Date and Future Directions, Clin. Pharmacokinet. 53 (2014) 961–973. doi:10.1007/s40262-014-0177-7.

[9] N.G.L. Jager, H. Rosing, S.C. Linn, J.H.M. Schellens, J.H. Beijnen, Dried blood spot self-sampling at home for the individualization of tamoxifen treatment, Ther. Drug Monit. 37 (2015) 1. doi:10.1097/FTD.0000000000000224.

[10] J. van der Heijden, Y. de Beer, K. Hoogtanders, M. Christiaans, G.J. de Jong, C. Neef, L. Stolk, Therapeutic drug monitoring of everolimus using the dried blood spot method in combination with liquid chromatography-mass spectrometry, J. Pharm. Biomed. Anal. 50 (2009) 664–670. doi:10.1016/j.jpba.2008.11.021.

[11] J.C.G. Den Burger, A.J. Wilhelm, A. Chahbouni, R.M. Vos, A. Sinjewel, E.L. Swart, Analysis of cyclosporin A, tacrolimus, sirolimus, and everolimus in dried blood spot samples using liquid chromatography tandem mass spectrometry, Anal. Bioanal. Chem. 404 (2012) 1803–1811. doi:10.1007/s00216-012-6317-8.

[12] R.A. Koster, J.W.C. Alffenaar, B. Greijdanus, D.R.A. Uges, Fast LC-MS/MS analysis of tacrolimus, sirolimus, everolimus and cyclosporin A in dried blood spots and the influence of the hematocrit and immunosuppressant concentration on recovery, Talanta. 115 (2013) 47–54. doi:10.1016/j.talanta.2013.04.027.

[13] N.G.L. Jager, H. Rosing, J.H.M. Schellens, J.H. Beijnen, Procedures and practices for the validation of bioanalytical methods using dried blood spots: a review., Bioanalysis. 6 (2014) 2481–2514. doi:10.4155/bio.14.185.

[14] P. Denniff, N. Spooner, Volumetric Absorbtive Micro Sampling (VAMS): A Novel Dried Sample Collection Technique for Quantitative Bioanalysis, Anal. Chem. 86 (2014) 8489–8495. doi:10.1021/ac5022562.

[15] P.M.M. De Kesel, W.E. Lambert, C.P. Stove, Does volumetric absorptive microsampling

eliminate the hematocrit bias for caffeine and paraxanthine in dried blood samples? A comparative study, Anal. Chim. Acta. 881 (2015) 65–73. doi:10.1016/j.aca.2015.04.056.

[16] E.M. Kemper, B. Jansen, K.R. Brouwer, J.H.M. Schellens, J.H. Beijnen, O. Van Tellingen, Bioanalysis and preliminary pharmacokinetics of the acridonecarboxamide derivative GF120918 in plasma of mice and humans by ion-pairing reversed-phase high-performance liquid chromatography with fluorescence detection, J. Chromatogr. B Biomed. Sci. Appl. 759 (2001) 135–143. doi:10.1016/S0378-4347(01)00207-9.

[17] Committee for Medicinal Products for Human Use (CHMP) European Medicines Evaluation Agency, Guideline on Bioanalytical Method Validation, (2011). http://www.ema.europa.eu/docs/en_GB/document_library/Scientific_guideline/2011/08/WC500109686.pdf.

[18] Center for Drug Evaluation and Research (CDER) Food and Drug Administration, Guidance for Industry Bioanalytical Method Validation, (2001). http://www.fda.gov/downloads/Drugs/Guidance/ucm070107.pdf.

[19] R.B. Verheijen, F. Atrafi, J.H.M. Schellens, J.H. Beijnen, A.D.R. Huitema, R.H.J. Mathijssen, N. Steeghs, Pharmacokinetic Optimization of Everolimus Dosing in Oncology: A Randomized Crossover Trial, Clin. Pharmacokinet. (2017). doi:10.1007/s40262-017-0582-9.

[20] R.B. Verheijen, S. Bins, B. Thijssen, H. Rosing, L. Nan, J.H. Schellens, R.H. Mathijssen, M.P. Lolkema, J.H. Beijnen, N. Steeghs, A.D. Huitema, Development and clinical validation of an LC – MS / MS method for the quantification of pazopanib in DBS, Bioanalysis. (2016) 369–374. doi:10.1016/j.jchromb.2008.12.032.

[21] C.M. Nijenhuis, A.D.R. Huitema, S. Marchetti, C. Blank, J.B.A.G. Haanen, J. V. van Thienen, H. Rosing, J.H.M. Schellens, J.H. Beijnen, The Use of Dried Blood Spots for Pharmacokinetic Monitoring of Vemurafenib Treatment in Melanoma Patients, J. Clin. Pharmacol. (2016) 1307–1312. doi:10.1002/jcph.728.

[22] A.E. Kip, K.C. Kiers, H. Rosing, J.H.M. Schellens, J.H. Beijnen, T.P.C. Dorlo, Volumetric absorptive microsampling (VAMS) as an alternative to conventional dried blood spots in the quantification of miltefosine in dried blood samples, J. Pharm. Biomed. Anal. 135 (2017) 160–166. doi:10.1016/j.jpba.2016.12.012.

[23] P. Denniff, S. Parry, W. Dopson, N. Spooner, Quantitative bioanalysis of paracetamol in rats using volumetric absorptive microsampling (VAMS) Volumetric absorptive microsampling, J. Pharm. Biomed. Anal. 108 (2015) 61–69. doi:10.1016/j.jpba.2015.01.052.

[24] A.E. Kip, H. Rosing, M.J.X. Hillebrand, S. Blesson, B. Mengesha, E. Diro, A. Hailu, J.H.M. Schellens, J.H. Beijnen, T.P.C. Dorlo, Validation and clinical evaluation of a novel method to measure miltefosine in leishmaniasis patients using dried blood spot sample collection, Antimicrob. Agents Chemother. 60 (2016) 2081–2089. doi:10.1128/AAC.02976-15.

Chapter 3.2

Pharmacokinetic Optimization of Everolimus Dosing in Oncology: a Randomized Crossover Trial

R.B. Verheijen[1], F. Atrafi[2], J.H.M. Schellens[3,4], J.H. Beijnen[1,4], A.D.R. Huitema[1,5], R.H.J. Mathijssen[2], N. Steeghs[3]

[1]Department of Pharmacy & Pharmacology, The Netherlands Cancer Institute - Antoni van Leeuwenhoek, Louwesweg 6, 1066 EC Amsterdam, The Netherlands.
[2]Department of Medical Oncology, Erasmus MC Cancer Institute, Rotterdam, The Netherlands.
[3]Department of Medical Oncology and Clinical Pharmacology, The Netherlands Cancer Institute - Antoni van Leeuwenhoek, Amsterdam, The Netherlands.
[4]Department of Pharmaceutical Sciences, Utrecht University, Utrecht, The Netherlands.
[5]Department of Clinical Pharmacy, University Medical Center Utrecht, Utrecht, The Netherlands.

Abstract

Background: The mTOR-inhibitor everolimus is used in the treatment of breast cancer, neuro-endocrine tumors and renal cancer. The approved 10 mg once daily (QD) dose is associated with considerable adverse effects. It has been suggested that these are associated with the C_{max} of everolimus. Bi-daily (BID) dosing might be an alternative strategy with improved tolerability. However, a direct pharmacokinetic comparison of 10 mg QD with 5 mg BID dosing is lacking.

Methods: We performed a prospective randomized pharmacokinetic crossover trial comparing everolimus 10 mg QD with 5 mg BID. Patients received the first dose schedule for two weeks and then switched to the alternative regimen for two weeks. Pharmacokinetic sampling was performed on days 14 and 28.

Results: Eleven patients were included. Of these, 10 patients were evaluable for pharmacokinetic analysis. On the 10 mg QD schedule C_{max}, C_{min} and $AUC_{0\text{-}24h}$ were (mean (CV%)) 61.5 (29.6) ng/mL, 9.6 (35.0) ng/mL, 435 (28.1) ng*h/mL. Switching to the 5 mg BID schedule resulted in a reduction of C_{max} to 40.3 (46.6) ng/mL (p=0.013), whilst maintaining $AUC_{0\text{-}24h}$ at 436 (34.8) ng*h/mL (p=0.952). C_{min} increased to 13.7 (53.9) ng/mL (p=0.018). Overall the reduction in C_{max} was 21.2 ng/mL or 32.7%. The C_{max}/C_{min} ratio was reduced from 6.44 (36.2) to 3.18 (35.5), p<0.001.

Conclusions: We demonstrate that switching from a QD to a BID everolimus dose schedule reduces C_{max} without negatively impacting C_{min} or $AUC_{0\text{-}24h}$. These results merit further investigation of the BID schedule in an effort to reduce everolimus toxicity whilst maintaining treatment efficacy.

Background

Everolimus is an mammalian target of rapamycin (mTOR)-inhibitor approved for the treatment of renal cell carcinoma [1], neuroendocrine tumors [2] and hormone receptor positive, human epidermal growth factor receptor 2 (HER2) negative, breast cancer [3].

Inhibition of mTOR has been shown to enhance the effectiveness of hormonal based therapies for breast cancer patients who have become resistant to endocrine therapy [4].

The BOLERO-2 trial showed that addition of everolimus to exemestane increased progression free survival in patients with hormone positive, HER2-negative advanced breast cancer compared to placebo.[3] This improvement from 4.1 to 11.1 months resulted in a hazard ratio of 0.38 (95% confidence interval 0.31-0.48), p <0.0001 in the final analysis [5].

Nonetheless, the 10 mg once daily (QD) dose in combination with 25 mg QD exemestane resulted in significant adverse events (AEs) (any grade): 56% of patients developed stomatitis, 36% developed rash, 33% fatigue and 30% diarrhea. These events were severe (grade 3) in 8, 1, 3 and 2% respectively and a considerable 19% of patients discontinued treatment due to toxicity.

Moreover, a meta-analysis of over 900 patients included in various everolimus phase II trials by Ravaud et al estimated the overall incidence of stomatitis at 57% (any grade) and the incidence of severe (grade 3-4) stomatitis at 6% [6].

Adverse effects and in particular stomatitis have been shown to be related with pharmacokinetic exposure to everolimus [6,7]. Specifically, these adverse events may be associated with high maximum plasma concentrations (C_{max}) [8]. Thus reducing C_{max}, while maintaining efficacious trough concentrations (C_{min}), could be an effective method to optimize the treatment of everolimus by reducing toxicity yet retaining efficacy.

Generally, the various pharmacokinetic parameters C_{min}, C_{max} and area under the whole blood concentration-time curve (AUC) will be strongly interrelated (i.e. a higher dose will increase all 3 and conversely a dose reduction will reduce all 3). However, in contrast to lowering the QD dose (the current strategy to reduce toxicity in clinical practice) switching to a BID schedule could specifically reduce C_{max} without negatively impacting C_{min} or AUC and thereby theoretically reduce toxicity whilst not reducing efficacy.

A strategy to reduce the C_{max}/C_{min} ratio could be the use of an extended or sustained release formulation [8] or splitting the intake moments from QD to twice daily (BID).

We hypothesized, that given the pharmacological properties of everolimus, the latter approach could reduce the C_{max}, whilst maintaining the C_{min} and total exposure, measured as AUC at similar levels. This could lead to reducing the C_{max}/C_{min} ratio without the need to develop a new sustained release formulation and thereby preventing a costly patent extension.

To test this hypothesis, we performed a randomized pharmacokinetic crossover trial of 10 mg QD of everolimus versus 5 mg BID in cancer patients.

Methods

Study design

We performed a prospective, multicenter, randomized, crossover trial. An overview of the trial design is given in figure 1. Patients were randomized to start either with a 10 mg QD or 5 mg BID dose. Each patient was be treated for at least 2 weeks with each dose schedule. Patients were instructed to take everolimus daily at the same time with a low-fat meal. Patients requiring a dose reduction due to toxicity were considered non-evaluable for the pharmacokinetic endpoint and were replaced.

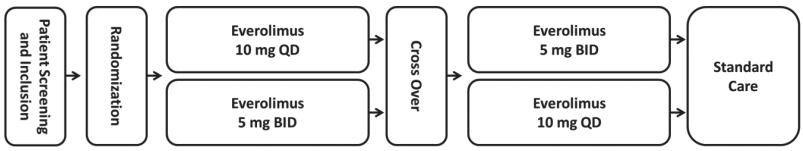

Figure 1: Trial design. Patients were randomized according to start either with a 2 week period of a 5 mg BID everolimus dose or a 10 mg QD everolimus dose. Pharmacokinetic sampling was performed after each 2 week period (day 14 and 28).

Patient population

Patients with histopathologically confirmed advanced cancer for whom everolimus was considered standard of care were eligible for inclusion. Further inclusion criteria were: age > 18 years, minimal acceptable safety laboratory values, defined as: absolute neutrophil count $\geq 1.5 \cdot 10^9$/L, platelet count of $>100 \cdot 10^9$/L, billirubin <1.5 times upper limit of normal (ULN), aspartate aminotransferase (AST) and alanine aminotransferase (ALT) <2.5 times ULN, creatinine <1.5 times ULN, or creatinine clearance >50 ml/min.

Exclusion criteria were the use of any concomitant medication (including over the counter and herbal medication) which would induce or inhibit the function of CYP3A4.

Pharmacokinetics

At the end of each two week period (day 14 and day 28) blood samples were collected for pharmacokinetic analysis. In the 10 mg QD schedule, samples (3 mL) were collected at 0, 0.5, 1, 2, 3, 4, 5, 6, 12 and 24 hours after drug administration. In the 5 mg BID schedule, sampling times were 0, 0.5, 1, 2, 3, 4, 5, 6, 12, 12.5, 13, 14, 15, 16 and 24 hours after ingestion of the last dose. On the days of pharmacokinetic sampling everolimus was taken concomitantly with a low-fat meal. Whole blood everolimus concentrations were measured using a validated liquid chromatography tandem mass spectrometry (LC-MS/MS) method.

Bioanalysis

A 200 µL aliquot of whole blood was transferred to an Eppendorf tube. A volume of 40 µL of 75 ng/mL internal standard ($^{13}C,^{2}H_3$-Everolimus) in methanol and 1.0 mL of *tert*-buthyl methyl ether was added. Samples were vortexed and shaken for 5 minutes at 1500 rpm, before being centrifuged at 23,100 G for 5 minutes. Liquid-liquid extraction was then followed by snap freezing the samples and transferring the organic phase to a new Eppendorf tube. The organic phase was then evaporated under a gentle stream of nitrogen. The residue was reconstituted in water with 20 nM ammonium formate and methanol (1:1, v/v) of which 5 µL was injected in the LC-MS/MS system (HPLC 1100 series (Agilent) and API3000 mass spectrometer (Sciex)). Chromatographic separation was performed on a Sunfire C18 column (Waters) using a 20 nM ammonium formate in water and a gradient of 50 to 100% methanol. The bioanalytical assay was validated in accordance with Food and Drug Administration guidelines for bioanalytical method validation. The analytical range was 1 to 100 ng/mL. Inter-run and intra-run precision were ≤8.5% and overall and intra-run bias within ±11%. Carry-over was ≤5.3% of the lower limit of quantitation (1 ng/mL) and matrix effect (quantified as the CV of the internal standard normalized matrix factor) was ≤1.7%.

Study endpoint

The primary end-point of this trial was to describe and compare the pharmacokinetics of everolimus in whole blood after a 10 mg QD and a 5 mg BID dose. Parameters of particular interest were C_{max}, C_{min}, $AUC_{0\text{-}24h}$. The safety of both dose schedules was included as an exploratory endpoint.

Safety assessments

Recording of AEs, physical examination, hematology and blood chemistry assessments were performed every two weeks. The incidence, severity, start and end dates of all serious AEs (SAEs) and of non-serious AEs were recorded. AEs were graded according to the Common Terminology Criteria for Adverse Events (CTCAE v4.02).

Statistics

All statistical analyses were performed in R version 3.3.2[9]. Pharmacokinetic parameters were calculated using non-compartmental analysis. C_{max} was defined as the higher of the two observed

peaks for the BID schedule. C_{min} was defined as the average of t= 0 and 24 hours and t= 0, 12 and 24 hours, for the QD and BID schedule respectively. Two-sided, paired t-tests were used to assess the difference between calculated pharmacokinetic parameters of the two dose schedules.

Given the descriptive nature of the pharmacokinetic end point in this pilot study it was unfeasible to perform a meaningful formal power analysis. Hence no calculation for the exact number of patients is given. The proposed number of patients is therefore based on comparable pharmacokinetic pilot studies and a conservative estimate of number of eligible patients. However, in an exploratory analysis it was calculated that with a sample size of 5 evaluable subjects in each sequence group (a total sample size of 10 subjects), a 2 x 2 crossover design will have 80% power to detect a difference in mean C_{max} of 17.5 ng/mL (the difference between a mean, μ_1, of 61 ng/mL for one treatment and a mean, μ_2, of 43.5 ng/mL for the other treatment) assuming that the √mean standard error is 12.021 (the Standard deviation of differences, σ_d, is 17[10] using a two group t-test with a 0.050 two-sided significance level. The sample size calculation was performed using the nQuery Advisor software package version 7.0.

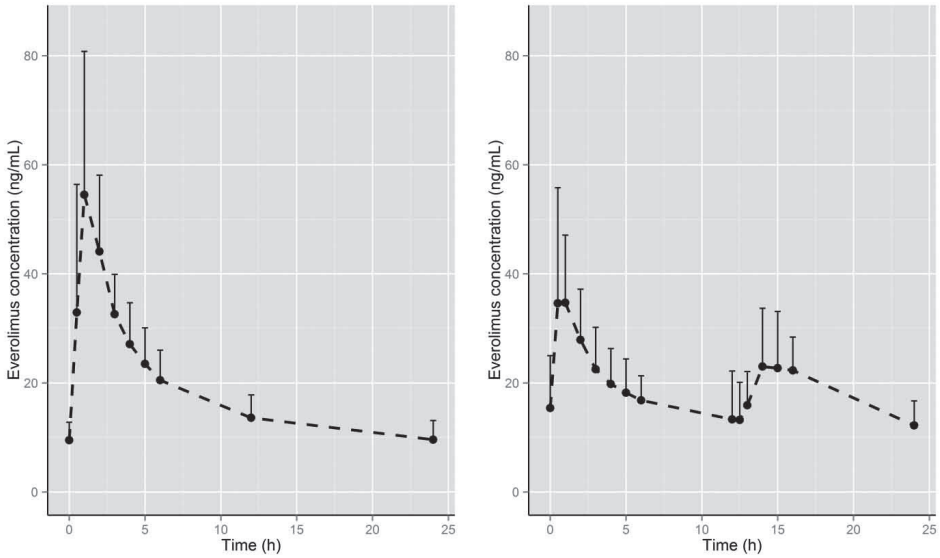

Figure 2: Whole blood concentration-time curves (mean + SD) of the 10 mg QD (left) and 5 mg BID (right) dose schedules (n=10).

Study conduct and registry

This trial was conducted in accordance with the World Medical Organization declaration of Helsinki, compliant with Good Clinical Practice and approved by the Medical Ethics Committee of the each participating medical center (The Netherlands Cancer Institute and Erasmus MC Cancer Institute). All patients provided written informed consent before enrollment. This trial was registered in the EudraCT database (2014-004833-25) and the Netherlands Trial Registry (NTR4908).

Results

Patient population

In total 11 patients signed written informed consent. Of these patients 4 had breast cancer, 4 renal cell cancer and 3 had neuro-endocrine tumors. One (breast cancer) patient withdrew consent after pharmacokinetic sampling on day 14. The remaining 10 patients were evaluable in both dose schedules. None of the patients required a dose reduction. An overview of the characteristics of the evaluable patients is provided in table 1. The 4 breast cancer patients used everolimus in combination with 25 mg exemestane in accordance with the summary of product characteristics. Of all the enrolled patients, 30% had already received everolimus prior to inclusion in the trial.

Table 1: Baseline characteristics of evaluable patients (n=10).

Characteristic	n (%) or mean (range)
Sex	
Male	5 (50%)
Female	5 (50%)
Age (years)	56 (43 – 78)
Height (cm)	171 (161 – 192)
Weight (kg)	76 (52 – 92)
WHO performance status	
0	4 (40%)
1	6 (60%)
Tumor type	
Breast cancer	3 (30%)
Renal cell carcinoma	4 (40%)
Neuroendocrine tumor	3 (30%)
Previous systemic therapy	
Chemotherapy	6 (60%)
Targeted therapy	5 (50%)
Endocrine therapy	4 (40%)

Pharmacokinetics

Absolute and relative change in C_{max} for each individual patient are displayed in table 2. The mean reduction in C_{max} achieved by switching from a QD to a BID dose was 21.2 ng/mL or 32.7%, p=0.013. All but one patient showed a reduction in C_{max}. For the single patient that did not show a reduction in C_{max}, only one of the two peak values on the BID schedule (79.4 and 40.2 ng/mL) was above the C_{max} the QD schedule (56.9 ng/mL). However, the highest of both peaks was used for calculation of the change in C_{max}.

Table 2: Absolute and relative change in C_{max} after switching from the 10 mg QD to the 5 mg BID for each individual patient in concentration (ng/mL) and percent.

ID	C_{max} reduction (ng/mL)†	C_{max} reduction (%)
1	5.5	12.1
2	14.9	48.1
3	35.1	47.5
4	21.1	47.4
5	3.4	5.5
6	-22.5	-39.5
7	30.1	44.1
8	48.4	67.6
9	31.4	47.4
10	44.5	46.6
Mean	**21.2 ng/mL**	**32.7 %**

† C_{max} is defined as the highest of the two observed peaks for the BID schedule.

An overview of the pharmacokinetic parameters for each of the dose schedules is provided in table 3. Changes in $AUC_{0\text{-}24h}$ and T_{max} were not statistically significant p=0.70 and 0.95, respectively. Box plots comparing selected pharmacokinetic parameters of the QD and BID schedule are shown in figure 3.

Table 3: Selected pharmacokinetic properties of everolimus in the 10 mg QD and 5 mg BID schedules, data are represented as mean (CV%).

Pharmacokinetic parameter	10 mg QD	5 mg BID	*P*
C_{max} (ng/mL) †	61.5 (29.6)	40.3 (46.6)	**0.013**
T_{max} (h)	1.4	2.2	0.703
C_{min} (ng/mL) ‡	9.6 (35.0)	13.7 (53.9)	**0.018**
$AUC_{0\text{-}24h}$ (ng*h/mL)	435 (28.1)	436 (34.8)	0.952
C_{max}/C_{min} ratio	6.44 (36.2)	3.18 (35.5)	**<0.001**

† C_{max} is defined as the higher of the two observed peaks for the BID schedule.

‡ C_{min} is defined as the average of t= 0 and 24 hours and t= 0, 12 and 24 hours, for the QD and BID schedule respectively

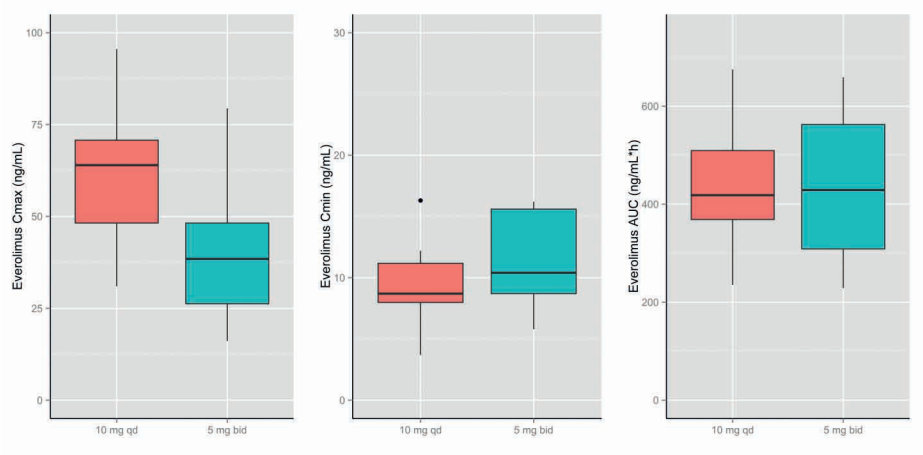

Figure 3: Box plots of C_{max}, C_{min} and $AUC_{0\text{-}24h}$ for both dose schedules. C_{min} is defined as the average of t= 0 and 24 hours and t= 0, 12 and 24 hours, for the QD (orange boxes) and BID schedule (green boxes) respectively. C_{max} was defined as the higher of the two observed peaks for the BID schedule.

Inter-patient variability (CV%) for $AUC_{0\text{-}24h}$, C_{max} and C_{min} were 28.1%, 29.6% and 36.2, respectively, for the 10 mg QD and 35.5%, 46.6% and 53.9%, respectively, for the 5 mg BID dose level.

Intra-patient variability (quantified as an intra-patient CV% on t=0 and t=24 for each schedule) was relatively small with a mean intra-patient CV of 11.1% on the BID schedule and 6.8% on the QD schedule.

Patients' hematocrit values (which could impact whole blood pharmacokinetics of everolimus) did not show marked changes between the two pharmacokinetic visits. Median fold change was 1.05 ranging from 0.97 to 1.17. Overall mean hematocrit during the trial was 36.6%.

Five patients were randomized to each treatment arm. Randomization sequence did not seem it impact the outcome of the primary endpoint, as the absolute and relative mean C_{max} reductions in the QD-BID arm were 19.4 ng/mL and 26.8% compared to 23.0 ng/mL and 38.5% in the BID-QD sequence arm.

Adverse events

An overview of all treatment related adverse events is provided in table 4. Only one patient did not experience any treatment related adverse events. The most common event was oral stomatitis (in all cases limited to grade 1). Only one grade 3 event (ALT elevation) and two grade 2 events (neuropathy and increased AST) occurred during the trial period. Due to the low number of events in the trial period, no distinct differences in toxicity between the two dosing arms or exposure-safety relationships could be distinguished.

Table 4: Toxicity data per dose schedule, graded according to CTCAE v 4.02, only treatment related toxicities are shown.

Adverse event	5 mg BID Any grade (n)	Grade ≥3 (n)	10 mg QD Any grade (n)	Grade ≥3 (n)
Stomatitis	2	0	2	0
AST increase	1	0	0	0
ALT increase	0	1	0	0
Neuropathy	1	0	0	0
Fatigue	1	0	0	0
Nausea	1	0	0	0
Constipation	0	0	1	0
Dry skin	2	0	0	0
Dry mouth	1	0	0	0
Pruritus	0	0	1	0

Discussion

The hypothesis of this study was that switching patients from a 10 mg QD to a 5 mg BID would lead to a reduction in C_{max}, which is probably responsible for most of the dose-limiting toxicities, whilst still maintaining AUC and C_{min}, to guarantee similar efficacy.

We have shown that splitting everolimus intake results in a large reduction in C_{max} and a modest, yet statistically significant increase in C_{min} (table 2, figure 2 and 3**)**. This resulted in an approximately 50% reduction in the C_{max}/C_{min} ratio of 6.44 on the QD schedule to 3.18 on the BID schedule ($p<0.001$).

No significant difference in total exposure measured as AUC was detected by splitting the dose into a 5 mg BID regimen. This was the intended outcome and in concordance with the pharmacokinetics data in the phase 1 study, which showed no dose-dependent change in bioavailability over a dose range of 5-70 mg [10]. Subsequently, these results support the view that a switch from 10 mg QD to 5 mg BID is feasible, and could improve specific pharmacokinetic parameters, without affecting overall exposure.

Previous studies have shown a large inter-patient variability in everolimus pharmacokinetics [7,10–12]. Our trial confirms the high inter-patient variability with CVs ranging from 28.1% to 53.9%. (**table 2**). CVs were numerically higher in the BID arm than on the QD arm. Most likely this difference is driven by the single outlier patient (see table 4) which had an increased C_{max} on the BID schedule. As food is known to affect everolimus pharmacokinetics[13], patients were instructed to take everolimus with a low-fat meal during the study period. To further reduce a possible effect of this and other environmental factors on everolimus pharmacokinetic variability we used a crossover design for the current study. Using this design only intra-patient pharmacokinetic variability could possibly influence the outcome.

As shown in figure 2, the C_{max} achieved on the BID schedule in the evening seemed lower compared to the C_{max} in the morning. This is most likely due to the larger meal size in the evening, as food is known to reduce everolimus absorption.[13]

Everolimus was well tolerated in the current study in both dose regimens. However, some patients had already received everolimus before enrollment. This limits the comparison of toxicity between the two dose regimens, as most everolimus associated AEs occur soon after initiation of therapy [14]. Moreover, in the current trial patients were only treated on each dose schedule for a short duration of merely two weeks.

Everolimus C_{min} has been linked to treatment efficacy in several studies. An analysis of 44 renal cell carcinoma patients proposed a threshold for efficacy of 14.1 ng/mL [15]. Although not statistically significant, a difference in progression free survival of 13.3 versus 3.9 months was seen. In pediatric oncology, everolimus is dosed based on whole blood concentrations and a C_{min} window of 5 – 15 ng/mL is used as the pharmacokinetic target [16]. In pancreatic neuro-endocrine tumors median progression free survival was 22.7 months in patients with a C_{min} of 10 - 30 ng/mL compared to only 13.8 months in patients with a C_{min} < 10 ng/mL [6]. In a meta-analysis of published phase II trials in various tumor types, a two-fold increase in C_{min} increased the probability of tumor size reduction by 40% and reduced the risk of progression free survival events by 10% [6].
These findings underscore the need to maintain C_{min} levels. Fortunately, the current strategy of 5 mg BID dosing even increased C_{min} compared to the once daily dosing, potentially leading to a better progression free survival. However, a prospective clinical trial is needed to conclusively demonstrate a reduction in toxicity and improved efficacy for the BID everolimus administration schedule.

A drawback of switching to a BID dose schedule might be that it could reduce treatment compliance. However, the effect of QD dosing on adherence has been shown to be modest in other therapeutic areas (e.g. only a 2.9% increase in adherence was seen in a meta-analysis of antiretroviral drugs)[17]. Moreover, it also could be argued that a reduction in toxicity could help maintain treatment adherence and even prevent dose reductions or treatment discontinuation, which are common in everolimus treatment [3,7].

Limitations of the current study include its limited size and duration and the fact that patients could already have received everolimus before enrollment. Although the endpoint of reduced C_{max}/C_{min} ratio has been achieved, the relationship between this ratio and toxicity cannot be assessed based on these data.

An alternative strategy to manage toxicity could be to individualize the everolimus dose based on measured C_{min} levels, also known as therapeutic drug monitoring. Given the high inter-patient variability in exposure [10] and the established exposure-efficacy and exposure-toxicity relationships, this would be a rational approach. Moreover, this has already been implemented in

everolimus therapy in transplantation medicine [18] and pediatric oncology [16]. BID dosing could be combined with therapeutic drug monitoring to further manage the pharmacokinetic exposure in everolimus treatment and interestingly, in transplantation medicine everolimus is already routinely administered in a BID schedule, albeit at a lower total dose [18].

Conclusion

In summary, this randomized pharmacokinetic crossover study in cancer patients indicates that switching from 10 mg QD to a 5 mg BID dose schedule significantly reduces everolimus C_{max} without negatively impacting C_{min} or $AUC_{0\text{-}24h.}$ These results merit further investigation of the BID everolimus schedule in oncology in an effort to reduce everolimus toxicity whilst maintaining treatment efficacy.

Compliance with Ethical Standards

This trial was conducted in accordance with the World Medical Organization declaration of Helsinki, compliant with Good Clinical Practice and approved by the Medical Ethics Committee of the each participating medical center (The Netherlands Cancer Institute and Erasmus MC Cancer Institute). All patients provided written informed consent before enrollment. This trial was registered in the EurdaCT database (2014-004833-25) and the Netherlands Trial Registry (NTR4908).

Funding Statement

This investigator initiated study was supported by Novartis. The funding source had no involvement in the study design, collection, analysis and interpretation of data, the writing of the report or in the decision to submit the article for publication.

Conflicts of Interest

N. Steeghs received funding from Novartis as principal investigator for this investigator initiated study. R.B. Verheijen, F. Atrafi, J.H.M. Schellens, J.H. Beijnen, A.D.R. Huitema and R.H.J. Mathijssen all declare they have no conflicts to disclose.

Acknowledgements

We thank all patients for their participation in this study.

References

1. Motzer RJ, Escudier B, Oudard S, Hutson TE, Porta C, Bracarda S, et al. Efficacy of everolimus in advanced renal cell carcinoma: a double-blind, randomised, placebo-controlled phase III trial. Lancet. 2008;372:449–56.
2. Yao JC, Shah MH, Ito T, Bohas CL, Wolin EM, Van Cutsem E, et al. Everolimus for advanced pancreatic neuroendocrine tumors. N Engl J Med. 2011;364:514–23.
3. Baselga J, Campone M, Piccart M, Burris HA 3rd, Rugo HS, Sahmoud T, et al. Everolimus in postmenopausal hormone-receptor-positive advanced breast cancer. N. Engl. J. Med. 2012;366:520–9.
4. Steelman LS, Martelli AM, Cocco L, Libra M, Nicoletti F, Abrams SL, et al. The Therapeutic Potential of mTOR Inhibitors in Breast Cancer. Br. J. Clin. Pharmacol. 2016;1–24.
5. Yardley DA, Noguchi S, Pritchard KI, Burris HA, Baselga J, Gnant M, et al. Everolimus plus exemestane in postmenopausal patients with HR+ breast cancer: BOLERO-2 final progression-free survival analysis. Adv. Ther. 2013;30:870–84.
6. Ravaud A, Urva SR, Grosch K, Cheung WK, Anak O, Sellami DB. Relationship between everolimus exposure and safety and efficacy: Meta-analysis of clinical trials in oncology. Eur. J. Cancer. 2014;50:486–95.
7. de Wit D, Schneider TC, Moes DJAR, Roozen CFM, den Hartigh J, Gelderblom H, et al. Everolimus pharmacokinetics and its exposure–toxicity relationship in patients with thyroid cancer. Cancer Chemother. Pharmacol. 2016;78:63–71.
8. Diederich A, Liechti K, Kuehl P, Cheung W. Pharmaceutical compositions comprising 40 - o - (2 - hydroxy) ethyl - rapamycin [Internet]. 2013. Available from: https://www.google.com/patents/WO2013050419A1?cl=en
9. Verheijen RB, Bins S, Mathijssen RHJ, Lolkema MP, van Doorn L, Schellens JHM, et al. Individualized Pazopanib Dosing: A Prospective Feasibility Study in Cancer Patients. Clin. Cancer Res. 2016;22:5738–46.
10. O'Donnell A, Faivre S, Burris HA, Rea D, Papadimitrakopoulou V, Shand N, et al. Phase I pharmacokinetic and pharmacodynamic study of the oral mammalian target of rapamycin inhibitor everolimus in patients with advanced solid tumors. J. Clin. Oncol. 2008;26:1588–95.
11. Kirchner GI, Meier-wiedenbach I, Manns MP. Clinical Pharmacokinetics of Everolimus. Clin. Pharmacokinet. 2004;43:83–95.
12. Moes DJAR, Press RR, Den Hartigh J, Van Der Straaten T, De Fijter JW, Guchelaar HJ. Population pharmacokinetics and pharmacogenetics of everolimus in renal transplant patients. Clin. Pharmacokinet. 2012;51:467–80.
13. Kovarik JM, Hartmann S, Figueiredo J, Rordorf C, Golor G, Lison A, et al. Effect of Food on Everolimus Absorption : Quantification in Healthy Subjects and a Confirmatory Screening in Patients With Renal Transplants. Pharmacotherapy. 2002;22:154–9.
14. Rugo HS, Pritchard KI, Gnant M, Noguchi S, Piccart M, Hortobagyi G, et al. Incidence and time course of everolimus-related adverse events in postmenopausal women with hormone receptor-positive advanced breast cancer: Insights from BOLERO-2. Ann. Oncol. 2014;25:808–15.
15. Thiery-Vuillemin A, Mouillet G, Nguyen Tan Hon T, Montcuquet P, Maurina T, Almotlak H, et al. Impact of everolimus blood concentration on its anti-cancer activity in patients with metastatic renal cell carcinoma. Cancer Chemother. Pharmacol. 2014;73:999–1007.
16. Krueger DA, Care MM, Holland K, Agricola K, Tudor C, Mangeshkar P, et al. Everolimus for Subependymal Giant-Cell Astrocytomas in Tuberous Sclerosis. N Engl J Med. 2010;363:1801–11.
17. Parienti JJ, Bangsberg DR, Verdon R, Gardner EM. Better Adherence with Once Daily Antiretroviral Regimens: A Meta Analysis. Clin. Infect. Dis. 2009;48:484–8.
18. Shipkova M, Hesselink DA, Holt DW, Billaud EM, van Gelder T, Kunicki PK, et al. Therapeutic Drug Monitoring of Everolimus: A Consensus Report. Ther. Drug Monit. 2016;38:143–69.

Chapter 4

Clinical Pharmacology of Kinase Inhibitors in Real-World Patient Cohorts

Chapter 4.1

Monitoring of EGFR Mutations in Circulating Tumor DNA of Non-Small Cell Lung Cancer Patients Treated With EGFR Inhibitors

R.B. Verheijen[1], T.T. van Duijl[1], M.M. van den Heuvel[2], D. Vessies[3], M. Muller[2], J.H. Beijnen[1,4], J.M. Janssen[1], J.H.M. Schellens[4,5], N. Steeghs[5], D. van den Broek[3], A.D.R. Huitema[1,6]

[1] Department of Pharmacy & Pharmacology, The Netherlands Cancer Institute - Antoni van Leeuwenhoek, Louwesweg 6, 1066 EC Amsterdam, The Netherlands.

[2] Department of Thoracic Oncology, The Netherlands Cancer Institute - Antoni van Leeuwenhoek, Amsterdam, The Netherlands.

[3] Department of Clinical Chemistry, The Netherlands Cancer Institute - Antoni van Leeuwenhoek, Amsterdam, The Netherlands.

[4] Department of Pharmaceutical Sciences, Utrecht University, Utrecht, The Netherlands.

[5] Department of Medical Oncology and Clinical Pharmacology, The Netherlands Cancer Institute - Antoni van Leeuwenhoek, Amsterdam, The Netherlands.

[6] Department of Clinical Pharmacy, University Medical Center Utrecht, Utrecht, The Netherlands.

Abstract

We studied EGFR mutations in circulating tumor DNA (ctDNA) and explored their role in predicting progression free survival (PFS) of non-small cell lung cancer (NSCLC). NSCLC patients treated with erlotinib or gefitinib were included. The L858R, T790M mutations and exon 19 deletions were quantified in plasma using digital droplet polymerase chain reaction (ddPCR). The dynamics of ctDNA mutations over time and relationships with PFS were explored. In total 249 plasma samples (1-13 per patient) were available from 68 NSCLC patients. The T790M and L858R or exon 19 deletion were found in the ctDNA of 49% and 56% patients, respectively. The median [range] concentration in these samples were 7.3 [5.1 - 3688.7], 11.7 [5.1 – 12393.3] and 27.9 [5.9 – 2896.7] copies/mL, respectively. Using local polynomial regression, the number of copies of EGFR mutations per mL increased several months prior to progression on standard response evaluation. This change was more pronounced for the driver mutations than for the resistance mutations. In conclusion, quantification of EGFR mutations in plasma ctDNA was predictive of treatment outcomes in NSCLC patients. In particular, an increase in driver mutation copy number may predict disease progression.

Introduction

Non-small cell lung cancer (NSCLC) is the single most common histological subtype of lung cancer. Approximately 5-20% of patients present with an activating mutation in the epidermal growth factor receptor (EGFR) gene.[1,2] The most abundant activating (or driver) mutations are the L858R point mutation on exon 21 and deletions on exon 19 of the EGFR gene.[3–5] Once such an EGFR mutation is found in the tumor, first-line therapy consists of a tyrosine kinase inhibitor (TKI) specifically targeting these EGFR mutations.[6] Erlotinib and gefitinib are TKIs that are commonly used for this purpose in the treatment of NSCLC. Despite the fact that patients often show impressive initial responses to treatments with these TKIs, resulting in significant improvements in progression free and overall survival, the tumor will inevitably develop resistance and relapse.[7–9]

The occurrence of the T790M mutation has been identified as a crucial resistance mutation, which has been shown to account for a large proportion of the acquired resistance to EGFR inhibitors.[10–12] Although standard tumor genotyping is still being performed by taking a needle or surgical biopsy from a tumor lesion, the possibilities for 'liquid' biopsies, i.e. tumor genotyping through analyzing tumor cells or DNA fragments in the systemic circulation, are expanding rapidly.[13,14] These technologies could be used as a more patient friendly alternative to determine the EGFR genotype of tumors, forgoing the need for traditional invasive biopsies. Furthermore, the less invasive nature of these types of techniques allows for repeated measurements over time to study quantitative changes before, during and after treatment with anti-cancer drugs. An example of this liquid biopsy technology is using digital droplet polymerase chain reaction (ddPCR) to detect mutations in circulating tumor DNA (ctDNA) in blood or plasma of patients with cancer.[15,16] Using ddPCR, quantitative monitoring of selected genes such as the EGFR gene during treatment, could for instance predict which patients are likely to respond to treatment with targeted EGFR inhibitors. Additionally, patients that may benefit from switching to another therapy can be selected, as specific inhibitors of the most common T790M EGFR resistance mutation have become available.[17] Even though it is apparent that techniques like these will impact and improve the manner in which patients with EGFR inhibitors are treated, the precise ways in which ctDNA monitoring could guide treatment remains unclear.

The aim of this study was to measure the most important EGFR driver and resistance mutations in ctDNA in a cohort of NSCLC patients treated with the EGFR inhibitors erlotinib and gefitinib. The ultimate goal was to analyze the quantitative dynamics of these mutations over time and explore the roles of EGFR driver and resistance mutations in predicting disease progression.

Subjects and Methods

Patient population

An observational study was performed in the outpatient clinic of the Netherlands Cancer Institute, Amsterdam, The Netherlands. All patients with NSCLC who received erlotinib or gefitinib as first-line anti-EGFR therapy for whom at least one plasma sample was available were included. Clinical visits and response evaluations were scheduled in accordance with standard treatment guidelines. Clinical characteristics including demographic data, medical history, tumor characteristics (stage, EGFR mutational status), erlotinib and/or gefitinib dose and administration schedule, plasma sampling date, treatment duration, reason for discontinuation and progression free survival (PFS) were collected retrospectively from medical records. For this retrospective observational study no informed consent was required in accordance with code of conduct for responsible use of human tissue and medical research.[18]

Sample collection

Surplus plasma was collected from samples obtained during treatment with an EGFR-inhibitor as part of routine care. These plasma samples had been collected into EDTA tubes and stored at (at least) -20 °C until DNA isolation.

Circulating DNA analysis

For mutation analysis, cell-free DNA was extracted from plasma samples (circa 1 mL) in elution buffer using QIAsymphony circulating DNA Nucleic Acid Kits (Qiagen). Quantification of the *a priori* selected EGFR mutants (T790M, L858R and exon 19 deletions) in purified DNA was performed using ddPCR assays. To detect EGFR target alleles, TaqMan hydrolysis mutant (T790M or L858R) and wildtype probes labelled with FAM/HEX were used (Bio-Rad). Variants of in-frame exon 19 deletions were detected using a FAM/HEX drop-off assay (PrimeTime, Integrated DNA Technologies). This assay enabled detection and quantification of (amongst others) the following frame deletions and indels: c.2235_2249del15, c.2236_2250del15, c.2239_2256del18, c.2239-2251del13 ins C, c.2240-2254del15 and c.2240-2257del18.[19]

Samples were partitioned into circa 20.000 water in oil droplets using a Droplet Generator (Bio-Rad). The target gene was amplified in each droplet with PCR thermocycling using a C1000 Touch Thermal Cycler. The cycles temperatures used were, 95 ºC for polymerase activation and denaturation, 55 ºC for annealing, 98 ºC for incubation and 12 ºC for the final hold. FAM/HEX fluorescence intensity was measured for every droplet with a QX100 Droplet Reader (Bio-Rad). In a two-dimensional fluorescence intensity histogram, thresholds were set manually (lasso tool) according to amplitude guidelines within our lab. ddPCR results were evaluated based on the quantity of positive droplets for mutation and wildtype, double positive droplets and total accepted droplets in the assay. The read-out was converted to allele concentration using the initial plasma sample volume from which

the ctDNA was extracted. Absolute quantification of the mutation was presented as copies of mutant allele per mL plasma.

Table 1: Characteristics of included patients, n=68.

	Patients, n (%), [range]
Age (median in years)	62 [37-83]
Gender	
female	50 (74%)
male	18 (26%)
Stage at start treatment	
IIIA	5 (7%)
IIIB	8 (12%)
IV	55 (81%)
EGFR driver mutation‡	
exon 19 del	37 (54%)
L858R	22 (32%)
other/uncommon*	4 (6%)
unknown	5 (7%)
Treatment	
erlotinib	38 (56%)
gefitinib	24 (35%)
erlotinib & gefitinib†	6 (9%)
Previous lines of therapy	
none	48 (71%)
chemotherapy	15 (22%)
other/unknown	5 (7%)

‡ These were the EGFR activating mutations based on solid biopsies taken as part of routine patient care.

**G719A (c.2156G>C); L747P (2239_2240 TT>CC); A840T (c.2518G>A); L861Q (c.2582T>A)*

† These patients switched from erlotinib to gefitinib or vice versa due to toxicity.

Data Analysis & Statistics

The distribution of the concentrations (mutant copies/mL plasma) in ctDNA were studied for each of the studied EGFR mutations. The dynamics of these ctDNA mutations over time were examined by plotting the ctDNA concentrations versus the normalized time to progression of disease (as measured by routine CT scans). Trends over time would be identified using locally weighted polynomial regression or LOESS regression fits in resulting scatter plots.

Exploratory survival analyses were conducted to investigate the relationship between EGFR copy numbers in ctDNA and PFS. Specifically, the relationship between the occurrence of the T790M mutation at any time during treatment were studied. Also, comparisons were made between

patients whose EGFR driver mutations reached concentrations below the limit of detection versus patients whose mutations were above this limit in all available samples. All statistical analyses were performed in R 3.2.2.[20]

Results

Patient Population

From September 2012 to March 2016, 68 patients with NSCLC were enrolled. Descriptive characteristics of the included patients are shown in table 1. Based on solid biopsies at diagnosis, 37 patients (54%) carried a deletion in exon 19, 22 patients (32%) harbored an EGFR L858R mutation and for 9 patients (13%) the original driver EGFR mutation was uncommon or unknown. In our cohort, median PFS on anti-EGFR therapy was 14.1 [range 1.2 – 93.7] months and at time of analysis 10 patients had ongoing response on erlotinib or gefitinib.

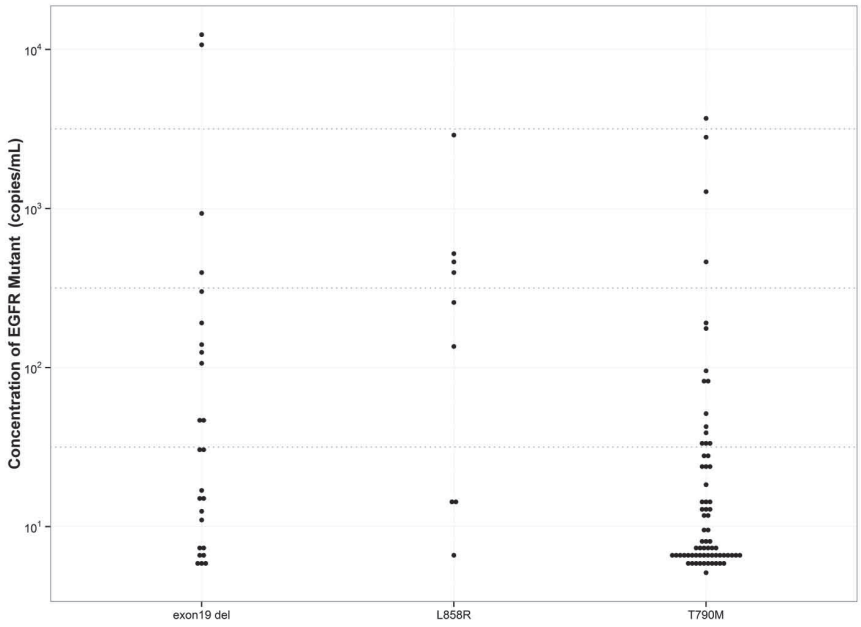

Figure 1: Non-zero EGFR mutant concentrations (in copies/mL plasma) plotted on a log scale for a cohort of non-small cell lung cancer patients treated with EGFR inhibitors. The T790M and L858R or exon 19 deletion were found in the ctDNA of 49% and 56% patients, respectively. The median [range] concentrations were 7.3 [5.1 - 3688.7], 11.7 [5.1 – 12393.3] and 27.9 [5.9 – 2896.7] for the T790M, exon 19 del and L858R mutation respectively.

EGFR mutations in ctDNA

Of the 68 evaluable patients, a total of 249 plasma samples were collected during treatment and samples were distributed among the patients with a mean of 3.7 [range 1 -13] samples per patient. For 33 patients (49%) the EGFR T790M mutant was detected in at least one plasma sample collected during first TKI treatment (Table 2). The median concentration of EGFR T790M mutant positive samples was 7.3 [range 5.1 - 3688.7] copies per mL plasma (figure 1).

In total, 59 patients had the L858R or exon 19 del activating mutations detected in solid biopsies (table 1). For 54 of these, additional plasma was available for quantitative mutation analysis of the original EGFR driver mutation. In 30 patients of these 54 patients (56%) the L858R or exon 19 deletion mutant was detectable in at least one plasma sample.

The median concentration of the mutant allele was 11.7 [range 5.1 – 12393.3] and 27.9 [range 5.9 – 2896.7] copies per mL plasma, for the exon 19 deletion and L858R mutant, respectively (figure 1).

In 42 of the 54 patients (78%) the concentration of the EGFR activating mutation was or eventually dropped under the limit of detection in ctDNA during treatment.

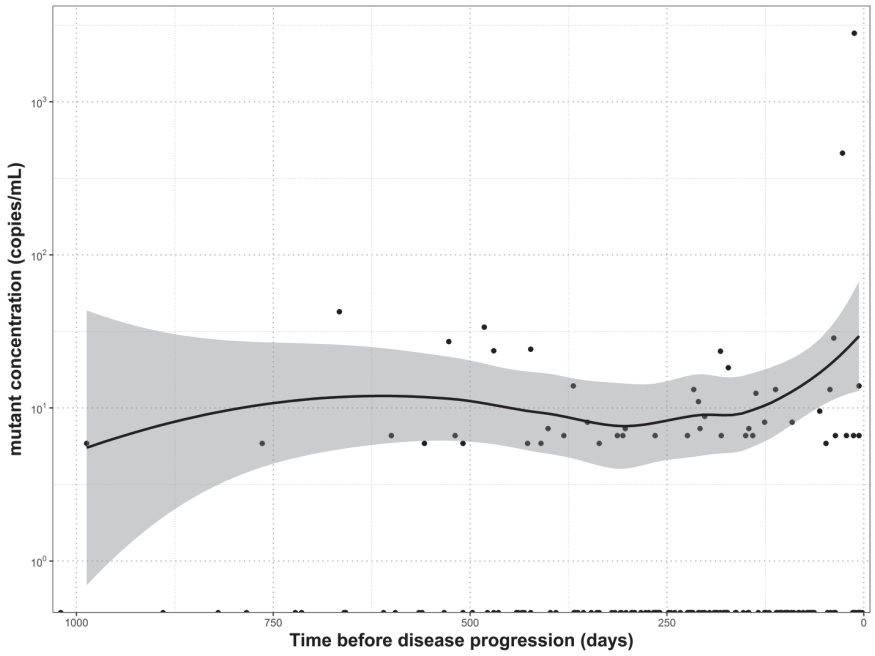

Figure 2: Semi-log scatter plot of the concentration (in copies/mL plasma) of the EGFR T790M mutation, over time before disease progression (in days). Each dot represents a single sample from a patient. The line indicates the locally weighted polynomial regression or LOESS regression plus 95% confidence interval (shaded area). Approximately 125 days before clinical progression, an increase in the mutant concentration is observable, suggesting the possibility of early prediction of treatment failure using T790M concentrations.

Dynamics of EGFR mutations in ctDNA over time

To explore the association between occurrence of EGFR mutations in plasma and treatment response, data of all patients was combined and normalized at the date of progression on CT scan (t = 0). Separate plots were made for the EGFR resistance (figure 2) and activating mutations (figure 3). After application of local regression to the data, a modest yet distinct increase in T790M mutant concentrations was noticed approximately 80-120 days before progression of disease observed on CT scan (figure 2). Remarkably, two patients with very high T790M mutation concentrations showed rapid relapse of the tumor. As shown in figure 2.

The same plot is shown for the L858R or exon19 deletion in figure 3. Here a clear rise in EGFR copy numbers is seen approximately 5 months before progression using standard response evaluation.

Survival Analyses

Survival analyses using the EGFR driver mutations did not result in a significant relationship with PFS. In total 42 patients reached concentrations below the limit of detection during treatment, whilst 12 did not. Median PFS was 14.0 months in the former versus 11.8 months in the latter group (p=0.134). Detection of the T790M mutation at any time during treatment was also unable to predict PFS in Kaplan-Meier analysis (median 14.0 months, n=35 versus 14.2 months n=33, p=0.648).

Discussion

We show the feasibility of ddPCR quantification of EGFR driver and resistance mutations in ctDNA of NSCLC patients treated with erlotinib and/or gefitinib. In contrast to what may have been expected, the occurrence of detectable (at any concentration above the limit of detection) T790M levels in plasma did not seem to predict imminent treatment failure (figure 2). In Kaplan-Meier analysis, measurement of T790M (without specifying the sampling time point) also did not predict shorter PFS. The presence of a T790M resistant sub clone in the tumor apparently does not translate into immediate progression of tumor growth as measured by standard imaging techniques. This observations is supported by previous preclinical studies into the growth dynamics of T790M mutated tumor cells which, though resistant to therapy, exhibited remarkably slow growth rates.[21] However, very high concentrations (>100 copies/mL) of T790M in plasma did seem to result in rapid relapse of the tumor, as illustrated by two cases in our cohort (figure 2).

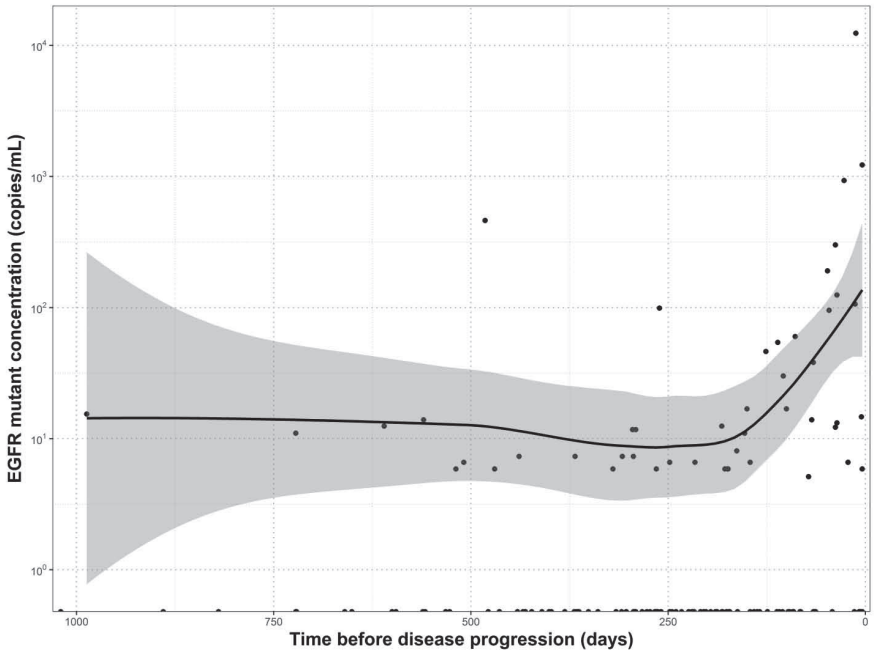

Figure 3: Semi-log scatter plot of the concentration (in copies/mL plasma) of the EGFR driver mutations, L858R and exon 19 del over time before disease progression (in days). Each dot represents a single sample from a patient. The line indicates the locally weighted polynomial regression or LOESS regression plus 95% confidence interval (shaded area). Approximately 150 days before clinical progression, an increase in the mutant concentration is observable, suggesting the possibility of early prediction of treatment failure.

Changes in concentrations of the EGFR mutations in ctDNA over time seemed to be able to predict clinical progression several months before progression of disease was determined using standard CT scans (figure 2 & 3). This effect seemed particularly pronounced for the L858R mutation and exon 19 deletions (figure 3). This observation indicates that quantitative monitoring of EGFR activating mutations could serve as an early predictor of disease progression and could possibly serve a role similar to that prostate specific antigen in prostate cancer. However, future prospective studies are needed to confirm this hypothesis.

These early signals of progressive disease could enable an early switch to second line treatment, in particular to an EGFR inhibitor that also targets the T790M mutations such as osimertinib.[17] If such an early change in treatment translates into increased patient survival is still unknown. This effect is studied in the currently ongoing APPLE trial. In this trial, patients are randomized to start directly on osimertinib, an EGFR inhibitor specifically targeting the T790M mutation (arm A), or to gefitinib until the T790M mutation is detected in ctDNA (arm B) or to gefitinib until progressive disease on CT is observed (arm C).[22] Trials like these will increasingly be needed to study the effects of treatment changes based on ctDNA measurements on patient outcomes.

Although our study focused on quantification of the most important EGFR activating and resistance mutations, future studies could also take non-classical EGFR activating mutations or mutations in non-EGFR genes such as KRAS into account. As these mutations have previously been linked to outcomes in NSCLC patients treated with EGFR inhibitors.[4,23]

Future efforts could also focus on using more advanced mathematical methods to explore the quantitative nature of ctDNA dynamics and treatment outcomes. Non-linear mixed effect modelling, which is at the moment mainly employed for pharmacokinetic and pharmacodynamic data, could be an attractive strategy to this end.[24]

Conclusion

We show that ddPCR quantification of EGFR activating and resistance mutations in plasma ctDNA could be a relevant predictor of treatment outcomes in NSCLC patients. In particular, an increase in the copies/mL of the EGFR driver mutation over time may predict clinical progression, suggesting ctDNA monitoring could be used as an early read out of treatment failure. ctDNA monitoring of EGFR activating mutations could therefore possibly serve a role similar to that prostate specific antigen in prostate cancer. However, future prospective studies are needed to confirm this hypothesis.

Conflicts of interest

The authors declare they have no interests to disclose.

References

1 Dearden S, Stevens J, Wu YL, Blowers D. Mutation incidence and coincidence in non small-cell lung cancer: Meta-analyses by ethnicity and histology (mutMap). *Ann Oncol* 2013; **24**: 2371–2376.

2 Boch C, Kollmeier J, Roth a., Stephan-Falkenau S, Misch D, Gruning W *et al.* The frequency of EGFR and KRAS mutations in non-small cell lung cancer (NSCLC): routine screening data for central Europe from a cohort study. *BMJ Open* 2013; **3**: e002560–e002560.

3 Arcila ME, Nafa K, Chaft JE, Rekhtman N, Lau C, Reva B a *et al.* EGFR exon 20 insertion mutations in lung adenocarcinomas: prevalence, molecular heterogeneity, and clinicopathologic characteristics. *Mol Cancer Ther* 2013; **12**: 220–9.

4 Kuiper JL, Hashemi SMS, Thunnissen E, Snijders PJF, Grünberg K, Bloemena E *et al.* Non-classic EGFR mutations in a cohort of Dutch EGFR-mutated NSCLC patients and outcomes following EGFR-TKI treatment. *Br J Cancer* 2016; **115**: 1504–1512.

5 Murray S, Dahabreh IJ, Linardou H, Manoloukos M, Bafaloukos D, Kosmidis P. Somatic Mutations of the Tyrosine Kinase Domain of Epidermal Growth Factor Receptor and Tyrosine Kinase Inhibitor Response to TKIs in Non-small Cell Lung Cancer: An Analytical Database. *J Thorac Oncol* 2008; **3**: 832–839.

6 Novello S, Barlesi F, Califano R, Cufer T, Ekman S, Levra MG *et al.* Metastatic non-small-cell lung cancer: ESMO Clinical Practice Guidelines for diagnosis, treatment and follow-up. *Ann Oncol* 2016; **27**: V1–V27.

7 Zhou C, Wu YL, Chen G, Feng J, Liu XQ, Wang C *et al.* Final overall survival results from a randomised, phase III study of erlotinib versus chemotherapy as first-line treatment of EGFR mutation-positive advanced non-small-cell lung cancer (OPTIMAL, CTONG-0802). *Ann Oncol* 2015; **26**: 1877–1883.

8 Zhao H, Fan Y, Ma S, Song X, Han B, Cheng Y *et al.* Final Overall Survival Results from a Phase III, Randomized, Placebo-Controlled, Parallel-Group Study of Gefitinib Versus Placebo as Maintenance Therapy in Patients with Locally Advanced or Metastatic Non–Small-Cell Lung Cancer (INFORM; C-TONG 0804). *J Thorac Oncol* 2015; **10**: 655–664.

9 Greenhalgh J, Dwan K, Boland A, Bates V, Vecchio F, Dundar Y *et al.* First-line treatment of advanced epidermal growth factor receptor (EGFR) mutation positive non-squamous non-small cell lung cancer (Review). *Cochrane Database Syst Rev* 2016; **5**. doi:10.1002/14651858.CD010383.pub2.

10 Sequist L V, Waltman B a, Dias-Santagata D, Digumarthy S, Turke AB, Fidias P *et al.* Genotypic and histological evolution of lung cancers acquiring resistance to EGFR inhibitors. *Sci Transl Med* 2011; **3**: 75ra26.

11 Yu HA, Arcila ME, Hellmann MD, Kris MG, Ladanyi M, Riely GJ. Poor response to erlotinib in patients with tumors containing baseline EGFR T790M mutations found by routine clinical molecular testing. *Ann Oncol* 2014; **25**: 423–428.

12 Wang Z, Chen R, Wang S, Zhong J, Wu M, Zhao J *et al.* Quantification and dynamic monitoring of EGFR T790M in plasma cell-free DNA by digital PCR for prognosis of EGFR-TKI treatment in advanced NSCLC. *PLoS One* 2014; **9**: 1–7.

13 Crowley E, Di Nicolantonio F, Loupakis F, Bardelli A. Liquid biopsy: monitoring cancer-genetics in the blood. *Nat Rev Clin Oncol* 2013; **10**: 472–484.

14 Murtaza M, Dawson S-J, Tsui DWY, Gale D, Forshew T, Piskorz AM *et al.* Non-invasive analysis of acquired resistance to cancer therapy by sequencing of plasma DNA. *Nature* 2013; **497**: 108–12.

15 Oxnard GR, Paweletz CP, Kuang Y, Mach SL, O'Connell A, Messineo MM *et al.* Noninvasive detection of response and resistance in egfrmutant lung cancer using quantitative next-generation genotyping of cell-free plasma DNA. *Clin Cancer Res* 2014; **20**: 1698–1705.

16 Lee JY, Qing X, Xiumin W, Yali B, Chi S, Bak SH *et al.* Longitudinal monitoring of EGFR mutations in plasma predicts outcomes of NSCLC patients treated with EGFR TKIs: Korean Lung Cancer Consortium (KLCC-12-02). *Oncotarget* 2016; **7**: 6984–6993.

17 Mok TS, Wu Y-L, Ahn M-J, Garassino MC, Kim HR, Ramalingam SS *et al.* Osimertinib or Platinum–Pemetrexed in EGFR T790M–Positive Lung Cancer. *N Engl J Med* 2016; **376**. doi:10.1056/NEJMoa1612674.

18 Federation of Dutch Medical Scientific Societies. Human Tissue and Medical Research: Code of conduct for responsible use (2011). 2011. http://www.federa.org/sites/default/files/

digital_version_first_part_code_of_conduct_in_uk_2011_12092012.pdf.

19 Yung TK, Chan KA, Mok TS, Tong J, To KF, Lo YD. Single-molecule detection of epidermal growth factor receptor mutations in plasma by microfluidics digital PCR in non–small cell lung cancer patients. *Clin Cancer Res* 2009; **15**: 2076–2084.

20 R Core Development Team. A Language and Environment for Statistical Computing. Vienna, Austria R Found. Stat. Comput. 2016.https://www.r-project.org/.

21 Chmielecki J, Foo J, Oxnard GR, Hutchinson K, Ohashi K, Somwar R *et al.* Optimization of Dosing for EGFR-Mutant Non-Small Cell Lung Cancer with Evolutionary Cancer Modeling. *Sci Transl Med* 2011; **3**. doi:10.1126/scitranslmed.3002356.

22 Remon J, Menis J, Hasan B, Peric A, De Maio E, Novello S *et al.* The APPLE Trial: Feasibility and Activity of AZD9291 (Osimertinib) Treatment on Positive PLasma T790M in EGFR -mutant NSCLC Patients. EORTC 1613. *Clin Lung Cancer* 2017; **9291**: 1–6.

23 Brugger W, Triller N, Blasinska-Morawiec M, Curescu S, Sakalauskas R, Manikhas GM *et al.* Prospective molecular marker analyses of EGFR and KRAS from a randomized, placebo-controlled study of erlotinib maintenance therapy in advanced non-small-cell lung cancer. *J Clin Oncol* 2011; **29**: 4113–4120.

24 Barbolosi D, Ciccolini J, Lacarelle B, Barlési F, André N. Computational oncology - mathematical modelling of drug regimens for precision medicine. *Nat Rev Clin Oncol* 2015; : 242–254.

Chapter 4.2

Imatinib Pharmacokinetics in a Large Observational Cohort of Gastrointestinal Stromal Tumor Patients

Sheima Farag[1], Remy B. Verheijen[2], J. Martijn Kerst[1], Annemiek Cats[3], Alwin D.R. Huitema[2], Neeltje Steeghs[1]

[1] *Department of Medical Oncology and Clinical Pharmacology, The Netherlands Cancer Institute-Antoni van Leeuwenhoek, Plesmanlaan 12, 1066 CX Amsterdam, The Netherlands.*

[2] *Department of Pharmacy & Pharmacology, The Netherlands Cancer Institute - Antoni van Leeuwenhoek, Louwesweg 6, 1066 EC Amsterdam, The Netherlands*

[3] *Department of Gastroenterology, The Netherlands Cancer Institute - Antoni van Leeuwenhoek, Plesmanlaan 12, 1066 EC Amsterdam, The Netherlands*

Abstract

Background: Low imatinib trough levels (C_{min}) have been associated with decreased clinical outcome in Gastrointestinal stromal tumor (GIST) patients. This study describes pharmacokinetics of imatinib in a large cohort of GIST patients in routine care.

Methods: An observational study was performed in imatinib treated GIST patients. Patient and tumor characteristics were derived from the Dutch GIST registry and medical records. Imatinib levels were measured by LC-MS/MS. Analyses included occurrence of low imatinib C_{min} (<1000 ug/L), change in C_{min} over time and correlation between exposure and response.

Results: In total, 421 plasma samples were available from 108 GIST patients. Most patients (79.6%) received imatinib dose of 400 mg. Inter- and intrapatient variability of C_{min} were 54% and 23%, respectively. 44.4% of patients presented with C_{min} <1000 µg/L in the first steady state sample, 32.4% of patients was <1000 µg/L in over 75% of the samples. Only 33.3% of patients had C_{min} levels ≥1000 µg/L in all measured samples. No decrease of C_{min} over time was found ($p>0.05$). 57 of 62 (91.9%) palliative treated patients had a tumor response (median C_{min} 1271 µg/L). 5 (8.1%) palliative patients did not respond (median C_{min} 920 µg/L). Given the limited number of non-responders in this cohort, no statistically significant association with clinical benefit could be demonstrated.

Conclusions: In routine clinical care one third of GIST patients is systematically underexposed with the fixed dose of imatinib. Prospective clinical studies are needed to investigate the value of C_{min} guided imatinib dosing in GIST patients.

Introduction

Gastrointestinal stromal tumors (GISTs) are the most common mesenchymal malignancies arising from the gastrointestinal tract. Activating mutations in KIT or platelet derived growth factor receptor (PDGFR), resulting in activation of the tyrosine kinase signaling pathway, are considered to be the main molecular drivers in GIST. Imatinib is a tyrosine kinase inhibitor (TKI) that targets protein kinases such as Bcr-Abl, KIT and PDGFR- A and B[1]. Since the introduction of imatinib survival has spectacularly improved in advanced GIST patients and improved recurrence free survival in the adjuvant setting. The recommended dose of imatinib is 400 mg based on previous phase III studies [2,3]. However, large variability is observed in imatinib plasma concentrations during treatment [4,5]. This variability may be caused by a range of factors. Imatinib is metabolized by CYP3A4 and CYP3A5 and is also a substrate for drug transporters such as PgP and BCRP (ABCB1 and ABCG2), exposure might therefore be influenced by genetic polymorphisms and co-administered drugs [6,7]. In addition, patients undergoing a major gastrectomy have been shown to have significantly lower C_{min} than other patients [8] and one study reported a significant decrease of imatinib exposure over time [9].

Several trials have found a correlation between higher imatinib plasma concentrations and better response to treatment in GIST [4,10–12] and CML[13–15]. Given the increasing evidence that exposure is relevant to clinical outcome and the large variability in pharmacokinetics, which may be even larger in routine care than in clinical trials, measuring imatinib plasma concentrations may be useful to guide treatment of this drug. Over the last 3 years plasma samples were drawn from GIST patients at routine outpatient visits at our institute. This study describes the pharmacokinetics and occurrence of underexposure of imatinib in a large observational cohort of GIST patients with over 400 levels measured in more than 100 patients during routine outpatient care.

Methods

Patients

All GIST patients treated with imatinib in the outpatient clinic of the Netherlands Cancer Institute (NKI) were retrospectively identified and included. Identification was done through search in the database of the Dutch GIST Registry, containing all patients diagnosed with GIST from 2009 to 2014 treated in five GIST centers in the Netherlands. Only patients treated in the NKI were included. Patients who were diagnosed before 2009 and had one or more imatinib plasma concentration measured, were separately identified and their data were manually added.

Variables

Patient characteristics (gender and ethnicity) and tumor characteristics (location, size, mitotic index and mutation status) were extracted from the Dutch GIST registry. The mutation analysis protocol

included analysis of *KIT* (exons 9, 11, 13 and 17) and *PDGFRA* (exons 12, 14 and 18) by Sanger Sequencing. Sequencing was performed on a capillary sequencer (ABI 3730 DNA Analyzer, Life Technologies, USA), mutation analysis was performed using specific software (MutationSurveyer, Softgenetics, USA).

Also treatment objective (palliative or (neo-)adjuvant), imatinib dose, dose schedule and adverse events were included in the analysis. Past surgeries for GIST and surgery results were entered and so were concomitant medication and medical history. For patients diagnosed before 2009, patients' files were used for extracting abovementioned variables. Response evaluations were derived from regularly performed computed tomography scans (CT-scans) and were performed according to RECIST 1.1. Best overall response was defined as the best response recorded from the start of imatinib treatment until disease progression/recurrence. Patients were classified as responders if best response was found to be complete response (CR) or partial response (PR). Patients were classified as non-responders if stable disease (SD) or progressive disease (PD) was best response.

Pharmacokinetics

Blood samples were drawn at regularly scheduled visits to the outpatient clinic. Time of last intake of imatinib dose and the time of blood sampling were recorded. Plasma imatinib plasma concentrations were determined using a validated LC-MS/MS assay[16]. An estimate of the imatinib C_{min} was calculated based on the measured concentration and interval between last ingested dose and sample time using the algorithm developed by Wang et al [17]. Adequate imatinib plasma concentrations were defined as imatinib ≥1000 µg/L as described in previous studies [13,15,18]. For the analysis the first steady state imatinib C_{min} level was used. A representative C_{min} level was defined as the first representative sample at least 2 weeks after start of imatinib treatment.

Statistical Analysis

Statistical analyses were executed using IBM SPSS Statistics 20 and R 3.2.2 [19]. Univariate and multivariate Cox regression, using relevant characteristics such as KIT mutational status, imatinib dose, were used for assessing the correlation between imatinib exposure and time on imatinib and time to progression. Also, exploratory analyses using non-linear mixed effects modeling were conducted to evaluate changes in imatinib C_{min} over time. Interpatient and intra-patient variability was calculated using the coefficient of variation. An association between imatinib C_{min} trough levels and clinical and demographic variables, such as age, gender, tumor site, surgery and tumor characteristics, was assessed using the independent Mann-Whitney U tests. All tests were two-sided and a p-value of <0.05 was considered significant.

Results

Between January 2009 and May 2014, 111 patients who received imatinib therapy were identified from the Dutch GIST registry database. Not all patients had known trough imatinib plasma concentrations. From August 2012 to December 2014, 582 imatinib plasma concentrations of 123 GIST patients were measured. An additional 33 patients who started imatinib treatment before 2009 and have had imatinib drug level measured were identified in the outpatient clinic. All samples below the lower limit of quantification were excluded in case this was due to a planned end of treatment or interruption due to adverse events. Also, samples with missing time of last dose or sampling and samples drawn within two weeks after start of imatinib treatment were excluded. This resulted in representative 421 imatinib plasma concentrations of 108 patients included in the analysis. Median sample frequency per patient was 3 (range: 1-11).

Patient and tumor characteristics are described in table 1. More than half of the cohort consisted of men (n=60, 56.5%) and median age was 60 (range: 28-87) (table 1).

Table 1: Patient characteristics

Characteristic		Patients (n=108)
Gender (m)		60 (55.6%)
Age (median, range)		60 (28-87)
Tumor status		
	Localized	59 (54.6%)
	Metastasized	49 (45.4%)
Treatment objective		
	Neo-adjuvant	16 (14.8%)
	Adjuvant	30 (27.8%)
	Palliative	62 (57.4%)
Location primary tumor		
	Stomach	46 (42.6%)
	Small bowel	44 (40.7%)
	Duodenum	2 (1.9%)
	Rectum	7 (6.5%)
	Esophagus	2 (1.9%)
	Colon	1 (0.9%)
	Unknown	6 (5.5%)
Primary tumor size in mm's (median, range)		100 (19-300)
Mutation status		
	KIT exon 11	76 (70.4%)
	KIT exon 9	9 (8.3%)
	KIT exon 13	1 (0.9%)
	KIT exon 17	3 (2.8%)
	PDGFR exon 14	1 (0.9%)
	PDGFR exon 18	5 (4.6%)
	Wildtype	3 (2.8%)
	Unknown	10 (9.3%)

An overview of the distribution of the calculated imatinib C_{min} of the patients studied in this cohort is given in table 2. Median steady state C_{min} was 1082 µg/L. A total of 60 patients (55.6%) had adequate C_{min} levels at steady state. (Figure 1) Overall, 32.4% of patients showed low imatinib C_{min} levels in over 75% of the samples, and 33.3% of patients showed adequate imatinib C_{min} levels in all measured samples. Imatinib exposure showed high inter- and intrapatient variability with a relative standard deviation of 54% and 23%, respectively. No significant change over time was found. Slope was estimated at a neglible 0.00004 day-1, with an RSE of 25%, p>0.05

Median time on imatinib was 27 months (range: 1-161). Within recorded follow up, 12 patients treated with palliative intent had stopped imatinib due to progressive disease. No statistically significant difference in time to progression (TTP) was found between patients with low steady state C_{min} levels (n=27) and adequate C_{min} levels (n=35) in univariate Cox regression (hazard ratio 1.64, 95%CI 0.611- 5.61, p=0.43). (Figure 2) In multivariate analysis correcting for imatinib dose, gender and KIT mutational status, the association between C_{min} and TTP remained not significant (hazard ratio 0.60, 95%CI 0.53 – 6.35, p=0.34).

Of the 62 evaluable patients treated with palliative intent, 5 (8.1%) patients were non-responders. Median C_{min} in patients showing radiological response was 1270 µg/L and in non-responders this was 920 µg/L, p=0.23 (Figure 3). In the neo-adjuvant setting no difference in imatinib C_{min} levels was found between responders and non-responders, as all but 2 patients had a response.

No clinical characteristic (age, type of surgery, gender, extend of resection) was predictive for low imatinib C_{min}. Also, no association for tumor characteristics such as location (p=0.54), tumor status a registry entry (p=0.23) and mutation status (p=0.48) was found. Four patients (3.7%) had ended imatinib treatment due to adverse events. No association with imatinib C_{min} was found (p=0.40).

Discussion

Several studies have linked higher imatinib C_{min} to better treatment outcomes[4,10–13,15]. In CML, a threshold of ≥1000 µg/L is recommended based on several studies [20–22]. In GIST patients a threshold of ≥1100 µg/L has been suggested [20–22]. This is based on a study by Demetri et al in which patients with in the lowest C_{min} quartile (<1100 µg/L) had shorter time to progression and decreased clinical benefit [4].

In our cohort we found that a large proportion of patients was underexposed to imatinib even when using the relatively low threshold of ≥1000 µg/L (table 2, figure 1). Although 92.6% of patients received imatinib dose of 400 mg or higher, over 40% of our patients had imatinib C_{min} levels <1000 µg/L at first steady state sample and only one third of our patients had adequate C_{min} levels in every sample (table 2). This suggests that GIST patients in routine care have a higher risk for underexposure, which may even result in less clinical benefit [4].

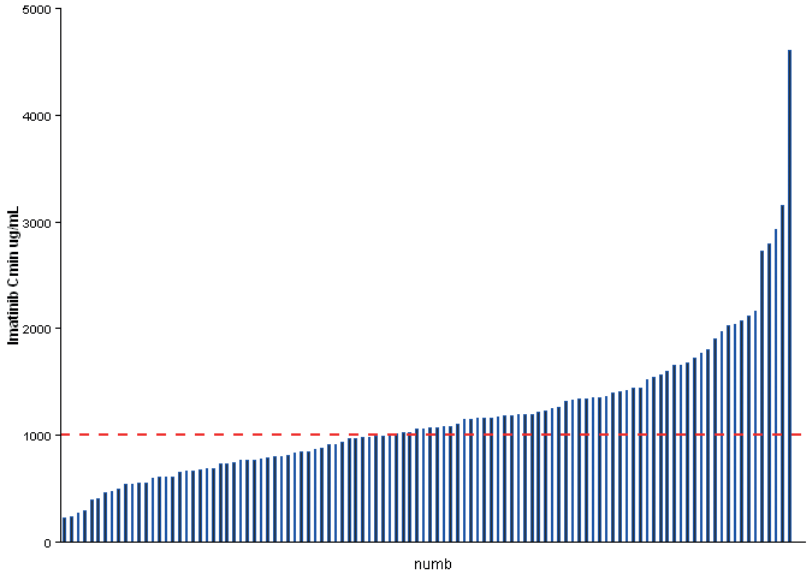

Figure 1: Distribution of first representative imatinib C_{min} (µg/L) levels per patient (n=108).The dotted red line indicates a C_{min} of 1000 µg/L.

Table 2: Characteristics of the 421 available imatinib plasma samples

Characteristic	Patients (108)
Mean C_{min}† in µg/L (range)	1193 (227-4606)
Categorical Cmin (n) (%)	
<1000 µg/L	48 (44.4%)
≥1000 µg/L	60 (55.6%)
C_{min} <1000 µg/L in >75% of the samples (n) (%)	35 (32.4%)
C_{min} ≥1000 µg/L in all samples (n) (%)	36 (33.3%)
Categorical received dose in mg (n) (%)	
<400 mg	8 (7.4%)
400 mg	86 (79.6%)
>400-800 mg	14 (13.0%)

†Calculated trough level (C_{min}). Unless otherwise specified first representative C_{min} was used.

In the case of Demetri et al. the higher average C_{min} may be due to a higher imatinib dose, as patients were randomized to either 400 or 600 mg QD. But other studies in both CML and GIST patients have also described higher levels than those in our cohort [11,15]. This could be explained by the fact that these previous studies were performed in a selected and regulated trial setting. In our cohort, no patient selection was made other than the diagnosis of GIST and treatment with imatinib. Although, concomitant medication was strictly monitored to prevent possible interactions, no strict exclusion

criteria for this study were set considering concomitant medication causing interaction for which no replacement was possible. Also, no exclusion criteria were made for comorbidities and laboratory results. Moreover in clinical care lack of patient compliance could be a factor.
Besides the large percentage of underexposure at first steady state sample (RSD of 54%), we also found large intrapatient variability of 23%. Only one third of patients had adequate C_{min} levels in every sample. This is in accordance with a study by Yoo et al[8], who also found a high inter- and intrapatient variability of 44.7% and 26.5% respectively.

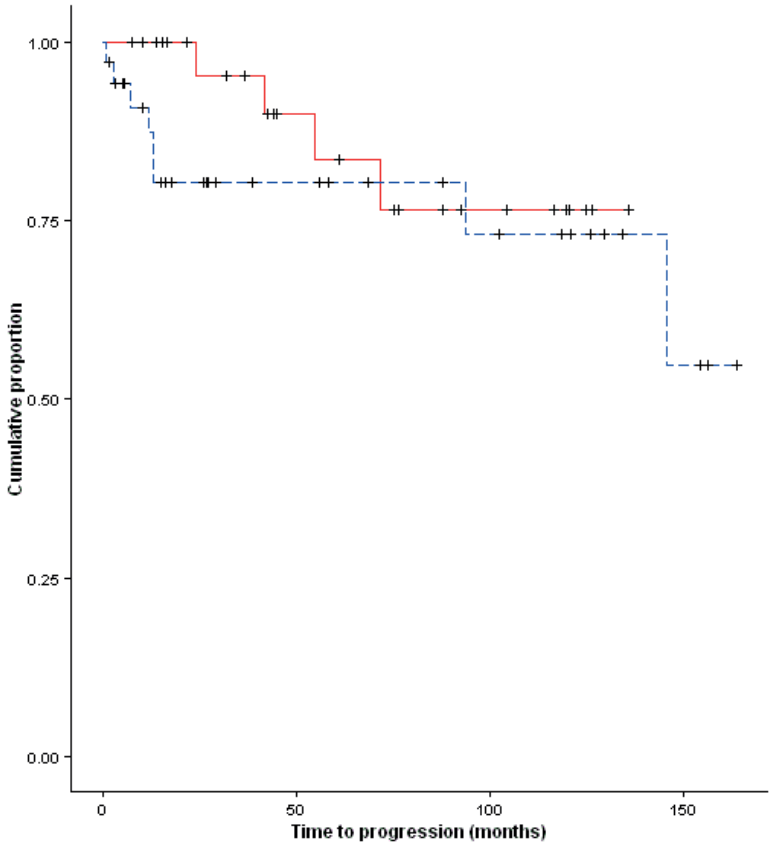

Figure 2: Time to progression (months) of GIST patients on imatinib treated with palliative intent as a function of imatinib C_{min} at steady state. The blue dashed line indicates patients with an imatinib C_{min} ≥1000 µg/L (n=35), the red line patients with an imatinib C_{min} <1000 µg/L (n=27).

An earlier prospective pharmacokinetic study found a significant decrease of systemic imatinib exposure of almost 30% within 90 days [9]. The authors hypothesized that this was a consequence of lower oral bioavailability with time, possibly due to upregulation of drug transporters or CYP3A4.

Another explanation could be that decrease of imatinib exposure is a result of decrease of alfa1-acid glycoproteint (AGP) as a consequence of impressive activity of imatinib treatment.[23] In our cohort, the large variability could not be explained by a change of C_{min} levels over time. A later study also did not find a time dependent decrease in exposure in a cohort of 65 patients, supporting our finding [24].

No clinical characteristic was found to be predictive for low imatinib C_{min}. Although prior studies have shown lower imatinib C_{min} levels after major gastrectomy, no correlation was found between C_{min} levels and extend of surgery in our study [8].

As prior studies have found a correlation between higher imatinib C_{min} levels and better clinical outcome [4,10–12], our results show that in daily clinic underexposure seems to be a substantial issue. Although no statistically significant relationships were found between imatinib exposure and treatment response, we found a trend toward responders having a higher C_{min} compared to non-responders in palliative setting (figure 3) and the same trend was found in neo-adjuvant patients. However, no correlation between TTP and C_{min} could be found in the palliative subgroup of patients (figure 2). This lack of statistically significant differences could be caused by low number of non-responders and limited amount of progression events.

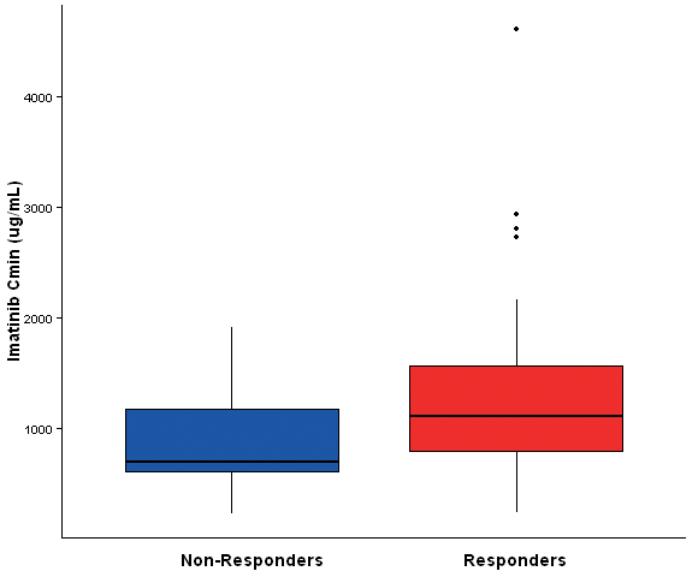

Figure 3: Box plot of imatinib C_{min} levels measured in palliative treated patients at steady state in responders (n=57) and non-responders (n=5). Median C_{min} levels were 920 µg/L for non-responders and 1271 µg/L for responders.

Our study gives new and representative insight into the underexposure of imatinib in GIST patients in routine clinical care. We showed that underexposure is a substantial problem in daily clinic and that

inter- and intrapatient variability is high. Given the fact that several studies described a correlation between C_{min} levels and response, pharmacokinetically guided dose individualization also known as therapeutic drug monitoring (TDM) should therefore be considered. One study attempted to demonstrate the benefits of TDM of imatinib, but failed due to small patient numbers and limited physician adherence to TDM recommendations [25].

A prospective clinical trial to assess the benefit of C_{min} guided imatinib dose adjustments in GIST patients is needed. Ideally using a relevant clinical endpoint such as PFS because previous studies have found clear correlations between imatinib exposure and efficacy and we now show that underexposure is a frequent problem in routine clinical care of imatinib treated GIST patients.

Compliance with ethical standards

Funding

A research grant for the Dutch GIST Registry is received from Novartis, Pfizer and Bayer
An unconditional research grant for PK sampling is received from Fonds NutsOhra

Conflicts of interest

N. Steeghs: As PI received a research grant from Pfizer, Novartis and Bayer for the Dutch GIST Registry. The other authors have no interests to disclose.

References

1. Corless CL, Barnett CM, Heinrich MC. Gastrointestinal stromal tumours: origin and molecular oncology. Nat. Rev. Cancer. 2011;11:865–78.
2. Blanke CD, Rankin C, Demetri GD, Ryan CW, von Mehren M, Benjamin RS, et al. Phase III randomized, intergroup trial assessing imatinib mesylate at two dose levels in patients with unresectable or metastatic gastrointestinal stromal tumors expressing the kit receptor tyrosine kinase: S0033. J. Clin. Oncol. 2008;26:626–32.
3. Patel S, Zalcberg JR. Optimizing the dose of imatinib for treatment of gastrointestinal stromal tumours: lessons from the phase 3 trials. Eur. J. Cancer. 2008;44:501–9.
4. Demetri GD, Wang Y, Wehrle E, Racine A, Nikolova Z, Blanke CD, et al. Imatinib plasma levels are correlated with clinical benefit in patients with unresectable/metastatic gastrointestinal stromal tumors. J. Clin. Oncol. 2009;27:3141–7.
5. Lankheet NAG, Knapen LM, Schellens JHM, Beijnen JH, Steeghs N, Huitema ADR. Plasma Concentrations of Tyrosine Kinase Inhibitors Imatinib , Erlotinib , and Sunitinib in Routine Clinical Outpatient Cancer Care. 2013;0:1–9.
6. Peng B, Lloyd P, Schran H. Clinical Pharmacokinetics of Imatinib. Clin. Pharmacokinet. 2005;44:879–94.
7. Eechoute K, Sparreboom A, Burger H, Franke RM, Schiavon G, Verweij J, et al. Drug transporters and imatinib treatment: implications for clinical practice. Clin. Cancer Res. 2011;17:406–15.
8. Yoo C, Ryu M-H, Kang BW, Yoon S-K, Ryoo B-Y, Chang H-M, et al. Cross-sectional study of imatinib plasma trough levels in patients with advanced gastrointestinal stromal tumors: impact of gastrointestinal resection on exposure to imatinib. J. Clin. Oncol. 2010;28:1554–9.
9. Eechoute K, Fransson MN, Reyners AK, de Jong F a, Sparreboom A, van der Graaf WT a, et al. A long-term prospective population pharmacokinetic study on imatinib plasma concentrations in GIST patients. Clin. Cancer Res. 2012;18:5780–7.
10. Delbaldo C, Chatelut E, Ré M, Deroussent A, Séronie-Vivien S, Jambu A, et al. Pharmacokinetic-pharmacodynamic relationships of imatinib and its main metabolite in patients with advanced gastrointestinal stromal tumors. Clin. Cancer Res. 2006;12:6073–8.
11. von Mehren M, Widmer N. Correlations between imatinib pharmacokinetics, pharmacodynamics, adherence, and clinical response in advanced metastatic gastrointestinal stromal tumor (GIST): an emerging role for drug blood level testing? Cancer Treat. Rev. 2011;37:291–9.
12. Widmer N, Decosterd L a, Csajka C, Montemurro M, Haouala a, Leyvraz S, et al. Imatinib plasma levels: correlation with clinical benefit in GIST patients. Br. J. Cancer. 2010;102:1198–9.
13. Picard S, Titier K, Etienne G, Teilhet E, Ducint D, Lassalle R, et al. Trough imatinib plasma levels are associated with both cytogenetic and molecular responses to standard-dose imatinib in chronic myeloid leukemia. Blood. 2007;109:3496–9.
14. Singh N, Kumar L, Meena R, Velpandian T. Drug monitoring of imatinib levels in patients undergoing therapy for chronic myeloid leukaemia: comparing plasma levels of responders and non-responders. Eur. J. Clin. Pharmacol. 2009;65:545–9.
15. Larson RA, Druker BJ, Guilhot F, O'Brien SG, Riviere GJ, Krahnke T, et al. Imatinib pharmacokinetics and its correlation with response and safety in chronic-phase chronic myeloid leukemia: a subanalysis of the IRIS study. Blood. 2008;111:4022–8.
16. Lankheet NAG, Hillebrand MJX, Rosing H, Schellens JHM, Beijnen JH, Huitema ADR. Method development and validation for the quantification of dasatinib, erlotinib, gefitinib, imatinib, lapatinib, nilotinib, sorafenib and sunitinib in human plasma by liquid chromatography coupled with tandem mass spectrometry. Biomed. Chromatogr. 2013;27:466–76.
17. Wang Y, Chia YL, Nedelman J, Schran H. A Therapeutic Drug Monitoring Algorithm for Refining the Imatinib Trough Level Obtained at Different Sampling Times. Ther. Drug Monit. 2009;31:579–84.
18. Takahashi N, Wakita H, Miura M, Scott SA, Nishii K, Masuko M, et al. Correlation between imatinib pharmacokinetics and clinical response in Japanese patients with chronic-phase chronic myeloid leukemia. Clin. Pharmacol. Ther. 2010;88:809–13.

19. R Core Development Team. A Language and Environment for Statistical Computing. Vienna, Austria R Found. Stat. Comput. 2008.

20. Teng T, Mabasa VH, Mary H, Ensom H, Pharm BS. The Role of Therapeutic Drug Monitoring of Imatinib in Patients with Chronic Myeloid Leukemia and Metastatic or Unresectable Gastrointestinal Stromal Tumors. Ther. Drug Monit. 2012;34:85–97.

21. Yu H, Steeghs N, Nijenhuis CM, Schellens JHM, Beijnen JH, Huitema ADR. Practical guidelines for therapeutic drug monitoring of anticancer tyrosine kinase inhibitors: focus on the pharmacokinetic targets. Clin. Pharmacokinet. 2014;53:305–25.

22. de Wit D, Guchelaar H-J, den Hartigh J, Gelderblom H, van Erp NP. Individualized dosing of tyrosine kinase inhibitors: are we there yet? Drug Discov. Today. 2015;20:18–36.

23. Chatelut E, Gandia P, Gotta V, Widmer N. Long-term prospective population PK study in GIST patients - Letter. Clin. Cancer Res. 2013;19:949.

24. Yoo C, Ryu M-H, Ryoo B-Y, Beck MY, Chang H-M, Lee J-L, et al. Changes in imatinib plasma trough level during long-term treatment of patients with advanced gastrointestinal stromal tumors: correlation between changes in covariates and imatinib exposure. Invest. New Drugs. 2012;30:1703–8.

25. Gotta V, Widmer N, Decosterd L a, Chalandon Y, Heim D, Gregor M, et al. Clinical usefulness of therapeutic concentration monitoring for imatinib dosage individualization: results from a randomized controlled trial. Cancer Chemother. Pharmacol. 2014;74:1307–19.

Chapter 5

Improving Delivery of Kinase Inhibitors to the Central Nervous System

Chapter 5.1

Clinical Pharmacokinetics of an Amorphous Solid Dispersion Tablet of Elacridar

Emilia Sawicki[1], Remy B. Verheijen[1], Alwin D.R. Huitema[1,2], Olaf van Tellingen[3], Jan H.M. Schellens[2,4,5], Bastiaan Nuijen[1], Jos H. Beijnen[1,2,4,5] and Neeltje Steeghs[2,4]

[1] Department of Pharmacy & Pharmacology, The Netherlands Cancer Institute / MC Slotervaart, Louwesweg 6, 1066 EC, Amsterdam, The Netherlands.
[2] Department of Clinical Pharmacology, Antoni van Leeuwenhoek - The Netherlands Cancer Institute, Plesmanlaan 121, 1066 CX, Amsterdam, The Netherlands
[3] Department of Clinical Chemistry/Preclinical Pharmacology, The Netherlands Cancer Institute, Plesmanlaan 121, 1066 CX, Amsterdam, The Netherlands
[4] Department Medical Oncology, Antoni van Leeuwenhoek - The Netherlands Cancer Institute, Plesmanlaan 121, 1066 CX, Amsterdam, The Netherlands
[5] Utrecht Institute of Pharmaceutical Sciences (UIPS), David de Wied building, Universiteitsweg 99, 3584 CG, Utrecht, The Netherlands

Abstract

Elacridar is an inhibitor of the Permeability Glycoprotein (P-gp) and the Breast Cancer Resistance Protein (BCRP) and is a promising absorption enhancer of drugs that are substrates of these drug-efflux transporters. However, elacridar is practically insoluble in water, resulting in low bioavailability which currently limits its clinical application. We evaluated the *in vitro* dissolution and clinical pharmacokinetics of a novel amorphous solid dispersion (ASD) tablet containing elacridar. The dissolution from ASD tablets was compared to that from a crystalline powder mixture in a USP type II dissolution apparatus. The pharmacokinetics of the ASD tablet were evaluated in an exploratory clinical study at oral doses of 25 mg, 250 mg or 1000 mg in 12 healthy volunteers. A target C_{max} was set at ≥ 200 ng/mL based on previous clinical data. The *in vitro* dissolution from the ASD tablet was 16.9 ± 3.7 times higher compared to that from a crystalline powder mixture. C_{max} and $AUC_{0-\infty}$ increased linearly with dose over the explored range. The target C_{max} of ≥ 200 ng/mL was achieved at the 1000 mg dose level. At this dose the C_{max} and $AUC_{0-\infty}$ were 326 ± 67 ng/mL and 13.4 ± 8.6 · 10^3 ng·h/mL respectively. In summary, the ASD tablet was well tolerated, resulted in relevant pharmacokinetic exposure and can be used for proof-of-concept clinical studies.

Introduction

Permeability Glycoprotein (P-gp; ABCB1) and the Breast Cancer Resistance Protein (BCRP; ABCG2) are two membrane-associated drug-efflux transporters that are expressed on epithelial cells lining the gastro-intestinal tract, in the endothelial cells that form the blood brain barrier, in stem cells and in cancer cells [1]. Consequently, they limit the oral bioavailability, reduce uptake in the central nervous system (CNS) of various drugs and may cause multidrug resistance of tumor cells [2]. Elacridar is a third generation inhibitor of P-gp developed in the 1990s for treatment of multidrug resistant cancers [3]. Later, it was also found to be an inhibitor of BCRP [4]. Clinical trials with transporter inhibitors to reverse multidrug resistance of tumors have been unsuccessful, but it was demonstrated that elacridar was an effective absorption enhancer of paclitaxel and topotecan at C_{max} values of ≥ 200 ng/mL [5–7]. Based on preclinical work it is also expected that elacridar may enhance drug delivery of substrate drugs to the CNS, which might increase the efficacy of treating brain tumors [2]. Further commercial development of elacridar was abandoned, possibly due to its challenging pharmaceutical properties. Elacridar is practically insoluble in water ($12.3 \cdot 10^{-5}$ mg/mL) [8] and appears to have a poor membrane permeability [9], suggesting it is a class IV drug according to the Biopharmaceutics Classification System (BCS) [10]. Moreover, the conventional tablet (containing elacridar hydrochloride) demonstrated poor and unpredictable oral absorption [6,11,12]. Currently no formulation is available for clinical trials. Although two new formulations are in preclinical development, according to our knowledge these have not yet been evaluated in humans [8,9].

Several formulation strategies can improve solubility-limited absorption, one of them being an amorphous solid dispersion (ASD) [13,14]. Here, the drug is dispersed in a biologically inactive hydrophilic amorphous polymer. When administered, this creates a temporarily supersaturated state with a high degree of solubilization, generating a time window for increased absorption [15,16].

ASDs have been developed for many poorly soluble drugs [17] and over 20 are already commercially available [18], underlining the feasibility and success of this approach. Because of this, we developed an ASD tablet formulation containing 25 mg elacridar hydrochloride (23.5 mg elacridar).

In this study we first evaluated the *in vitro* dissolution characteristics from the ASD tablet and based on the promising results we conducted a pharmacokinetic study in healthy volunteers.

Materials and methods

Chemicals and materials

Elacridar hydrochloride was synthesized according to previously reported procedures [19]. Povidone K30 (PVPK30) was purchased from BASF Chemtrade (Ludwigshafen, Germany); sodium dodecyl sulfate (SDS) from Merck (Darmstadt, Germany); dimethyl sulfoxide (DMSO) from VWR (Amsterdam, The Netherlands); lactose monohydrate SuperTab® 30GR from DFE Pharma (Goch,

Germany); anhydrous colloidal silicon dioxide and magnesium stearate from Fagron (Capelle a/d Ijssel, The Netherlands); croscarmellose sodium from FMC (Philadelphia, USA); demineralized water from B. Braun (Melsungen, Germany). Simulated Intestinal Fluid without pancreatic enzymes (SIFsp, pH 6.8) was prepared as described in USP-NF [20]. Stainless steel boxes were from Gastronorm (The Netherlands).

Preparation of elacridar ASD tablets

Elacridar hydrochloride, PVPK30 and SDS were dissolved in DMSO (1:6:1, w/w/w) to yield an elacridar hydrochloride concentration of 10 mg/ml. The solution was dried by lyophilization in a Lyovac GT4 (GEA Lyophil, Hürth, Germany) by a method described previously [21]. This yielded the ASD powder which was immediately grinded and stored in dark airtight glass containers in a desiccator at 2 – 8 °C. The ASD powder, lactose monohydrate, croscarmellose sodium, anhydrous colloidal silicon dioxide and magnesium stearate (30:63:5:1:1, w/w/w/w/w) were weighted in a hermetically sealed 2 L stainless steel vessel and mixed in a Turbula T10B mixer (Willy A. Bachofen AG Maschinenfabrik, Muttenz, Switzerland). Tablets were pressed on an eccentric tablet press (Korsch, EK10, Berlin, Germany). Each ASD tablet contained 25 mg elacridar hydrochloride (23.5 mg elacridar). Tablets were stored in aluminum blisters with polyvinylchloride sealing at – 20 °C. The production process and storage were performed according to Good Manufacturing Practices (GMP) and batch size was 200 – 300 tablets.

In vitro dissolution

Dissolution was studied by using a type II paddle dissolution apparatus as described in the European Pharmacopoeia [22] at rotation speed of 100 rpm. One tablet was placed in 500 mL SIFsp at 37 °C. Samples of 1 mL were taken through a 0.45 µm PVDF filter, diluted with 2 mL DMSO and measured on a previously described validated HPLC-UV system [23].

Clinical study

The pharmacokinetics of ASD formulation were assessed in healthy volunteers in a dose-escalation design, with 3 subjects per dose level. The aim was to achieve a target C_{max} of ≥ 200 ng/mL. The first dose level was 25 mg and each next level was based on the mean C_{max} of the previous dose level. A maximum dose was set at 1000 mg as previous clinical data indicated this is safe and well tolerated [5–7]. The dose level that reached the target C_{max} was expanded to a total of 6 volunteers. All subjects were instructed to fast 2 hours before and 2 hours after ingestion of the tablets. This study was approved by the Medical Ethics Committee of MC Slotervaart (Amsterdam, The Netherlands) and all volunteers provided written informed consent before enrolment. This trial was registered in the European Clinical Trial Database (EudraCT, registration number 2013-001131-47).

Pharmacokinetics

Blood samples (3 mL) were taken at t = 0, 0.5, 1, 1.5, 2, 4, 6, 8, 12, 24 and 48 hours after administration of the formulation. These were centrifuged at 1500 rpm for 10 minutes and the plasma was stored at - 20°C. Elacridar concentrations were measured using a validated LC-MS/MS method as previously described [24]. Non-compartmental analysis of data was performed in R version 3.0.0, calculated parameters were C_{max}, T_{max}, $AUC_{0\text{-}48h}$ and $AUC_{0\text{-}\infty}$. These parameters were compared to values of previous clinical studies with the same once daily oral dose. To assess dose linearity and proportionality, individual observations of C_{max} and $AUC_{0\text{-}\infty}$ were plotted versus dose and a one-way ANOVA was executed on the dose normalized values of C_{max} and $AUC_{0\text{-}\infty}$ at each dose level.

Results

In vitro dissolution

Figure 1 shows the dissolution from a crystalline physical mixture compared to the ASD tablets (98.8 ± 0.8 % content and 99.7 ± 0.5 % purity). The physical mixture resulted in 1.4 ± 0.1 % dissolution, whereas the dissolution from ASD tablets reached 23.7 ± 3.7 %, with a maximum at 30 to 60 minutes. The dissolution from ASD tablets was 16.9 ± 3.7 times higher than from a physical mixture.

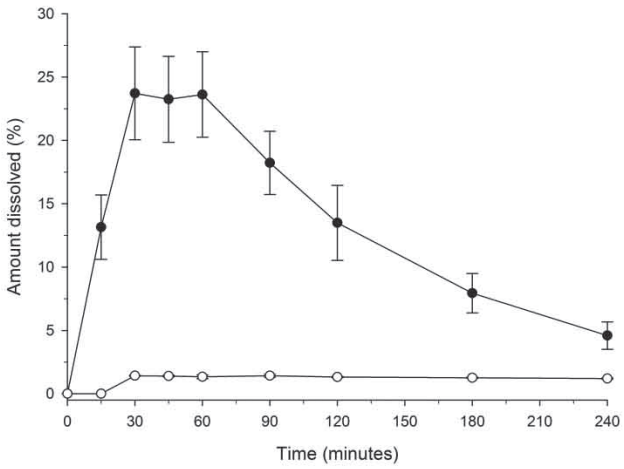

Figure 1. In vitro dissolution as mean ±standard deviation of the amount dissolved from the ASD tablets (3 batches, 6 tablets per batch, ●●●) and from a physical mixture of crystalline elacridar hydrochloride:PVPK30:crystalline SDS (1:6:1, w/w/w) (n = 3, ○○○) measured in a European Pharmacopoeia dissolution apparatus type II paddle 100 rpm 37 °C.

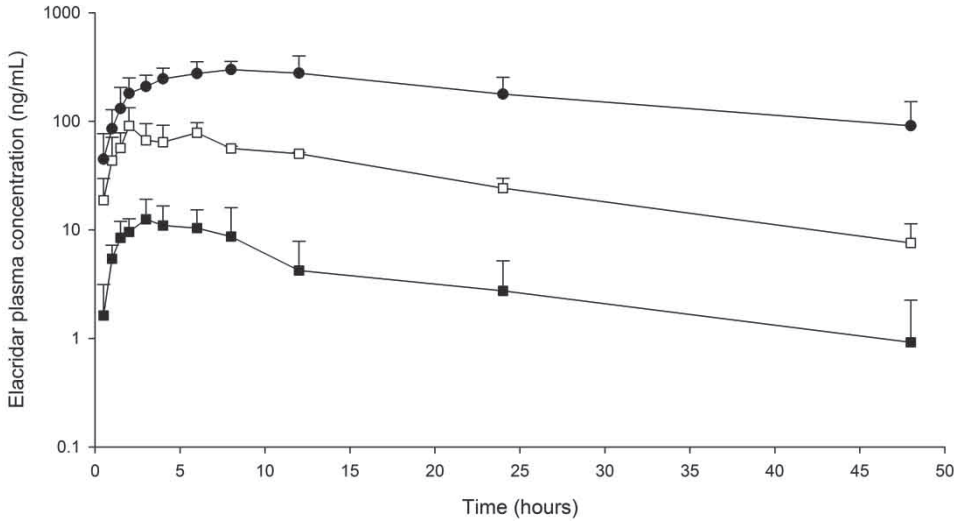

Figure 2. Elacridar plasma concentrations + standard deviation plotted on a semi-log scale for the 25 mg (n = 3, ■■■), 250 mg (n=3, □□□) and 1000 mg (n=6, ●●●) mg dose levels in the healthy volunteers.

Clinical study

Thirteen healthy volunteers provided written informed consent. One volunteer withdrew from the trial due to problems with venous access, before taking the study medication. Of the remaining twelve volunteers 10 were female and 2 were male with a mean (± SD) age of 42 (± 9) years.

The ASD tablets were well tolerated. Adverse events were observed only at the 1000 mg dose level (nausea, dyspepsia and flatulence), they were limited to the day of ingestion and none of them exceeded grade 1 (CTC-AE v4.03).

Pharmacokinetics

Calculated pharmacokinetic parameters for each dose level are shown in Table 1. The dose levels were 25 mg, 250 mg and 1000 mg (corresponding to 23.5 mg, 235 mg and 940 mg elacridar). Plasma concentration time curves of each dose are presented in Figure 2. The 25 mg dose was taken by 3 volunteers and resulted in a C_{max} of 12.6 ± 6.52 ng/mL which was considerably below the target C_{max}. We therefore increased the dose 10-fold to 250 mg in the next 3 volunteers. Here, the C_{max} was 97.0 ± 32.1 ng/mL. The third dose level of 1000 mg (taken by 3 volunteers) resulted in a C_{max} of 350 ± 65.2 ng/mL. This level was expanded with 3 extra volunteers and the overall C_{max} was 326.0 ± 67.4 ng/mL. Figures 3 a and b show individual observations of C_{max} and $AUC_{0-\infty}$ as a function of dose. C_{max} and $AUC_{0-\infty}$ both increased linearly. Dose normalized values of C_{max} and $AUC_{0-\infty}$ (Table 1) did not deviate significantly from dose proportionality over the tested dose range (p = 0.277 and 0.399 respectively,

ANOVA), though the C_{max}/dose ratio seemed to decline at higher doses. Table 2 compares the pharmacokinetic results of this study with earlier clinical trials with once daily orally administered elacridar.

Discussion

Inhibition of P-gp and BCRP by elacridar could be a valuable tool to improve drug delivery to the CNS and increase oral bioavailability of drugs which are substrates of these transporters. However, elacridar's low aqueous solubility currently limits its clinical application. The aim of this study was to assess whether the ASD tablet increases the dissolution and whether this formulation results in relevant pharmacokinetic exposure in healthy volunteers.
In vitro, the ASD formulation resulted in considerably higher dissolution (16.9 ± 3.7 fold) compared to that from a crystalline physical mixture (Figure 1). This indicated that the ASD could be a suitable approach to enhance the absorption of elacridar and supported investigation of its pharmacokinetics in a clinical trial.

In healthy volunteers, the targeted C_{max} of ≥ 200 ng/mL was achieved at a dose of 1000 mg, without grade > 1 toxicity. In fact, C_{max} and AUC at this dose were higher than values reported in most earlier clinical studies with elacridar (Table 2) [6,7] and similar to one study where elacridar was administered orally together with a paclitaxel formulation that contained polyethoxylated castor oil (Cremophor®) [5]. In contrast to previous trials, the ASD tablets showed a linear dose-dependent increase in C_{max} and $AUC_{0-\infty}$ (Figure 3). The previously used clinical formulation displayed no clear relationship between dose, C_{max} and AUC [6]. That study only found an approximate threefold increase in C_{max} and AUC over a dose range of 100-1000 mg. Furthermore, variability of in C_{max} and exposure seemed lower in the current than in previous trials (Table 2). These observations indicate that the ASD formulation strategy resulted in more reliable absorption pharmacokinetics of elacridar. In this study the high number of tablets at the 1000 mg dose was considered manageable as only a single administration was required and no alternative GMP-compliant formulation of elacridar was available. Nonetheless this is a limitation of the current formulation and will restrict its use to small proof-of-concept studies. For clinical applications involving daily oral administration further research into a new formulation will be needed.

Table 1. Pharmacokinetic parameters calculated from each dose level of elacridar

Dose	C_{max} ± SD ng/ml (CV %)	$AUC_{0-\infty}$ ± SD ng·h/ml ·10^3 (CV %)	T_{max} ± SD h (CV %)	$AUC_{0-\infty}$ /Dose ratio ± SD	C_{max} /Dose ratio ± SD
25 mg (n = 3)	12.6 ± 6.52 (52 %)	0.205 ± 0.172 (84 %)	2.7 ± 0.58 (22 %)	8.21 ± 6.87	0.504 ± 0.261
250 mg (n = 3)	97.0 ± 32.1 (33 %)	1.70 ± 0.401 (24 %)	3.3 ± 2.3 (70 %)	6.82 ± 1.60	0.388 ± 0.128
1000 mg (n = 6)	326.0 ± 67.4 (21 %)	13.4 ± 8.64 (65 %)	9.0 ± 3.5 (39 %)	13.4 ± 8.64	0.326 ±0.0674

$AUC_{0-\infty}$: Area under the curve (extrapolated to infinity)

C_{max}: Maximum concentration

CV: Coefficient of variation

SD: Standard deviation

T_{max}: Time to maximum plasma concentration

Table 2. Pharmacokinetic parameters of the current study compared with previous clinical trials

Dose (mg)	N	C_{max} ± SD, (range) or (CV %) ng/mL	AUC_{0-t} ± SD, (range) or (CV %) ·10^3 ng·h/mL	T_{max} ± SD, (range) or (CV %)	Formulation	Reference
1000	**6**	**326 ± 67.4 (21%)**	**0-24 h: 5.58 ± 1.71 (31%) 0-48 h: 8.80 ± 3.03 (34%)**	**9.0 ± 3.5 (39%)**	**ASD tablet**	**This study**
1000	4	140 (114 – 171) NA	2.11 (1.77 – 2.51[a] (11%)	6.0 (6.0 – 8.2)	GSK tablet	[6]
1000	4	185 (138 – 248) NA	2.63 (1.66 – 4.17) [a] (32%)	6.0 (3.0 – 9.1)	GSK tablet	[6]
1000	8	157 ± 93 (59%)	2.41 ± 1.11[a] (46%)	3.6 ± 3.4 (94%)	GSK tablet	[7]
1000	8	242 ± 122 (50%)	4.25 ± 2.04[a] (48%)	4.6 ± 2.2 (48%)	GSK tablet	[7]
1000	6	434 ± 267 (62%)	9.43 ± 5.43[b] (58%)	7.7 ± 2.5 (32%)	GSK tablet	[5]

SD = standard deviation, CV = variation coefficient, NA = not available

a AUC_{0-24h}

b AUC_{0-48h}

The ASD formulation reached the prespecified target C_{max} of ≥ 200 ng/mL in healthy volunteers, however the increase in absorption did not approach the 17-fold increase as seen in the *in vitro* dissolution experiment. This could have several reasons:

Supersaturated solutions of BCS II/IV substances can be unstable *in vivo* and can recrystallize earlier than *in vitro*, thereby limiting absorption [25]. It has been proposed that with increasing degree of supersaturation the risk of *in vivo* fast nucleation and recrystallization also increases [26,27]. As the ASD tablet showed a rapid and a very high degree of supersaturation (Figure 1), the resulting system

might have been particularly unstable *in vivo*, leading to recrystallization before the solubilized drug could be absorbed, causing suboptimal absorption.

The lower than expected absorption could also be due to limited membrane permeability. Though this seems unlikely based on the high log P (5.55) of elacridar [28], in an *in vitro* assay the membrane permeability was similar to that of the leakage marker inulin [9]. This could indicate that strategies aiming to improve the dissolution (such as ASDs and other supersaturating formulations) of elacridar may be insufficient to increase absorption and that future formulation efforts should also focus on increasing permeability.

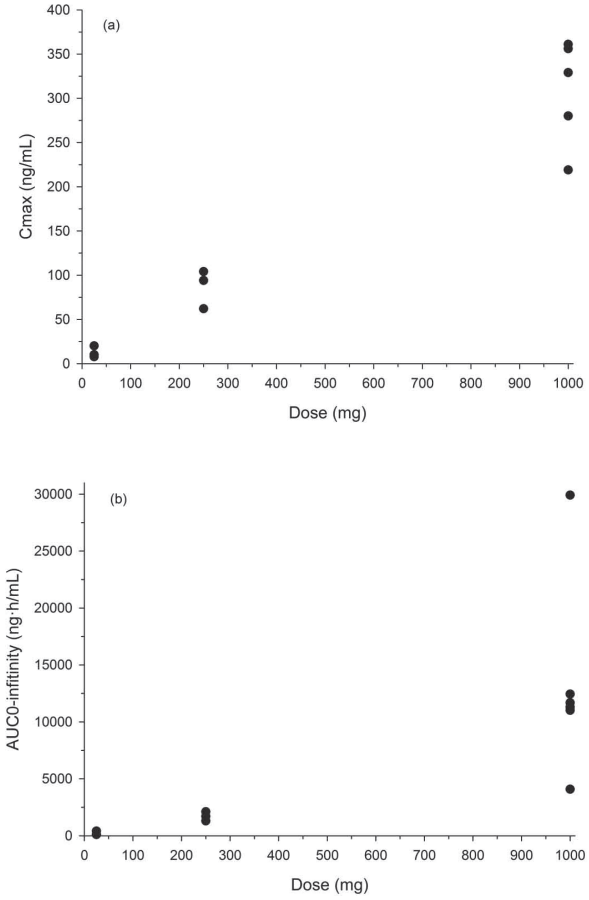

Figure 3. The relation of elacridar dose on the C_{max} (a) and $AUC_{0-\infty}$ (b) of ASD tablets administered to healthy volunteers at three different doses (25 mg n = 3, 250 mg n = 3 and 1000 mg, n = 6).

Conclusion

The ASD tablet considerably improved dissolution *in vitro*. In healthy volunteers, the target C_{max} of 200 ng/mL was reached and C_{max} and $AUC_{0-\infty}$ increased linearly with dose. In summary, the ASD tablet was well tolerated, resulted in relevant pharmacokinetic exposure and can be used for proof-of-concept clinical studies.

Compliance with ethical standards

The experiments comply with the current laws of the country in which they were performed.
All procedures were conducted in accordance with the ethical standards of the responsible committee on human experimentation (institutional and national) and with the Helsinki Declaration of 1975, as revised in 2000 (5). Informed consent was obtained from all human volunteers for being included in the study.

Acknowledgements

Funding for this research was provided by a personal grant from The Netherlands Cancer Institute to Dr. N. Steeghs.

References

1. Shukla S, Ohnuma S, Ambudkar SV. Improving cancer chemotherapy with modulators of ABC drug transporters. Curr. Drug Targets. 2011;12:621–30.
2. van Tellingen O, Yetkin-Arik B, de Gooijer MC, Wesseling P, Wurdinger T, de Vries HE. Overcoming the blood-brain tumor barrier for effective glioblastoma treatment. Drug Resist. Updat. 2015;19:1–12.
3. Hyafil F, Vergely C, Du Vignaud P, Grand-Perret T. In vitro and in vivo reversal of multidrug resistance by in vitro and in vivo reversal of multidrug resistance by GF120918, an acridonecarboxamide derivative. Cancer Res. 1993;53:4595–602.
4. de Bruin M, Miyake K, Litman T, Robey R, Bates SE. Reversal of resistance by GF120918 in cell lines expressing the ABC half-transporter, MXR. Cancer Lett. 1999;146:117–26.
5. Malingré MM, Beijnen JH, Rosing H, Koopman FJ, Jewell RC, Paul EM, et al. Co-administration of GF120918 significantly increases the systemic exposure to oral paclitaxel in cancer patients. Br. J. Cancer. 2001;84:42–7.
6. Kuppens IE, Witteveen EO, Jewell RC, Radema SA, Paul EM, Mangum SG, et al. A phase I, randomized, open-label, parallel-cohort, dose-finding study of elacridar (GF120918) and oral topotecan in cancer patients. Clin. cancer Res. 2007;13:3276–85.
7. Kruijtzer CMF, Beijnen JH, Rosing H, Ten Bokkel Huinink WW, Schot M, Jewell RC, et al. Increased oral bioavailability of topotecan in combination with the breast cancer resistance protein and P-glycoprotein inhibitor GF120918. J. Clin. Oncol. 2002;20:2943–50.
8. Sane R, Mittapalli RK, Elmquist WF. Development and evaluation of a novel microemulsion formulation of elacridar to improve its bioavailability. J. Pharm. Sci. 2013;102:1343–54.
9. Bunt AMG, Tellingen O van. Efflux inhibitor compositions and methods of treatment use the same, Patent number US 2014/0235631 A1. p. 1–33.
10. FDA. Waiver of in vivo bioavailability and bioequivalence studies for immediate-release solid oral dosage forms based on a biopharmaceutics classification system guidance for industry. 2015; Available from: http://www.fda.gov/downloads/Drugs/.../Guidances/ucm070246.pdf
11. Ward KW, Azzarano LM. Preclinical pharmacokinetic properties of the P-glycoprotein inhibitor GF120918A (HCl salt of GF120918, 9,10-dihydro-5-methoxy-9-oxo-N-[4-[2-(1,2,3,4-tetrahydro-6,7-dimethoxy-2-isoquinolinyl)ethyl]phenyl]-4-acridine-carboxamide) in the mouse, rat,dog(...). J. Pharmacol. Exp. Ther. 2004;310:703–9.
12. Planting AST, Sonneveld P, van der Gaast A, Sparreboom A, van der Burg MEL, Luyten GPM, et al. A phase I and pharmacologic study of the MDR converter GF120918 in combination with doxorubicin in patients with advanced solid tumors. Cancer Chemother. Pharmacol. 2005;55:91–9.
13. Kawabata Y, Wada K, Nakatani M, Yamada S, Onoue S. Formulation design for poorly water-soluble drugs based on biopharmaceutics classification system: basic approaches and practical applications. Int. J. Pharm. 2011;420:1–10.
14. van Hoogevest P, Liu X, Fahr A. Drug delivery strategies for poorly water-soluble drugs: the industrial perspective. Expert Opin. Drug Deliv. 2011;8:1481–500.
15. Chiou WL, Riegelman S. Pharmaceutical applications of solid dispersion systems. J. Pharm. Sci. 1971;60:1281–302.
16. Janssens S, van den Mooter G. Review: physical chemistry of solid dispersions. J. Pharm. Pharmacol. 2009;61:1571–86.
17. Alam MA, Ali R, Al-Jenoobi FI, Al-Mohizea AM. Solid dispersions: a strategy for poorly aqueous soluble drugs and technology updates. Expert Opin. Drug Deliv. 2012;9:1419–40.
18. He Y, Ho C. Amorphous solid dispersions: utilization and challenges in drug discovery and development. J. Pharm. Sci. 2015;104:3237–58.
19. Sharp MJ, Mader CJ, Strachan C. Synthesis of acridine derivative multidrug-resistant inhibitors, Patent number WO98/52923. 1998. p. 1–21.
20. USP. United States Pharmacopoeia National Formulary Online, www.usp.org/usp-nf. 2015; Available from: www.usp.org/usp-nf
21. den Brok MWJ, Nuijen B, Lutz C, Opitz HG, Beijnen JH. Pharmaceutical development of a lyophilised

dosage form for the investigational anticancer agent Imexon using dimethyl sulfoxide as solubilising and stabilising agent. J. Pharm. Sci. 2005;94:1101–14.

22. PhEur. European Pharmacopoeia Online. 2016; Available from: http://online.edqm.eu
23. Sawicki E, Hillebrand MJ, Rosing H, Schellens JHM, Nuijen B, Beijnen JH. Validation of a liquid chromatographic method for the pharmaceutical quality control of products containing elacridar. J. Pharm. Anal. 2016;6:268–75.
24. Stokvis E, Rosing H, Causon RC, Schellens JHM, Beijnen JH. Quantitative analysis of the P-glycoprotein inhibitor Elacridar (GF120918) in human and dog plasma using liquid chromatography with tandem mass spectrometric detection. J. Mass Spectrom. 2004;39:1122–30.
25. Sun DD, Lee PI. Haste makes waste: the interplay between dissolution and precipitation of supersaturating formulations. AAPS J. 2015;17:1317–26.
26. Patel DD, Anderson BD. Maintenance of supersaturation II: indomethacin crystal growth kinetics versus degree of supersaturation. J. Pharm. Sci. 2013;102:1544–53.
27. Brouwers J, Brewster ME, Augustijns P. Supersaturating drug delivery systems: the answer to solubility-limited oral bioavailability? J. Pharm. Sci. 2009;98:2549–2472.
28. Padowski JM, Pollack GM. Examination of the ability of the nasal administration route to confer a brain exposure advantage for three chemical inhibitors of P-glycoprotein. J. Pharm. Sci. 2010;99:3226–33.

Chapter 5.2

Molecular Imaging of ABCB1/ABCG2 Inhibition at the Human Blood Brain Barrier using Elacridar and ^{11}C-Erlotinib PET

Remy B Verheijen[1], Maqsood Yaqub[2], Emilia Sawicki[1], Olaf van Tellingen[3], Adriaan A Lammertsma[2], Bastiaan Nuijen[1], Jan HM Schellens[4,5], Jos H Beijnen[1,5], Alwin DR Huitema[1,6], N Harry Hendrikse[2,7], Neeltje Steeghs[4]

[1] Department of Pharmacy & Pharmacology, The Netherlands Cancer Institute - Antoni van Leeuwenhoek, Amsterdam, The Netherlands
[2] Department of Radiology & Nuclear Medicine, VU University Medical Center, Amsterdam, The Netherlands
[3] Department of Bio-Pharmacology/ Mouse Cancer Clinic, The Netherlands Cancer Institute - Antoni van Leeuwenhoek, Amsterdam, The Netherlands
[4] Department of Clinical Pharmacology & Medical Oncology, The Netherlands Cancer Institute - Antoni van Leeuwenhoek, Amsterdam, The Netherlands
[5] Department of Pharmaceutical Sciences, Utrecht University, Utrecht, The Netherlands
[6] Department of Clinical Pharmacy, Utrecht University Medical Center, Utrecht, The Netherlands.
[7] Department of Clinical Pharmacology and Pharmacy, VU University Medical Center, Amsterdam, The Netherlands

Abstract

Transporters such as ABCB1 and ABCG2 limit the exposure of several anti-cancer drugs to the brain, leading to suboptimal treatment in the central nervous system. The purpose of this study was to investigate the effects of the ABCB1/ABCG2 inhibitor elacridar on erlotinib uptake in the brain using ^{11}C-erlotinib PET.

Methods: Elacridar and cold erlotinib were administered orally to wild type (WT) and *Abcb1a/b;Abcg2* knockout (KO) mice. In addition, brain uptake was measured using ^{11}C-erlotinib imaging and *ex vivo* scintillation counting in KO and WT mice.

Six patients with advanced solid tumors underwent ^{11}C-erlotinib PET scans before and after a 1000 mg dose of elacridar. ^{11}C-erlotinib brain uptake was quantified by pharmacokinetic modeling using volume of distribution (V_T) as outcome parameter. In addition, ^{15}O-H_2O scans were acquired prior to each ^{11}C-erlotinib scan, to measure cerebral blood flow .

Results: Brain uptake of ^{11}C-erlotinib was 2.6-fold higher in *Abcb1a/b;Abcg2* KO mice than in WT mice, measured as % of injected dose/gram tissue (p=0.01). In WT mice, addition of elacridar (at systemic plasma concentrations of ≥200 ng/mL) resulted in increased brain concentration of erlotinib, without affecting erlotinib plasma concentration.

In patients, V_T of ^{11}C-erlotinib did not increase after intake of elacridar (0.216±0.12 versus 0.205±0.07, mean±SD, p=0.91). ^{15}O-H_2O PET showed no significant changes in cerebral blood flow. Elacridar exposure in patients was 401±154 ng/mL (mean ±SD). No increase in V_T with increased elacridar plasma exposure was found over the 271–619 ng/mL range.

Conclusion: In line with previous preclinical reports, when Abcb1 and Abcg2 were disrupted in mice, brain uptake increased both at a tracer and pharmacological erlotinib dose. In patients, brain uptake of ^{11}C-erlotinib was not higher after administration of elacridar. The more pronounced role that ABCG2 appears to play at the human blood-brain barrier and the lower potency of elacridar to inhibit ABCG2 may be an explanation of these inter-species differences.

Introduction

Leptomeningeal and central nervous system (CNS) metastases occur frequently in cancer patients, even in subjects whose extra cranial lesions are responsive to treatment and are known to result in a dismal prognosis . This can partly be explained by the pharmacokinetic properties of anti-cancer drugs, in particular their limited distribution into the brain.
The blood-brain barrier (BBB) is a major impediment to achieving pharmacologically active concentrations in cerebrospinal fluid and brain tissue(1,2). The BBB consists of endothelial cells that form a physical barrier for molecules due to the tight intercellular junctions, lack of fenestrations and very low pinocytic activity (3). An additional hurdle for brain uptake of drugs is the expression of efflux transporters at the BBB endothelium, such as the adenosine triphosphate-binding cassette (ABC) transporters, ABCB1 known as P-Glycoprotein and ABCG2 known as Breast Cancer Resistance Protein (1–3). These efflux transporters restrict access to the brain even of small lipophilic compounds, which would otherwise be able to penetrate cellular membranes by passive diffusion. Brain tumors and metastases can disrupt the integrity of the BBB. However, this disruption is heterogeneous and occurs predominantly in the tumor core where (abundant) microvascular proliferation results in vessel leakiness (1,4). Brain tissue adjacent to the tumor may therefore contain tumor cells that benefit from protection by a (more) intact BBB. Hence, the CNS is regarded as a sanctuary site for anti-cancer drugs (5).

Elacridar is an inhibitor of ABCB1(6) and ABCG2 (7). Numerous preclinical studies have shown that elacridar is able to enhance the brain penetration of substrate drugs including erlotinib (8,9). Erlotinib is an epidermal growth factor receptor inhibitor used in the treatment of advanced non-small cell lung cancer. Although non-small cell lung cancer frequently metastasizes to the brain, erlotinib exposure in the CNS is limited (10,11), as it is a substrate of both ABCB1 and ABCG2 (12–14). ^{11}C-erlotinib has been developed as a radiotracer to non-invasively study the biodistribution and target binding of erlotinib *in vivo* (15,16) and has been used to non-invasively study epidermal growth factor receptor mutations in tumor lesions of cancer patients (17,18).

The purpose of our study was to assess whether ^{11}C-erlotinib PET could quantify erlotinib uptake in the brain, particularly as readout of ABCB1/ABCG2 inhibition at the BBB. First preclinical experiments in mice were performed to establish the elacridar concentration needed to achieve Abcb1a/b and Abcg2 inhibition. Next, *in vivo* imaging in wild type (WT) and *Abcb1a/b* and *Abcg2* knock out (KO) mice was performed to establish the feasibility of monitoring drug transporter inhibition at the BBB using ^{11}C-erlotinib PET. Finally, a clinical trial in cancer patients using ^{11}C-erlotinib PET was performed to non-invasively study the effects of ABCB1/ABCG2-inhibition on the human brain penetration of erlotinib.

Materials and methods

Preclinical Pharmacology

Preclinical experiments were performed using female Friend Virus B mice, between 10 and 14 weeks of age, which were either WT or *Abcb1a/1b;Abcg2* $^{-/-}$ double KO mice.

Elacridar suspensions were prepared in vehicle solution (1% m/v hydroxypropyl methyl cellulose, 2%v/v polysorbate 80 in water) at concentrations of 1, 2.5 and 5 mg/mL. An erlotinib suspension was prepared at 2 mg/mL in the same vehicle solution.

Non-fasted animals received 10 µl per gram (body weight) of elacridar (0, 10, 25 or 50 mg/kg) orally by gavage, followed 30 min later by 10 µl per gram (body weight) of oral erlotinib (20 mg/kg). At 4 hours after erlotinib dosing blood was sampled by cardiac puncture. Animals were sacrificed and brain tissue was collected. Brain tissue was homogenized in 3 mL of 1% v/v BSA in water using a Fastprep 24 homogenizer (MPBio, Santa Ana, CA, USA). Erlotinib and elacridar were quantified *ex vivo* in both plasma and brain homogenates by LC-MS/MS. Each elacridar treated group (0, 10, 25, 50 mg/kg) consisted of 4 mice. A group of *Abcb1a/1b;Abcg2* KO mice (n=5) was used as positive control.

Preclinical Imaging

Abcb1a/b;Abcg2 WT and KO mice (n=2 for each group) were positioned in pairs in a double lutetium oxyorthosilicate/Lu1.8Y0.2SiO5(Ce) or LSO-LYSO layer high resolution research tomograph (Siemens/CTI, Knoxville, TN, USA) PET scanner (19). First, a transmission scan was acquired using a 740 MBq 2-dimensional fan-collimated ^{137}Cs (662 keV) moving point source (20). Next, a dynamic emission scan was acquired immediately following administration of 8-10 MBq ^{11}C-erlotinib (specific activity >18.5 GBq/µmol) to each animal. Emission data were acquired for 60 min in 3-dimensional (3D) list mode and rebinned into the following frame sequence: 4×30, 3×60, 2×150 and 4×300 s. Following corrections for decay, dead time, attenuation, randoms and scatter, scans were reconstructed using a 3D ordinary Poisson ordered subsets expectation maximization algorithm for mice (20). This resulted in images with an average spatial resolution of 3 mm full width at half maximum (19).

After the PET scans, mice were sacrificed and the brain was removed. Brains were weighed and radioactivity was measured in a 1282 Compugamma CS (LKB Wallac, Turku, Finland) using 5 × 10 µL aliquots of the injected formulation as internal standard. Results were expressed as % injected dose/gram brain (%ID/g brain) corrected for decay to time of injection.

Clinical Elacridar Formulation

Elacridar hydrochloride was formulated as an (unpatented) tablet formulation of which the pharmaceutical development has been described earlier.(21) These tablets were shown to be well tolerated and resulted in relevant pharmacokinetic exposure in healthy volunteers, with a mean C_{max} (±SD) of 326±67 ng/mL and $AUC_{0\text{-}48h}$ of 8800±3020 ng/mL*h (22).

Clinical Study Design

An overview of the clinical study design is presented in figure 1. After a screening visit (day -7), patients were scheduled for ^{11}C-erlotinib PET scans at two consecutive days (day 1 and 2). The ^{11}C-erlotinib was given at a specific activity of >18.5 GBq/µmol without adding additional unlabeled erlotinib.

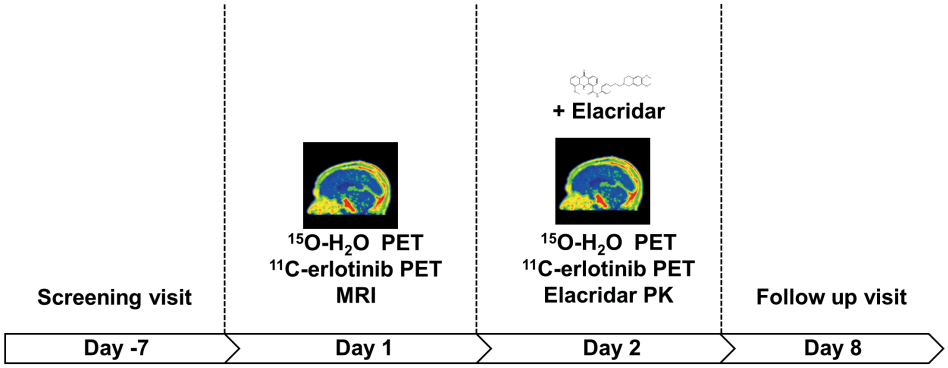

Figure 1: Schematic of the clinical study design.

As elacridar plasma concentrations have been shown to peak at 8-12 hours after intake of the present formulation (22), patients took a single oral 1000 mg elacridar dose 8 to 12 hours before the second PET scan. An MRI of the brain was acquired on day 1. The purpose of this was to exclude any brain metastases as these might have compromised the function of the BBB. Each ^{11}C-erlotinib scan was preceded by a ^{15}O-H_2O scan to assess possible effects of elacridar on cerebral blood flow. At the start and end of the second ^{11}C-erlotinib scan a venous blood sample was drawn to measure elacridar plasma concentrations, using LC-MS/MS (23).

On day 8 (a week after first PET scan) a follow up visit was scheduled. Each visit, patients were evaluated for safety, including assessment of adverse events, physical examination, performance status, blood pressure and heart rate measurements, and clinical laboratory tests. The incidence, severity, start and end dates of all adverse events (AEs) were recorded. AEs were graded according to the Common Terminology Criteria for Adverse Events (CTCAE v4.02).

Patient Population

Patients with advanced or metastatic solid tumors were eligible for enrollment if no standard therapy was available or if a tyrosine kinase inhibitor (if a ABCB1/ABCG2 substrate) was the standard therapeutic option. Furthermore patients had to be 18 years of age with the following lab values: absolute neutrophil count of ≥1.5x10^9 /L, platelet count of ≥75x10^9 /L, serum bilirubin ≤2.0xupper limit of normal (ULN), ASAT and ALAT ≤2.5xULN, serum creatinine ≤2.0xULN or creatinine clearance ≥40 mL/min. Exclusion criteria were known brain metastases and/or previous treatment with

central nervous system irradiation, as this could have compromised the function of the BBB. Patients discontinued any medication which induced, inhibited or was a substrate for ABCB1 and/or ABCG2 at least three plasma elimination half-lives before the first PET scan.

Tracer Preparation & Scanning Procedure in Cancer Patients

^{11}C-erlotinib was synthesized and prepared as described previously (17). Scans were performed on a Gemini TF-64 PET/CT scanner (Philips Medical Systems, Best, the Netherlands), which is a high performance, time-of-flight, fully 3-dimensional PET scanner together with a 16-slice Brilliance CT scanner. PET data were reconstructed using all appropriate corrections applied for normalization, dead time, decay, randoms, scatter and attenuation. PET data were reconstructed using the 3D RAMLA algorithm with CT based attenuation correction, at a final voxel size of 4x4x4 mm^3 and a spatial resolution of 5-7 mm full width at half maximum. First a low dose CT scan (50 mAs, without contrast) was performed for attenuation correction of the subsequent PET data. Following the CT scan, 370 MBq of ^{15}O-H_2O was injected intravenously, starting a 10 min emission scan in 3D mode. Next, after a 10 min period to allow for physical decay of ^{15}O, 370 MBq of ^{11}C-erlotinib was injected intravenously, simultaneously starting a 60 min emission scan in 3D mode. The ^{15}O-H_2O and ^{11}C-erlotinib emission scans were acquired in list-mode and sorted retrospectively into 26 (1x10, 8x5, 4x10, 2x15, 3x20, 2x30 and 6x60 s) and 36 (1x10, 8x5, 4x10, 2x15, 3x20, 2x30, 6x60, 4x150, 4x300 and 2x600 s) frames, respectively. No corrections for patient motion and/or respiratory motion were applied.

All patients received an indwelling radial artery cannula, for arterial blood sampling (17). In addition, a venous cannula was inserted, which was used for tracer injection and sampling of venous blood. The arterial input function was measured using online continuous blood sampling (at 300 mL/hour for the first 5 minutes, then at 150 ml/hour for 15 minutes)(24). At discrete time points (5, 10, 20, 40, and 60 minutes after injection), manual samples were obtained for online calibration of the measured whole blood input function, determination of plasma/whole blood ratios, and measurement of metabolite fractions. Plasma analysis of ^{11}C-erlotinib and polar radioactive metabolites were counted using a Wizard 1480 gammacounter (Perkin Elmer, Waltham, USA).

PET Data Analysis

To investigate whole brain uptake, three-dimensional regions of interest were defined manually around the whole brain, as seen on CT and MRI scans, and projected onto the dynamic PET scan, thereby generating ^{11}C-erlotinib time-activity curves.

Pharmacokinetic modeling was performed using in-house software, developed within the Matlab (The MathWorks Inc., Natick, MA, USA) environment. Data were fitted with single tissue, two tissue reversible and two tissue irreversible metabolite corrected plasma input models. The optimal plasma input model was determined on basis visual analysis of the time-activity curves, akaike criteria and sensitivity of the kinetic parameters. In case of the reversible models the volume of distribution, V_T

(dimensionless quantity), was used as the outcome parameter describing erlotinib uptake in tissue, as described previously (17,25). Results obtained with and without elacridar pretreatment were compared.

Study Conduct and Registration

All animal experiments were approved by the animal ethics committee of the Netherlands Cancer Institute, performed according to institutional guidelines and in compliance with Dutch legislation. The clinical trial was conducted in accordance with the declaration of Helsinki and approved by the medical ethics review committee of each of the participating medical centers. The trial was registered in the EUdraCT clinical trial database (2014-000281-21) and Netherlands trial registry (NTR4780). All patients provided written informed consent before enrollment.

Results

Preclinical Pharmacology

Increasing the dose of elacridar resulted in an increased plasma concentration of elacridar (figure 2, left panel). At 4 hours after dosing, the plasma elacridar concentrations were 216±46, 275±60 and 455±44 ng/mL for the 10, 25 and 50 mg/kg dose, respectively. The erlotinib plasma concentration was 1020±350 in WT mice receiving elacridar vehicle and was 2610±710, 2610±290 and 1900±830 ng/mL at the 10, 25 and 50 mg/kg elacridar dose. The erlotinib plasma concentration in KO mice was 1700±120 ng/mL.

The erlotinib brain-to-plasma ratios were 0.25±0.06, 0.31±0.05 and 0.37±0.04 for the increasing doses of elacridar (figure 2, right panel). The ratio for untreated WT mice was 0.09±0.01. Each dose was significantly higher ratio compared to vehicle, ($p<0.002$ for each dose, independent sample t-tests). The *Abcb1a/b;Abcg2* KO mice had a brain-to-plasma ratio of 0.45±0.02.

Preclinical Imaging

Representative summed images of a WT and a Abcb1a/b;Abcg2 KO mouse are shown in figure 3, left panel. ^{11}C-erlotinib PET scans showed increased cerebral uptake in KO compared to WT mice. The ^{11}C-erlotinib %ID/gr of brain tissue was determined ex vivo in KO and WT mice. ^{11}C-erlotinib brain uptake was increased 2.6-fold in the KO mice compared with WT mice ($p=0.01$, independent sample t-test) as shown in figure 3, right panel.

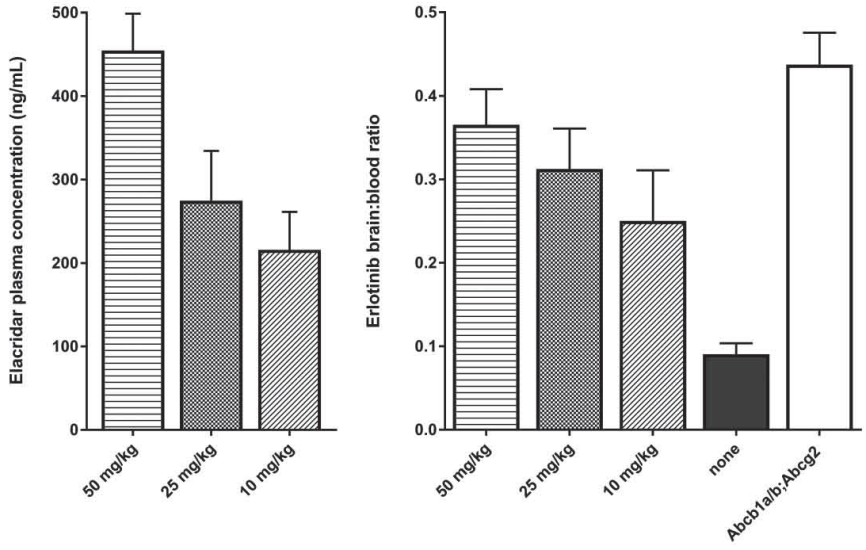

Figure 2: Preclinical pharmacology of elacridar and erlotinib in mice. *Left:* Elacridar plasma concentrations in ng/mL for increasing oral dose of elacridar (0, 10, 25 and 50 mg/kg). *Right*: Erlotinib brain-to-plasma ratios at the same increasing doses of elacridar in WT mice (n=4). A group of *Abcb1a/b;Abcg2* KO mice was used as positive controls (n=5).

Clinical Trial Results

From September 2014 to March 2015, seven patients signed informed consent. One patient dropped out before the first administration of ^{11}C-erlotinib due to unsuccessful placement of the arterial catheter. The six remaining patients all underwent the entire protocol. Due to problems with the arterial sampling, no input function was available for one patient. PET-data from the remaining five patients were available for evaluation, of which four in both scans. After analysis of the data of these patients, enrollment was terminated due to lack of effect.

The evaluable patients were all male and had a mean±SD age of 57±8 years and weighed 81±14 kg. Four patients had a gastro-intestinal stromal tumor and one had advanced colorectal cancer. The gastro-intestinal stromal tumor patients interrupted imatinib treatment three days before inclusion and restarted after the trial. The colorectal cancer patient did not receive active treatment.

None of the patients experienced adverse events related to the tracer dose of erlotinib. All AEs related to elacridar were ≤ grade 1, reversible and similar to those observed in previous trials with elacridar (26–28).

Clinical Imaging

Averaged ^{11}C-erlotinib PET images (5-60 minutes, corrected for ^{11}C-erlotinib dose) before and after a 1000 mg dose of elacridar for the subject with the largest increase in V_T are shown in figure 4. ^{11}C-erlotinib activity was markedly lower in the brain than in the surrounding tissues. The ^{11}C-erlotinib dose was not significantly different between the first and second scans, 363±37 versus 333±55 MBq (p=0.28, paired sample t-test). Moreover, no differences were observed in specific activity before (55.68 GBq/µmol) and after elacridar (50.65 GBq/µmol) resulting in comparable erlotinib doses of 2.54 and 2.61 µg respectively.

The optimal plasma input model for fitting ^{11}C-erlotinib data in the brain is the single tissue model (89% preference) followed by the two tissue reversible model (11%), according to the Akaike criterion. However, the fitted V_T was highly correlated between the single and two tissue reversible model (r^2 = 0.9979). An overview of ^{11}C-erlotinib brain V_T values before and after elacridar administration are summarized in table 1. V_T of ^{11}C-erlotinib did not increase after administration of elacridar (0.216±0.121 versus 0.205±0.071, p=0.91 paired sample t-test). ^{11}C-erlotinib whole brain activity curves as standardized uptake value (SUV) versus time of patients before and after a 1000 mg dose of elacridar are shown in figure 5. The metabolism of erlotinib was unaffected by elacridar. Curves of the percentage parent erlotinib versus time during the scan before and after the elacridar dose are provided in supplementary figure 1.

Cerebral blood flow was unaffected by administration of elacridar, ^{15}O-H_2O K_1 was 0.48±0.10 before and 0.44±0.13 after the 1000 mg dose of elacridar (p=0.21, paired sample t-test). For patient evaluable in both scans mean elacridar plasma concentrations on the day of the PET scan (averages of the samples at the start and end of the scan) were 401±154 ng/mL. The ratio of V_T (after/before elacridar) versus elacridar plasma concentration is plotted in figure 6. No increase in V_T ratio with higher elacridar plasma concentration was found over the 271 – 619 ng/mL range.

Discussion

It was hypothesized that inhibition of ABCB1 and ABCG2 by elacridar should result in increased erlotinib brain exposure in mice and in humans. In mice, we showed increased brain uptake both at a pharmacological (figure 2) and tracer (figure 3) erlotinib dose. These findings are supported by previous studies in mice and non-human primates (8,12,29). However, these preclinical data could not be reproduced in humans (table 1, figure 4 and 5).

This is the first study performed in human brain using ^{11}C-erlotinb using dynamic images in combination with metabolite corrected plasma input function. The optimal pharmacokinetic model for use in the brain was the single tissue compartment model according to the Akaike criterion. However, the differences in the estimated V_T between the two tissue compartment model and the

single tissue compartment models were small. Furthermore, it is expected that the two tissue model will perform better for regions with higher specific uptake. Therefore, our initial assessment shows that the two tissue reversible model is the preferred model to be used with ^{11}C-Erlotininb in the brain. Previously the test-retest variability for ^{11}C-erlotinib V_T in tumor lesions was quantified at 12%. Variability in V_T was relatively higher in this study compared to previous trials (17,25). This is probably due to the lower V_T (<0.5) values for erlotinib V_T in the brain compared to the previously explored tumor images.

Table 1: V_t of brain ^{11}C-erlotinib before and after elacridar administration in cancer patients (n=5).

Patient	^{11}C-Erlotinib V_T Before Elacridar	^{11}C-Erlotinib V_T After Elacridar	V_T Ratio†
1	0.395	0.312	0.790
2	0.179	0.198	1.106
3	-	0.179	-
4	0.160	0.221	1.381
5	0.128	0.116	0.906
Mean ±SD	**0.216 ± 0.121**	**0.205 ±0.071**	**0.999 ±0.236**

V_T: Brain volume of distribution

SD: Standard deviation

†The ratio is calculated based on patients evaluable in both scans.

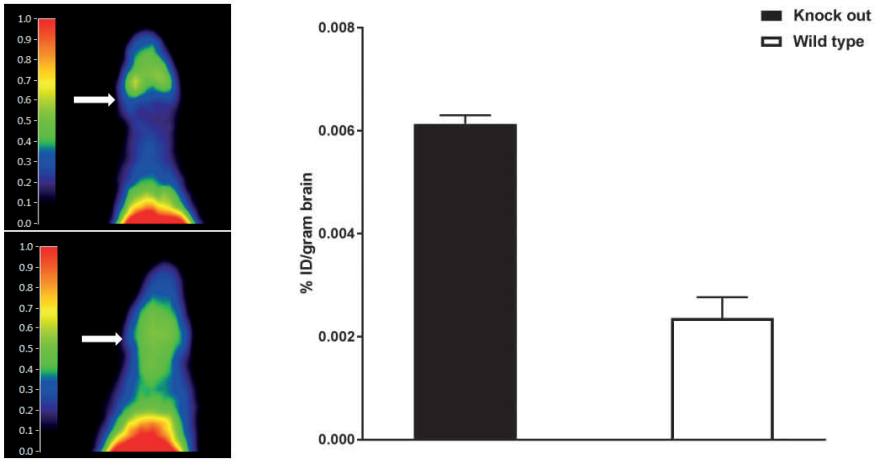

Figure 3: Preclinical imaging using ^{11}C-erlotinib PET. *Left:* Representative summation images of a *Abcb1a/b;Abcg2* KO (*lower panel*) and WT mouse (*upper panel*). Arrows indicate the brain. *Right:* ^{11}C-erlotinib percent of injected dose per gram of brain tissue (%ID/gr) determined *ex vivo* in KO and WT mice. Erlotinib brain penetration was significantly higher in the KO mice (n=2, per group).

There was no effect of ABCB1/ABCG2 inhibition on V_T in the clinical study and no relationship between erlotinib V_T-ratio and elacridar exposure, even though plasma concentrations as high as 600 ng/mL were measured (figure 6). This could be due to several factors: insufficient elacridar exposure, non-linear pharmacokinetics of erlotinib or inter-species differences in the BBB. Low free plasma concentrations of the inhibitor and non-linearity of transporter inhibition could be suggested as possible explanations for the lack of effect (30). However, it is unlikely that this applies to the combination of elacridar and erlotinib. Previously, Kuntner et al performed a dose finding study of elacridar using ^{11}C-verapamil imaging as readout (31). Elacridar was found to increase brain uptake at concentrations at or above 200 ng/mL. Similarly, our preclinical data show an increased erlotinib brain exposure at elacridar plasma concentrations of 200 – 400 ng/mL (figure 2) and the plasma levels of elacridar in our clinical trial were similar, if not higher. Moreover, no trend towards an increasing V_T-ratio with increasing elacridar concentration was seen over the 94 – 619 ng/mL range. A species difference in free drug concentrations is also unlikely because protein binding of erlotinib and its major metabolite desmethyl erlotinib are similar in mice and humans (95 versus 92% for erlotinib and 73 versus 90% for desmethyl erlotinib)(32).

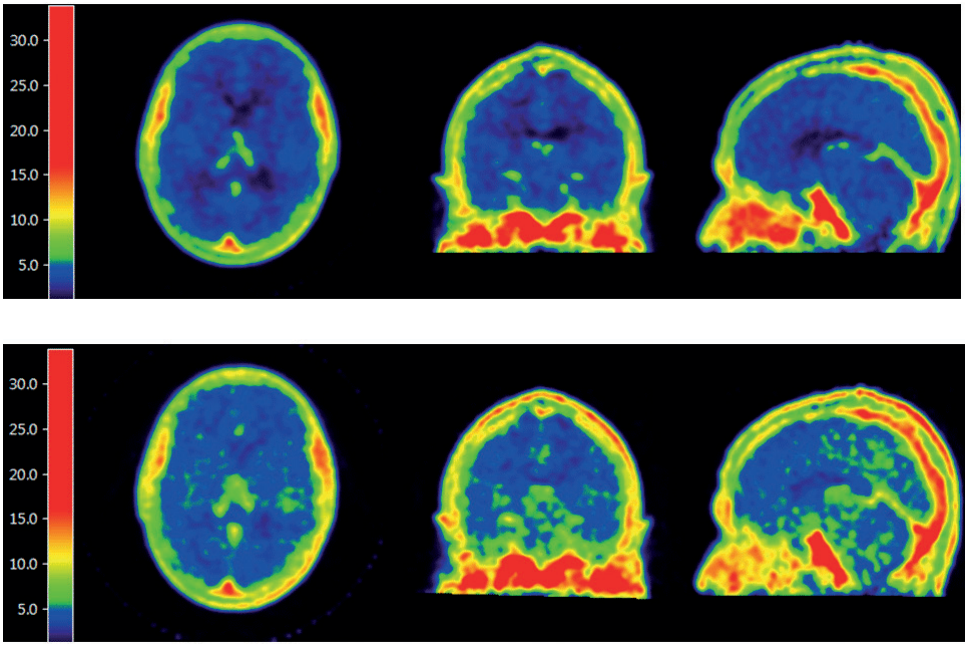

Figure 4: ^{11}C-erlotinib PET before (upper panel) and after elacridar (lower panel) for subject 4.

The considerations above seem to eliminate limited elacridar exposure as an explanation for the lack of increased brain exposure in the clinical study. Yet, inhibition by elacridar resulted in a 3.5-fold increase in ^{11}C-erlotinib brain V_T in primates (29). However, these results were achieved at an extremely high elacridar plasma concentration of maximally 10.0±1.5 µg/mL, using an intravenous infusion. Unfortunately, the study in monkeys did not further interrogate the relationship between elacridar plasma levels and erlotinib brain distribution. Although it is possible that such high elacridar levels in humans may also cause a better brain uptake of erlotinib, these will be hard to achieve via oral dosing given the unbeneficial pharmaceutical properties of elacridar. The concentrations observed in the current trial (401±154 ng/mL, figure 6) were already higher than most of the C_{max} values in previous clinical trials of 140 – 434 ng/mL (22,26–28,33).

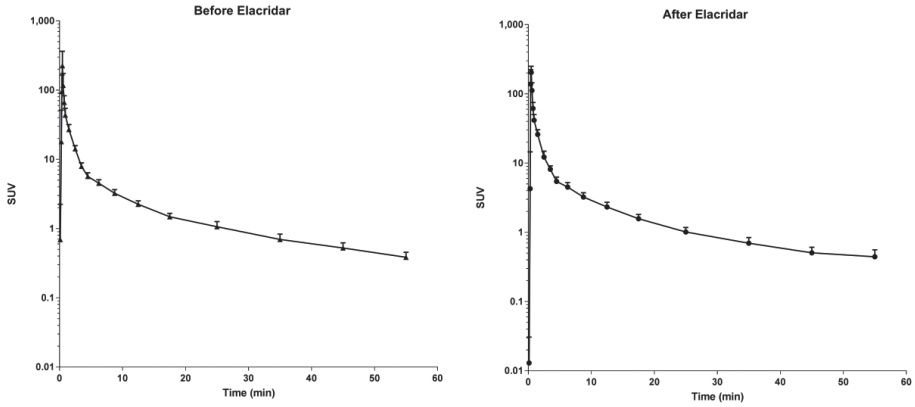

Figure 5: ^{11}C-erlotinib whole brain activity as standardized uptake value (SUV) versus time (in minutes) of patients before and after a 1000 mg dose of elacridar (n=5).

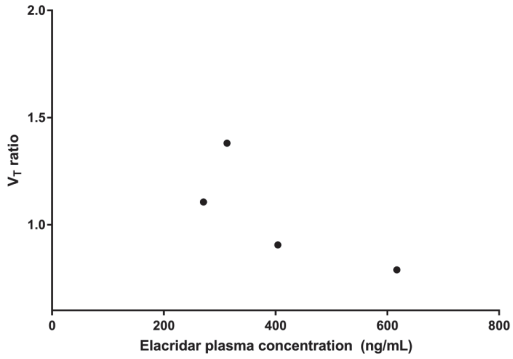

Figure 6: ^{11}C-erlotinib brain V_T ratio (after/before administration of elacridar) versus elacridar exposure (n=5). .

We used a tracer dose of erlotinib in the clinical study. Therefore, non-linear pharmacokinetics of erlotinib could be an explanation for the absence of an effect on V_T (as it could be argued that a higher dose of erlotinib would have shown an increase in brain uptake). However, this is less likely given the fact that we show increased brain uptake both at a pharmacological (figure 2) and tracer (figure 3) dose of erlotinib in preclinical studies. A previous study of ^{11}C-erlotinib in mice (8) suggested that erlotinib pharmacokinetics is non-linear and that erlotinib itself may be an inhibitor of ABCB1 and ABCG2. However, inhibition of these transporters by erlotinib is unlikely at tracer doses and probably also at pharmacological doses, as this conflicts with our preclinical experiments and with clinical observations that erlotinib cerebral spinal fluid concentrations are markedly lower than levels in plasma (10,11). Additionally, one study found that erlotinib induced the expression of ABCB1(34), but this is unlikely to occur in this short period of time.
A high dose of erlotinib did result in an increased erlotinib brain V_T in primates, but this effect was markedly smaller than that of elacridar (only 1.7-fold compared to a 3.5-fold increase). In a previous clinical ^{11}C-erlotinib study, addition of cold erlotinib resulted in markedly lower V_T in tumor lesions of cancer patients (18), supporting the choice to not add a pharmacological erlotinib dose in this trial.

The considerations listed above leave interspecies differences as the most likely explanation for the discrepancy between the preclinical and clinical results. Firstly, interspecies differences in drug transporter efficiency have been shown for various substrates even when corrected for protein expression levels (35). Secondly, Uchida et al. used mass spectrometry to quantify absolute protein levels of ABCB1 and ABCG2 in mice and human brain tissue (36). ABCG2 expression was found to be 1.8 fold higher and ABCB1 expression was 2.33 fold lower in the human compared to mice BBB. If ABCG2 indeed plays a more prominent role in the human BBB and/or if human ABCG2 is an efficient transporter of erlotinib, insufficient inhibition of ABCG2 could explain the lack of effect in the clinical trial. This hypothesis is supported by reports suggesting that elacridar inhibits ABCB1 at 50-100 nM, but that 250 nM is required for inhibition of ABCG2 (6,7), albeit likely that the inhibitory potency will be different for each substrate.
Thirdly, ABCG2 is known to compensate for ABCB1-inhibition for double substrates (37). This effect has also been shown for erlotinib in preclinical experiments (12). Importantly, in mice the largest gain in the erlotinib brain accumulation was seen when ABCB1 was absent with a moderate further increase when both ABCB1 and ABCG2 were absent. Very likely, the increase of erlotinib in mice that occurs by elacridar results predominantly by the inhibition of ABCB1 by elacridar. This could is also in line with other studies using ^{11}C-verapamil (a substrate for ABCB1, but not ABCG2) in humans showing statistically significant, albeit small, increases in brain uptake in ABCB1/ABCG2 inhibition (38). Besides species differences in substrate affinities and transporter expression other unknown factor may contribute to the observed differences. However, based om these observations we advise that future clinical trials aiming to increase brain exposure by administration of elacridar should try to avoid using strong ABCG2 substrates and focus primarily on ABCB1 and/or weak ABCG2 substrates.

Conclusion

Results of our preclinical studies are in accordance with previous reports that have shown a significant effect of combined Abcb1a/b;Abcg2 inhibition by elacridar on erlotinib brain penetration. To our knowledge this is the first study investigating the effect of BBB transporter inhibition on ^{11}C-erlotinib in the clinical setting. Here no increased brain V_T was found in cancer patients treated with elacridar. The more pronounced role that ABCG2 appears to play at the human BBB and the lower potency of elacridar to inhibit ABCG2 may be an explanation of these inter-species differences.
Future trials in this area should take into account the pharmacokinetic exposure of the inhibitor, the possible non-linearity of substrate and transporter kinetics and the possibility that an increased brain exposure can be achieved more easily for single ABCB1 than for dual ABCB1/ABCG2 substrates.

Financial disclosure

This research was funded by personal grant from the Netherlands Cancer Institute to Dr. N Steeghs.

Disclaimer

Olaf van Tellingen is co-inventor of a patent application (Bunt and Van Tellingen, 2014; US 20140235631A1) dealing with development of an improved oral formulation for elacridar. All other authors declare they have no conflict of interest.

Acknoledgements

We thank all patients for their participation in the clinical trial.

References

1. Van Tellingen O, Yetkin-Arik B, De Gooijer MC, Wesseling P, Wurdinger T, De Vries HE. Overcoming the blood-brain tumor barrier for effective glioblastoma treatment. Drug resist updat. 2015;19:1–12.
2. Milojkovic Kerklaan B, van Tellingen O, Huitema ADR, Beijnen JH, Boogerd W, Schellens JHM, et al. Strategies to target drugs to gliomas and CNS metastases of solid tumors. J neurol. 2016;263:428–40.
3. Deeken JF, Löscher W. The blood-brain barrier and cancer: Transporters, treatment, and trojan horses. Clin cancer res. 2007;13:1663–74.
4. Lockman PR, Mittapalli RK, Taskar KS, Rudraraju V, Gril B, Bohn KA, et al. Heterogeneous blood-tumor barrier permeability determines drug efficacy in experimental brain metastases of breast cancer. Clincancer res. 2010;16:5664–78.
5. Gainor JF, Ou SH, Logan J, Borges LF, Shaw AT. The central nervous system as a sanctuary site in ALK-positive non-small-cell lung cancer. J thorac oncol. 2013;8:1570–3.
6. Hyafil F, Vergely C, Du Vignaud P, Grand-Perret T. In vitro and in vivo reversal of multidrug resistance by GF120918, an acridonecarboxamide derivative. Cancer res. 1993;53:4595–602.
7. de Bruin M, Miyake K, Litman T, Robey R, Bates SE. Reversal of resistance by GF120918 in cell lines expressing the ABC half-transporter, MXR. Cancer lett.; 1999;146:117–26.
8. Traxl A, Wanek T, Mairinger S, Stanek J, Filip T, Sauberer M, et al. Breast Cancer Resistance Protein and P-glycoprotein Influence In Vivo Disposition of 11C-Erlotinib. J nucl med. 2015;56:1930–6.
9. Sane R, Mittapalli RK, Elmquist WF. Development and Evaluation of a Novel Microemulsion Formulation of Elacridar to imrpove its Bioavailability. J pharm sci. 2013;102:1343–54.
10. Broniscer A, Panetta JC, O'Shaughnessy M, Fraga C, Bai F, Krasin MJ, et al. Plasma and cerebrospinal fluid pharmacokinetics of erlotinib and its active metabolite OSI-420. Clin cancer res. 2007;13:1511–5.
11. Togashi Y, Masago K, Masuda S, Mizuno T, Fukudo M, Ikemi Y, et al. Cerebrospinal fluid concentration of gefitinib and erlotinib in patients with non-small cell lung cancer. Cancer chemother pharmacol. 2012;70:399–405.
12. De Vries NA, Buckle T, Zhao J, Beijnen JH, Schellens JHM, Van Tellingen O. Restricted brain penetration of the tyrosine kinase inhibitor erlotinib due to the drug transporters P-gp and BCRP. Invest new drugs. 2012;30:443–9.
13. Kodaira H, Kusuhara H, Fujita T, Ushiki J, Fuse E, Sugiyama Y. Quantitative evaluation of the impact of active efflux by p-glycoprotein and breast cancer resistance protein at the blood-brain barrier on the predictability of the unbound concentrations of drugs in the brain using cerebrospinal fluid concentration as a. J pharmacol exp ther. 2011;339:935–44.
14. Kodaira H, Kusuhara H, Ushiki J, Fuse E, Sugiyama Y. Kinetic Analysis of the Cooperation of P-Glycoprotein (P-gp / Abcb1) and Breast Cancer Resistance Protein (Bcrp / Abcg2) in Limiting the Brain and Testis Penetration of Erlotinib, Flavopiridol and Mitoxantrone. J pharmacol exp ther. 2010;333:788–96.
15. Abourbeh G, Itamar B, Salnikov O, Beltsov S, Mishani E. Identifying erlotinib-sensitive non-small cell lung carcinoma tumors in mice using [11C] erlotinib PET. EJNMMI res. 2015;5:1–10.
16. Memon AA, Jakobsen S, Dagnaes-Hansen F, Sorensen BS, Keiding S, Nexo E. Positron emission tomography (PET) imaging with [11C]-labeled erlotinib: A micro-PET study on mice with lung tumor xenografts. Cancer res. 2009;69:873–8.
17. Bahce I, Smit EF, Lubberink M, Van Der Veldt AAM, Yaqub M, Windhorst AD, et al. Development of [11C]erlotinib positron emission tomography for in vivo evaluation of EGF receptor mutational status. Clin cancer res. 2013;19:183–93.
18. Bahce I, Yaqub M, Errami H, Schuit RC, Schober P, Thunnissen E, et al. Effects of erlotinib therapy on [(11)C]erlotinib uptake in EGFR mutated, advanced NSCLC. EJNMMI res. 2016;6:10.
19. de Jong HWAM, van Velden FHP, Kloet RW, Buijs FL, Boellaard R, Lammertsma AA. Performance evaluation of the ECAT HRRT: an LSO-LYSO double layer high resolution, high sensitivity scanner. Phys med biol. 2007;52:1505–26.
20. van Velden FHP, Kloet RW, van Berckel BNM, Lammertsma AA, Boellaard R. Accuracy of 3-Dimensional Reconstruction Algorithms for the High-Resolution Research Tomograph. J nucl med. 2008;50:72–80.

21. Sawicki E, Schellens JHM, Beijnen JH, Nuijen B. Pharmaceutical development of an amorphous solid dispersion formulation of elacridar hydrochloride for proof-of-concept clinical studies. Drug dev ind pharm. 2017;43:584–94.
22. Sawicki E, Verheijen RB, Huitema ADR, van Tellingen O, Schellens JHM, Nuijen B, et al. Clinical pharmacokinetics of an amorphous solid dispersion tablet of elacridar. Drug deliv transl res. 2016;
23. Stokvis E, Rosing H, Causon R, Schellens J, Beijnen J. Quantitative analysis of the P-glycoprotein inhibitor Elacridar (GF120918) in human and dog plasma using liquid chromatography with tandem mass spectrometric detection. J mass spectrom. 2004;39:1122–30.
24. Boellaard R, Van Lingen A, Van Balen SCM, Hoving BG, Lammertsma AA. Characteristics of a new fully programmable blood sampling device for monitoring blood radioactivity during PET. Eur j nucl ned. 2001;28:81–9.
25. Yaqub M, Bahce I, Voorhoeve C, Schuit RC, Windhorst AD, Hoekstra OS, et al. Quantitative and simplified analysis of 11C-erlotinib studies. J nucl ned. 2016;1–20.
26. Kemper EM, Van Zandbergen AE, Cleypool C, Mos HA, Boogerd W, Beijnen JH, et al. Increased penetration of paclitaxel into the brain by inhibition of P-glycoprotein. Clin cancer res. 2003;9:2849–55.
27. Malingré MM, Beijnen JH, Rosing H, Koopman FJ, Jewell RC, Paul EM, et al. Co-administration of GF120918 significantly increases the systemic exposure to oral paclitaxel in cancer patients. Br j cancer. 2001;84:42–7.
28. Kruijtzer CMF, Beijnen JH, Rosing H, ten Bokkel Huinink WW, Schot M, Jewell RC, et al. Increased oral bioavailability of topotecan in combination with the breast cancer resistance protein and P-glycoprotein inhibitor GF120918. J clin oncol. 2002;20:2943–50.
29. Tournier N, Goutal S, Auvity S, Traxl A, Mairinger S, Wanek T, et al. Strategies to inhibit ABCB1- and ABCG2-mediated efflux transport of erlotinib at the blood-brain barrier: a PET study in non-human primates. J nucl med. 2016;1–24.
30. Kalvass JC, Polli JW, Bourdet DL, Feng B, Huang S-M, Liu X, et al. Why clinical modulation of efflux transport at the human blood-brain barrier is unlikely: the ITC evidence-based position. Clin pharmacol ther. 2013;94:80–94.
31. Kuntner C, Bankstahl JP, Bankstahl M, Stanek J, Wanek T, Stundner G, et al. Dose-response assessment of tariquidar and elacridar and regional quantification of P-glycoprotein inhibition at the rat blood-brain barrier using (R)-[11C]verapamil PET. Eur j nucl med mol imaging. 2010;37:942–53.
32. EMA - Committee for Medicinal Products for Human Use. European Public Assessment Report Tarceva. 2005;
33. Kuppens IELM, Witteveen EO, Jewell RC, Radema SA, Paul EM, Mangum SG, et al. A phase I, randomized, open-label, parallel-cohort, dose-finding study of elacridar (GF120918) and oral topotecan in cancer patients. Clin cancer res. 2007;13:3276–85.
34. Harmsen S, Meijerman I, Maas-Bakker RF, Beijnen JH, Schellens JHM. PXR-mediated P-glycoprotein induction by small molecule tyrosine kinase inhibitors. Eur j pharm sci. 2013;48:644–9.
35. Katoh M, Suzuyama N, Takeuchi T, Yoshitomi S, Asahi S, Yokoi T. Kinetic analyses for species differences in P-glycoprotein-mediated drug transport. J pharm sci. 2006;95:2673–83.
36. Uchida Y, Ohtsuki S, Katsukura Y, Ikeda C, Suzuki T, Kamiie J, et al. Quantitative targeted absolute proteomics of human blood-brain barrier transporters and receptors. J neurochem. 2011;117:333–45.
37. Agarwal S, Elmquist WF. Insight into the cooperation of P-glycoprotein (ABCB1) and breast cancer resistance protein (ABCG2) at the blood-brain barrier: A case study examining sorafenib efflux clearance. Mol pharm. 2012;9:678–84.
38. Römermann K, Wanek T, Bankstahl M, Bankstahl JP, Fedrowitz M, Müller M, et al. (R)-[11C] verapamil is selectively transported by murine and human P-glycoprotein at the blood-brain barrier, and not by MRP1 and BCRP. Nucl med biol. 2013;40:873–8.

Supplemental figures

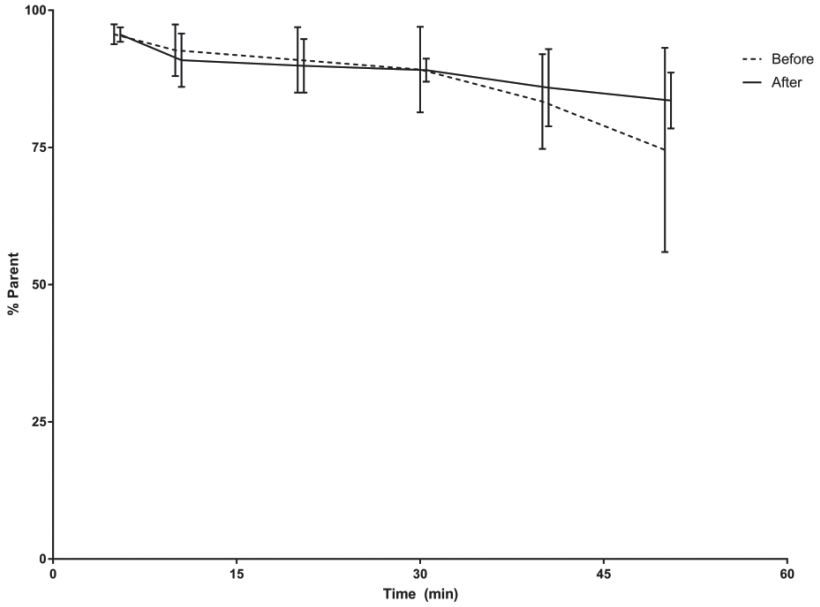

Supplemental figure 1: Erlotinib metabolism, plotted as percent parent erlotinib in the first (dashed line) and second (filled line) ^{11}C-erlotinib PET scan.

Chapter 6

Clinical Pharmacokinetics of the FAK-Inhibitor BI 853520

Chapter 6.1

Randomized, Open-Label, Crossover Studies Evaluating the Effect of Food and Liquid Formulation on the Pharmacokinetics of the Novel Focal Adhesion Kinase (FAK)-Inhibitor BI 853520

R.B. Verheijen[1], D.A.J. van der Biessen[2], S.J. Hotte[3], L.L. Siu[4], A. Spreafico[4], M.J.A. de Jonge[5], L.C. Pronk[6], F.Y.F.L. De Vos[7], D. Schnell[8], H.W. Hirte[3], N. Steeghs[1], M.P. Lolkema[2,5]

[1] Department of Medical Oncology and Clinical Pharmacology, Netherlands Cancer Institute, Plesmanlaan 121, 1066 CX Amsterdam, The Netherlands.

[2] Department of Medical Oncology, Erasmus MC Cancer Institute, Rotterdam, The Netherlands. a.vanderbiessen@erasmusmc.nl

[3] Division of Medical Oncology, Juravinski Cancer Centre, , Ontario Canada.

[4] Division of Medical Oncology and Haematology, Princess Margaret Cancer Centre, Toronto, Ontario, Canada.

[5] Department of Internal Oncology, Erasmus MC Cancer Institute, Rotterdam, The Netherlands.

[6] Clinical Development Oncology, Boehringer Ingelheim España S.A., Madrid, Spain.

[7] Department of Medical Oncology, University Medical Center Utrecht Cancer Center, Utrecht, The Netherlands.

[8] Department of Translational Medicine and Clinical Pharmacology, Boehringer Ingelheim Pharma GmbH & Co. KG, Birkendorfer Biberach, Germany.

Abstract

Background: BI 853520 is a potent inhibitor of focal adhesion kinase (FAK) currently under clinical development. Two randomized, open-label, crossover studies were conducted to evaluate the effect of food and liquid dispersion on the pharmacokinetics of BI 853520.

Methods: Sixteen patients with advanced solid tumors were enrolled in each sub-study. The order of administration was randomized and pharmacokinetic samples collected for 48 hours after a 200 mg dose of BI 853520. Lack of effect would be demonstrated if the 90% confidence interval (90% CI) of the ratio of the geometric mean (GMR) of the area under the plasma curve (AUC_{0-48} and $AUC_{0-\infty}$) and maximum concentration (C_{max}) did not cross the 80–125% (bioequivalence) boundaries.

Results: Administration of BI 853520 as a liquid dispersion did not affect AUC_{0-48}, $AUC_{0-\infty}$ and C_{max} compared to a tablet, resulting in GMRs (90% CIs) of 1.00 (0.92-1.09), 0.98 (0.90-1.07) and 0.93 (0.86-1.01) respectively. GMRs plus 90% CIs for the fed versus fasted state were 0.95 (0.77-1.19), 0.96 (0.77-1.19) and 0.92 (0.76-1.11) for the same parameters. Although the 90% CIs were not within bioequivalence limits, after administration with a high-fat meal, the limited size of the reductions in AUC_{0-48}, $AUC_{0-\infty}$ and C_{max} are unlikely to be clinically relevant.

Conclusions: These studies demonstrate that BI 853520 can be used effectively as a liquid dispersion and no food restrictions need to be provided to patients. These favorable pharmacokinetic properties contribute to the convenience and flexibility of the posology of BI 853520.

Introduction

The focal adhesion kinase (FAK), also known as protein tyrosine kinase 2 (PTK2), is a non-receptor cytokine tyrosine kinase that comprises a structural component of focal adhesions. These focal adhesions are protein complexes containing cell surface integrins, which are essential for interaction with the extracellular matrix and transduction of signaling pathways.[1] FAK plays a vital role in proliferation, survival and migration of tumor cells.[2] In cancer, dysregulation and activation of focal adhesions facilitate cell motility and promote invasive tumor growth.[1] Increased expression of FAK is found in various tumor types and the extent of expression has been related to the extent of disease progression and metastasis.[3] In particular, FAK overexpression has been implicated in the development of sarcomas, and prostate, colorectal, ovarian and breast cancer.[4–9]

In mice, genetic knock out of FAK has been shown to be embryonically lethal, underscoring its role in development, in particular in the formation of blood vessels.[10] Chemical inhibition of FAK has been shown to reduce FAK activity and block tumor growth in a range of xenograft models. [11–14] Moreover, inhibition of FAK on endothelial cells has been shown to improve sensitivity of tumor cells to chemotherapy and immunotherapy in preclinical models.[15,16] Several inhibitors of FAK have been evaluated in cancer patients,[17–19] both as monotherapy and in combination with chemotherapy, targeted and immune therapies. [20] BI 853520 is a potent inhibitor of FAK and clinical exploration has shown biomarker engagement and anti-tumor activity in the phase 1 studies reported by de Jonge et al and Doi et al in this issue.

A major determinant of drug absorption is the impact of concomitant administration with or without food.[21] Food, amongst other factors, may influence gastric pH, emptying and motility. Moreover, the presence of a high-fat meal may improve the solubility of lipophilic drugs thereby increasing (relative) bioavailability. All these factors can influence the rate and extent of gastrointestinal absorption and indicate the need to study the effects of food on drug bioavailability during clinical drug development.[22,23] A marked influence of food on absorption has been reported for several orally dosed anti-cancer drugs.[24–27] In particular, in the case of abiraterone, a 1000% increase in area under the plasma concentration time curve (AUC) was demonstrated when the drug was administered with food compared to a fasted state, illustrating a clinically relevant food effect.[25] The requirement to administer drugs in the fasting state can have a major impact on patients' well-being, especially if the fasting state has to be continued for several hours after drug administration.

Further, oral administration of drugs can be problematic for those who cannot swallow whole tablets. This may be particularly relevant in patients with some advanced cancers such as head and neck cancer or esophageal cancer, or in pediatric patients. Therefore development of an alternative oral formulation could increase convenience of administration for patients. However, any alternative

formulation should first be tested clinically to demonstrate it achieves appropriate pharmacokinetic exposure.

We report on two randomized, open-label, crossover studies evaluating the effect of administration with or without a high calorie meal and the effect of administration as a liquid dispersion on the pharmacokinetics of the novel FAK-inhibitor BI 853520.

Patients and methods

Patients

Patients who were treated in the expansion cohorts of the phase 1 dose-finding study of BI 853520 (NCT01335269; see the article by de Jonge in this issue) were eligible for enrollment if they had a confirmed diagnosis of advanced, measurable or evaluable, non-resectable and/or metastatic non-hematologic malignancy, and disease progression in the last 6 months before study entry demonstrated by serial imaging. Patients needed to have failed conventional treatment or be unamenable to established treatment options or have no proven therapy available to them. Moreover, patients needed to have an Eastern Cooperative Oncology Group (ECOG) performance score of 0 or 1, have recovered from reversible toxicities (alopecia excluded) from prior anti-cancer therapies (Common Terminology Criteria for Adverse Events grade < 2), be at least 18 years of age and have a life expectancy of at least 3 months.

The main exclusion criteria were serious concomitant illness, active infections, pregnancy, breastfeeding, active or symptomatic brain metastases, second malignancies, congestive heart failure of grade III or IV, myocardial infarction within 6 months of inclusion, absolute neutrophil count <1500/mm^3, platelet count <100,000/mm^3, total bilirubin >1.5 times the upper limit of normal (ULN), aspartate transferase and/or alanine transferase >3 times ULN or >5 times ULN in patients with liver metastases.

Study design

An overview of the design of both studies is provided in Figure 1. The effect of food on the pharmacokinetics of BI 853520 was investigated in a randomized, open-label, crossover, single-dose study in patients with advanced solid tumors. Patients received a single 200 mg tablet of BI 853520 either in a fed or fasted state (see details of the conditions of drug administration below) with a wash-out period of 7 days between each administration. The order of fasted-fed or fed-fasted was established through randomization.

The pharmacokinetics of a single 200 mg dose of BI 853520 in a liquid dispersion were studied in the same randomized, open-label, crossover design using the 200 mg tablet as reference. The order of

administration (liquid-tablet or tablet-liquid) was randomized and a 7 day wash-out period applied as described above.

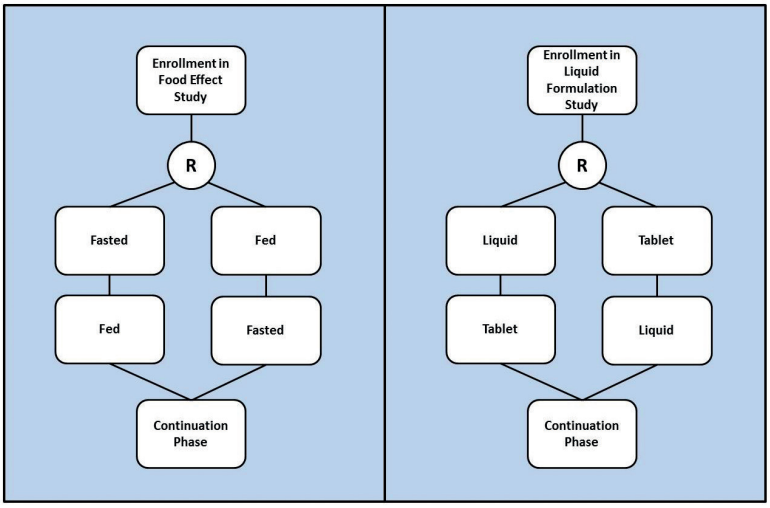

Figure 1: Schematic of randomized, open-label, crossover trials to evaluate the effect of food and formulation on the pharmacokinetics of a 200 mg dose of the FAK-inhibitor BI 853520. The order of administration (fasted-fed versus fed-fasted [left panel] or tablet-liquid versus liquid-tablet [right panel]) was randomized (R) and a wash-out period of 1 week applied between the two treatments. After the pharmacokinetic studies, patients continued on a daily dose of 200 mg BI 853520 (as a tablet) until disease progression, intolerability of the study medication or withdrawal of consent.

After the last pharmacokinetic sample of each pharmacokinetic study, patients continued treatment with a daily dose of 200 mg BI 853520 until disease progression, intolerability of the study medication or withdrawal of consent.

Drug administration

In the food-effect study, BI 853520 was administered either after an overnight fast with approximately 240 mL of water or with a standardized high calorie meal. No food was allowed for 4 hours after intake of the drug. Water was allowed 1 hour after taking the drug. The high calorie meal was a high-fat breakfast containing approximately 950 kilocalories (at least half of which were from fat) and was ingested in no more than 30 minutes. Directly after the meal, the single 200 mg tablet of BI 853520 was administered.

In the tablet versus liquid formulation study, patients received BI 853520 in a fasted state, as described above. Patients remained fasted for 4 hours after intake of the drug. The liquid formulation was prepared by dissolution of the tablet in 20 mL of a reconstitution solution containing sucralose

(4 mg/mL), menthol (2 mg/mL) and benzoic acid (1 mg/mL). The tablet was submersed in the solution in a child-resistant screw-cap bottle, without being crushed. The bottle was then closed and shaken thoroughly for 30 seconds. After shaking, the bottle was set aside for 10 minutes. If the tablet was not dispersed completely, the bottle would be shaken for another 30 seconds and set aside for 5 minutes. This procedure was resumed until the tablet was dispersed completely into a homogeneous dispersion without noticeable lumps. No further dilution of the dispersion was allowed.

Pharmacokinetic sampling

In both studies, blood samples were collected before and at 0.5, 1, 2, 3, 4, 6, 8, 10, 24 and 48 hours after drug administration. Plasma concentrations of BI 853520 were measured by validated assays based on liquid chromatography coupled to tandem mass spectrometry (LC-MS/MS). The lower limit of detection for the assay was 1 nmol/L for plasma.

Data analysis

Based on the plasma concentration time-curves, pharmacokinetic parameters were calculated using non-compartmental analysis. Parameters of interest were time to maximum plasma concentration (T_{max}), maximum plasma concentration (C_{max}), AUC calculated from 0 to 48 hours and extrapolated to infinity (AUC_{0-48} and $AUC_{0-\infty}$ respectively), and the plasma half-life ($T_{1/2}$).

The 90% confidence interval (CI) was calculated for the ratio of the geometric mean C_{max}, $AUC_{0-\infty}$ and AUC_{0-48} for a 200 mg dose under fed and fasted conditions and for the 200 mg tablet and liquid formulation respectively. In each study, only patients evaluable for both treatment states (fasted and fed) or both formulations (liquid and tablet) were included in calculation of the ratio. Lack of difference was demonstrated if the 90% CI of the geometric means of C_{max}, $AUC_{0-\infty}$ and AUC_{0-48} were within the 80–125% limits, in accordance with Food and Drug Administration guidelines for food effect and bioequivalence studies.[28,29]

Trial conduct and registry

This trial was conducted in accordance with the WHO Declaration of Helsinki and Good Clinical Practices. All patients provided written informed consent before enrollment in accordance with International Conference on Harmonization Good Clinical Practice and local legislation. This trial was registered in the United States National Institutes of Health clinical trial registry under the ClinicalTrials.gov identifier: NCT01335269.

Results

In total, 16 patients were enrolled in both studies. In the food effect study, 15 patients were evaluable for treatment in at least one state (fed or fasted), while in the liquid-tablet study 16 patients were evaluable for treatment with at least one dose (liquid or tablet) of BI 853520. Reasons for exclusion from the pharmacokinetic analysis included vomiting within 4 hours after ingestion, failure to take the full BI 853520 dose and expired sample stability. In the food effect sub-study, one plasma concentration-time profile was excluded for one patient due to vomiting after drug administration, and in the liquid-tablet sub-study one plasma concentration-time profile was excluded for one patient due to incomplete drug administration.

The patient characteristics are presented in Table 1. An overview of all plasma-concentration time curves is provided in Figure 2 and a summary of all pharmacokinetic parameters of interest is given in Figure 3.

Table 1: Characteristics of evaluable patients in both studies

	Food effect study	**Liquid formulation study**
Patient (n)	15	16
Gender (n, %)		
Male	5 (33.3)	8 (50)
Female	10 (66.6)	8 (50)
Age (mean, range)	56 [25 – 72]	60 [55 – 89]
Weight (mean, CV)	70 (24.5)	71 (15.3)
Height (mean, CV)	169 (6.6)	172 (5.9)
Tumor type (n, %)		
Soft tissue sarcoma	11 (73.3)	-
Esophageal carcinoma	-	6 (37.5)
Pancreatic adenocarcinoma	2 (13.3)	4 (25.0)
Ovarian carcinoma	1 (6.7)	6 (37.5)
Other	1 (6.7)	-

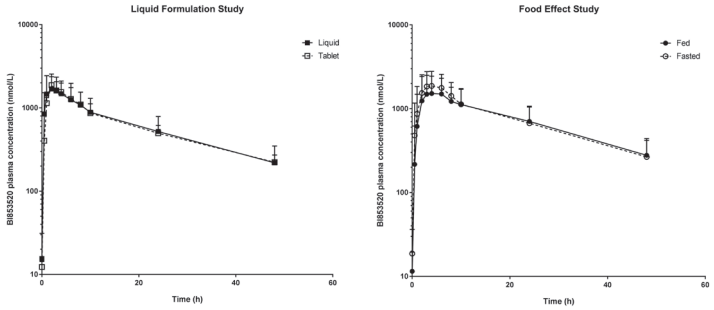

Figure 2: Plasma concentration-time curves for BI 853520 (200 mg) in the food effect and liquid formulation studies. Mean plus standard deviation of the plasma concentration-time curves for a 200 mg BI 853520 tablet administered to patients in a fed and fasted state (left) and a 200 mg dose of BI 853520 administered as a liquid dispersion and tablet (right).

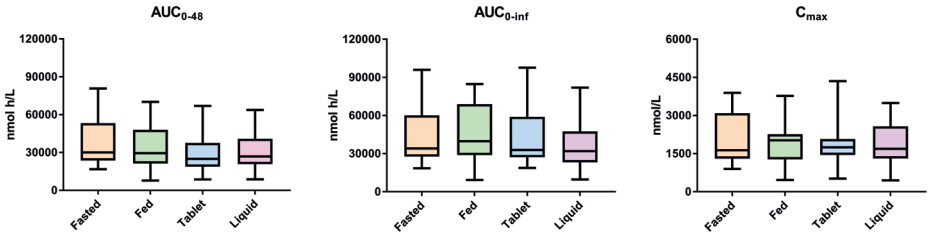

Figure 3: AUC_{0-48}, $AUC_{0-\infty}$ and C_{max} of BI 853520 (200 mg) in the food effect and liquid formulation studies. Boxplots of area under the plasma concentration time curve (AUC) from 0 to 48 hours (AUC_{0-48}) and extrapolated to infinity ($AUC_{0-\infty}$), and the maximum plasma concentration of BI 853520 (C_{max}) following a single 200 mg dose of BI 853520 administered as a liquid (lilac) or tablet (blue) in the liquid formulation study, and under fed (green) or fasted (orange) conditions (both as a tablet) in the food effect study.

Food effect

Plasma-concentration time curves of patients receiving 200 mg of BI 853520 under fed and fasted conditions are presented in Figure 2. The plasma profile of BI 853520 was not markedly influenced by concomitant administration of the high-calorie meal. A summary of the pharmacokinetic parameters of interest is provided in Table 2. The ratio of the geometric means plus 90% CI were 0.95 (0.77–1.19), 0.96 (0.77–1.19) and 0.92 (0.76–1.11) for AUC_{0-48}, $AUC_{0-\infty}$ and C_{max}, respectively. All 90% CIs crossed the lower of the 80–125% boundaries. T_{max} and $T_{1/2}$ of BI 853520 administered after a high calorie meal were not different from those in fasted patients.

Table 2: Pharmacokinetic parameters for a 200 mg tablet of BI 853520 administered under fasted and fed conditions.

	Fasted	Fed	Ratio†
Patients (n)	15	14	-
T_{max*}	3 [1-6]	4 [1-24]	-
AUC_{0-48} (nmol*h/L)	33300 (47.8)	30700 (65.3)	0.95 [0.77-1.19]
$AUC_{0-\infty}$ (nmol*h/L)	39700 (49.4)	38900 (65.3)	0.96 [0.77-1.19]
C_{max} (nmol/L)	1860 (52.1)	1630 (68.6)	0.92 [0.76-1.11]
$T_{1/2}$ (h)	18.0 (22.6)	18.0 (16.1)	-

*Unless otherwise specified, data are presented as geometric mean and coefficient of variation (%). * Median [range], - Not calculated, † geometric means of fasted/fed ratio plus 90% confidence interval. Only data from patients evaluable in both treatment administrations were included (n=14).*

Table 3: Pharmacokinetic parameters of 200 mg BI 853520 administered as a tablet or liquid formulation.

	Tablet	Liquid	Ratio†
N	16	14	-
T_{max*}	2 [1–6]	2 [1–6]	-
AUC_{0-48} (nmol*h/L)	26600 (54.5)	27300 (56.5)	1.00 [0.92–1.09]
$AUC_{0-\infty}$ (nmol*h/L)	32200 (56.5)	32600 (59.3)	0.98 [0.90–1.07]
C_{max} (nmol/L)	1740 (55.0)	1620 (57.1)	0.93 [0.86–1.01]
$T_{1/2}$ (h)	19.5 (16.4)	18.4 (22.7)	-

Unless otherwise specified, data are presented as geometric mean and coefficient of variation (%).

** Median [range], - not calculated, † geometric means of liquid/tablet ratio plus 90% confidence interval. Only data from patients evaluable in both treatment administrations was included (n=14).*

Liquid formulation

Plasma concentration-time curves for the liquid formulation study are provided in Figure 2. Calculated parameters for the pharmacokinetics of the liquid dispersion and tablet are presented in Table 3. T_{max} and $T_{1/2}$ were not affected by dispersing BI 853520 in a liquid. Geometric mean ratios plus 90% CIs of AUC_{0-48}, $AUC_{0-\infty}$ and C_{max} were 0.98 (0.90–1.07), 1.00 (0.92–1.09) and 0.93 (0.86–1.01), respectively. All 90% CIs were within the 80–125% limits, indicating no statistically significant impact on pharmacokinetic exposure.

Discussion

The possible effect of food and formulation (liquid dispersion vs tablet) on pharmacokinetic parameters of BI 853520 were assessed in two randomized, open-label, crossover pharmacokinetic studies. A total of 16 patients were planned for each study. This planned sample size was not based on a power calculation, but was judged to be appropriate to achieve the aims of this exploratory sub-study, and as being adequate to provide a minimum of 12 evaluable patients for the analysis, as required by FDA guidance.

The plasma profile, T_{max} and $T_{1/2}$, of BI 853520 when taken after a high-calorie meal was not markedly different from that in fasted patients. The 90% CI for the ratio of the geometric means of the AUC_{0-48}, $AUC_{0-\infty}$ and C_{max} all crossed the lower of the 80–125% boundaries. However, we consider the reductions not to result in clinically meaningful differences in exposure. Our data, therefore, seem to support the view that BI 853520 may be administered orally without the need for stringent conditions regarding food intake.

Administration of BI 853520 after dispersion of the tablet in a reconstitution solvent did not significantly impact any pharmacokinetic parameters (Table 3, Figure 3). None of the 90% CIs of the calculated pharmacokinetic parameters crossed the predefined 80–125% limits. This indicates that the bioavailability of BI 853520 is unaffected by liquid dispersion and supports the use of the reconstitution liquid to facilitate drug administration in patients having problems swallowing.

Overall, the pharmacokinetic profile of BI 853520 was favorable and unlikely to be influenced by the type of formulation and concomitant administration with food. This will allow for a patient friendly posology without strict requirements for administration under fasted conditions. Also, administration of BI 853520 as a liquid dispersion may be especially convenient for patients who experience problems swallowing or for pediatric patients.

In conclusion, these randomized, open-label, crossover studies indicate no significant effect of liquid dispersion on the pharmacokinetics of BI 853520, and only minimal effect after a high calorie meal. These favorable pharmacokinetic properties contribute to the convenience and flexibility of the posology of BI 853520.

Acknowledgements

Medical writing and editing assistance, supported financially by Boehringer Ingelheim, was provided by Lynn Pritchard of GeoMed, an Ashfield Company, part of UDG Healthcare plc, during the preparation of this article.

Financial support: This work was supported by Boehringer Ingelheim, Ingelheim am Rhein, Germany. BI 853520 is an asset of Boehringer Ingelheim.

References

[1] Lim ST, Mikolon D, Stupack DG, Schlaepfer DD. FERM control of FAK function: Implications for cancer therapy. Cell Cycle 2008;7:2306–14.

[2] Zhang J, Hochwald SN. The role of FAK in tumor metabolism and therapy. Pharmacol Ther 2014;142:154–63.

[3] Sulzmaier FJ, Jean C, Schlaepfer DD. FAK in cancer: mechanistic findings and clinical applications. Nat Rev Cancer 2014;14:598–610.

[4] Oktay MH, Oktay K, Hamele-Bena D, Buyuk A, Koss LG. Focal adhesion kinase as a marker of malignant phenotype in breast and cervical carcinomas. Hum Pathol 2003;34:240–5.

[5] Owens L V, Xu L, Craven RJ, Tumors H, Xu L, Craven RJ, et al. Overexpression of the Focal Adhesion Kinase (p125 FAK) in Invasive Human Tumors. Cancer Res 1995;55:2752–5.

[6] Lark AL, Livasy CA, Calvo B, Caskey L, Moore DT, Yang X, et al. Overexpression of Focal Adhesion Kinase in Primary Colorectal Carcinomas and Colorectal Liver Metastases: Immunohistochemistry and Real-Time 2003;9:215–22.

[7] Judson PL, He X, Cance WG, Van Le L. Overexpression of focal adhesion kinase, a protein tyrosine kinase, in ovarian carcinoma. Cancer 1999;86:1551–6.

[8] Tremblay L, Hauck W, Aprikian AG, Begin LR, Chapdelaine A, Chevalier S. Focal adhesion kinase (pp125FAK) expression, activation and association with paxillin and p50CSK in human metastatic prostate carcinoma. Int J Cancer 1996;68:164–71.

[9] Weiner TM, Liu ET, Craven RJ, Cance WG. Expression of focal adhesion kinase gene and invasive cancer. Lancet (London, England) 1993;342:1024–5.

[10] Ilic D, Kovacic B, McDonagh S, Jin F, Baumbusch C, Gardner DG, et al. Focal adhesion kinase is required for blood vessel morphogenesis. Circ Res 2003;92:300–7.

[11] Golubovskaya VM, Figel S, Ho BT, Johnson CP, Yemma M, Huang G, et al. A small molecule focal adhesion kinase (FAK) inhibitor, targeting Y397 site: 1-(2-hydroxyethyl)-3, 5, 7-triaza-1-azoniatricyclo [3.3.1.1(3,7)]decane; bromide effectively inhibits FAK autophosphorylation activity and decreases cancer cell viability, clonog. Carcinogenesis 2012;33:1004–13.

[12] Golubovskaya VM, Ho B, Zheng M, Magis A, Ostrov D, Morrison C, et al. Disruption of focal adhesion kinase and p53 interaction with small molecule compound R2 reactivated p53 and blocked tumor growth. BMC Cancer 2013;13:342.

[13] Walsh C, Tanjoni I, Uryu S, Tomar A, Nam J-O, Luo H, et al. Oral delivery of PND-1186 FAK inhibitor decreases tumor growth and spontaneous breast to lung metastasis in pre-clinical models. Cancer Biol Ther 2010;9:778–90.

[14] Roberts WG, Ung E, Whalen P, Cooper B, Hulford C, Autry C, et al. Antitumor activity and pharmacology of a selective focal adhesion kinase inhibitor, PF-562,271. Cancer Res 2008;68:1935–44.

[15] Tavora B, Reynolds LE, Batista S, Demircioglu F, Fernandez I, Lechertier T, et al. Endothelial-cell FAK targeting sensitizes tumours to DNA-damaging therapy. Nature 2014;514:112–6.

[16] Jiang H, Hegde S, Knolhoff BL, Zhu Y, Herndon JM, Meyer MA, et al. Targeting focal adhesion kinase renders pancreatic cancers responsive to checkpoint immunotherapy. Nat Med 2016;22:1–13.

[17] Jones SF, Siu LL, Bendell JC, Cleary JM, Razak ARA, Infante JR, et al. A phase i study of VS-6063, a second-generation focal adhesion kinase inhibitor, in patients with advanced solid tumors. Invest New Drugs 2015;33:1100–7.

[18] Infante JR, Camidge DR, Mileshkin LR, Chen EX, Hicks RJ, Rischin D, et al. Safety, pharmacokinetic, and pharmacodynamic phase I dose-escalation trial of PF-00562271, an inhibitor of focal adhesion kinase, in advanced solid tumors. J Clin Oncol 2012;30:1527–33.

[19] Soria JC, Gan HK, Blagden SP, Plummer R, Arkenau HT, Ranson M, et al. A phase I, pharmacokinetic and pharmacodynamic study of GSK2256098, a focal adhesion kinase inhibitor, in patients with advanced solid tumors. Ann Oncol Off J Eur Soc Med Oncol 2016:1–7.

[20] Roy-Luzarraga M, Hodivala-Dilke K. Molecular Pathways: Endothelial Cell FAK-A Target for Cancer Treatment. Clin Cancer Res 2016;22:3718–24.

[21] Singh BN, Malhotra BK. Effects of food on the clinical pharmacokinetics of anticancer agents. Clin Pharmacokinet 2004;43:1127–56.

[22] Parsad S, Ratain MJ. Food Effect Studies for Oncology Drug Products. Clin Pharmacol Ther 2017.

[23] Szmulewitz RZ, Ratain MJ. Playing Russian Roulette With Tyrosine Kinase Inhibitors. Clin Pharmacol Ther 2013;93:242–4.

[24] Heath EI, Chiorean EG, Sweeney CJ, Hodge JP, Lager JJ, Forman K, et al. A phase I study of the pharmacokinetic and safety profiles of oral pazopanib with a high-fat or low-fat meal in patients with advanced solid tumors. Clin Pharmacol Ther 2010;88:818–23.

[25] Chi KN, Spratlin J, Kollmannsberger C, North S, Pankras C, Gonzalez M, et al. Food effects on abiraterone pharmacokinetics in healthy subjects and patients with metastatic castration-resistant prostate cancer. J Clin Pharmacol 2015;55:1406–14.

[26] Kovarik JM, Hartmann S, Figueiredo J, Rordorf C, Golor G, Lison A, et al. Effect of Food on Everolimus Absorption : Quantification in Healthy Subjects and a Confirmatory Screening in Patients With Renal Transplants. Pharmacotherapy 2002;22:154–9.

[27] Lewis LD, Koch KM, Reddy NJ, Cohen RB, Lewis NL, Whitehead B, et al. Effects of food on the relative bioavailability of lapatinib in cancer patients. J Clin Oncol 2009;27:1191–6.

[28] Food and Drug Administration. Guidance for Industry. Food-Effect Bioavailability and Fed Bioequivalance Studies 2002. https://www.fda.gov/downloads/RegulatoryInformation/Guidances/UCM126833.pdf.

[29] Food and Drug Administration. Bioavailability and Bioequivalence Studies submitted in NDAs or INDs - General considerations (Draft) 2014. http://www.fda.gov/downloads/drugs/guidancecomplianceregulatoryinformation/guidances/ucm389370.pdf.

Chapter 7

Conclusion & Perspectives

Conclusion and Perspectives

The introduction of targeted anti-cancer therapies, such as kinase inhibitors, has unrecognizably changed and improved the treatment of cancer. Yet, challenges remain in selecting those patients who may benefit most from these treatments and how to best deploy these agents in the treatment of patients. This thesis describes a range of clinical pharmacological studies to optimize and to personalize the treatment of cancer using kinase inhibitors.

Overall, the first four chapters of this thesis illustrate that there is room for improvement when determining the appropriate dose for kinase inhibitors in oncology. **Chapter 1** shows that the currently used fixed dosing paradigm is far from perfect. First of all, the standard methods to arrive at this fixed dose are based on a strikingly small number of patients. Second, these studies do not formally take into account the optimal efficacious dose, as they focus on determining a maximum tolerable dose. Furthermore, after choosing this fixed dose in the aforementioned small dose-escalation study, this dose is then not reconsidered throughout further drug development nor during the post-approval life cycle. Even though data from hundreds to thousands of patients may have become available before market-entry approval has been granted. **Chapters 2** and **3** of this thesis describe how the standard approved dose of kinase inhibitors could be optimized by further investigating the clinical pharmacology of these drugs. The focus of **chapter 2** is on the oral kinase inhibitor pazopanib and aimed to personalize dosing for this drug. **Chapter 3** aimed to optimize specific pharmacokinetic parameters of everolimus to improve efficacy and to reduce toxicity in cancer patients. **Chapter 4** focusses on real-world patients cohorts and identifies that not all patients benefit optimally from current dosing strategies.
First, multiple bioanalytical methods to quantify pazopanib concentrations in patient samples were developed, validated and applied in **chapters 2.2** and **2.3**. Then, exposure-survival relations were identified in patients routinely treated with pazopanib at the Netherlands Cancer Institute. These analyses indicated that patients with higher pazopanib minimal plasma concentrations (C_{min}) had a longer progression free survival than patients with lower C_{min} (**chapter 2.4**). The following **chapter 2.5** demonstrates in a prospective study in cancer patients that personalizing the pazopanib dose, based on measured C_{min} was feasible, safe and lead to additional patients reaching the targeted pharmacokinetic exposure. Also, we found that patients who reached the targeted exposure had a larger reduction in tumor size than those patients who did not reach this target.
Chapter 3.1 describes a method for the quantification of everolimus concentrations in patients samples using a less invasive sampling technique only requiring a finger prick. Then in **chapter 3.2** we describe a clinical pharmacokinetic study to optimize everolimus dosing in oncology. It was hypothesized that this could be achieved by lowering the maximal concentration (C_{max}) which could easily be achieved by splitting the schedule for once daily (QD) to bi-daily (BID) dosing. To confirm this hypothesis we performed a prospective randomized pharmacokinetic crossover trial comparing everolimus 10 mg QD with 5 mg BID. Switching to a BID schedule significantly

reduced everolimus C_{max} without negatively impacting either total exposure measured as area under the concentration-time curve (AUC) or C_{min}, which are thought to be related to treatment efficacy. Moreover, BID dosing could be combined with therapeutic drug monitoring to further manage the pharmacokinetic exposure in everolimus treatment. Interestingly, in transplantation medicine everolimus is already routinely administered in a BID schedule. These results merit further investigation of the BID everolimus schedule in oncology in an effort to reduce everolimus toxicity whilst maintaining treatment efficacy.
As shown in **chapter 4,** clinical pharmacological properties of kinase inhibitors can also be studied in routine patient care. First we show in **chapter 4.1** that monitoring of circulating tumor DNA could be informative to predict which non-small cell lung cancer patients may benefit optimally from erlotinib or gefitinib treatment. Then in **chapter 4.2** we showed that gastro-intestinal stromal tumor patients are systematically underexposed when treated with the standard imatinib fixed dose. Although these studies separately study either tumor genetics or drug pharmacokinetics, future studies could also integrate these two strategies for an even more detailed monitoring of treatment. One could hypothesize for example that specific thresholds could exist for genetically different tumor types, where more aggressive tumors would need treatment at higher concentrations (at a risk of more toxicity) whilst less aggressive tumors could be treated at a more patient friendly lower dose. To study these dynamic quantitative effects more advanced mathematical methods such as non-linear mixed effect modelling could be an attractive strategy.

These first four chapters indicate that treatment outcomes for cancer patients could be improved further by optimizing and personalizing the dose of kinase inhibitors. Not only could the fixed dosing schedules be improved by optimizing important pharmacokinetic parameters such as the maximum concentrations (C_{max}) and C_{min} as demonstrated for everolimus, but more importantly this optimization should not stop at the population level. Since it has been demonstrated that pharmacokinetic parameters are related to treatment outcomes and that these parameters vary between patients on the same fixed dose, it logically follows that personalizing the dose to achieve these pharmacokinetic targets could improve treatment outcomes. This paradigm is currently already accepted to determine the dose on a group level in special patient populations, such as pediatric patients or patients with renal or hepatic impairment.
To facilitate the implementation of individualized dosing, we have provided recommendations for personalized dosing of kinase inhibitors based on their pharmacokinetic and pharmacodynamic properties in **chapter 1.1**. Although individualized dosing is based on solid scientific reasoning and has shown merit in multiple exploratory clinical trials, some of which are referenced in this thesis (**chapters 1.1** and **2.5**), it is unlikely that these will be sufficient to overcome the fixed dosing paradigm in oncology. Before individualized adaptive dosing schedules can become the new standard of care, further confirmatory clinical trials may be needed, using relevant clinical efficacy endpoints such as progression-free and overall survival. These could then decisively validate the

personalized dosing paradigm and facilitate its implementation as standard care of cancer patients treated with kinase inhibitors.

Leptomeningeal (LM) and central nervous system (CNS) metastases are a frequent occurrence in cancer patients, even in subjects whose extra-cranial lesions are responsive to treatment. LM and CNS lesions are known to result in a dismal prognosis for patients, which can partly be explained by the pharmacokinetic properties of anti-cancer drugs, in particular their limited distribution into the cerebrospinal fluid (CSF) and brain parenchyma. A large part of this limited distribution can be explained by the fact that many kinase inhibitors are substrates for efflux transporters, such as the ATP-binding cassette (ABC) transporters ABCB1 and ABCG2 present in the blood-brain barrier. Co-administration of an inhibitor of these transporters could increase the concentration of kinase inhibitors in the CNS and allow for more effective treatment of LM and CNS metastases.
Elacridar is an inhibitor of both ABCB1 and ABCG2. **Chapter 5.1** describes the phase I dose-escalation study in healthy volunteers to investigate the clinical pharmacokinetics of a novel amorphous solid dispersion formulation of elacridar. The clinical application of this formulation was found to be safe and the 1000 mg dose level resulted in pharmacokinetic exposure which, based on the available data, would be pharmacologically relevant. To proof the concept of ABCB1 and ABCG2 inhibition at the blood-brain barrier, a clinical imaging study using carbon-11 labeled erlotinib as a PET-probe was conducted in cancer patients, which is presented in **chapter 5.2**. In contrast to many preclinical studies in mice and primates, no increase in brain uptake of erlotinib was seen after administration of elacridar in patients. Moreover, no trend towards increased CNS uptake was seen with increasing elacridar plasma concentrations. Thorough analysis of the possible cause of lack of effect, pointed towards a more prominent role of ABCG2 in the human blood-brain barrier. Unfortunately, this weakens the heretofore promising concept of ABCB1 and ABCG2 inhibition in the brain for double substrates. Furthermore, our observations suggest that future clinical trials aiming to increase brain exposure by administration of elacridar should avoid using strong ABCG2 substrates and focus primarily on ABCB1 and/or weak ABCG2 substrates.

Clinical pharmacological research not only focuses on current clinical practice. Clinical pharmacokinetic research can also be beneficial early in drug development to optimize the formulation, dosing and posology of drug candidates. **Chapter 6** studied the clinical pharmacokinetics of BI 853520 in two randomized crossover studies. These indicated that the pharmacokinetic profile of BI 852520 was favorable and unlikely to be strongly influenced by the type of formulation and concomitant administration with food. This will allow for a patient friendly posology without strict requirements for administration under fasted conditions. Also, administration of BI 853520 as a liquid dispersion may be especially convenient for further studies in esophageal cancer, or other tumor types were patient may be likely to experience problems swallowing. Taken together, these favorable pharmacokinetic properties encourage further clinical development of BI 853520 in oncology.

Taken as a whole, this thesis testifies to the relevant contributions the discipline of clinical pharmacology can make to the development of novel anti-cancer drugs and the treatment of cancer patients with already approved agents. In particular, the clinical pharmacokinetic and pharmacodynamic properties of existing drugs and novel drug candidates should be taken into account to further enhance treatment results.

Currently these clinical pharmacological studies are already an integral part of the development and application of anti-cancer drugs. Yet, this thesis provides clear examples and recommendations how and where more emphasis on clinical pharmacology could be leveraged to further improve treatment outcomes by reducing toxicity, improving efficacy and personalizing the treatment of cancer patients treated with kinase inhibitors.

Appendix

Summary
Nederlandse samenvatting
List of publications
Curriculum vitae

Summary

The introduction of targeted anti-cancer therapies has unrecognizably changed and improved the treatment of cancer. Yet, challenges remain in selecting those patients who may benefit most from these treatments and how to best deploy these agents in the treatment of patients. An important class of drugs within these new category of targeted therapies is that of the kinase inhibitors (KIs). This thesis describes clinical pharmacological studies to optimize and personalize the treatment of cancer patients with this class of agents.

Despite the fact that pharmacokinetic exposure of kinase inhibitors is highly variable and clear relationships exist between exposure and treatment outcomes, fixed dosing is still standard practice. **Chapter 1.1** aims to summarize the available clinical pharmacokinetic and pharmacodynamic data into practical guidelines for individualized dosing of KIs through therapeutic drug monitoring (TDM). Additionally, we provide an overview of prospective TDM trials and discuss the future steps needed for further implementation of TDM of KIs.

Chapter 2 of this thesis focusses on pazopanib, a small molecule tyrosine kinase inhibitor targeting the vascular endothelial growth factor receptor (VEGFR)-1,2,3, platelet derived growth factor receptor (PDGFR) α/β, fibroblast growth factor receptor (FGFR) and the stem cell receptor/ c-Kit. **Chapter 2.1** provides an overview of the complex pharmacokinetic and pharmacodynamic profiles of pazopanib and based on the available data we propose optimized dosing strategies. **Chapter 2.2** describes the validation and clinical application of a fast and straightforward method for the quantification of pazopanib in human plasma for the purpose of TDM and bioanalytical support of clinical trials. All validated parameters were within pre-established limits and fulfilled the Food and Drug Administration (FDA) and European Medicines Agency (EMA) requirements for bioanalytical method validation. After completion of the validation, the routine application of the method was tested by analyzing clinical study samples which were collected for the purpose of therapeutic drug monitoring.
For routine monitoring of individual pazopanib exposure plasma sampling may not be ideal, as it is invasive and requires a trained nurse or other healthcare professional to draw the sample. Dried blood spot (DBS) analyses, where a patient draws the blood sample by a simple finger prick is a more convenient alternative. Therefore we developed a DBS assay as a patient friendly approach to guide treatment, described in **chapter 2.3**. The method was validated according to FDA and EMA guidelines and European Bioanalysis Forum recommendations. Influence of spot homogeneity, spot volume and hematocrit were shown to be within acceptable limits. Analysis of paired clinical samples showed a good correlation between the measured plasma and DBS concentrations. The method has been applied to over 300 clinical samples, demonstrating that it is suitable to support TDM and clinical trials of cancer patients treated with pazopanib.

The aim of **chapter 2.4** was to explore the pharmacokinetics and exposure-survival relationships of pazopanib in a real-world patient cohort. In total 61 patients were included in the analysis, of whom 35 had renal cell carcinoma and 26 soft tissue sarcoma. Our study confirmed that the previously established threshold of C_{min} >20 mg/L is related to longer progression free survival in renal cell carcinoma patients. Furthermore, the results showed that at the currently approved fixed dose regimen, a relevant subgroup of 16.4% of patients treated with pazopanib is underexposed in routine care and may be at risk of suboptimal treatment efficacy. Moreover, our data pointed towards a similar association of increased progression free survival with higher exposure in soft tissue sarcoma patients. Plasma C_{min} monitoring of pazopanib can help to identify patients with low C_{min} for whom treatment at a higher dose may be appropriate.
This hypothesis was tested in **chapter 2.5**. Here, we conducted a prospective multicenter trial in 30 patients with advanced solid tumors. An individualized pazopanib dosing algorithm was applied, where C_{min} was measured weekly and the dose was increased if C_{min} was <20 mg/L and toxicity < grade 3.
The dosing algorithm led to patients receiving dosages of 400 to 1800 mg daily. Patients whose dose was increased had a significant increase in exposure. Patients who required a dose reduction for toxicity could in many cases be treated at a reduced dose whilst maintaining adequate exposure. Individualized pazopanib dosing was feasible and safe. Future randomized clinical trials are needed to investigate the effect of individualized dosing on a clinical endpoint such as progression free or overall survival.

Chapter 3 of this thesis studied everolimus. Everolimus is a mammalian target of rapamycin (mTOR)-inhibitor approved for the treatment of renal cell carcinoma, neuroendocrine tumors and hormone receptor positive, human epidermal growth factor receptor 2 (HER2) negative, breast cancer.
Chapter 3.1 shows the bioanalytical validation and clinical application of an LC-MS/MS method to quantify everolimus using the less invasive sampling technique volumetric absorptive microsampling (VAMS). The VAMS method met all pre-specified validation criteria and was successfully applied to several samples from cancer patients treated with everolimus. Unfortunately, no superiority compared to DBS sampling could be demonstrated as a clear effect of hematocrit on analytical performance was also found for the VAMS method.
The currently approved 10 mg once daily (QD) dose is associated with considerable adverse effects, in particular with stomatitis. It has been suggested that these adverse events are associated with the C_{max} of everolimus. Bi-daily (BID) dosing might be an alternative strategy with improved tolerability. In an attempt to improve this, we performed a prospective randomized pharmacokinetic crossover trial comparing everolimus 10 mg QD with 5 mg BID in **chapter 3.2**. Patients received the first dose schedule for two weeks and then switched to the alternative regimen for two weeks. Switching to the 5 mg BID schedule resulted in a significant reduction of C_{max} of 33% whilst maintaining AUC_{0-24h} whilst C_{min} increased. Overall the C_{max}/C_{min} ratio was reduced by 50%. These results merit further

investigation of the BID everolimus schedule in oncology in an effort to reduce everolimus toxicity whilst maintaining treatment efficacy.

Chapter 4 contains clinical pharmacological studies of kinase inhibitors conducted during routine care of cancer patients. In **chapter 4.1**, we monitored the dynamics of circulating tumor (ct) DNA in plasma samples of NSCLC patients treated with erlotinib or gefitinib. In particular, an increase in the EGFR activating mutations over time predicted clinical progression, suggesting ctDNA monitoring could be used as an early read-out of treatment failure. **Chapter 4.2** describes pharmacokinetics of imatinib in a large cohort of gastro-intestinal stromal tumor (GIST) patients in routine care. In total, 421 plasma samples were available from 108 GIST patients. In daily clinical care 32.4% of imatinib treated GIST patients were systematically underexposed, with C_{min} levels <1000 µg/L. This study showed that underexposure is a frequent problem in routine clinical care of imatinib treated GIST patients and future prospective clinical studies are needed to investigate the value of C_{min} guided imatinib dosing in these patients.

Chapter 5 described efforts to improve the delivery of kinase inhibitors across the blood-brain barrier (BBB) into the central nervous system (CNS) to improve prevention and treatment of CNS metastases and tumors. A major hurdle to delivery of kinase inhibitors to the CNS is the active efflux by the ATP-binding cassette (ABC) transporters ABCB1 and ABCG2. Elacridar is an inhibitor of the ABCB1 and ABCG2 and is a promising CNS absorption enhancer of drugs that are substrates of these drug-efflux transporters. **Chapter 5.1** describes the phase I dose-escalation study of an amorphous solid dispersion (ASD) tablet formulation in healthy volunteers. C_{max} and $AUC_{0-\infty}$ increased linearly with dose over the explored range. The target C_{max} of ≥ 200 ng/mL was achieved at the 1000 mg dose level. The ASD tablet was well tolerated, resulted in relevant pharmacokinetic exposure, and suitable for us in proof-of-concept clinical studies.

The proof-of-concept study is described in **chapter 5.2**. The purpose of the present study was to assess whether ^{11}C-erlotinib PET could also be used to quantify erlotinib uptake in the brain, particularly as readout of ABCB1/ABCG2 inhibition at the BBB. To address this question, first preclinical experiments in mice were performed to establish the elacridar concentration needed to achieve Abcb1a/b and Abcg2 inhibition. Next, *in vivo* imaging in wild type and Abcb1a/b and Abcg2 knock out mice was performed to establish the feasibility of monitoring drug transporter inhibition at the BBB using ^{11}C-erlotinib PET. Finally, a clinical trial in cancer patients using ^{11}C-erlotinib PET was performed to non-invasively study the effects of ABCB1/ABCG2-inhibition on the human brain penetration of erlotinib.

Results of our preclinical studies were in accordance with previous reports that have shown a significant effect of combined Abcb1a/b;Abcg2 inhibition by elacridar on erlotinib brain penetration. However, these findings did not translate into an increased brain uptake of erlotinib in cancer patients co-treated with elacridar. The more pronounced role that ABCG2 appears to play at

the human BBB and the lower potency of elacridar to inhibit ABCG2 may be an explanation of these inter-species differences.
These results show that future trials in this area should take into account the pharmacokinetic exposure of the inhibitor, the possible non-linearity of substrate and transporter kinetics and the possibility that an increased brain exposure can be achieved more easily for single ABCB1 than for dual ABCB1/ABCG2 substrates.

Two randomized crossover clinical trials with the novel focal adhesion kinase inhibitor BI 853520 are described in **chapter 6**. The aim of these studies was to evaluate the effect of liquid dispersion and food on the pharmacokinetics of BI 853520. Sixteen patients with advanced solid tumors were enrolled in each sub-study. The order of administration was randomized and pharmacokinetic samples collected for 48 hours after a 200 mg dose of BI 853520. Although minor differences in AUC_{0-48}, $AUC_{0-\infty}$ and C_{max} were found, these are unlikely to be clinically relevant, demonstrating that BI 853520 can be used effectively as a liquid dispersion and no food restrictions need to be provided to patients. These favorable pharmacokinetic properties contribute to the convenience and flexibility of the posology of BI 853520.

In summary, this thesis demonstrates the relevant contributions the discipline of clinical pharmacology can make to the development of novel anti-cancer drugs and the treatment of cancer patients with already approved agents. Although clinical pharmacological studies are already an integral part of the development and application of anti-cancer drugs, this thesis provides clear examples and recommendations how and where more emphasis on clinical pharmacology could be leveraged to further improve treatment outcomes by reducing toxicity, improving efficacy and personalizing the treatment of cancer patients treated with kinase inhibitors.

Samenvatting

De introductie van doelgerichte anti-kankergeneesmiddelen heeft de behandeling van kanker onherkenbaar veranderd en verbeterd. Maar het selecteren van patiënten die het meeste baat hebben bij deze behandelingen en het bepalen hoe deze middelen het best ingezet kunnen worden, blijkt nog steeds cruciaal. Een belangrijke klasse van doelgerichte anti-kankergeneesmiddelen is die van de kinaseremmers. Dit proefschrift beschrijft klinische farmacologische studies ter optimalisatie en personalisatie van deze klasse van geneesmiddelen.

De farmacokinetische blootstelling van kinaseremmers is sterk variabel tussen patiënten en de blootstelling is duidelijk gerelateerd aan de effectiviteit en bijwerkingen van de behandeling. Dit maakt dat sommige patiënten met een hoge blootstelling het risico lopen op bijwerken en anderen met een lage blootstelling het risico lopen op verminderen effectiviteit. Desondanks worden deze middelen in standaardzorg nog steeds gegeven in een vaste dosis. **Hoofdstuk 1.1** geeft een overzicht van de farmacokinetische en farmacodynamische eigenschappen van kinaseremmers en vertaalt deze naar praktische aanbevelingen voor het individualiseren van de dosis op basis van de bloedspiegel, beter bekend als *therapeutic drug monitoring* (TDM). Daarnaast wordt een overzicht gegeven van alle prospectieve klinische TDM studies en beschrijven we de toekomstige stappen die nodig zijn voor de verdere implementatie van TDM voor kinaseremmers in de oncologie.

Hoofdstuk 2 gaat over pazopanib, een remmer van de *vascular endothelial growth factor receptor, platelet derived growth factor receptor, fibroblast growth factor receptor* en de stamcelreceptor/ c-Kit. **Hoofdstuk 2.1** geeft een overzicht van het complexe farmacokinetische en farmacodynamische profiel van pazopanib en gebaseerd op de beschikbare data worden aanbevelingen gedaan voor het optimaliseren van de behandeling met dit middel. **Hoofdstuk 2.2** beschrijft de analytische validatie en klinische toepassing van een methode voor het kwantificeren van pazopanib in humaan plasma ten behoeve van TDM en het ondersteunen van klinische studies met pazopanib. Alle validatieparameters waren binnen de vooraf bepaalde limieten en voldeden aan de *Food & Drug Administration* (FDA) en *European Medicine Agency* (EMA) vereisten voor de validatie van bioanalytische methoden. Na de validatie werd de toepasbaarheid van deze methode aangetoond op een groot aantal plasma monsters van patiënten behandeld met pazopanib.
Voor het monitoren van de pazopanib blootstelling in routinezorg is het afnemen van een plasmamonster mogelijk niet ideaal, omdat hiervoor een getrainde verpleegkundige (of andere zorgmedewerker) nodig is om het monster af te nemen. *Dried blood spot* (DBS) analyses zouden een passend alternatief kunnen zijn. Hier wordt bloed afgenomen door een prik op de vingertop van de patiënt. In **hoofdstuk 2.3** wordt de ontwikkeling en toepassing van een DBS methode voor pazopanib als patiëntvriendelijk alternatief voor de plasmamethode beschreven. De methode werd gevalideerd in overeenkomst met FDA en EMA richtlijnen en *European Bioanalysis Forum* aanbevelingen. Ook de invloed van druppelhomogeniteit, -volume en hematocriet werden

onderzocht. Analyse van meer dan 300 gepaarde plasma en DBS monsters liet zien dat er een goede overeenkomst was tussen beide methoden en dat de DBS methode geschikt was voor het toepassing in TDM en het ondersteunen van klinische studies met patiënten die behandeld worden met pazopanib.

Het doel van **hoofdstuk 2.4** was het onderzoeken van de farmacokinetiek en de relatie tussen de blootstelling en overleving in een cohort van patiënten behandeld met pazopanib. In totaal werden 61 patiënten geïncludeerd, waarvan 35 nierkanker en 26 een wekedelen sarcoom hadden. Onze studie bevestigde dat de streefwaarde van een dalspiegel (C_{min}) van >20 mg/L gerelateerd was aan progressievrije overlevering in nierkankerpatiënten. Verder toonden de resultaten aan dat op de huidige standaarddosering 16.4% van de patiënten een blootstelling onder deze streefwaarde had. Bovendien wezen onze resultaten naar een vergelijkbare associatie van langere progressievrije overleving bij hogere C_{min} in patiënten met een wekedelen sarcoom. Op basis hiervan werd geconcludeerd dat het monitoren van pazopanib C_{min} zinvol is en dat patiënten met een lagere C_{min} mogelijk baat hebben bij een hogere dosis.

Deze hypothese werd vervolgens getest in **hoofdstuk 2.5**. Hier werd een prospectieve klinische studie uitgevoerd in 30 patiënten waarbij een geïndividualiseerd pazopanib doseeralgoritme werd toegepast. Wekelijks werd de C_{min} gemeten waarbij de dosis werd verhoogd als deze <20 mg/L en de toxiciteit <graad 3 was. Het doseeralgoritme leidde tot doseringen uiteenlopend van 400 tot 1800 mg per dag. Patiënten waarbij de dosis verhoogd werd, hadden een significante stijging van de C_{min}. Patiënten bij wie een dosisreductie noodzakelijk was, konden in nagenoeg alle gevallen succesvol behandeld worden op een lagere dosis met adequate blootstelling. Het geïndividualiseerd doseren van pazopanib was haalbaar, veilig en leidde tot een groter aantal patiënten dat de streefwaarde haalde

In **hoofdstuk 3** worden studies naar optimalisatie van de behandeling met everolimus beschreven. Everolimus is een remmer van het *mammalian target of rapamycin* (mTOR) en wordt gebruikt bij de behandeling van nierkanker, neuro-endocriene tumoren en borstkanker. **Hoofdstuk 3.1** laat de validatie en klinische toepassing van een bioanalytische methode voor het kwantificeren van everolimus zien. De methode maakte gebruik van de minder invasieve *volumetric absorptive microsampling* (VAMS) techniek. De methode voldeed aan alle validatiecriteria en werd toegepast op een set monsters van kankerpatiënten die behandeld werden met everolimus. Hoewel de methode dus succesvol gevalideerd en toegepast kon worden, kon er helaas geen superioriteit ten opzichte van DBS methoden aangetoond worden, aangezien er ook voor VAMS een duidelijk effect van hematocriet op de analytische resultaten aantoonbaar was.

De huidige dosis van everolimus is 10 mg eenmaal daags (QD). Deze dosis is geassocieerd met aanzienlijke bijwerkingen, zoals stomatitis. Het wordt gesuggereerd dat deze bijwerkingen vooral het gevolg zijn van een hoge topspiegel (C_{max}). Tweemaal daags doseren (BID) zou hierdoor een geschikt alternatief kunnen zijn met betere tolerantie. Om dit te onderzoeken hebben we in **hoofdstuk 3.2** een gerandomiseerde farmacokinetische crossover studie gedaan die 5 mg BID

met 10 mg QD vergeleek. Overstappen naar het BID schema leidde tot een significante daling van de C_{max} van 33% terwijl de totale blootstelling gemeten als *area under the concentration time curve* (AUC_{0-24h}) gelijk bleef en de C_{min} steeg. De ratio van C_{max}/C_{min} daalde met 50%. Op basis van deze veelbelovende resultaten kan verder onderzocht worden of dit zou kunnen leiden tot verminderde toxiciteit bij gelijke effectiviteit.

Hoofdstuk 4 bevat klinisch farmacologische studies met kinaseremmers die uitgevoerd zijn gedurende de routinezorg van patiënten. In **hoofdstuk 4.1** wordt de dynamiek van circulerend tumor DNA (ctDNA) in patiënten met een niet-kleincellig longcarcinoom die behandeld werden met de *epidermal growth factor receptor* (EGFR) remmers erlotinib of gefitinib beschreven. In het bijzonder is gekeken naar patiënten waar de concentratie van de activerende EGFR mutatie in bloed toenam in de tijd. Dit fenomeen leek voorspellend te zijn voor tumorprogressie en suggereerde dat het monitoren van ctDNA gebruikt zou kunnen worden als vroege voorspeller van therapiefalen. **Hoofdstuk 4.2** beschrijft de farmacokinetiek van de kinaseremmer imatinib in een groot cohort van gastro-intestinale stromale tumor (GIST) patiënten. In totaal waren 421 monsters van 108 patiënten beschikbaar. In de praktijk bleken 32.4% van de patiënten systematisch niet de drempelwaarde van 1000 µg/L te halen. Dit toonde aan dat lage blootstelling een frequent probleem is in routine zorg van GIST patiënten die met imatinib behandeld worden en dat toekomstige klinische studies nodig zijn om de waarde van het doseren van imatinib op basis van de C_{min} aan te tonen.

Naast het suboptimale *one-size-fits-all* doseren van kinaseremmers is een andere tekortkoming van deze middelen dat ze vaak maar in beperkte mate effectief zijn tegen tumoren en metastasen in het centrale zenuwstelsel. Het feit dat ze door de aanwezigheid van de bloed-hersenbarrière vaak maar in lage concentraties deze laesies bereiken speelt hier belangrijke rol in.
Hoofdstuk 5 beschrijft studies die tot doel hadden om de blootstelling van kinaseremmers in het centrale zenuwstelsel te bevorderen met als streven het verbeteren van de behandeling van hersentumoren en –metastasen. Elacridar is een potente remmer van ABCB1 en ABCG2, beide belangrijke geneesmiddeltransporters in de bloed-hersenbarrière. **Hoofdstuk 5.1** laat de fase I dosisescalatie studie van een *amorphous solid dispersion* (ASD) tablet van elacridar in gezonde vrijwilligers zien. De C_{max} en $AUC_{0-\infty}$ namen lineair toe met de dosis en de beoogde blootstelling van een C_{max} van ≥ 200 ng/mL werd behaald op een dosis van 1000 mg. De ASD tablet werd goed getolereerd en resulteerde in relevante farmacokinetische blootstelling en werd daarmee geschikt bevonden voor het gebruik in *proof-of-concept* studies in patiënten.

Deze *proof-of-concept* studie wordt beschreven in **hoofdstuk 5.2**. Het doel was om te onderzoeken of door middel van ^{11}C-erlotinib PET een toename in de hersenconcentratie van erlotinib kon worden aangetoond in patiënten na een eenmalige dosis van de ABCB1/ABCG2 remmer elacridar. Eerst werd in muisexperimenten gekeken welke concentratie elacridar nodig was voor optimale remming van deze transporters. Daarnaast werd met *in vivo* ^{11}C-erlotinib PET imaging gekeken of het haalbaar

was om de hersenopname van erlotinib te visualiseren. Uiteindelijk werd in een klinische studie ^{11}C-erlotinib PET toegepast om het effect van ABCB1/ABCG2 remming op het menselijke brein te bestuderen, door voor en na een dosis elacridar scans te maken.
De resultaten van de preklinische experimenten waren in overeenstemming met data uit de literatuur en lieten een stijging van de erlotinib opname in het brein zien na toediening van elacridar. Maar in de klinische studie kon na inname van elacridar geen toename van ^{11}C-erlotinib in het brein worden aangetoond. De meer prominente rol van ABCG2 in de humane bloed-hersenbarrière en lagere potentie van elacridar voor ABCG2 zijn een mogelijke oorzaak van het verschil tussen de preklinische en klinische resultaten.
Deze studie wijst op het belang voor toekomstige studies in dit veld om rekening te houden met de farmacokinetische blootstelling van de transportremmer, de mogelijke non-lineariteit van transporter- en substraatkinetiek en het feit dat het waarschijnlijk makkelijker is om de breinconcentratie te verhogen voor pure ABCB1 dan voor ABCB1/ABCG2 substraten.

In **hoofdstuk 6** worden 2 gerandomiseerde crossover studies met de *focal adhesion kinase* remmer BI 853520 weergegeven. Het doel was om het effect van voedsel en het toedienen als een vloeistof op de farmacokinetiek van BI 853520 te evalueren. Hoewel er kleine verschillen in $AUC_{0\text{-}48}$, $AUC_{0\text{-}\infty}$ en C_{max} werden gevonden, is het onwaarschijnlijk dat deze klinisch relevant zullen zijn. Hiermee toonde deze studies aan dat BI 853520 effectief toegediend kan worden als een vloeistof en dat er wat betreft inname met voedsel geen extra voorzorgsmaatregelen nodig zijn. Deze gunstige farmacokinetische eigenschapen dragen bij aan het gebruiksgemak voor patiënten en de flexibiliteit van de posologie van BI 853520.

Samengevat laat dit proefschrift concreet zien hoe klinisch farmacologisch onderzoek kan bijdragen aan de optimalisatie van de behandeling van kankerpatiënten met kinaseremmers. Klinisch farmacologische studies zijn in beperkte mate al een standaard onderdeel van de ontwikkeling van nieuwe geneesmiddelen. Toch geeft dit proefschrift praktische voorbeelden hoe de verdere toepassing van de klinische farmacologie, door middel van het optimaliseren en personaliseren van het gebruik van kinaseremmers, kan bijdragen aan het verbeteren van de behandeling van patiënten met kanker.

Dankwoord

Boven alles wil ik alle patiënten bedanken, die gedurende een zeer moeilijke tijd in hun leven deelnamen aan de studies die de basis vormen van dit proefschrift. Zonder hun deelname was dit onderzoek niet mogelijk geweest.

Neeltje en Alwin, ik wil jullie bedanken voor de mogelijkheid om dit onderzoek te hebben kunnen doen. Het was uitdagend om projecten zowel in de kliniek als in het lab op te zetten (met hier en daar nog een sponsorstudie of andersoortig randproject erbij). Gelukkig waren jullie er altijd voor mij met de nodige ondersteuning, ervaring, expertise en bereidheid om mij op te rapen en af te stoffen als ik weer eens omviel. Samen vormen jullie wat mij betreft het dreamteam voor de farmacologische oncologie in Nederland. Ik ben ervan overtuigd dat jullie nog veel zullen bereiken!

Jos en Jan, de kwaliteit en kwantiteit van het farmacologisch onderzoek in het AvL is indrukwekkend dankzij de onderzoeksgroep die jullie gedurende de jaren, samen met de eerdere generaties onderzoekers en OIOs, hebben opgebouwd. Ik wil jullie bedanken voor jullie expertise en input op mijn projecten, presentaties en manuscripten.

Graag wil ik alle collega's van het AvL bedanken die meegewerkt hebben aan dit onderzoek in de eerste plaats de artsen, VS-en, verpleegkundigen en anderen van de Farmacologie afdeling en CRU, maar ook de wetenschappelijke administratie, het klinisch lab en de pathologie. Ook de afdeling de radiologie, in het bijzonder Annemarie, zou ik willen bedanken voor de ondersteuning bij het uitvoeren van dit onderzoek.
Ook wil ik iedereen van het apotheeklab, in het bijzonder Hilde, Bas en Niels bedanken voor het ondersteunen (en doorstaan?) van mijn projecten aldaar.

Ook de onderzoekers uit de andere centra, het ErasmusMC, UMCU en VUMC wil ik bedanken voor hun bijdrage aan dit proefschrift, met name Harry, Maqsood, Sander, Florence en Ron.

Liefste OIOs, uit de keet, balzaal, O1 en tot slot H3,
Bedankt voor alle inhoudelijke en vooral niet-inhoudelijke ondersteuning de afgelopen jaren. Bij uitstek gaat mijn liefde uit naar alle OIOs uit room 5 en mijn paranimfen Sven en Niels! Mijn excuses als ik soms onuitgenodigd wetenschappelijk of non-wetenschappelijk advies gegeven heb. Mijn bedoelingen waren altijd goed. Vooral bedankt ook voor alle koffie, vrijdagen, weekenden en surprises. Zonder jullie had ik het niet kunnen en willen doen!

Beste clowntjes (jullie weten wel wie jullie zijn), bedankt voor de broodnodige afleiding en ontspanning gedurende het zwoegen de afgelopen jaren.

Pap, Mam, Max en Tris,
Bedankt dat jullie mij altijd gesteund en in mij geloofd hebben. Als ik ooit iets bereikt heb, is dat dankzij jullie!

List of publications

- Pharmacokinetic optimization of everolimus dosing in oncology: a randomized crossover trial.
  Verheijen RB, Atrafi F, Schellens JHM, Beijnen JH, Huitema ADR, Mathijssen RHJ, Steeghs N.
  Clin Pharmacokinet. 2017 Jul 31. [Epub ahead of print]
- Practical recommendations for therapeutic drug monitoring of kinase inhibitors in oncology.
  Verheijen RB, Yu H, Schellens JHM, Beijnen JH, Steeghs N, Huitema ADR.
  Clin Pharmacol Ther. 2017 Jul 12 [Epub ahead of print].
- Clinical pharmacokinetics & pharmacodynamics of pazopanib: towards optimized dosing.
  Verheijen RB, Beijnen JH, Schellens JH, Huitema ADR, Steeghs N.
  Clin Pharmacokinet. 2017 Feb 10 [Epub ahead of print].
- Imatinib pharmacokinetics in a large observational cohort of gastrointestinal stromal tumor patients.
  Farag S, **Verheijen RB**, Martijn Kerst J, Cats A, Huitema ADR, Steeghs N.
  Clin Pharmacokinet. 2017 Mar;56(3):287-292.
- Clinical pharmacokinetics of an amorphous solid dispersion tablet of elacridar.
  Sawicki E, **Verheijen RB**, Huitema ADR, van Tellingen O, Schellens JHM, Nuijen B, Beijnen JH, Steeghs N.
  Drug Deliv Transl Res. 2017 Feb;7(1):125-131.
- Individualized pazopanib dosing: a prospective feasibility study in cancer patients.
  Verheijen RB, Bins S, Mathijssen RHJ, Lolkema MP, van Doorn L, Schellens JHM, Beijnen JH, Langenberg MH, Huitema ADR, Steeghs N.
  Clin Cancer Res. 2016 Dec 1;22(23):5738-5746.
- Individualized pazopanib dosing-response.
  Verheijen RB, Huitema ADR, Steeghs N.
  Clin Cancer Res. 2016 Dec 15;22(24):6299.
- Development and clinical validation of an LC-MS/MS method for the quantification of pazopanib in DBS.
  Verheijen RB, Bins S, Thijssen B, Rosing H, Nan L, Schellens JHM, Mathijssen RHJ, Lolkema MP, Beijnen JH, Steeghs N, Huitema ADR.
  Bioanalysis. 2016 Jan;8(2):123-34.
- In vivo visualization of MET tumor expression and anticalin biodistribution with the MET-specific anticalin 89Zr-PRS-110 PET tracer.
  Terwisscha van Scheltinga AG, Lub-de Hooge MN, Hinner MJ, **Verheijen RB**, Allersdorfer A, Hülsmeyer M, Nagengast WB, Schröder CP, Kosterink JG, de Vries EGE, Audoly L, Olwill SA.
  J Nucl Med. 2014 Apr;55(4):665-71.

Curriculum vitae

Remy Verheijen was born on July 27th 1989 in Wilnis (De Ronde Venen). After graduating from grammar school at the Stedelijk Gymnasium Nijmegen in 2007, he went on to study Pharmacy at the University of Groningen, where he received his Bachelor and Master of Science, both cum laude. He conducted his scientific internship at the departments of Medical Oncology, Nuclear Medicine & Molecular Imaging and Clinical Pharmacy & Pharmacology of the University Medical Center Groningen, where he investigated molecular imaging of investigational medicinal proteins using Zirconium-89 in xenograft models. Subsequently, he started his PhD research at the department of Pharmacy & Pharmacology of the Netherlands Cancer Institute – Antoni van Leeuwenhoek and MC Slotervaart, supervised by dr. N. Steeghs, prof.dr. J.H. Beijnen, prof.dr. J.H.M. Schellens and prof. dr. A.D.R. Huitema. His PhD research resulted in this thesis, which he will defend at the University of Utrecht on November 29th 2017.